

APPENDIX 3.B - ANALYSIS OF DAMAGED FUEL CONTAINER

3.B.1 Introduction

This appendix contains an analysis of the damaged fuel container that is used for the HI-STAR 100 MPC. The objective of the analysis is to demonstrate that the storage container is structurally adequate to support the loads that develop during normal lifting operations and during an end drop.

The upper closure assembly is designed to meet the requirements set forth for Special Lifting Devices in Nuclear Plants [2]. The remaining components of the damaged fuel container are governed by ASME Code Section III, Subsection NG.

3.B.2 Composition

This appendix was created using the Mathcad (version 6.0+) software package. Mathcad uses the symbol ':=' as an assignment operator, and the equals symbol '=' retrieves values for constants or variables.

3.B.3 References

1. Crane Manufacture's of America Association, Specifications for Electric Overhead Traveling Cranes #70.
2. ANSI N14-6, Special Lifting Devices for Loads Greater than 10000 lbs. in Nuclear Plants.
3. ASME Boiler and Pressure Vessel Code, Section III Subsection NG, July 1995

3.B.4 Assumptions

1. Buckling is not a concern during an accident since during a drop the canister will be supported by the walls of the fuel basket.
2. The strength of the weld is assumed to decrease the same as the base metal as the temperature is increased.

3.B.5 Method

Three cases are considered: 1) normal handling of container, 2) evaluation of lifting attachment to ANSI N14-6 criteria, and 3) accident drop event.

3.B.6 Acceptance Criteria

1) Normal Handling -

a) Container governed by ASME NG[3] allowables:
shear stress allowable is 60% of membrane stress intensity

b) Welds are governed by NG Code allowables with appropriate quality factors;
stress limit = 60% of tensile stress intensity (per Section III, Subsection NG-3227.2).

2) Drop Accident -

a) Container governed by ASME Section III, Appendix F allowables:
(allowable shear stress = 0.42 S_u)

3.B.7 Input Data

The damaged fuel container is only handled while still in the spent fuel pool. Therefore, its design temperature for lifting considerations is the temperature of the fuel pool water (150°F). The design temperature for accident conditions is 725°F. All dimensions are taken from the design drawings and bill of materials in Chapter 1. The basic input parameters used to perform the calculations are:

Design stress intensity of SA240-304 (150°F)	$S_{m1} := 20000 \cdot \text{psi}$	Table 1.A.1
Design stress intensity of SA240-304 (725°F)	$S_{m2} := 15800 \cdot \text{psi}$	
Yield stress of SA240-304 (150°F)	$S_{y1} := 27500 \cdot \text{psi}$	Table 1.A.3
Yield stress of SA240-304 (725°F)	$S_{y2} := 17500 \cdot \text{psi}$	
Ultimate strength of SA240-304 (150°F)	$S_{u1} := 73000 \cdot \text{psi}$	Table 1.A.2
Ultimate strength of SA240-304 (725°F)	$S_{u2} := 63300 \cdot \text{psi}$	
Ultimate strength of weld material (150°F)	$S_{u_w} := 70000 \cdot \text{psi}$	
Ultimate strength of weld material (725°F)	$S_{u_{wacc}} := S_{u_w} \frac{S_{u2}}{S_{u1}}$	
Weight of a BWR fuel assembly	$W_{fuel} := 400 \cdot \text{lbf}$	
Weight of the damaged fuel container	$W_{container} := 150 \cdot \text{lbf}$	

Wall thickness of the container sleeve	$t_{\text{sleeve}} := 0.12 \cdot \text{in}$
Thickness of the base	$t_{\text{base}} := 0.12 \cdot \text{in}$
Inner dimension of the container sleeve	$id_{\text{sleeve}} := 4.93 \cdot \text{in}$
Wall thickness of container collar	$t_{\text{collar}} := 0.12 \cdot \text{in}$
Distance from end of sleeve to top of engagement slot	$d_{\text{slot}} := 0.44 \cdot \text{in}$
Diameter of the shear pin	$D_{\text{pin}} := 0.375 \cdot \text{in}$
Diameter of the lead-in	$D_{\text{leadin}} := 0.75 \cdot \text{in}$
Wall thickness of the lead-in (Sch. 160 pipe)	$t_{\text{leadin}} := 0.218 \cdot \text{in}$
Thickness of weld between lead-in ext. and collar	$t_{\text{weld1}} := 0.125 \cdot \text{in}$
Length of the load tab	$l_{\text{tab}} := 2.15 \cdot \text{in}$
Height of the load tab	$h_{\text{tab}} := 0.5 \cdot \text{in}$
Width of the load tab	$w_{\text{tab}} := 0.5 \cdot \text{in}$
Thickness of weld between locking shaft and load tab	$t_{\text{weld2}} := 0.1875 \cdot \text{in}$
Thickness of fuel spacer tubing	$t_{\text{tube}} := 0.25 \cdot \text{in}$
Size of fuel spacer (square) tubing	$s_{\text{tube}} := 4.0 \cdot \text{in}$
Size of square cutout in fuel spacer tubing	$s_{\text{cutout}} := 1.75 \cdot \text{in}$
Quality factor for full penetration weld (visual inspection)	$n := 0.5$
Quality factor for single fillet weld (visual inspection)	$nf := 0.35$
Dynamic load factor for lifting [1]	$DLF := 1.15$

Table NG-3352-1

3.B.7 Calculations

3.B.7.1 Lifting Operation (Normal Condition)

The critical load case under normal conditions is the lifting operation. The key areas of concern are the container sleeve, the weld between the sleeve and the base of the container, the container collar, and the upper closure assembly. All calculations performed for the lifting operation assume a dynamic load factor of 1.15.

3.B.7.1.1 Container Sleeve

During a lift, the container sleeve is loaded axially, and the stress state is pure tensile membrane. For the subsequent stress calculation, it is assumed that the full weight of the damaged fuel container and the fuel assembly are supported by the sleeve. The magnitude of the load is

$$F := \text{DLF} \cdot (W_{\text{container}} + W_{\text{fuel}}) \quad F = 632 \text{ lbf}$$

The cross sectional area of the sleeve is

$$A_{\text{sleeve}} := (\text{id}_{\text{sleeve}} + 2 \cdot t_{\text{sleeve}})^2 - \text{id}_{\text{sleeve}}^2 \quad A_{\text{sleeve}} = 2.42 \text{ in}^2$$

Therefore, the tensile stress in the sleeve is

$$\sigma := \frac{F}{A_{\text{sleeve}}} \quad \sigma = 261 \text{ psi}$$

The allowable stress intensity for the primary membrane category is S_m per Subsection NG of the ASME Code. The corresponding safety factor is

$$\text{SF} := \frac{S_m}{\sigma} \quad \text{SF} = 76.6$$

3.B.7.1.2 Base Weld

The base of the container must support the amplified weight of the fuel assembly. This load is carried directly by the full penetration weld which connects the base to the container sleeve. The magnitude of the load is

$$F := \text{DLF} \cdot W_{\text{fuel}} \quad F = 460 \text{ lbf}$$

The area of the weld, with proper consideration of quality factors, is

$$A_{\text{weld}} := n \cdot 4 \cdot d_{\text{sleeve}} \cdot t_{\text{base}} \quad A_{\text{weld}} = 1.18 \text{ in}^2$$

Therefore, the amplified shear stress in the weld, including the quality factor, is

$$\sigma := \frac{F}{A_{\text{weld}}} \quad \sigma = 389 \text{ psi}$$

From the ASME Code the allowable weld shear stress, under normal conditions (Level A), is 60% of the membrane strength of the base metal. The corresponding safety factor is

$$SF := \frac{0.6 \cdot S_{m1}}{\sigma} \quad SF = 30.9$$

3.B.7.1.3 Container Collar

The load tabs of the upper closure assembly engage the container collar during a lift. The load transferred to the engagement slot, by a single tab, is

$$F := \frac{DLF \cdot (W_{\text{container}} + W_{\text{fuel}})}{2} \quad F = 316.25 \text{ lbf}$$

The shear area of the container collar is

$$A_{\text{collar}} := 2 \cdot d_{\text{slot}} \cdot (t_{\text{sleeve}} + t_{\text{collar}}) \quad A_{\text{collar}} = 0.211 \text{ in}^2$$

The shear stress in the collar is

$$\sigma := \frac{F}{A_{\text{collar}}} \quad \sigma = 1497 \text{ psi}$$

The allowable shear stress from Subsection NG, under normal conditions, is

$$\sigma_{\text{allowable}} := 0.6 \cdot S_{m1} \quad \sigma_{\text{allowable}} = 12000 \text{ psi}$$

Therefore, the safety factor is

$$SF := \frac{\sigma_{\text{allowable}}}{\sigma} \quad SF = 8$$

3.B.7.1.4 Upper Closure Assembly

The upper closure assembly is classified as a special lifting device [2]. As such the allowable tensile stress for design is the lesser of one-third of the yield stress and one-fifth of the ultimate strength.

$$\sigma_1 := \frac{S_{y1}}{3} \qquad \sigma_2 := \frac{S_{u1}}{5}$$
$$\sigma_1 = 9167 \text{ psi} \qquad \sigma_2 = 14600 \text{ psi}$$

For SA240-304 material the yield stress governs at the lifting temperature.

$$\sigma_{\text{allowable}} := \sigma_1$$

The total lifted load is

$$F := \text{DLF} \cdot (W_{\text{container}} + W_{\text{fuel}}) \qquad F = 632 \text{ lbf}$$

The shear stress in the shear pin under this load is calculated as

$$A_{\text{pin}} := \frac{\pi}{4} \cdot D_{\text{pin}}^2 \qquad A_{\text{pin}} = 0.11 \text{ in}^2$$
$$\sigma := \frac{F}{2 \cdot A_{\text{pin}}} \qquad \sigma = 2863 \text{ psi}$$

The safety factor is

$$\text{SF} := \frac{0.6 \sigma_{\text{allowable}}}{\sigma} \qquad \text{SF} = 1.92$$

The bearing stress in the lead-in and the corresponding safety factor are

$$\sigma := \frac{F}{2 \cdot D_{\text{pin}} \cdot t_{\text{leadin}}} \qquad \sigma = 3869 \text{ psi}$$
$$\text{SF} := \frac{\sigma_{\text{allowable}}}{\sigma} \qquad \text{SF} = 2.37$$

The stress in the full penetration weld between the lead-in extension and the lead-in collar is (quality factor is 0.5) is computed from the available weld area and the force F

$$A_{\text{weld}} := \pi \cdot D_{\text{leadin}} \cdot t_{\text{weld1}} \quad A_{\text{weld}} = 0.295 \text{ in}^2$$

The shear stress in the weld is

$$\sigma := \frac{F}{A_{\text{weld}}} \quad \sigma = 2148 \text{ psi}$$

The safety factor is

$$\text{SF} := \frac{n \cdot \sigma_{\text{allowable}}}{\sigma} \quad \text{SF} = 2.13$$

The shear stress in the load tabs due to the lifted weight is computed as follows:

$$A_{\text{tab}} := h_{\text{tab}} \cdot w_{\text{tab}} \quad A_{\text{tab}} = 0.25 \text{ in}^2$$

$$\sigma := \frac{F}{2 \cdot A_{\text{tab}}} \quad \sigma = 1265 \text{ psi}$$

The safety factor is

$$\text{SF} := \frac{.6 \cdot \sigma_{\text{allowable}}}{\sigma} \quad \text{SF} = 4.35$$

If the full weight of the lift is supported by the fillet welds between the locking shaft and the load tabs, the shear stress in the welds is

$$A_{\text{weld}} := 2 \cdot h_{\text{tab}} \cdot t_{\text{weld2}} \quad A_{\text{weld}} = 0.187 \text{ in}^2 \quad \sigma := \frac{F}{2 \cdot A_{\text{weld}}} \quad \sigma = 1687 \text{ psi}$$

The safety factor is

$$\text{SF} := \frac{n \cdot .6 \cdot \sigma_{\text{allowable}}}{\sigma} \quad \text{SF} = 1.14$$

3.B.7.2 60g End Drop (Accident Condition)

The critical member of the damaged fuel container during the drop scenario is the lower fuel spacer. It is subjected to direct compression due to the amplified weight of the fuel assembly. The lower fuel spacer has four leg members at the corners of the tube. The load per leg due to a 60g end drop is

$$F := \frac{60 \cdot W_{\text{fuel}}}{4}$$

$$F = 6000 \text{ lbf}$$

The cross sectional area of each leg is

$$A_{\text{leg}} := (s_{\text{tube}} - s_{\text{cutout}}) \cdot t_{\text{tube}}$$

$$A_{\text{leg}} = 0.56 \text{ in}^2$$

The stress in the member is

$$\sigma := \frac{F}{A_{\text{leg}}}$$

$$\sigma = 10667 \text{ psi}$$

The allowable primary membrane stress from Subsection NG of the ASME Code, for accident conditions (Level D), is

$$\sigma_{\text{allowable}} := 2.4 \cdot S_{m2}$$

$$\sigma_{\text{allowable}} = 37920 \text{ psi}$$

The safety factor is

$$SF := \frac{\sigma_{\text{allowable}}}{\sigma}$$

$$SF = 3.6$$

3.B.8 Conclusion

The damaged fuel container and the upper closure assembly are structurally adequate to withstand the specified normal and accident condition loads. All calculated safety factors are greater than one, which demonstrates that all acceptance criteria have been met or exceeded.

APPENDIX 3.C - RESPONSE OF CASK TO TORNADO WIND LOAD AND LARGE MISSILE IMPACT

3.C.1 Introduction

The objective of this analysis is to determine the response of the cask to the combined load of the wind due to the design basis tornado and the large missile impact (loading case B) specified in Section 2.2.3. It is demonstrated that under this loading condition, the cask will not tip over. The case of large missile impact plus the instantaneous pressure drop due to the tornado passing the cask is also considered. The two cases need not be combined.

Impacts from two types of smaller missiles are considered in Appendix 3.G.

3.C.2 Method

In this analysis, the cask is simultaneously subjected to a missile impact at the top of the cask and either a constant wind force or an instantaneous pressure drop leading to an impulsive adder to the initial angular velocity imparted by a missile strike. The configuration of the system just prior to impact by the missile is shown in Figure 3.C.1.

The first step of the analysis is to determine the post-strike angular velocity of the cask, which is the relevant initial condition for the solution of the post-impact cask equation of motion. There are certain limiting assumptions that we can make to compute the post-impact angular velocity of the cask. There are three potential limiting options available.

- a. Assume a coefficient of restitution (ratio of velocity of separation to velocity of approach) = 1. This assumption results in independent post impact motion of both the cask and the missile with the change in kinetic energy of the missile being entirely transmitted to the cask.
- b. Assume a coefficient of restitution = 0. This assumption results in the missile and the cask moving together after the impact with a certain portion of the kinetic energy lost by the missile being dissipated during the collision so that the post impact kinetic energy is less than the energy change in the missile.
- c. Assume a coefficient of restitution = mass of missile/mass of cask. This assumption brings the missile to rest after the impact. There is kinetic energy dissipated during the impact process but the kinetic energy acquired by the cask is larger than in case b.

Missile impact tests conducted under the auspices of the Electric Power Research Institute (see EPRI NP-440, Full Scale Tornado Missile Impact Tests", 1977) have demonstrated that case c above matches the results of testing.

Determination of the force on the cask due to the steady tornado wind is the next step. The primary tornado load is assumed to be a constant force due to the wind, acting on the projected area of the cask and acting in the direction that tends to cause maximum propensity for overturning.

The equation of motion of the cask under the wind loading is developed, and using the initial angular velocity of the cask due to the missile strike, the time-dependent solution for the post-impact position of the cask centroid is obtained.

In the second scenario, the missile impact occurs at the same instant that the cask sees the pressure drop due to the passing of the tornado.

3.C.3 Assumptions

The assumptions for the analysis are stated here; further explanation is provided in the subsequent text.

1. The cask is assumed to be a rigid solid cylinder, with uniform mass distribution. This assumption implies that the cask sustains no plastic deformation (i.e. no absorption of energy through plastic deformation of the cask occurs).
2. The angle of incidence of the missile is assumed to be such that its overturning effect on the cask is maximized.
3. The missile is assumed to strike at the highest point of the cask, again maximizing the overturning effect.
4. The cask is assumed to pivot about a point at the bottom of the baseplate opposite the location of missile impact and application of wind force in order to conservatively maximize the propensity for overturning.
5. Inelastic impact is assumed, indicating that the missile velocity is reduced to zero after impact. This assumption conservatively lets the missile impart the maximum amount of momentum to the cask.
6. The missile does not adhere to the cask, even though the coefficient of restitution is assumed to be zero.
7. The analysis is performed for a cask without fuel. A lighter cask will tend to rotate further after the missile strike. The weight of the missile is not included in the total post-impact weight. A lower bound weight of 189,000 lbs is used in this analysis.

8. Planar motion of the cask is assumed; any loads from out-of-plane wind forces are neglected. In typical impacts, a portion of the energy will be expended in rotating the cask. No such energy dissipation is assumed.

9. The drag coefficient for a cylinder in turbulent crossflow is conservatively taken as 0.6. Per Mark's Standard Handbook for Mechanical Engineers [3.C.1], the drag coefficient (C_d) for a cylinder in crossflow at the calculated Reynold's number is less than 0.5. The use of a higher drag coefficient results in a greater overturning force.

10. The missile and wind loads are assumed to be perfectly aligned in direction.

11. The instantaneous pressure drop is converted to an initial angular motion of the cask by an impulse-momentum relation.

12. The coefficient of friction between the cask and the foundation is assumed to be infinite. In other words, there is no conversion of the missile kinetic energy into translational motion of the cask.

It is recognized that the above assumptions taken together impose a large measure of conservatism in the dynamic model, but render the analysis highly simplified. In a similar spirit of simplification, the calculations are performed by neglecting the geometry changes which occur due to the dynamic motion of the cask. This linearity assumption is consistent with the spirit of the simplified model used herein.

Certain overseas and domestic sites may have different missile and wind load requirements. The evaluation for the specific site shall consider its design basis loads, but shall utilize the methodology presented in this appendix.

3.C.4 Input Data

The following input data is used to perform the analysis. All dimensions are obtained from the Design Drawings in Section 1.5.

The weight of the cask plus contents, $W_c := 189000 \cdot \text{lbf}$

The cask total height, $L := 203.125 \cdot \text{in}$

The diameter of the cask base in contact with the supporting surface, $a := 83.25 \cdot \text{in}$

The maximum diameter of the overpack, $D := 96.0 \cdot \text{in}$

Gravitational acceleration, $g := 386.4 \cdot \frac{\text{in}}{\text{sec}^2}$

The weight of the large missile (1800 kg, from Table 2.2.5), $W_m := 3960 \cdot \text{lbf}$

The maximum tornado wind speed (from Table 2.2.4), $v_t := 360 \text{ mph}$

The pre-impact missile velocity (from Table 2.2.5), $v_m := 126 \text{ mph}$

The translation speed of the tornado (from Table 2.2.4), $V_{tr} := 70 \text{ mph}$

The drag coefficient for cylinder in turbulent crossflow, $C_d := 0.6$

The density of air, $\rho_{air} := 0.075 \frac{\text{lbf}}{\text{ft}^3}$ ("lbf" indicates pounds "force")

The viscosity of air, $\mu_{air} := 4.18 \cdot 10^{-7} \frac{\text{lbf}}{\text{ft} \cdot \text{sec}}$

Maximum instantaneous pressure drop (from Table 2.2.4), $dp := 3 \text{ psi}$

The total mass of the cask and its contents (M_c) can be calculated from the total weight and gravitational acceleration as:

$$M_c := \frac{W_c}{g}$$

Similarly, the mass of the large missile (M_m) can be calculated from its weight and gravitational acceleration as:

$$M_m := \frac{W_m}{g}$$

3.C.5 Solution for Post-Missile Strike Motion of Cask

The missile imparts the maximum angular momentum to the cask when the initial angle of the strike is defined by the relation:

$$\phi_0 := \text{atan}\left(\frac{a}{L}\right)$$

Substituting the values of a and L defined above, the missile strike angle $\phi_0 = 22.286 \text{ deg}$

The distance between the missile impact location and the cask pivot point, as shown on Figure 3.C.1, is calculated as:

$$d := (a^2 + L^2)^{0.5}$$

The centroidal mass moment of inertia of a cylindrical object about an axis parallel to and intersecting its axial midplane (I_z), for rotation about z, is given by:

$$I_z := \frac{1}{12} \cdot M_c \cdot \left[3 \cdot \left(\frac{D}{2} \right)^2 + L^2 \right]$$

Using the parallel axis theorem, the moment of inertia of the cask after the missile strike about the rotation point can be determined as:

$$I_r := I_z + M_c \cdot \left(\frac{d}{2} \right)^2$$

$$I_r = 3.033 \times 10^9 \text{ lb} \cdot \text{in}^2 \quad (\text{"lb" indicates pounds "mass"})$$

As stated in Section 3.C.3, it is conservatively assumed that the missile does not remain attached to the cask after impact. Using balance of angular momentum, the post-impact initial angular velocity of the cask can be determined using:

$$\omega := \frac{M_m \cdot v_m \cdot d}{I_r}$$

Thus, the post-impact initial angular velocity, $\omega = 0.635 \frac{1}{\text{sec}}$

For subsequent dynamic analysis, this angular velocity is used as the initial condition on the equation for the angular rotation of the cask as a function of time.

3.C.6 Calculation of Pressure due to Tornado Wind

The drag coefficient of a cylinder in turbulent crossflow is a function of the Reynold's Number, which can be calculated using the relation:

$$Re := \frac{\rho_{\text{air}} \cdot v_t \cdot D}{\mu_{\text{air}}} \quad Re = 7.579 \times 10^8$$

The drag coefficient (C_d) for a cylinder in crossflow for this Reynold's Number is less than 0.5 [3.C.1], so a conservatively higher value of 0.6 is used.

$$C_d := 0.6$$

The pressure on the side of the cask (p_{\max}), due to wind loading, is determined using:

$$p_{\max} := \frac{1}{2} \cdot C_d \cdot \frac{\rho_{\text{air}}}{g} \cdot v_t^2$$

and the resulting force on the projected area of the cask is therefore given by:

$$F_{\max} := p_{\max} \cdot D \cdot L$$

Thus, the force due to tornado wind, $F_{\max} = 2.638 \times 10^4$ lbf

3.C.7 Post Impact Plus Steady Wind Solution

The solution of the post-impact dynamics problem for the period of time when the horizontal displacement of the cask mass center is greater than or equal to zero is obtained by solving the following equation of motion:

$$I_r \alpha := \left(-W_c \cdot \frac{a}{2} \right) + F_{\max} \cdot \left(\frac{L}{2} \right)$$

where I_r is the cask moment of inertia about the rotation point and α is the angular acceleration of the cask. The above equation arises from summation of dynamic moments about the cask pivot point. The steady wind enters into the above equation through F_{\max} , and the impacting missile enters into the equation through the initial angular velocity.

The angular position of the cask is examined through 250 time steps of 0.005 sec duration.

Let $i := 1..250$

$$t_i := \frac{i}{200} \cdot \text{sec}$$

Let θ = the angular rotation variable of the cask subsequent to the impact. The analytical solution of the above equation is therefore:

$$\theta_i := \omega \cdot t_i + \frac{(t_i)^2}{2 \cdot I_r} \cdot \left(-W_c \cdot \frac{a}{2} + F_{\max} \cdot \frac{L}{2} \right)$$

3.C.8 Results

Once the angular rotation with respect to time is known, the horizontal displacement of the cask center of gravity can be calculated as:

$$x_i := \frac{D}{2} - \frac{d}{2} \cdot \cos\left(\arccos\left(\frac{D}{d}\right) + \theta_i\right)$$

Figure 3.C.2 shows a plot of the motion of the cask center versus time.

3.C.9 Missile Impact Plus Pressure Drop

The case of instantaneous pressure drop plus impact by a missile is studied by finding the increment of initial angular speed imparted to the cask by the pressure wave. Using a balance of angular momentum relation, the increment of angular speed is determined and added to that of the missile strike.

Time of pressure wave to cross cask body $dt := \frac{D}{V_{tr}} \quad dt = 0.078 \text{ sec}$

Increment of angular velocity imparted to cask in time dt

$$d\omega := \frac{(dp \cdot D \cdot L) \cdot \left(\frac{L}{2}\right) \cdot dt}{I_r} \quad d\omega = 0.059 \text{ sec}^{-1}$$

Therefore, for this case the initial angular speed is

$$\omega_1 := \omega + d\omega \quad \omega_1 = 0.694 \text{ sec}^{-1}$$

The angular position of the cask is examined through 250 time steps of 0.005 sec duration.

Let $i := 1..250$

$$t_i := \frac{i}{200} \cdot \text{sec}$$

Let θ_1 = the angular rotation variable of the cask subsequent to the impact. The analytical solution of the above equation is therefore:

$$\theta_{1i} := \omega_1 \cdot t_i + \frac{(t_i)^2}{2 \cdot I_r} \cdot \left(-W_c \cdot \frac{a}{2} \right)$$

3.C.8 Results

Once the angular rotation with respect to time is known, the horizontal displacement of the cask center of gravity can be calculated as:

$$x_{1i} := \frac{D}{2} - \frac{d}{2} \cdot \cos \left(\arccos \left(\frac{D}{d} \right) + \theta_{1i} \right)$$

Figure 3.C.3 shows a plot of the motion of the cask center versus time.

3.C.9 Conclusion

As is shown in Figure 3.C.2, the maximum horizontal excursion of the cask centroid under the given loading is less than 2.8 feet. In order for a cask tipover accident to occur, the centroid must undergo a horizontal displacement of 3.3 feet. Therefore, the combined tornado wind and missile strike events will not result in cask tipover. The case of missile strike plus tornado passing the cask is not a bounding case.

3.C.10 References

[3.C.1] E. Avallone and T. Baumeister, Marks' Standard Handbook for Mechanical Engineers, McGraw-Hill, Inc., Ninth Edition, 1987, p. 11-77.

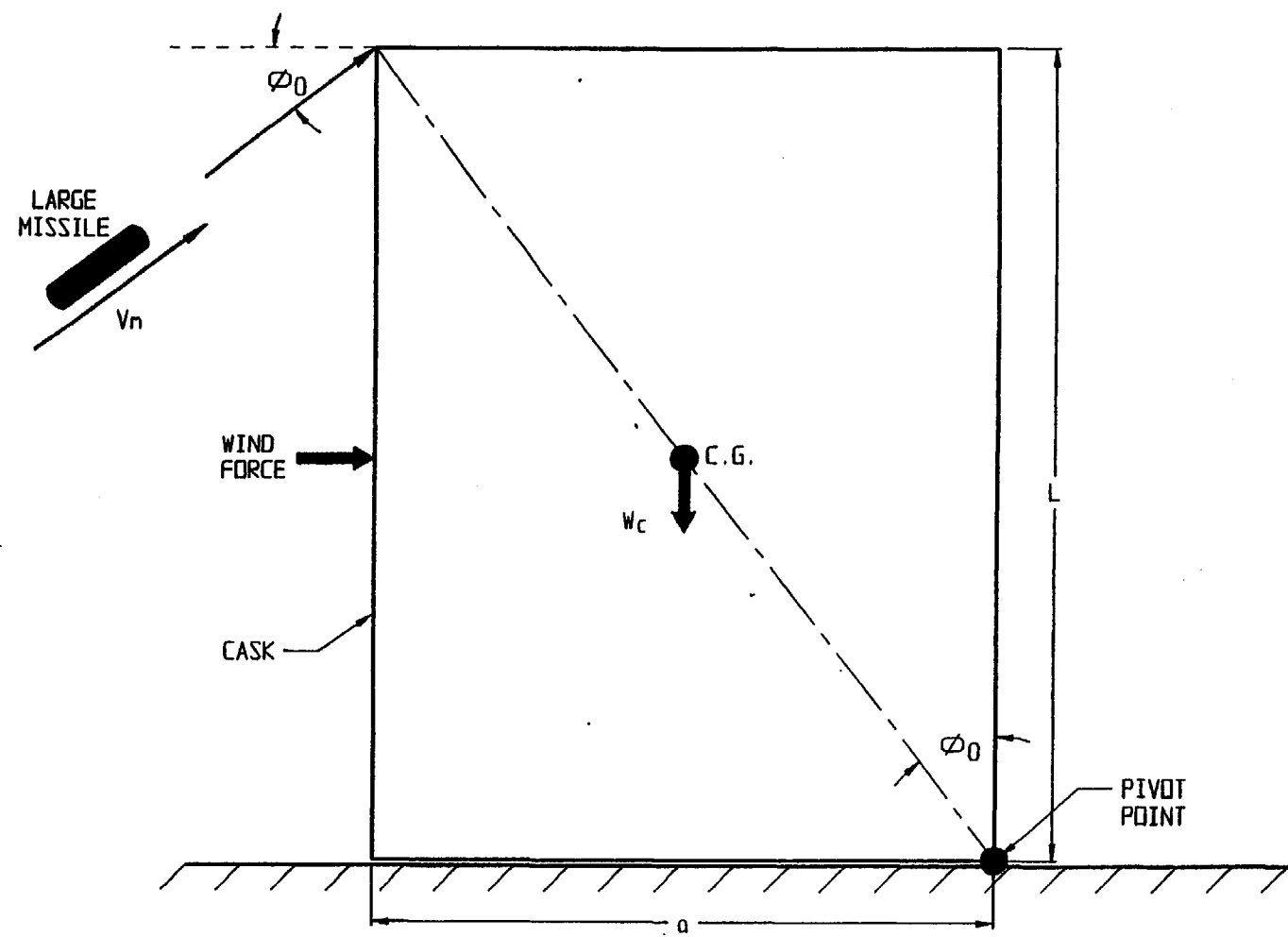


FIGURE 3.C.1; FREE BODY DIAGRAM OF CASK FOR LARGE MISSILE STRIKE/TORNADO EVENT

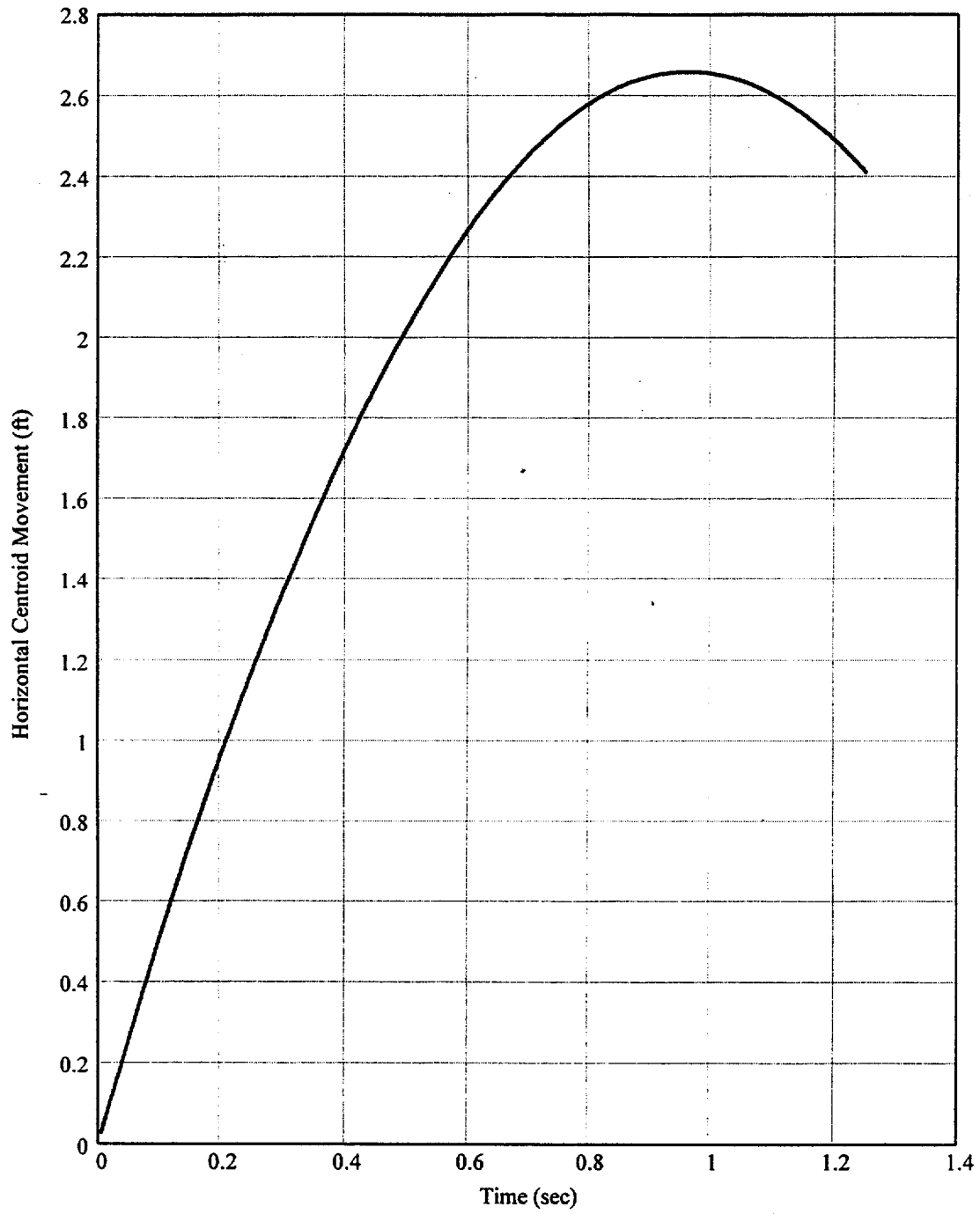


Fig. 3.C.2 Horizontal Motion of Centroid

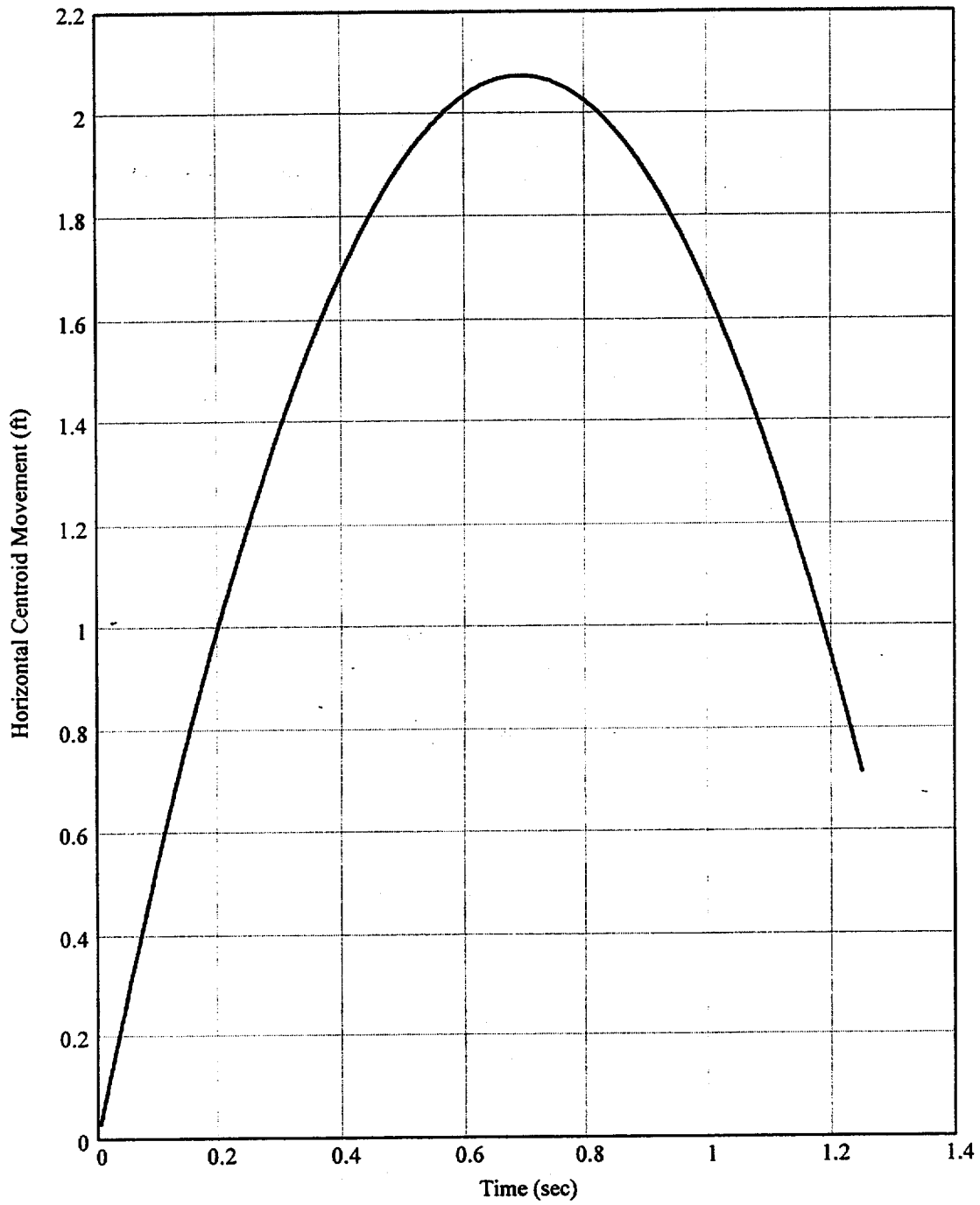


Fig. 3.C.3 Horizontal Motion of Centroid

APPENDIX 3.D - LIFTING TRUNNION STRESS ANALYSIS

3.D.1 Introduction and Description

This appendix contains a stress analysis of the upper lifting trunnions on the HI-STAR 100 Overpack. The objective of this analysis is to show that under any cask lifting condition, the stress in the trunnions and in the surrounding overpack forging do not exceed allowable limits. Note that, to further demonstrate the robust nature of the cask, Appendix 3.Y, describes a lift at three times deadweight.

The appendix is self contained in that all references cited are listed in the appendix, and the necessary "free body" diagrams are shown by figures at the conclusion of the appendix. This Appendix is written using the Mathcad electronic scratchpad computer code [3.D.1]. The notation "==" represents the equal sign for a defined calculation. The notation "=" represents a computed response or answer.

3.D.2 Methodology and Acceptance Criteria

Methodology

The lifting trunnions are threaded into the forging. A locking plate, secured with attachment bolts, prevents the trunnions from backing out.

The lifting trunnions are analyzed using a mechanics of materials method with the trunnions considered as short beams. Stresses in both the trunnions and in the overpack top forging are calculated under the specified load. Sketches at the end of the appendix show the appropriate free body diagrams.

In this analyses, primary bending moments and shear forces in the trunnions are determined first. Then, local bearing stress, thread shear stress and stress due to internal pressure are calculated.

The global effects of the trunnion loading are considered as a load case in the finite element analysis of the HI-STAR 100 Overpack and are reported elsewhere.

Acceptance Criteria

The HI-STAR 100 Overpack trunnions are part of a non-redundant lifting system. NUREG-0612 [3.D.2], section 5.1.6(3), requires that the lifting trunnions be able to support a load of 10 times the actual lifted load without exceeding the material ultimate strength and 6 times the actual lifted load without exceeding yield. The ultimate strength criterion governs the trunnion and forging materials.

The lifted load should include a dynamic load factor to account for inertia effects. CMAA Specification #70 (1988) [3.D.3], recommends an appropriate minimum hoist load factor for lifted loads. Since cask lifting is a low speed operation the use of a minimum hoist load factor for dynamic effects is conservative.

Where the trunnions and the top forging interface, the top forging allowable strengths are used in the determination of structural margins; the limits on strength are those of the ASME Code, Section III, Subsection NB for the appropriate load combination.

3.D.3 Materials and Material Properties

Trunnions are SB-637-N07718 steel. The overpack top forging is SA-350-LF3 steel. Based on thermal analyses in Chapter 4 (see Table 4.4.16), the maximum normal operating temperature on the inside surface of the top forging in the vicinity of the lifting trunnion will not exceed 163 degrees F. The outer surface temperature of the top forging will be higher than the ambient environment temperature. In the calculations, a bulk metal temperature of 150 degrees F is assumed for determination of material properties. Material properties are extracted from the appropriate tables in Section 3.3.

The trunnion material yield strength,	$S_y := 147000 \cdot \text{psi}$	Table 3.3.5
The trunnion material ultimate strength,	$S_u := 181300 \cdot \text{psi}$	Table 3.3.5
The forging material yield strength,	$S_{yf} := 35850 \cdot \text{psi}$	Table 3.3.4
The forging material local membrane stress intensity,	$SI_f := 34600 \cdot \text{psi}$	Table 3.1.8

3.D.4 Assumptions

1. The trunnions are analyzed for strength as beam members.
2. The weight of the extended portion of the trunnion is conservatively neglected since it opposes the lifted load.
3. Any load carrying capacity of the locking plate is conservatively neglected in the analysis of the trunnion as a beam.
4. Trunnions are loaded equally.
5. The lifting yoke is conservatively set at the outer end of the trunnion so as to maximize the moment arm for the analysis of the trunnion as a beam member. The minimum thickness of the lifting yoke is specified. Therefore, the maximum value of the moment arm can be established
6. In the determination of local shear stress in the trunnion thread, the actual location of the lift point is used based on a conservative "worst case" analysis of the tolerance stack-up.
7. Trunnion stress analysis is based only on mechanical loads applied laterally to the trunnion axis.

3.D.5 References

[3.D.1] MATHCAD 7.02, Mathsoft, 1998.

[3.D.2] NUREG-0612, Control of Heavy Loads at Nuclear Power Plants Resolution of Generic Technical Activity A-36, Section 5.1.6(3), 1980.

[3.D.3] Crane Manufacturers Association of America (CMAA), Specification #70, 1988, Section 3.3.

[3.D.4] J.Shigley and C. Mischke, Mechanical Engineering Design, McGraw-Hill, 5th Edition, 1989, p.328.

3.D.6 Analysis

In this section, moments, forces, and stresses in the trunnion and the top forging material are determined. Moments and forces in the trunnions are compared to allowable strengths per NUREG-0612, and local stresses in the top forging are compared with appropriate allowable stress intensities.

3.D.6.1 Moments and Forces in the Trunnion

In this subsection, the geometry of the system is defined, and bending moments and shear forces in the lifting trunnions are determined.

3.D.6.1.1 Input Data

The trunnion outer diameter, $d := 5.75 \cdot \text{in}$

The minimum lift yoke connecting link yoke width, $t_f := 2.25 \cdot \text{in}$

The maximum lifted weight of the cask and contents, $W := 250000 \cdot \text{lbf}$ Table 3.2.4

The number of lifting trunnions, $n := 2$

The dynamic load factor (from Reference 3.D.3), $\text{DLF} := 0.15$

The exposed trunnion length (including locking plate), $L := 3.375 \cdot \text{in}$

The minimum clearance between lifting link and trunnion end $c := 0.25 \cdot \text{in}$

This minimum lift yoke connecting link width conservatively defines the contact patch on the trunnion and establishes the location of the concentrated lifting load. for the purpose of determining the bending moment at the root of the trunnion beam member. The maximum lifted weight bounds the actual maximum weights of the HI-STAR 100 systems.

The trunnion cross sectional area (Area), moment of inertia (I) and applied per trunnion load (P) can be determined using the following formulae:

$$\text{Area} := \frac{\pi \cdot d^2}{4} \qquad I := \frac{\pi \cdot \left(\frac{d}{2}\right)^4}{4} \qquad P := \frac{W \cdot (1 + \text{DLF})}{n}$$

Substituting the input values defined above into these three equations yields the following values:

$$\text{Area} = 25.97 \text{ in}^2 \qquad I = 53.65884 \text{ in}^4 \qquad P = 1.44 \times 10^5 \text{ lbf}$$

3.D.6.1.2 Bending Stress at the Root of the Trunnion

The lifting yoke arm is conservatively set at the outer end of the trunnion to maximize the moment arm. The applied moment arm (L_{arm}) is defined as the distance from the root of the trunnion to the centerline of the lifting yoke connecting link (see Figure 3.D.1).

$$L_{\text{arm}} := L - .5 \cdot t_f \qquad \text{Conservatively neglect the clearance "c"}$$

$$L_{\text{arm}} = 2.25 \text{ in}$$

The applied moment (M) at the root of the trunnion is therefore determined as:

$$M := P \cdot L_{\text{arm}} \qquad M = 3.23 \times 10^5 \text{ in} \cdot \text{lbf}$$

From beam theory, the maximum tensile stress occurs in an outer fiber at the root of the trunnion. The distance from the neutral axis to an outer fiber (y) is one-half of the trunnion diameter:

$$y := \frac{d}{2}$$

and the maximum bending stress due to the applied moment is therefore determined as:

$$\sigma := \frac{M \cdot y}{I} \qquad \sigma = 17329.51 \text{ psi}$$

Comparing the value of the bending stress with the yield strength of the material results in a safety factor of:

$$S_1 := \frac{S_y}{\sigma} \qquad S_1 = 8.48$$

This safety factor is greater than 6, which is the factor of safety on yield required by [3.D.2]. Note that the safety factor calculated above, and used elsewhere in this appendix, is defined as the allowable yield strength divided by the calculated stress (or stress intensity).

3.D.6.1.3 Shear Stress in the Trunnion

The maximum shear stress in the trunnion, which occurs at the neutral axis, is determined using beam theory. The first moment of the area above the neutral axis is determined as:

$$Q := \int_0^\pi \int_{0 \cdot \text{in}}^{\frac{d}{2}} r^2 \cdot \sin(\theta) \, dr \, d\theta \quad \text{or} \quad Q := \frac{1}{12} \cdot d^3$$

$$Q = 15.84 \text{ in}^3$$

The shear load (V) is equal to the applied per trunnion load (P) and the "thickness" of the beam (t) at the neutral axis is equal to the trunnion diameter (d).

$$V := P$$

$$t := d$$

From beam theory, the maximum shear stress is determined as:

$$\tau := \frac{V \cdot Q}{I \cdot t} \quad \tau = 7381.09 \text{ psi}$$

The shear yield strength is defined as 60% of the tensile yield strength. This definition of yield strength in shear is consistent with formulas given in ASME Section III, Subsection NG, NG-3227.2 and NG-3232.1(b) where the ratio of allowable shear strength to allowable tensile strength is 0.6. It is also consistent (and conservative) when compared to the same ratio given in ASME Section III, Subsection NF where the ratio of allowable shear/allowable average tension is $0.4/0.6 = 0.667$. Comparing the calculated shear stress value with the yield shear strength, result in a safety factor of:

$$S_2 := \frac{0.6 \cdot S_y}{\tau} \quad S_2 = 11.95$$

This safety factor is greater than 6, as required by [3.D.2].

In addition to a check based on yield strength, the calculated moment and shear force must be checked against the ultimate carrying capacity in bending and in shear. We calculate the ultimate moment from the following formula (which is easily derived from the classical principles of Limit Analysis applied to a circular section).

$$M_u := S_u \left[\frac{4}{3} \left(\frac{d}{2} \right)^3 \right] \quad M_u = 5.74 \times 10^6 \text{ lbf}\cdot\text{in}$$

Comparing the ultimate capacity with the applied moment gives

$$S_3 := \frac{M_u}{M} \quad S_3 = 17.76$$

Similarly, the ultimate shear force capacity is

$$V_u := .6 \cdot S_u \cdot \text{Area} \quad V_u = 2.82 \times 10^6 \text{ lbf}$$

Therefore the ultimate carrying capacity in shear is

$$S_4 := \frac{V_u}{V} \quad S_4 = 19.65$$

3.D.6.2 Local Stresses in the Top Forging

In the following subsection, stresses in the top forging due to bearing loads, thread shear loads, and internal pressure are determined.

3.D.6.2.1 Input Data

The number of threads per inch, $NTI := 4$

The trunnion length inserted into the top forging, $L_w := 5.875 \text{ in}$

The design internal pressure under normal handling, $p := 40 \text{ psi}$ Table 2.2.1

The overpack forging outer diameter, $D_o := 83.25 \text{ in}$

The overpack forging inner diameter, $D_i := 68.75 \text{ in}$

The mean diameter in thread region $d_m := d + 1.0 \text{ in}$

3.D.6.2.2 Bearing Stress

A longitudinal local bearing stress is developed in the base material, during cask handling, at the contact surface between the embedded portion of the trunnion and the cavity in the top forging. The effective diameter (for stress evaluation purposes) of the portion of the trunnion that is threaded into the top forging is determined as per [3.D.4] as:

$$dd := d_m - \frac{1.299038}{NTI} \cdot \text{in} \quad dd = 6.43 \text{ in}$$

The projected area supporting the bearing load is determined as:

$$A := L_w dd \quad A = 37.75 \text{ in}^2$$

and the average bearing stress on the top forging material is therefore determined as:

$$\sigma_d := \frac{V}{A} \quad \sigma_d = 3808.11 \text{ psi}$$

3.D.6.2.3 Thread Shear Stress Due to Trunnion Bending

The bending moment that is transferred from the trunnion to the top forging is reacted by a shear stress distribution on the threads. (see Figure 3.D.2, a free body of the portion of the trunnion inserted into the forging). We recalculate the bending moment using a bounding value for the actual location of the applied load. This bounding value considers that the maximum position of the lifting link on the trunnion will leave a clearance "c" between the edge of the link and the end of the trunnion.

$$c = 0.25 \text{ in}$$

The total bending moment applied to the trunnion threads is therefore defined by:

$$\text{Moment} := M \cdot \frac{(L_{\text{arm}} - c)}{L_{\text{arm}}} + V \cdot \left(\frac{L_w}{2} \right) \quad \frac{(L_{\text{arm}} - c)}{L_{\text{arm}}} = 0.89$$

The average shear stress in the threaded region is assumed to be a sinusoidal distribution around the periphery. Therefore, moment equilibrium yields:

$$\text{Moment} := \int_0^{2 \cdot \pi} \tau \cdot R \cdot \sin(\text{theta}) \cdot R \cdot (L_w) \, d\text{theta}$$

where the average shear stress along the threaded length, $\tau := \tau_{\text{max}} \cdot \sin(\text{theta})$

Integrating the moment expression above, over the required interval, yields the following expression for the total bending moment:

$$\text{Moment} := \tau_{\max} \cdot \pi \cdot d^2 \cdot \frac{(L_w)}{4}$$

Solving for the maximum shear stress existing around the circumference of the trunnion (averaged along the length of the insert) gives the stress at the root of the trunnion thread.

$$\tau_{\max} := 4 \cdot \frac{\text{Moment}}{\pi \cdot d^2 \cdot (L_w)} \quad \tau_{\max} = 3725.96 \text{ psi}$$

Similarly, the shear stress at the external root of the thread in the top forging is:

$$\tau_{\text{froot}} := 4 \cdot \frac{\text{Moment}}{\pi \cdot d_m^2 \cdot L_w} \quad \tau_{\text{froot}} = 3376.05 \text{ psi}$$

3.D.6.2.4 Local Stress in Forging Due to Internal Pressure

The stress in the top forging due to the design internal pressure is calculated using shell theory. This stress is approximated as a circumferential stress using a mean diameter and thickness of the top forging. The mean radius of the overpack forging is determined as:

$$r := \frac{D_o + D_i}{2} \quad r = 76 \text{ in}$$

and the thickness of the overpack forging is determined as:

$$t := \frac{D_o - D_i}{2} \quad t = 7.25 \text{ in}$$

From shell theory, the circumferential stress in the forging due to internal pressure is determined as:

$$\sigma_{\text{pres}} := p \cdot \frac{r}{t} \quad \sigma_{\text{pres}} = 419.31 \text{ psi}$$

3.D.6.2.5 Comparison with Allowable Stress Intensity Per ASME Subsection NB

The allowable local membrane stress intensity of the top forging material in the region supporting the lifting trunnions is set forth in Section 3.D.3 of this appendix as:

$$SI_f = 34600 \text{ psi}$$

The safety factor on membrane stress intensity in the top forging is calculated at the location of maximum shear stress and bearing stress, and uses the classical formula for stress intensity [3.D.4]. The three normal stresses acting on the point are defined as:

A longitudinal minimum normal stress, $\sigma_1 := -\sigma_d + .5 \cdot \sigma_{pres}$

A normal stress estimate on a surface perpendicular to a radial line, $\sigma_2 := -.5 \cdot p$

The normal "hoop" stress, $\sigma_3 := \sigma_{pres}$

Substituting the appropriate values of σ_d , σ_{pres} and p , the three normal stresses are:

$$\sigma_1 = -3598.46 \text{ psi} \quad \sigma_2 = -20 \text{ psi} \quad \sigma_3 = 419.31 \text{ psi}$$

The formula for maximum stress intensity in the plane of the shear stress involves σ_1 and σ_2 . For a bounding estimate of the safety factor, we use σ_1 and σ_3 instead since σ_3 adds to σ_1 . The maximum in-plane stress intensity is therefore calculated as:

$$SI_{calc} := \left[(\sigma_1 - \sigma_3)^2 + 4 \cdot \tau_{froot}^2 \right]^{0.5} \quad SI_{calc} = 7857.06 \text{ psi}$$

and the safety factor (must be > 1.0) is determined as:

$$SF_m := \frac{SI_f}{SI_{calc}} \quad SF_m = 4.4$$

Note that this calculation does not consider the global effect of the trunnion load on the top forging. The global analysis is considered as a load combination for the overpack finite element analysis, reported elsewhere.

The calculation above demonstrates that the local membrane stress intensity in the forging section, adjacent to the lifting trunnion, is within the limit required by the ASME Code, Section III, Subsection NB. Appendix 3.Y contains a finite element analysis of the top forging subject to a trunnion load equal to three times the dead weight of the cask.

3.D.6.2.5 Comparison with Yield Strength Per NUREG-0612

The allowable yield stress of the top forging material in the region supporting the lifting trunnions is set forth in Section 3.D.3 of this appendix as:

$$S_{yf} = 35850 \text{ psi}$$

The safety factor against yield in the top forging is calculated for bearing stress and for thread shear stress separately. The same calculation is also performed for the trunnion material at the interface.

We note that Regulatory Guide 3.61 only requires that the material anywhere in the cask not exceed 1/3 of the yield stress. Nevertheless, at the thread interface between the trunnion and the top forging, we conservatively apply the more stringent requirements of NUREG-0612.

Safety Factor Against Yielding for Bearing Stress in Forging at Interface

$$SF_{\text{bearing}} := \frac{S_{yf}}{\sigma_d} \quad SF_{\text{bearing}} = 9.41$$

Safety Factor Against Yielding for Thread Shear Stress in Forging at interface.

$$SF_{\text{thread_shear}} := .6 \cdot \frac{S_{yf}}{\tau_{\text{root}}} \quad SF_{\text{thread_shear}} = 6.37$$

Safety Factor Against Yielding for Bearing Stress in Trunnion

$$SF_{\text{bearing}} := \frac{S_y}{\sigma_d} \quad SF_{\text{bearing}} = 38.6$$

Safety Factor Against Yielding for Thread Shear Stress in Trunnion

$$SF_{\text{thread_shear}} := .6 \cdot \frac{S_y}{\tau_{\text{max}}} \quad SF_{\text{thread_shear}} = 23.67$$

The above calculations demonstrate that the local bearing stress and the thread shear stress at the trunnion-forging interface satisfy NUREG-0612 requirements on trunnion safety factors against material yield.

3.D.7 Conclusion

The lifting trunnions meet the requirements of NUREG 0612 for lifting heavy loads in a nuclear power plant.

The local membrane stress intensity limits in the top forging satisfy the required ASME Section III, Subsection NB limits.

The bearing stress and the thread shear stress satisfy NUREG-0612 requirements at the trunnion-forging interface. During the lift, these stresses are less than 1/6 the respective yield stress.

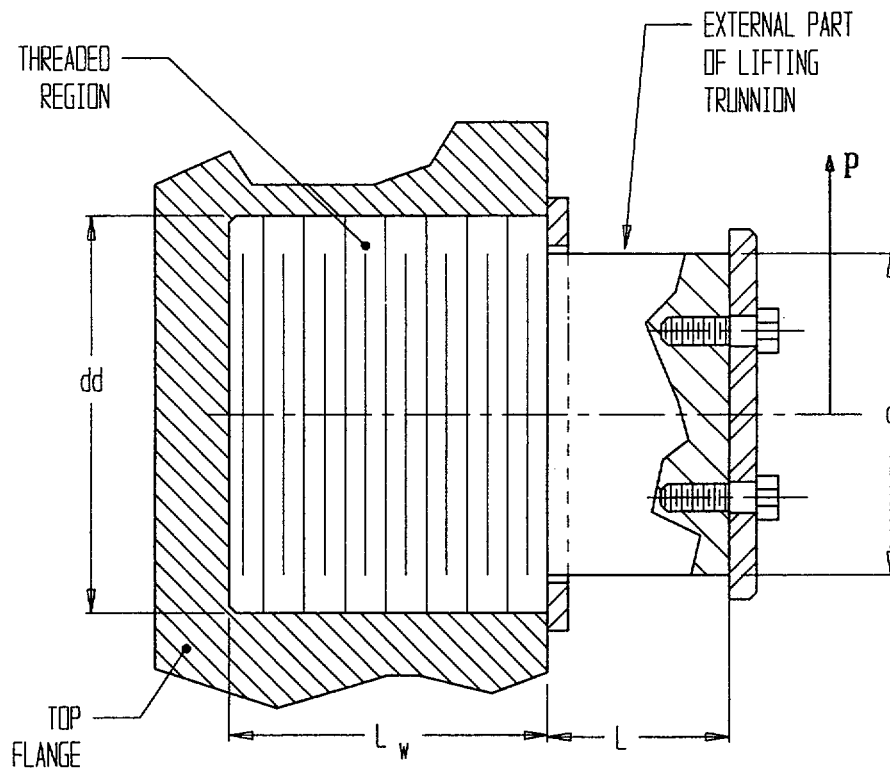


FIGURE 3.D.1; SKETCH OF LIFTING TRUNNION GEOMETRY SHOWING APPLIED LOAD

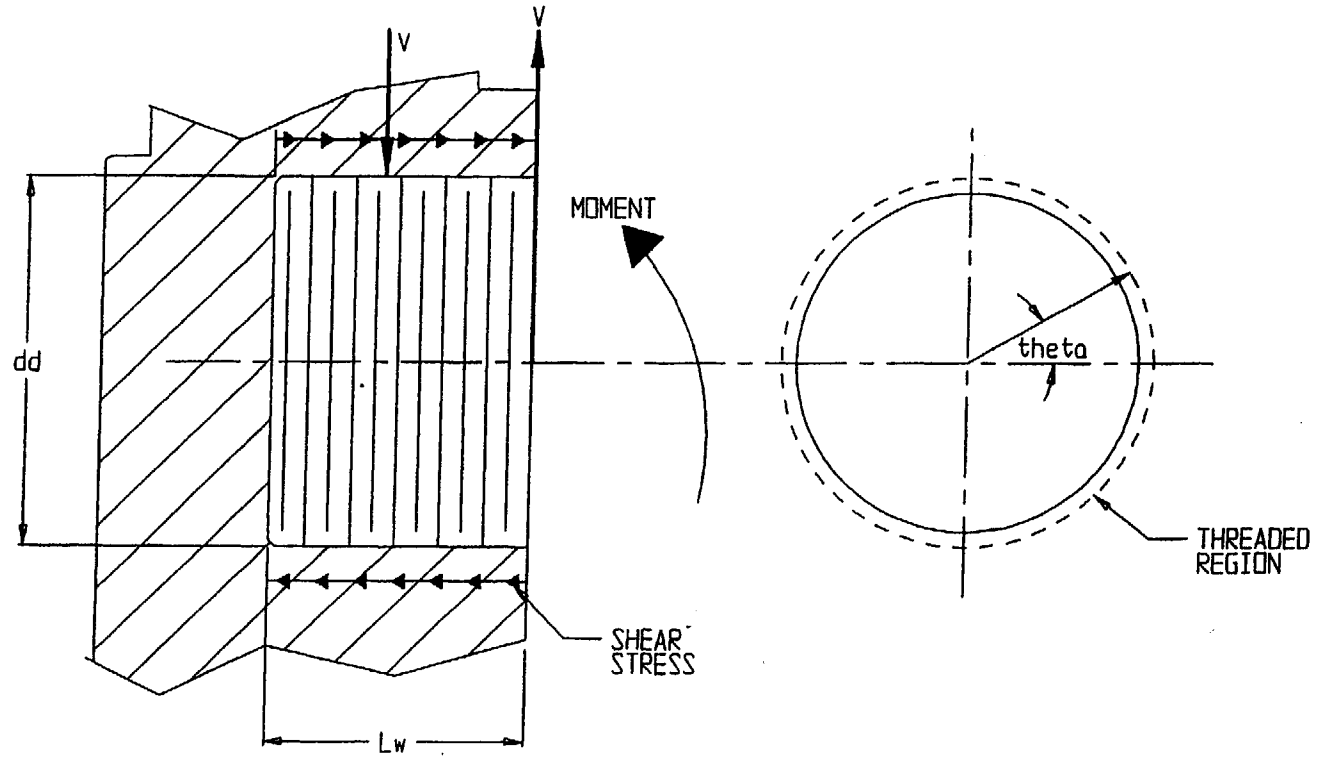


FIGURE 3.D.2; FREE BODY SKETCH OF LIFTING TRUNNION THREADED REGION SHOWING MOMENT BALANCE BY SHEAR STRESSES

APPENDIX 3.E: ANALYSIS OF MPC TOP CLOSURE

3.E.1 Scope

This appendix provides the stress analysis of the MPC top closure plate under bounding load cases for both storage and transport scenarios.

3.E.2 Methodology

Conservative values for stresses on the closure plate are obtained by using classical strength of materials formulations, which are sufficient for determining primary stresses in the component. The peripheral weld to the MPC shell is protected by a thin closure ring. The analysis of this ring is performed using a finite element model.

3.E.3 References

[3.E.1] S.P. Timoshenko, Strength of Materials, Vol. 2, Third Edition, Van Nostrand, 1956.

[3.E.2] ANSYS Finite Element Code, 5.0, Ansys, Inc., 1994.

3.E.4 Configuration, Geometry, and Input Weight Data

3.E.4.1 Configuration and Geometry

Figure 3.E.1 shows a sketch of the top closure lid with the the closure ring attached. The configuration is the same for all MPC types. The following dimensions are obtained from drawing no. 1393.

The outer radius of the lid, $R_{lid} := \frac{67.375}{2} \cdot \text{in}$

The inner radius of the closure ring, $R_i := \frac{53.03125}{2} \cdot \text{in}$

The outer radius of the closure ring, $R_o := \frac{67.875}{2} \cdot \text{in}$

The minimum thickness of the lid, $h := 9.5 \cdot \text{in}$

The closure ring thickness, $t := 0.375 \cdot \text{in}$

3.E.4.2 Input Weight Data

The bounding weight of the closure lid (MPC-68), $W_{lid} := 10400 \cdot \text{lb}$ Table 3.2.4

The bounding weight per square inch of lid, $P_{lid} := \frac{W_{lid}}{\pi \cdot R_{lid}^2}$ $P_{lid} = 2.917 \text{ psi}$

The bounding weight of the fuel basket plus fuel,

$$W_{fuel} := 13000 \cdot \text{lb} + 54000 \cdot \text{lb} \quad \text{Table 3.2.4}$$

The maximum total package weight of the MPC (including dynamic load factor),

$$W_{lift} := 1.15 \cdot 90000 \cdot \text{lb} \quad \text{Table 3.2.4}$$

The maximum lifted weight is the bounding MPC weight with an applied 0.15 inertia load factor to bound loads during an MPC transfer operation.

3.E.5 Acceptance Criteria

Level A or Level D primary stress intensity levels must not be exceeded under the defined load conditions. Load cases considered are set to bound all requirements for either storage or transport.

3.E.6 Allowable Strengths

Allowable strengths at the design temperature of 550°F and at the accident temperature of 775°F are used. The material used is Alloy X. The relevant allowable stress intensities for primary membrane stress and for combined primary bending and primary membrane stress, for ASME Section III, Subsection NB components, are therefore:

The Level A allowable stress intensity for combined stress (550°F), $S_{ac} := 25450 \cdot \text{psi}$

The Level A allowable stress intensity for membrane stress (550°F), $S_{am} := 16950 \cdot \text{psi}$

The Level D allowable stress intensity for combined stress (550°F), $S_{dc} := 61050 \cdot \text{psi}$

The Level D allowable stress intensity for membrane stress (550°F), $S_{dm} := 40700 \cdot \text{psi}$

The Level D allowable stress intensity for combined (775°F), $S_{firec} := 54225 \cdot \text{psi}$

The Level D allowable stress intensity for membrane (775°F), $S_{firem} := 36150 \cdot \text{psi}$

The closure ring, which functions as the secondary seal for the MPC, is located on the upper surface of the lid. The appropriate design temperature at this location is 400°F, which bounds all non-accident metal temperatures obtained at that location in the analyses of Chapter 4. The Level A membrane and membrane plus bending allowable stress intensities at this temperature are:

$$S_{amr} := 18700 \cdot \text{psi}$$

$$S_{acr} := 28100 \cdot \text{psi}$$

3.E.7 Load Cases

The following bounding loads are considered as potential limiting loads for the top closure plate structural qualification. Only the most limiting combinations are used for the qualification. For calculation purposes, the applied loads are considered as equivalent surface pressures.

The external pressure, $P_{ext} := 125 \cdot \text{psi}$

The internal pressure, $P_{int} := 100 \cdot \text{psi}$

The fire pressure, $P_{fire} := 125 \cdot \text{psi}$

A bottom end drop on the overpack baseplate gives a pressure of,

$$P_{sd} := \frac{60 \cdot W_{lid}}{\pi \cdot R_{lid}^2} \quad P_{sd} = 175.0 \text{ psi}$$

A top end drop on the overpack closure plate gives a pressure,

$$P_{td} := \frac{60 \cdot W_{fuel}}{\pi \cdot R_{lid}^2} \quad P_{td} = 1128 \text{ psi}$$

The center lift weight, $P_{lift} := W_{lift}$

Note that external pressure never governs because internal pressure adds a membrane stress component. The center lift weight load is included to incorporate a future fully-loaded lifting operation.

For the qualification of the closure ring, only a single load case need be considered. If the primary, load carrying MPC cover plate-to-MPC shell peripheral weld leaks, then the closure ring will be subjected to the internal pressure load, and behaves as an annular plate supported at its inner and outer periphery. While this case is amenable to manual calculations, the case is analyzed using the finite element method for simplicity.

3.E.8 Calculations

The stress analysis of the closure plate is performed by conservatively assuming that the closure plate acts as a simply supported plate. This will conservatively predict a higher stress at the center of the plate. In the plate analysis, it is assumed that the thickness is constant. This is slightly nonconservative at the outer periphery of the plate since the closure ring is a separate component; however, as will be seen from the results, the safety margins are large so that the effect is negligible.

In all of the following analyses, since the circumferential stress has the same sign as the radial stress, stress intensities differ from stresses only by the surface pressure, where applicable.

3.E.8.1 Level A Bounding Calculations

The design load is the internal pressure case, since there is a direct stress as well as a bending stress because of the peripheral weld. However, for a transfer operation, there exists the potential for a bounding Level A condition to be internal pressure plus a central lifted load.

3.E.8.1.1 Load Case E1.a, Table 3.1.4

This load case consists of internal pressure only. Reference [3.E.1] provides a formula for the maximum bending stress at the center of a simply supported circular plate. For the case of internal pressure alone, the stress intensity SI_1 and resultant margin of safety are determined as:

The Poisson's ratio of the material, $\nu := 0.3$

The bending stress due to internal pressure,
$$\sigma_b := \frac{3 \cdot (3 + \nu)}{8} \cdot (P_{int} + P_{lid}) \cdot \left(\frac{R_{lid}}{h} \right)^2$$

$$\sigma_b = 1601 \text{ psi}$$

The direct stress due to internal pressure,
$$\sigma_d := -P_{int} \quad \sigma_d = -100 \text{ psi}$$

The combined stress intensity,
$$SI_1 := (\sigma_b + |\sigma_d|) \quad SI_1 = 1701 \text{ psi}$$

The margin of safety, $MS_1 := \frac{S_{ac}}{SI_1} - 1$ $MS_1 = 14.0$

3.E.8.1.2 Load Case E2, Table 3.1.4

This load case consists of the combined internal pressure and lifting loads. From pp.106-107 of [3.E.1], the following stress result is conservative since it assumes the lifting load is applied at the center of the plate. In reality, the lifting load acts on the plate at some radial distance from the center point. Therefore, the value computed here overestimates the maximum stress.

$$\sigma_{lift} := \frac{P_{lift}}{h^2} \cdot (1 + \nu) \cdot \left(.485 \cdot \ln\left(\frac{R_{lid}}{h}\right) + 0.52 \right) + 1.5 \cdot \frac{P_{lift}}{\pi \cdot h^2} \quad \sigma_{lift} = 2238 \text{ psi}$$

This stress must be added to the stress intensity due to internal pressure to determine the total combined stress intensity SI_2 . The limiting stress intensity and resultant margin of safety are therefore determined as:

The limiting combined stress intensity, $SI_2 := \sigma_{lift} + SI_1$ $SI_2 = 3940 \text{ psi}$

The limiting margin of safety, $MS_2 := \frac{S_{ac}}{SI_2} - 1$ $MS_2 = 5.5$

3.E.8.2 Level D Bounding Calculations

3.E.8.2.1 Load Case E3.a, Table 3.1.4

3.E.8.2.1.1 Bounding 10CFR72 (Storage) Bottom End Drop

This load case corresponds to the 10CFR72 (storage) end drop on the overpack baseplate. The amplified weight of the lid, plus the external design pressure, give rise to a bending stress. This bending stress and the resultant margin of safety are determined as:

The bending stress due to the loading, $\sigma_b := \frac{3 \cdot (3 + \nu)}{8} \cdot (P_{sd} + P_{ext}) \cdot \left(\frac{R_{lid}}{h}\right)^2$

$$\sigma_b = 4669 \text{ psi}$$

The margin of safety, $MS_3 := \frac{S_{dc}}{\sigma_b} - 1$ $MS_3 = 12.1$

3.E.8.2.1.2 Bounding 10CFR71 (Transport) Top End Drop

For this case, the MPC closure plate is supported by the overpack closure plate over a peripheral band of support. It is conservative for the MPC qualification to assume that all support is at the outer edge. Therefore, the bending stress and resultant margin of safety due to the equivalent pressure of the fuel basket and fuel, the applied weight of the closure plate and the internal pressure is determined as:

The bending stress due to the loading, $\sigma_b := \frac{3 \cdot (3 + \nu)}{8} \cdot (P_{int} + P_{sd} + P_{td}) \cdot \left(\frac{R_{lid}}{h} \right)^2$

$\sigma_b = 21825 \text{ psi}$

The margin of safety, $MS_4 := \frac{S_{dc}}{(\sigma_b + P_{int})} - 1$ $MS_4 = 1.8$

3.E.8.2.1.3 Load Case E5, Table 3.1.4

This load case considers dead load, fire pressure, and fire temperature material properties.

The bending stress is, $\sigma_b := \frac{3 \cdot (3 + \nu)}{8} \cdot (P_{fire} + P_{lid}) \cdot \left(\frac{R_{lid}}{h} \right)^2$

$\sigma_b = 1.991 \times 10^3 \text{ psi}$

The margin of safety is, $MS_5 := \frac{S_{firec}}{\sigma_b} - 1$ $MS_5 = 26.2$

3.E.8.3 Peripheral Weld Stress

The area of the weld is computed by multiplying the total length of the weld (at radius R_{lid}) by the weld thickness. The weld capacity is found by multiplying this area by a quality factor (defined in ASME Subsection NG) and by the appropriate weld stress allowable from ASME Subsection NF. The weld between the MPC lid and the shell is a 3/4 inch (minimum) J-groove weld. For conservatism, a smaller weld size (i.e., 5/8 inch) is considered in the following stress evaluations.

The thickness of the weld, $t_{weld} := 0.625 \cdot \text{in}$

The quality factor for a single groove weld that is examined by root and final PT is $n := 0.45$

The allowable weld stresses for Level A and Level D conditions are S_a and S_d , respectively. The weld metal strength is assumed to decrease with temperature in the same manner as does the base metal (Alloy X)

$$S_a := 0.3 \cdot 70000 \cdot \left[1 - \left(\frac{75 - 63.3}{75} \right) \right] \cdot \text{psi} \quad S_a = 1.772 \times 10^4 \text{ psi}$$

$$S_d := .42 \cdot 70000 \cdot \left[1 - \left(\frac{75 - 63.3}{75} \right) \right] \cdot \text{psi} \quad S_d = 2.481 \times 10^4 \text{ psi}$$

The maximum load capacity of the weld, $LC_{weld} := n \cdot 2 \cdot \pi \cdot R_{lid} \cdot t_{weld} \cdot S_a$

$$LC_{weld} = 1.055 \times 10^6 \text{ lbf}$$

The margin of safety of this load capacity, for the Level A center lift loading case (Load Case E2, Table 3.1.4), is determined as:

$$MS_6 := \frac{LC_{weld}}{W_{lift} + \pi \cdot P_{int} R_{lid}^2} - 1 \quad MS_6 = 1.29$$

The bounding weld load for Level D conditions is determined by multiplying the equivalent pressure load for the load case by the area of the closure plate. The bottom end drop is taken by the welds, and the top end drop is taken by bearing on the overpack closure plate.

$$L_{weld} := P_{sd} \cdot \pi \cdot (R_{lid})^2 \quad L_{weld} = 624000 \text{ lbf}$$

$$MS_7 := \frac{S_d}{S_a} \cdot \frac{LC_{weld}}{L_{weld}} - 1 \quad MS_7 = 1.37$$

To further demonstrate the adequacy of the weld, its capacity is compared to a weld load that equals three times the total lifted weight. The margin of safety is

$$MS_8 := \frac{LC_{weld}}{3 \cdot W_{lift}} - 1 \quad MS_8 = 2.40$$

3.E.8.4 Fatigue Analysis of Weld

The welds will be subjected to cyclic stress each time the cask is lifted. The force difference is equal to W_{lift} . Pressure loads are not a fatigue consideration since they remain relatively constant during normal operation. Therefore, the effective fatigue stress can be determined as follows

The fatigue factor for a single groove weld that is examined by root and final PT is $f := 4$ and the alternating stress is

$$\sigma := \frac{\left(f \cdot \frac{W_{lift}}{2} \right)}{2 \cdot \pi \cdot R_{lid} \cdot t_{weld}} \quad \sigma = 1565 \text{ psi}$$

This stress is compared to curve B in Figure I-9.2.2 of the ASME Division I Appendices per Subsection NG. This curve shows that the welds have unlimited life at this stress level.

3.E.8.5 Closure Ring Analysis

The closure ring must be capable of withstanding the application of the full MPC internal pressure, to ensure that a leak in the primary closure plate weld will be contained. This condition is modeled as an annular ring subject to the design internal pressure. A finite element analysis of a thin ring with an applied pressure is performed using the ANSYS finite element code. The thin ring is simulated by four layers of PLANE42 axisymmetric quadrilateral elements (see Figure 3.E.2). The boundary condition is conservatively set as zero displacement at node locations 1 and 2 (see Figure 3.E.2). The bottom surface is subjected to a 100 psi pressure to simulate leakage of the primary MPC weld. The maximum stress intensity in the ring (occurring at the top center point) and the resultant margin of safety for Level A conditions are determined as:

The maximum stress intensity in the ring, $SI_{ring} := 20001 \cdot \text{psi}$

The margin of safety, $MS_9 := \frac{S_{acr}}{SI_{ring}} - 1$ $MS_9 = 0.405$

Since the actual support condition provides some clamped support, this result is very conservative.

The total load capacity of the closure ring weld is determined by calculating the total area of the two weld lines at radii R_i and R_o , multiplying by the allowable weld stress, and conservatively applying the specified weld efficiency.

The closure ring weld thickness, $t_{crw} := 0.125$ -in (this allows for fit-up)

The quality factor for a single groove or a single fillet weld that is examined by root and final PT is $n := 0.45$

The load capacity of the ring welds, $LC_{crw} := n \cdot 2 \cdot \pi \cdot \left(R_i + \frac{R_o}{\sqrt{2}} \right) \cdot t_{crw} \cdot S_a$

$$LC_{crw} = 3.164 \times 10^5 \text{ lbf}$$

The margin of safety of these welds for the applied loading condition (internal pressure only) is determined as:

$$MS_{10} := \frac{LC_{crw}}{\pi \cdot P_{int} (R_o^2 - R_i^2)} - 1 \quad MS_{10} = 1.24$$

3.E.9 Conclusions

The results of the evaluations presented in this appendix demonstrate the adequacy of the MPC closure plate, closure ring and associated weldments to maintain their structural integrity during applied bounding load cases considered. Positive safety margins exist for all components examined for all load cases considered.

The bending stress evaluation of the closure ring conservatively assumes a simple support condition at the peripheral welds. Therefore, any seal welds in the closure ring configuration need be sized based on positive margins on shear stress.

The seal weld size (0.125") adequately supports the expected shear load. Note that a closure ring peripheral weld thickness as small as 0.056" provides a small positive margin of safety.

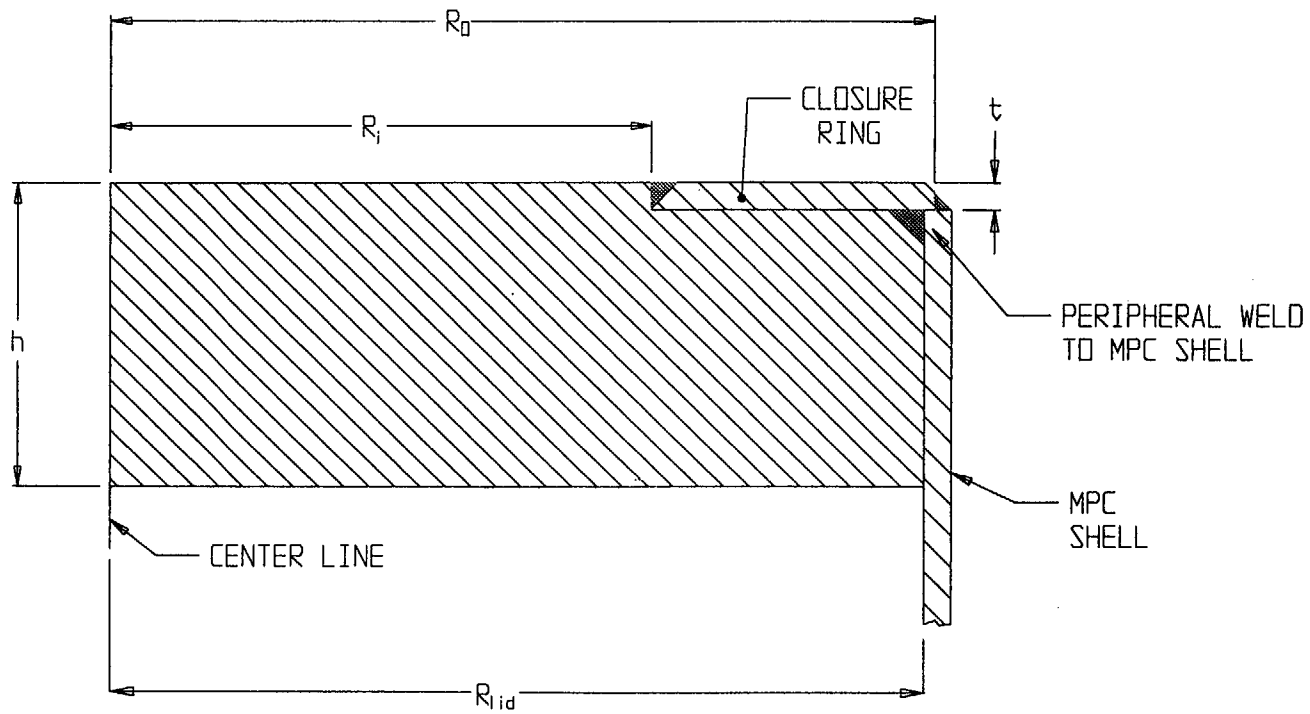


FIGURE 3.E.1; TOP CLOSURE LID WITH CLOSURE RING ATTACHED

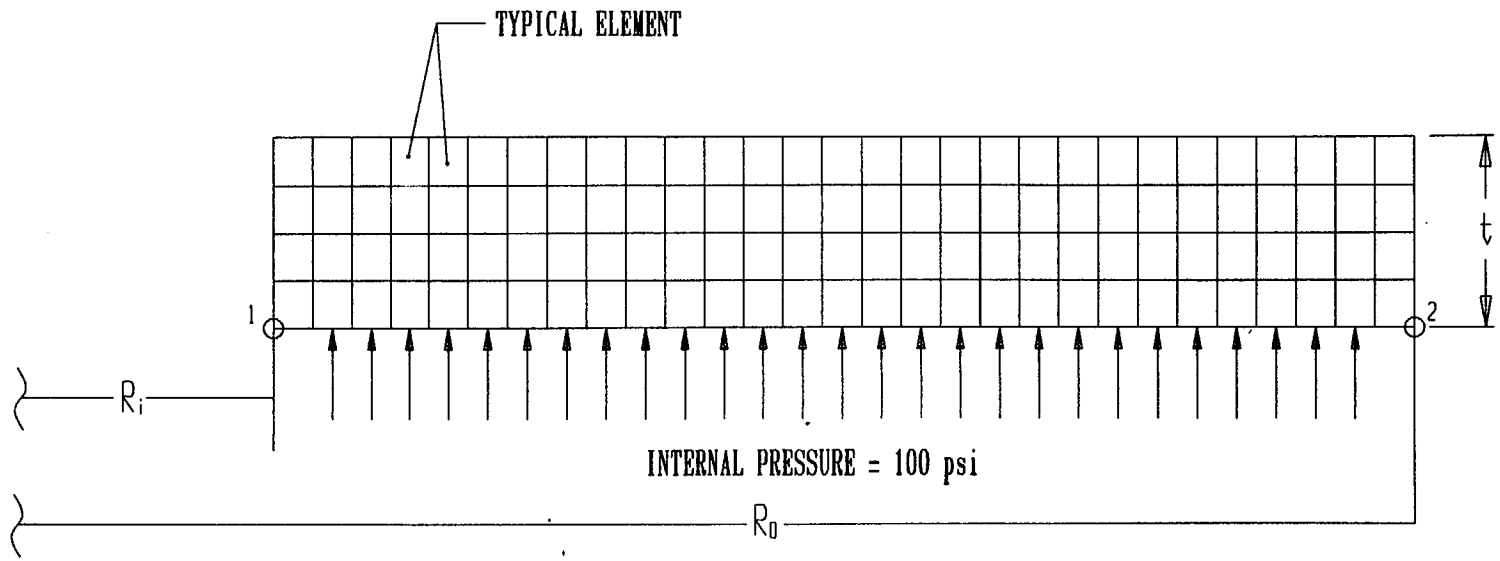


FIGURE 3.E.2; FINITE ELEMENT MODEL - CLOSURE RING

APPENDIX 3.F - STRESS ANALYSIS OF OVERPACK CLOSURE BOLTS

3.F.1 Introduction

This appendix contains a stress analysis of the HI-STAR 100 Overpack closure bolts. The purpose of the analysis is to demonstrate that stresses in the closure bolts do not exceed allowable maximums.

The HI-STAR 100 package can be used for both transportation and storage of spent nuclear fuel. Loadings from the normal and hypothetical accident conditions of transport as specified in Federal Regulation 10 CFR part 71 are more severe than the loadings placed on the bolts in the storage condition.

The complex interaction of forces and moments in bolted joints of shipping casks has been investigated in Reference 3.F.1, resulting in a comprehensive method of closure bolt stress analysis. That method is employed here. The analysis is presented in a step-by-step form for each loading combination considered. For each set of formulas or calculations used, reference to the appropriate table in [3.F.1] is given. Tables 4.3, 4.4, 4.5, and 4.7 are reproduced directly from [3.F.1] and placed at the end of this appendix to assist the reader. Where necessary, the formulas are modified to reflect the particulars of the HI-STAR system. For example, the loads due to impact from the MPC are applied as a pressure band near the bolt circle rather than as a uniform pressure load since the MPC contacts the overpack closure plate only around the periphery. Further, since the HI-STAR 100 closure lid has a raised face outside of the bolt circle, no prying forces can develop from loads directed outward (such as internal pressure or impact loads on the lid from the internals).

3.F.2 References

- [3.F.1] Mok, Fischer, Hsu, *Stress Analysis of Closure Bolts for Shipping Casks* (NUREG/CR-6007 UCRL-ID-110637), Lawrence Livermore National Laboratory/Kaiser Engineering, 1993.
- [3.F.2] Horton, H. (Ed.), *Machinery's Handbook*, 15th Ed., The Industrial Press, 1957.
- [3.F.3] FEL-PRO Technical Bulletin, N-5000 Nickel Based - Nuclear Grade Anti-Seize Lubricant, 8/97.
- [3.F.4] K.P. Singh and A.I. Soler, *Mechanical Design of Heat Exchangers and Pressure Vessel Components*, First Edition, Arcturus Publishers, Inc., 1984.

3.F.3 Assumptions

The assumptions used in the analysis are given as a part of Reference 3.F.1. The assumptions in that reference are considered valid for this analysis except where noted below.

1. No bolt prying can occur from outward directed loads since the closure lid has a raised face outside of the bolt circle which eliminates the potential for prying due to positive bending moments.

2. The forces and moments in the bolts due to the gasket load are included in the preload imposed.
3. Puncture forces are calculated using pressure equal to 3 times the lid yield strength. This is conservative since a dynamic analysis of the impact would demonstrate lower contact loads.
4. The forces and moments in the bolts due to vibration loads are small relative to the forces and moments generated by all other loads, and are considered negligible.
5. A recess is provided in the overpack closure plate that causes the MPC to contact the bottom face of the overpack closure plate over an annular region at the outer periphery of the closure plate. The formulas for plates under uniform pressure used in the reference are replaced here by formulas for plates loaded uniformly over an annular region at the outer periphery.
6. As the HI-STAR 100 Overpack includes a protected lid, shear bolt forces are defined to be zero.
7. The temperatures used in the analyses are taken from the thermal analysis of the HI-STAR.
8. The actual weight of the overpack closure plate is replaced by a somewhat larger weight in this analysis. This is conservative because loads on the bolts are increased with a heavier closure plate.
9. The impact load in this analysis is assumed to be 60 g. This is conservative because actual accelerations of the cask are less than 60 g. An impact angle of 80 degrees is assumed since the impact limiter will load the closure plate in the near top drop condition.

3.F.4 Terminology

Some terminology in Reference 3.F.1 differs from Holtec's terminology. In this analysis, the 'cask wall' is Holtec's 'main flange'. The 'cask' is Holtec's 'Overpack'. 'Closure lid' and 'closure plate' are used interchangeably.

Wherever possible, parameter names are consistent with Reference 3.F.1.

3.F.5 Composition

This appendix was created with the Mathcad (version 6.0+) software package. Mathcad uses the symbol ':=' as an assignment operator, and the equals symbol '=' retrieves values for constants or variables. Inequalities are also employed. Mathcad returns 0 for a false inequality, and 1 for a true inequality.

Units are also carried with Mathcad variables.

3.F.6 Analysis Procedure

The analysis procedure is taken from Section 6.4 of Reference 3.F.1. The following general steps are taken:

1. Identification of individual loadings.
2. Identification of critical combined load cases. Three critical combined load cases are considered in the HI-STAR bolt analysis.
3. Identification and evaluation of load parameters.
4. Determination of the forces and moments acting on the bolts due to each of individual loading.
5. Determination of the forces and moments acting on the bolts for the combined load case under analysis.
6. Evaluation of the stresses in the bolts for the combined load case.
7. Comparison with acceptance criteria.

3.F.7 Identification of Individual Loadings

The individual loadings acting on the cask closure are the following:

- a. Bolt preload. Bolt preload is present in all loadings and includes any gasket sealing loads.
- b. Pressure. Design internal pressure is applied to the overpack wall and lid for all load combinations.
- c. Temperature. Temperatures from an appropriate thermal analysis are used.
- d. Impact. An impact angle and g-level are specified. A near top end drop resulting in an 80 degree impact angle is consistent with the assumption that the impact limiter does not load the closure plate.
- e. Puncture. The cask is subjected to a puncture load from an 6 inch diameter mild steel punch. A punch angle of 90 degrees is used. This simulates the hypothetical puncture condition.

3.F.8 Identification of Critical Combined Load Cases

The critical combined load cases that apply to the HI-STAR 100 system in the transport mode are as follows:

1. Normal condition maximum stress analysis: Preload + pressure + temperature

2. Accident condition maximum stress analysis: Preload + pressure + temperature + puncture
3. Accident condition maximum stress analysis: Preload + pressure + temperature + impact

These three cases are examined below.

3.F.9 Geometry Parameters

The parameters which define the HI-STAR 100 closure geometry are given in this section. The following information is obtained from the design drawings in Section 1.5 unless otherwise noted.

The nominal closure bolt diameter, $D_b := 1.625$ ·in

The total number of closure bolts, $N_b := 54$

The stress area of a closure bolt (from [3.F.4], p. 100), $A_b := 1.680$ ·in²

The closure lid diameter at the bolt circle, $D_{lb} := 74.75$ ·in

Closure lid diameter at the location of the gasket load reaction, $D_{lg} := 71.565$ ·in

The HI-STAR overpack gasket system includes two concentric seals. The value for D_{lg} above locates the gasket load reaction between the two seal diameters.

The thickness of the cask wall, $t_c := 6.25$ ·in

The minimum thickness of the closure lid, $t_l := \left(6 - \frac{1}{16}\right)$ ·in

This value for the closure lid thickness accounts for the thickness reduction (recess) in the bottom face of the lid.

The effective thickness of the closure lid flange, $t_{lf} := 4.25$ ·in

The closure plate diameter at the inner edge, $D_{li} := 69.75$ ·in

The closure plate diameter at the inner edge is overpack inner diameter plus twice the width of the cut-out in the top flange which accommodates the inflatable annulus seal.

The closure plate diameter at the outer edge, $D_{lo} := 77.375$ ·in

The bolt length, $L_b := 4.25$ ·in

The bolt length is the length between the top and bottom surfaces of the closure plate, at the bolt circle location.

The number of bolt threads per inch, $n := 8 \cdot \frac{1}{\text{in}}$

The bolt thread pitch, $p := \frac{1}{n}$

The upper bound MPC weight (from Table 3.2.4), $W_c := 90000 \cdot \text{lb}$

The bounding weight used for closure plate (from Table 3.2.4), $W_l := 8000 \cdot \text{lb}$

The overpack closure lid recess inner diameter, $d_l := 52.75 \cdot \text{in}$

3.F.10 Material Properties

The overpack closure bolts are SB-637-N07718 steel, and the closure plate and top flange are SA-350-LF3 steel. The following material properties are used in the analysis based on a design temperature of 400 degrees F. The property values are obtained from Sections 3.1 and 3.3.

The Young's modulus of the cask wall material, $E_c := 26100000 \cdot \text{psi}$

The Young's modulus of the closure plate material, $E_l := 26100000 \cdot \text{psi}$

The Poisson's ratio of the closure plate material, $\text{NUI} := 0.3$

The closure bolt material coefficient of thermal expansion, $a_b := 7.45 \cdot 10^{-6} \cdot \text{R}^{-1}$

The cask wall material coefficient of thermal expansion, $a_c := 6.98 \cdot 10^{-6} \cdot \text{R}^{-1}$

The closure plate material coefficient of thermal expansion, $a_l := 6.98 \cdot 10^{-6} \cdot \text{R}^{-1}$

The zero points of the Fahrenheit and Rankine scales differ by a constant ($1 \text{ } ^\circ\text{F} = 1 \text{ R}$), therefore the above numbers are accurate with either unit.

Young's modulus of the closure bolt material, $E_b := 27600000 \cdot \text{psi}$

Yield strength of closure plate material, $S_{y1} := 32200 \cdot \text{psi}$

Tensile strength of closure plate material, $S_{u1} := 64600 \cdot \text{psi}$

Young's modulus of top flange material, $E_{lf} := 26100000 \cdot \text{psi}$

Bolt material minimum yield stress or strength (room temperature), $S_{y1} := 150000 \cdot \text{psi}$

Bolt material minimum yield stress or strength (design temperature), $S_{y2} := 138300 \cdot \text{psi}$

Bolt material minimum ultimate stress or strength (design temperature), $S_u := 170600 \cdot \text{psi}$

3.F.11 Combined Load Case 1

Normal Condition maximum stress analysis: Preload + pressure + temperature

3.F.11.1 Identification and Evaluation of Load Parameters, Combined Load Case 1

For each individual loading in this combined load case, the load parameters must be defined. The load parameters for the first individual load case in load combination 1 are as follows:

Loading parameters for preload:

The nominal value of the nut factor is 0.15 from Reference 3.F.3.

The minimum nut factor, based on a tolerance of +/- 5%, is $K := 0.1425$

The maximum bolt preload torque per bolt (Table 8.1.3), $Q := 2895 \cdot \text{ft} \cdot \text{lb} + 90 \cdot \text{ft} \cdot \text{lb}$

Loading parameters for pressure load:

The pressure inside the cask wall, $P_{ci} := 100 \cdot \text{psi}$

The pressure outside the cask wall, $P_{co} := 14.7 \cdot \text{psi}$

The pressure inside the closure lid, $P_{li} := 100 \cdot \text{psi}$

The pressure outside the closure lid, $P_{lo} := 14.7 \cdot \text{psi}$

Loading parameters for the normal condition temperature load: (bolt installation at 70 deg. F)

The maximum temperature rise of the main flange, $T_c := (155 - 70) \cdot R$

The maximum temperature rise of the closure lid inner surface, $T_{li} := (155 - 70) \cdot R$

The maximum temperature rise of the closure lid outer surface, $T_{lo} := (150 - 70) \cdot R$

The maximum temperature change of the closure lid, $T_l := \frac{T_{li} + T_{lo}}{2}$ $T_l = 82.5 R$

The maximum temperature change of the closure bolts, $T_b := \frac{T_l + T_c}{2}$ $T_b = 83.75 R$

As these parameters are all temperature differences, the Fahrenheit-to-Rankine conversion factor of 460° can be omitted. The temperature values are obtained from the normal steady state analysis of a bounding MPC (highest heat load and temperatures).

3.F.11.2 Determination of Bolt Forces and Moments for the Individual Loadings

Array parameters are used to account for the multiple individual loadings within one combined load case. In combined load case 1, there are three individual loadings, so let i include the range from 1 to 3 as follows:

Let $i := 1..3$

The forces and moments generated by each individual load case are represented by the following symbols:

The non-prying tensile bolt force per bolt = F_{a_i}

The shear bolt force per bolt = F_{s_i}

The fixed-edge closure lid force = F_{f_i}

Fixed-edge closure lid moment = M_{f_i}

The subscript i is used only to keep track of each individual load case within a load combination.

The first individual loading in this load combination is the residual load after the preload operation. The forces and moments generated by this load are defined as [3.F.1, Table 4.1]:

The non-prying tensile bolt force per bolt, $F_{a_1} := \frac{Q}{K \cdot D_b}$

The maximum residual tensile bolt force (preload) per bolt, $F_{a_r_1} := F_{a_1}$

The maximum residual torsional bolt moment per bolt, $M_{tr} := 0.5 \cdot Q$

The preload stress in each bolt (based on stress area), $Preload := \frac{F_{a_1}}{A_b}$

Substituting the appropriate input data, the values of these parameters are determined as:

$$F_{a_1} = 154688 \text{ lbf}$$

$$F_{a_r_1} = 154688 \text{ lbf}$$

$$M_{tr} = 17910 \text{ in}\cdot\text{lbf}$$

$$Preload = 92076 \text{ psi}$$

The second individual loading in this load combination is the pressure load. The forces and moments generated by this load are defined as follows [3.F.1, Table 4.3]:

The non-prying tensile force per bolt, $F_{a2} := \frac{\pi \cdot Dlg^2 \cdot (Pli - Plo)}{4 \cdot Nb}$

The shear bolt force per bolt, $F_{s2} := \frac{\pi \cdot El \cdot tl \cdot (Pci - Pco) \cdot Dlb^2}{2 \cdot Nb \cdot Ec \cdot tc \cdot (1 - NUI)}$

The fixed-edge closure lid force, $Ff_2 := \frac{Dlb \cdot (Pli - Plo)}{4}$

The fixed-edge closure lid moment, $Mf_2 := \frac{(Pli - Plo) \cdot Dlb^2}{32}$

Substituting the appropriate input data, the values of these parameters are determined as:

$$F_{a2} = 6354 \text{ lbf}$$

$$F_{s2} = 18816 \text{ lbf}$$

$$Ff_2 = 1594 \frac{\text{lbf}}{\text{in}}$$

$$Mf_2 = 14894 \text{ lbf}$$

The third individual loading in this load combination is the temperature load. The forces and moments generated by this load are defined as [3.F.1, Table 4.4]:

The non-prying tensile bolt force per bolt, $F_{a3} := 0.25 \cdot \pi \cdot Db^2 \cdot Eb \cdot (al \cdot Tl - ab \cdot Tb)$

The shear bolt force per bolt, $F_{s3} := \frac{\pi \cdot El \cdot tl \cdot Dlb \cdot (al \cdot Tl - ac \cdot Tc)}{Nb \cdot (1 - NUI)}$

The fixed-edge closure lid force, $Ff_3 := 0 \cdot \frac{\text{lbf}}{\text{in}}$

The fixed-edge closure lid moment, $Mf_3 := \frac{El \cdot al \cdot tl^2 \cdot (Tlo - Tli)}{12 \cdot (1 - NUI)}$

Substituting the appropriate input data, the values of these parameters are determined as:

$$F_{a3} = -2753 \text{ lbf}$$

$$F_{s3} = -16800 \text{ lbf}$$

$$Ff_3 = 0 \frac{\text{lbf}}{\text{in}}$$

$$Mf_3 = -3823 \text{ lbf}$$

3.F.11.3 Determination of Combined Bolt Forces and Combined Bolt Moments

The calculations in the following subsections are performed in accordance with Tables 4.9, 2.1 and 2.2 of Reference 3.F.1.

3.F.11.3.1 Tensile Bolt Force

First, combine the non-prying tensile bolt forces (F_{a_i}):

The total preload and temperature load, $F_{a_pt} := F_{a_1} + F_{a_3}$

$$F_{a_pt} = 151936 \text{ lbf}$$

The sum of the remaining forces (pressure), $F_{a_al} := F_{a_2}$

$$F_{a_al} = 6354 \text{ lbf}$$

The combined non-prying tensile bolt force, $F_{a_c} := F_{a_al} \cdot (F_{a_al} > F_{a_pt}) + F_{a_pt} \cdot (F_{a_pt} > F_{a_al})$

$$F_{a_c} = 151936 \text{ lbf}$$

If the combined non-prying tensile bolt force (F_{a_c}) is negative, set it equal to zero. Per Appendix 3 of Reference [3.F.1], inward directed loads are not reacted by the bolts, but the developed formulations are still valid if the spurious bolt forces < 0.0 are removed from the calculation.

$$F_{a_c} := F_{a_c} \cdot (F_{a_c} > 0 \cdot \text{lbf})$$

$$F_{a_c} = 151936 \text{ lbf}$$

Next, combine the prying tensile bolt forces and moments (these bolt forces develop due to F_{f_i} and M_{f_i}):

The sum of the fixed edge forces, $F_{f_c} := F_{f_1} + F_{f_2} + F_{f_3}$

$$F_{f_c} = 1594 \frac{\text{lbf}}{\text{in}}$$

If the combined fixed-edged force (F_{f_c}) is negative, set it equal to zero.

$$F_{f_c} := F_{f_c} \cdot \left(F_{f_c} > 0 \cdot \frac{\text{lbf}}{\text{in}} \right) + 0 \cdot \frac{\text{lbf}}{\text{in}} \cdot \left(F_{f_c} < 0 \cdot \frac{\text{lbf}}{\text{in}} \right)$$

$$F_{f_c} = 1.594 \times 10^3 \frac{\text{lbf}}{\text{in}}$$

The sum of fixed-edge moments, $M_{f_c} := M_{f_1} + M_{f_2} + M_{f_3}$

$$Mf_c = 11071 \frac{\text{lbf}\cdot\text{in}}{\text{in}}$$

Define the appropriate prying force moment arm depending on the direction of Mf_c . For inward directed loading, prying moments are developed by the lid rotating about the flange inner edge; for outward directed loading, prying moments are developed by the lid rotating about its outer edge. Thus, the moment arms are different in the two cases.

$$\text{Arm} := (Dlo - Dlb) \cdot (Mf_c > 0 \cdot \text{lbf}) + (Dlb - Dli) \cdot (Mf_c < 0 \cdot \text{lbf})$$

$$\text{Arm} = 2.625 \text{ in}$$

The prying tensile bolt force for the combined loading can therefore be determined as:

The constants C_1 and C_2 are: $C_1 := 1$

$$C_2 := \left[\frac{8}{3 \cdot (\text{Arm})^2} \right] \cdot \left[\frac{El \cdot t^3}{1 - \text{NUI}} + \frac{(Dlo - Dli) \cdot El \cdot t^3}{Dlb} \right] \cdot \left(\frac{Lb}{Nb \cdot Db^2 \cdot Eb} \right)$$

$$C_2 = 3.347$$

The bolt preload per unit length of bolt circle, $P := Fa_pt \cdot \left(\frac{Nb}{\pi \cdot Dlb} \right)$

$$P = 34938 \frac{\text{lbf}}{\text{in}}$$

The parameter P is the pressure/temperature force which is multiplied to determine preload per unit length of bolt circle (see Tables 2.1 and 4.9 in Section II.3 of Reference 3.F.1).

The non-prying tensile bolt force, $B := Ff_c \cdot (Ff_c > P) + P \cdot (P > Ff_c)$

$$B = 34938 \frac{\text{lbf}}{\text{in}}$$

The additional tensile bolt force per bolt caused by prying action of the closure lid, $Fap := \left(\frac{\pi \cdot Dlb}{Nb} \right) \cdot \left[\frac{\frac{2 \cdot Mf_c}{\text{Arm}} - C_1 \cdot (B - Ff_c) - C_2 \cdot (B - P)}{C_1 + C_2} \right]$

$$Fap = -24918 \text{ lbf}$$

The prying force must be tensile. If the result is negative, set it equal to zero.

$$Fab_c := Fap \cdot (Fap > 0 \cdot \text{lbf}) + 0 \cdot \text{lbf} \cdot (Fap < 0 \cdot \text{lbf})$$

$$Fab_c = 0 \text{ lbf}$$

The total tensile bolt force for stress analysis, $FA := Fa_c + Fab_c$

$$FA = 151936 \text{ lbf}$$

3.F.11.3.2 Bolt Shear Force

The sum of the shear forces, $Fs_c := Fs_1 + Fs_2 + Fs_3$

$$Fs_c = 2016 \text{ lbf}$$

$$Fs := 0 \text{ lbf} \quad (\text{protected cask lid})$$

3.F.11.3.3 Bolt Bending Moment

The calculations in this section are performed in accordance with Table 2.2 of Reference 3.F.1. The following relations are defined:

$$Kb := \left(\frac{Nb}{Lb} \right) \left(\frac{Eb}{Dlb} \right) \left(\frac{Db^4}{64} \right)$$

$$Kl := \frac{El \cdot tl^3}{3 \cdot \left[(1 - NUl^2) + (1 - NUl)^2 \cdot \left(\frac{Dlb}{Dlo} \right)^2 \right] \cdot Dlb}$$

$$Mbb_c := \left(\frac{\pi \cdot Dlb}{Nb} \right) \left(\frac{Kb}{Kb + Kl} \right) \cdot Mf_c$$

$$Mbb := Mbb_c$$

where Mbb is the bolt bending moment. Substituting the appropriate values, these parameters are calculated as:

$$Kb = 511136 \text{ lbf}$$

$$Kl = 17817619 \text{ lbf}$$

$$Mbb_c = 1.343 \times 10^3 \text{ lbf} \cdot \text{in}$$

$$Mbb = 1.343 \times 10^3 \text{ lbf} \cdot \text{in}$$

3.F.11.3.4 Bolt Torsional Moment

The torsional bolt moment is generated only by the preloading operation, therefore no combination is necessary.

3.F.11.4 Evaluation of Bolt Stresses

Per Table 5.1 of Reference 3.F.1, the average and maximum bolt stresses for comparison with the acceptance criteria are obtained. Inch-series threads are used and the maximum shear and bending are in the bolt thread.

The bolt diameter for tensile stress calculation [3.F.1, Table 5.1], $D_{ba} := D_b - 0.9743 \cdot p$

$$D_{ba} = 1.503 \text{ in}$$

The bolt diameter for shear stress calculation, $D_{bs} := D_{ba}$

$$D_{bs} = 1.503 \text{ in}$$

The bolt diameter for bending stress calculation, $D_{bb} := D_{ba}$

$$D_{bb} = 1.503 \text{ in}$$

The bolt diameter for torsional stress calculation, $D_{bt} := D_{ba}$

$$D_{bt} = 1.503 \text{ in}$$

The average tensile stress caused by the tensile bolt force F_A , $S_{ba} := 1.2732 \cdot \frac{F_A}{D_{ba}^2}$

$$S_{ba} = 85608 \text{ psi}$$

The average shear stress caused by the shear bolt force F_s , $S_{bs} := 1.2732 \cdot \frac{F_s}{D_{bs}^2}$

$$S_{bs} = 0 \text{ psi}$$

The maximum bending stress caused by the bending bolt moment M_b , $S_{bb} := 10.186 \cdot \frac{M_{bb}}{D_{bb}^3}$

$$S_{bb} = 4026 \text{ psi}$$

The maximum shear stress caused by the torsional bolt moment M_t , $S_{bt} := 5.093 \cdot \frac{M_{tr}}{D_{bt}^3}$

$$S_{bt} = 26854 \text{ psi}$$

The maximum stress intensity caused by the combined loading of tension, shear, bending and torsion can therefore be determined as:

$$S_{bi} := \left[(S_{ba} + S_{bb})^2 + 4 \cdot (S_{bs} + S_{bt})^2 \right]^{0.5}$$

$$S_{bi} = 104494 \text{ psi}$$

3.F.11.5 Comparison with Acceptance Criteria: Normal Conditions, Maximum Stress Analysis

These comparisons are performed in accordance with Table 6.1 of Reference 3.F.1.

The basic allowable stress limit for the bolt material, $S_m := \frac{2}{3} \cdot S_{y1} \cdot (S_{y1} \leq S_{y2}) + \frac{2}{3} \cdot S_{y2} \cdot (S_{y2} < S_{y1})$

$$S_m = 9.22 \times 10^4 \text{ psi}$$

The average tensile stress (must be $< S_m$), $S_{ba} = 85608 \text{ psi}$

The average shear stress (must be $< 0.6S_m$), $S_{bs} = 0 \text{ psi}$

For combined tensile and shear stress, the sum of the squares of the stress-to-allowable ratios (R_t and R_s) must be less than 1.0.

The tensile stress-to-allowable ratio, $R_t := \frac{S_{ba}}{S_m}$ $R_t = 0.929$

The shear stress-to-allowable ratio, $R_s := \frac{S_{bs}}{0.6 \cdot S_m}$

The sum of the squares of the ratios (must be < 1.0), $R_t^2 + R_s^2 = 0.862$

For combined tension, shear, bending and torsion loadings, the maximum stress intensity must be less than 1.35 times the allowable stress limit of the bolt material (S_m).

$$1.35 \cdot S_m = 124470 \text{ psi}$$

$$S_{bi} = 104494 \text{ psi}$$

3.F.11.6 Conclusion

For the first loading combination, allowable stress limits are not exceeded.

3.F.12 Critical Combined Load Case 2

Accident Condition maximum stress analysis: Preload + pressure + temperature + puncture

3.F.12.1 Identification and Evaluation of Load Parameters, Combined Load Case 2

The first three individual loadings in this combined load case are the same as the individual loadings in the previous load case. Therefore, only the puncture load parameters must be defined for this load combination. The load parameters for the puncture individual load case in load combination 2 are as follows:

The diameter of the puncture bar, $D_{pb} := 6 \cdot \text{in}$

The impact angle between the cask axis and the ground, $\xi := 90 \cdot \text{deg}$

3.F.12.2 Determination of Bolt Forces and Moments of Individual Loadings

Four individual loadings exist, so we define a range from 1 to 4 as follows:

Let $i := 0..4$

Bolt forces and moments for the preload, pressure, and temperature loads have already been calculated in the previous section. Determination of bolt forces and moments for the puncture load (the fourth individual load in this load combination) are required here [3.F.1, Table 4.7].

First, calculate the maximum puncture load generated by the puncture bar. The puncture force is assumed to be based on a dynamic flow stress S_y at the circular contact area between the bar and the lid surface. The dynamic flow stress is taken as the average of the yield strength and the ultimate strength of the lid material. Therefore, for this puncture analysis:

The dynamic flow stress, $S_y := .5 \cdot (S_{y1} + S_{u1})$

$$S_y = 4.84 \times 10^4 \text{ psi}$$

The puncture contact area, $P_{un} := 0.75 \cdot \pi \cdot D_{pb}^2 \cdot S_{y1}$

$$P_{un} = 2.731 \times 10^6 \text{ lbf}$$

The bolt forces and moments due to the puncture load can now be determined as:

The non-prying tensile bolt force per bolt, $F_{a4} := \frac{-\sin(\xi) \cdot P_{un}}{N_b}$

$$F_{a4} = -50580 \text{ lbf}$$

The shear bolt force per bolt, $F_{s4} := \frac{\cos(\xi) \cdot P_{un}}{N_b}$

$$F_{s4} = -1.936 \times 10^{-11} \text{ lbf}$$

The fixed-edge closure lid force, $F_{f4} := \frac{-\sin(\xi) \cdot P_{un}}{\pi \cdot D_{lb}}$

$$F_{f4} = -11631 \frac{\text{lbf}}{\text{in}}$$

The fixed-edge closure lid moment, $M_{f4} := \frac{-\sin(\xi) \cdot P_{un}}{4 \cdot \pi}$

$$Mf_4 = -217350 \frac{\text{lbf}\cdot\text{in}}{\text{in}}$$

3.F.12.3 Determination of Combined Bolt Forces and Combined Bolt Moments

3.F.12.3.1 Bolt Tensile Force

Combine the non-prying tensile bolt forces.

The total preload and temperature load, $Fa_{pt} := Fa_1 + Fa_3$

$$Fa_{pt} = 151936 \text{ lbf}$$

The sum of the remaining loads (pressure and puncture), $Fa_{al} := Fa_2 + Fa_4$

$$Fa_{al} = -44226 \text{ lbf}$$

The combined non-prying tensile bolt force, $Fa_c := Fa_{al} \cdot (Fa_{al} > Fa_{pt}) + Fa_{pt} \cdot (Fa_{pt} > Fa_{al})$

$$Fa_c = 151936 \text{ lbf}$$

If Fa_c is negative, set it equal to zero: $Fa_c := Fa_c \cdot (Fa_c > 0 \cdot \text{lbf})$

$$Fa_c = 151936 \text{ lbf}$$

Combine the prying tensile bolt forces.

The sum of the fixed-edge forces, $Ff_c := Ff_1 + Ff_2 + Ff_3 + Ff_4$

$$Ff_c = -10037 \frac{\text{lbf}}{\text{in}}$$

If Ff_c is negative, set it equal to zero: $Ff_c := Ff_c \cdot \left(Ff_c > 0 \cdot \frac{\text{lbf}}{\text{in}} \right) + 0 \cdot \frac{\text{lbf}}{\text{in}} \cdot \left(Ff_c < 0 \cdot \frac{\text{lbf}}{\text{in}} \right)$

$$Ff_c = 0 \frac{\text{lbf}}{\text{in}}$$

The sum of the fixed-edge moments, $Mf_c := Mf_1 + Mf_2 + Mf_3 + Mf_4$

$$Mf_c = -206279 \frac{\text{lbf}\cdot\text{in}}{\text{in}}$$

Determine the appropriate prying force moment arm depending on the direction of Mf_c .

$$\text{Arm} := (Dlo - Dlb) \cdot (Mf_c > 0 \cdot \text{lbf}) + (Dlb - Dli) \cdot (Mf_c < 0 \cdot \text{lbf})$$

$$\text{Arm} = 5 \text{ in}$$

Determine the prying tensile bolt force for the combined loading.

The non-prying tensile bolt force, $B := Ff_c \cdot (Ff_c > P) + P \cdot (P > Ff_c)$

$$B = 34938 \frac{\text{lbf}}{\text{in}}$$

The additional tensile force per bolt caused by prying action of the lid can now be determined as:

The constants C_1 and C_2 are: $C_1 := 1$

$$C_2 := \left[\frac{8}{3 \cdot (\text{Arm})^2} \right] \cdot \left[\frac{E \cdot t^3}{1 - \text{NU1}} + \frac{(\text{Dlo} - \text{Dli}) \cdot E \cdot f \cdot t^3}{\text{Dlb}} \right] \cdot \left(\frac{\text{Lb}}{\text{Nb} \cdot \text{Db}^2 \cdot \text{Eb}} \right)$$

$$C_2 = 0.923$$

The additional tensile force per bolt caused by prying action of the closure lid, $F_{ap} := \left(\frac{\pi \cdot \text{Dlb}}{\text{Nb}} \right) \cdot \left[\frac{\frac{2 \cdot \text{Mf_c}}{\text{Arm}} - C_1 \cdot (B - Ff_c) - C_2 \cdot (B - P)}{C_1 + C_2} \right]$

$$F_{ap} = -265668 \text{ lbf}$$

If the prying force is negative, set it equal to zero: $F_{ab_c} := F_{ap} \cdot (F_{ap} > 0 \cdot \text{lbf}) + 0 \cdot \text{lbf} \cdot (F_{ap} < 0 \cdot \text{lbf})$

$$F_{ab_c} = 0 \text{ lbf}$$

The total tensile bolt force for stress analysis, $F_A := F_{a_c} + F_{ab_c}$

$$F_A = 151936 \text{ lbf}$$

3.F.12.3.2 Bolt Shear Force

The sum of the shear forces, $F_{s_c} := F_{s1} + F_{s2} + F_{s3} + F_{s4}$

$$F_{s_c} = -1.936 \times 10^{-11} \text{ lbf}$$

$$F_s := 0 \cdot \text{lbf} \quad (\text{protected cask lid})$$

3.F.12.3.3 Bolt Bending Moment

The bolt bending moment can be determined as:

$$M_{bb_c} := \left(\frac{\pi \cdot \text{Dlb}}{\text{Nb}} \right) \cdot \left(\frac{\text{Kb}}{\text{Kb} + \text{Kl}} \right) \cdot \text{Mf_c}$$

$$M_{bb_c} = -25016 \text{ in} \cdot \text{lbf}$$

$$M_{bb} := M_{bb_c}$$

$$M_{bb} = -25016 \text{ in-lbf}$$

3.F.12.3.4 Bolt Torsional Moment

The torsional bolt moment is generated only by the preloading operation. No combination is necessary.

3.F.12.4 Evaluation of Bolt Stresses

Per Table 5.1 of Reference 3.F.1, the average and maximum bolt stresses are obtained for comparison to the acceptance criteria.

The average tensile stress caused by the bolt tensile force F_A ,
$$S_{ba} := 1.2732 \cdot \frac{F_A}{D_{ba}^2}$$

$$S_{ba} = 85608 \text{ psi}$$

The average shear stress caused by the bolt shear force F_s ,
$$S_{bs} := 1.2732 \cdot \frac{F_s}{D_{bs}^2}$$

$$S_{bs} = 0 \text{ psi}$$

The maximum bending stress caused by the bolt bending moment M_b ,
$$S_{bb} := 10.186 \cdot \frac{M_{bb}}{D_{bb}^3}$$

$$S_{bb} = -75018 \text{ psi}$$

The maximum shear stress caused by the bolt torsional moment M_t ,
$$S_{bt} := 5.093 \cdot \frac{M_{tr}}{D_{bt}^3}$$

$$S_{bt} = 26854 \text{ psi}$$

3.F.12.5 Comparison with Acceptance Criteria: Accident Conditions, Maximum Stress Analysis

the comparison with acceptance criteria is performed as per Table 6.3 of Reference 3.F.1.

Compute $0.7 \cdot S_u = 119420 \text{ psi}$

$$S_{y2} = 1.383 \times 10^5 \text{ psi}$$

The average tensile stress (must be < the smaller of $0.7S_u$ and S_{y2}), $S_{ba} = 85608 \text{ psi}$

Compute $0.42 \cdot S_u = 71652 \text{ psi}$

$$0.6 \cdot S_{y2} = 82980 \text{ psi}$$

The average shear stress (must be < the smaller of $0.42S_u$ and $0.6S_{y2}$), $S_{bs} = 0 \text{ psi}$

For combined tensile and shear stress, the sum of the squares of the stress-to-allowable ratios (R_t and R_s) must be less than 1.0.

$$\text{The tensile stress-to-allowable ratio, } R_t := \frac{S_{ba}}{0.7 \cdot S_u \cdot (0.7 \cdot S_u \leq S_y2) + S_y2 \cdot (S_y2 \leq 0.7 \cdot S_u)} \quad R_t = 0.717$$

$$\text{The shear stress-to-allowable ratio, } R_s := \frac{S_{bs}}{0.42 \cdot S_u \cdot (0.42 \cdot S_u \leq 0.6 \cdot S_y2) + 0.6 \cdot S_y2 \cdot (0.6 \cdot S_y2 \leq 0.42 \cdot S_u)}$$

The sum of the squares of the ratios (must be < 1.0), $R_t^2 + R_s^2 = 0.514$

3.F.12.6 Conclusion

For the second loading combination, allowable stress limits are not exceeded.

3.F.13 Critical Combined Load Case 3

Accident condition maximum stress analysis: Preload + pressure + temperature + impact

The preload, pressure, and temperature individual loadings in this combined load case are the same as in the two previous load cases. Therefore, only the impact load parameters must be defined for this load combination.

3.F.13.1 Identification and Evaluation of Impact Load Parameters

Impact load parameters are defined in Table 4.5 of Reference 3.F.1. Impact decelerations have been accurately computed elsewhere using a dynamic analysis. Nevertheless, an additional dynamic load factor is applied for conservatism in the results.

The applied dynamic load factor, $DLF := 1.05$

Impact angle between the cask axis and the target surface, $\xi := 80\text{-deg}$

Maximum rigid-body impact acceleration (g) of the cask, $a_i := 60\text{-g}$

We conservatively assume that if an impact limiter is in place, it will provide a reacting load at a location r_p , relative to the pivot point assumed in [3.F.1]. The distance from the pivot point to the center of pressure on an impact limiter r_p must therefore be specified. The following formula is used to ensure, for any given case, that r_p is underestimated.

$$r_p := \left(\frac{D_{lo}}{2} \right) \cdot \sin(\xi)^8$$

$$r_p = 34.228 \text{ in}$$

For conservatism, this offset is neglected since it will reduce the tensile load in the bolts.

$$r_p := 0 \cdot \text{in}$$

3.F.13.3 Determination of Bolt Forces and Moments of Individual Loadings

The fourth and final individual loading in this load combination is the impact load. The forces and moments generated by this load are determined (per Reference 3.F.1, Table 4.5) as:

$$\text{The non-prying force per bolt, } F_{a4} := \frac{1.34 \cdot \sin(\xi) \cdot \text{DLF} \cdot a_i \cdot (W_l + W_c)}{N_b} \cdot \frac{\frac{D_{lo}}{2} - r_p}{\left(\frac{D_{lb}}{2}\right)}$$

$$F_{a4} = 156178 \text{ lbf}$$

This formula has been modified by addition of the correct location of the load from the impact limiter (non zero r_p), although for storage, r_p is zero.

$$\text{The shear bolt force per bolt, } F_{s4} := \frac{\cos(\xi) \cdot a_i \cdot W_l}{N_b}$$

$$F_{s4} = 1544 \text{ lbf}$$

$$\text{The fixed-edge closure lid force, } F_{f4} := \frac{1.34 \cdot \sin(\xi) \cdot \text{DLF} \cdot a_i \cdot (W_l + W_c)}{\pi \cdot D_{lb}}$$

$$F_{f4} = 34695 \frac{\text{lbf}}{\text{in}}$$

$$\text{The fixed-edge closure lid moment, } M_{f4} := \frac{1.34 \cdot \sin(\xi) \cdot \text{DLF} \cdot a_i \cdot (W_l + W_c)}{8 \cdot \pi} \left[1 - \left(\frac{d_l}{D_{lb}} \right)^2 \right]$$

$$M_{f4} = 162740 \frac{\text{in} \cdot \text{lbf}}{\text{in}}$$

The above formula has been modified to reflect the physical fact that in the HI-STAR 100 system the MPC transfers load to the overpack closure plate only around the periphery, because of the recess at the center of the closure plate. Therefore, the formula for a fixed edge plate with a pressure load applied only around the surface greater than $r = d_l/2$ has been used.

3.F.13.4 Determination of Combined Bolt Forces and Combined Bolt Moments

3.F.13.4.1 Bolt Tensile Force

First, combine the non-prying bolt tensile forces.

The total preload and temperature load, $Fa_{pt} := Fa_1 + Fa_3$

$$Fa_{pt} = 151936 \text{ lbf}$$

The sum of the remaining loads (pressure and impact), $Fa_{al} := Fa_2 + Fa_4$

$$Fa_{al} = 162531 \text{ lbf}$$

The combined non-prying tensile bolt force, $Fa_c := Fa_{al} \cdot (Fa_{al} > Fa_{pt}) + Fa_{pt} \cdot (Fa_{pt} > Fa_{al})$

$$Fa_c = 162531 \text{ lbf}$$

If Fa_c is negative, set it equal to zero: $Fa_c := Fa_c \cdot (Fa_c > 0 \cdot \text{lbf})$

$$Fa_c = 162531 \text{ lbf}$$

Next, combine the prying bolt tensile forces.

The sum of the fixed-edge forces, $Ff_c := Ff_1 + Ff_2 + Ff_3 + Ff_4$

$$Ff_c = 36289 \frac{\text{lbf}}{\text{in}}$$

The sum of the fixed-edge moments, $Mf_c := Mf_1 + Mf_2 + Mf_3 + Mf_4$

$$Mf_c = 173811 \frac{\text{in} \cdot \text{lbf}}{\text{in}}$$

Define the appropriate prying force moment arm depending on the direction of Mf_c .

$$\text{Arm} := (Dlo - Dlb) \cdot (Mf_c > 0 \cdot \text{lbf}) + (Dlb - Dli) \cdot (Mf_c < 0 \cdot \text{lbf})$$

$$\text{Arm} = 2.625 \text{ in}$$

Determine the prying bolt tensile force for the combined loading.

The non-prying tensile bolt force, $B := Ff_c \cdot (Ff_c > P) + P \cdot (P > Ff_c)$

$$B = 3.629 \times 10^4 \frac{\text{lbf}}{\text{in}}$$

The additional tensile force per bolt caused by prying action of the closure lid can be determined as:

The constants C_1 and C_2 are: $C_1 := 1$

$$C_2 := \left[\frac{8}{3 \cdot (\text{Arm})^2} \right] \cdot \left[\frac{El \cdot t^3}{1 - \text{NUI}} + \frac{(Dlo - Dli) \cdot El \cdot t \cdot f^3}{Dlb} \right] \cdot \left(\frac{Lb}{Nb \cdot Db^2 \cdot Eb} \right)$$

$$C_2 = 3.347$$

The additional tensile force per bolt caused by prying action of the closure lid, $F_{ap} := \left(\frac{\pi \cdot D_{lb}}{N_b} \right) \left[\frac{\frac{2 \cdot M_{f_c}}{Arm} - C_1 \cdot (B - F_{f_c}) - C_2 \cdot (B - P)}{C_1 + C_2} \right]$

$$F_{ap} = 127955 \text{ lbf}$$

If the prying bolt force is negative, set it equal to zero: $F_{ab_c} := F_{ap} \cdot (F_{ap} > 0 \cdot \text{lbf}) + 0 \cdot \text{lbf} \cdot (F_{ap} < 0 \cdot \text{lbf})$

$$F_{ab_c} = 127955 \text{ lbf}$$

For a raised face flange outboard of the bolt circle, no prying force can be developed.

$$F_{ab_c} := 0 \cdot \text{lbf}$$

The total tensile bolt force for stress analysis, $F_A := F_{a_c} + F_{ab_c}$

$$F_A = 162531 \text{ lbf}$$

3.F.13.4.2 Bolt Shear Force

The sum of the shear forces, $F_{s_c} := F_{s_1} + F_{s_2} + F_{s_3} + F_{s_4}$

$$F_{s_c} = 1544 \text{ lbf}$$

$$F_s := 0 \cdot \text{lbf} \quad (\text{protected cask lid})$$

3.F.13.4.3 Bolt Bending Moment

The bolt bending moment can now be determined as:

$$M_{bb_c} := \left(\frac{\pi \cdot D_{lb}}{N_b} \right) \cdot \left(\frac{K_b}{K_b + K_l} \right) \cdot M_{f_c}$$

$$M_{bb_c} = 21079 \text{ in} \cdot \text{lbf}$$

$$M_{bb} := M_{bb_c}$$

$$M_{bb} = 21079 \text{ in} \cdot \text{lbf}$$

3.F.13.4.4 Bolt Torsional Moment

The torsional bolt moment is generated only by the preloading operation. No combination is necessary.

3.F.13.5 Evaluation of Bolt Stresses

Per Table 5.1 of Reference 3.F.1, obtain the average and maximum bolt stresses for comparison to the acceptance criteria.

The average tensile stress caused by the bolt tensile force F_A , $S_{ba} := 1.2732 \cdot \frac{F_A}{D_{ba}^2}$

$$S_{ba} = 91578 \text{ psi}$$

The average shear stress caused by the bolt shear force F_s , $S_{bs} := 1.2732 \cdot \frac{F_s}{D_{bs}^2}$

$$S_{bs} = 0 \text{ psi}$$

The maximum bending stress caused by the bolt bending moment M_b , $S_{bb} := 10.186 \cdot \frac{M_{bb}}{D_{bb}^3}$

$$S_{bb} = 63211 \text{ psi}$$

The maximum shear stress caused by the bolt torsional moment M_t , $S_{bt} := 5.093 \cdot \frac{M_{tr}}{D_{bt}^3}$

$$S_{bt} = 26854 \text{ psi}$$

3.F.13.5 Comparison with Acceptance Criteria: Accident Conditions, Maximum Stress Analysis

The comparison with acceptance criteria is performed as per Table 6.3 of Reference 3.F.1.

$$0.7 \cdot S_u = 119420 \text{ psi}$$

$$S_{y2} = 1.383 \times 10^5 \text{ psi}$$

The average tensile stress (must be $< 0.7S_u$ and S_{y2}), $S_{ba} = 91578 \text{ psi}$

$$0.42 \cdot S_u = 71652 \text{ psi}$$

$$0.6 \cdot S_{y2} = 82980 \text{ psi}$$

The average shear stress (must be $< 0.42S_u$ and $0.6S_{y2}$), $S_{bs} = 0 \text{ psi}$

For combined tensile and shear stress, the sum of the squares of the stress-to-allowable ratios (R_t and R_s) must be less than 1.0.

The tensile stress-to-allowable ratio, $R_t := \frac{S_{ba}}{0.7 \cdot S_u \cdot (0.7 \cdot S_u \leq S_{y2}) + S_{y2} \cdot (S_{y2} \leq 0.7 \cdot S_u)}$ $R_t = 0.767$

The shear stress-to-allowable ratio, $R_s := \frac{S_{bs}}{0.42 \cdot S_u \cdot (0.42 \cdot S_u \leq 0.6 \cdot S_{y2}) + 0.6 \cdot S_{y2} \cdot (0.6 \cdot S_{y2} \leq 0.42 \cdot S_u)}$

The sum of the squares of the ratios (must be < 1.0), $R_t^2 + R_s^2 = 0.588$

3.F.13.6 Conclusion

For the third loading combination, allowable stress limits are not exceeded.

3.F.14 Bolt Analysis Conclusion

Using the standard method presented in Reference 3.F.1, the above analysis demonstrates that stresses closure bolts for the HI-STAR 100 Overpack will not exceed allowable limits.

APPENDIX 3.G - MISSILE PENETRATION ANALYSES

3.G.1 Introduction

In this appendix, deformations and stresses in the HI-STAR 100 Overpack due to two missile strikes are investigated. The objective of the analysis is to show that deformations in the HI-STAR 100 system due to the missile strike events do not compromise the containment boundary of the system, and that global stresses that arise from the missile strikes do not exceed the appropriate limits.

The two missiles considered are a 1-in. diameter steel sphere and an 8-in. diameter rigid cylinder, both traveling at 126 miles per hour. The two missile impacts are separate events. No metal thinner than 0.25-in. is exposed to impact.

3.G.2 References

[3.G.1] Young, Warren C., Roark's Formulas for Stress and Strain, 6th Edition, McGraw-Hill, 1989.

[3.G.2] Rothbart, H., Mechanical Design and Systems Handbook, 2nd Edition, McGraw Hill, 1985.

[3.G.3] Working Model, v.3.0, Knowledge Revolution, 1995.

3.G.3 Composition

This appendix was created using the Mathcad (version 6.0+) software package. Mathcad uses the symbol ':=' as an assignment operator, and the equals symbol '=' retrieves values for constants or variables. Mathcad's built-in equation solver is also used.

3.G.4 General Assumptions

General assumptions that apply to all analyses in this appendix are stated here. Further assumptions are stated in the subsequent text.

1. Formulae taken from Reference 3.G.1 are based on assumptions that are delineated in that reference.
2. The missiles are assumed to strike the cask at the most vulnerable location, in a manner that imparts the largest amount of energy to the cask surface.
3. In missile strikes on the side of the overpack, no structural resistance is offered by the neutron absorber material.

4. All material property data are specified at the design temperature of the particular component. For components with multiple materials (i.e. the overpack), the properties for the material with the lowest strength are used.

3.G.5 1-in. Diameter Steel Sphere Impact

3.G.5.1 Method

The first step in the 1-in. diameter sphere missile impact analysis is an investigation of the elastic behavior of the cask component being impacted. By balancing the kinetic energy of the missile with the work done deforming the impacted surface, it is shown that the missile's energy will not be entirely absorbed by elastic deformation. Therefore, the small missile will dent the cask. The elastic impact of the sphere is treated as a contact problem. The geometry is shown in Figure 3.G.1.

Following the elastic investigation of the impact, a plastic analysis is performed to determine the depth of the dent.

3.G.5.2 Elastic Analysis

The input data is specified as follows:

The diameter of the sphere (from Table 2.2.5), $D := 1\text{-in}$

The mass of the sphere (from Table 2.2.5), $M := 0.22\text{-kg} \cdot 2.204 \frac{\text{lb}}{\text{kg}}$

The velocity of sphere before impact (from Table 2.2.5), $V_0 := 126\text{-mph}$

The density of steel (from Section 3.3), $\rho := 0.283 \frac{\text{lb}}{\text{in}^3}$

The modulus of elasticity of the material (from Table 3.3.4), $E := 26.1 \cdot 10^6 \text{-psi}$

The Poisson's ratio of steel (from Section 3.3), $\nu := 0.3$

The yield stress of the material (from Table 3.3.4), $S_y := 32600\text{-psi}$

In the 1-in. diameter sphere impact problem, the final velocity at which elastic deformation ends is assumed. This velocity is assumed to be 99.96% of the pre-impact velocity of the missile. Thus, the velocity at which the average surface stress reaches the yield stress of the material (V_f) is:

$$V_f := 125.95\text{-mph}$$

Using Table 33, case 1 (p. 650) of reference 3.G.1 for a sphere penetrating a flat plate, the spring constant K_2 relating the contact load to the local target deformation (raised to the power 1.5) is defined as:

$$K_2 := \left(\frac{E^2 \cdot D}{1.55^3} \right)^{0.5}$$

Balancing the kinetic energy with the work done deforming the bodies, we obtain the relation:

$$\frac{1}{2} \cdot M(dV)^2 := Fdx$$

where:

$$F := K_2 \cdot x^{\frac{3}{2}}$$

and x is the depth of penetration.

Integrating and applying the condition that $x = 0$ at time $t = 0$ gives:

$$\frac{M}{2} \cdot (V^2 - V_0^2) := \frac{2}{5} \cdot K_2 \cdot x^{2.5}$$

Solving this equation for x , the depth of penetration $x := \left[\frac{M \cdot \frac{(V_0^2 - V_f^2)}{2}}{0.4 \cdot K_2} \right]^{0.4}$

and the peak impact force $F := K_2 \cdot x^{1.5}$ Thus, the depth of penetration = 0.003 in

and the peak impact force $F = 2112.312$ lbf

The surface area of the cask/missile contact patch is determined as:

$$\text{Area} := \pi \cdot (D \cdot x - x^2) \quad \text{Area} = 0.009 \text{ in}^2$$

and the average pressure on the patch to elastically support the load is approximately given as:

$$P_{\text{avg}} := \frac{F}{\text{Area}}$$

$$P_{\text{avg}} = 232519 \text{ psi}$$

This average pressure is greater than the yield stress of the impacted material. Therefore, the impact produces an inelastic deformation at the missile/cask contact location and local yielding occurs almost immediately after impact. From this conclusion, the change in kinetic energy of the missile is assumed to be entirely absorbed by plastic deformation.

3.G.5.3 Plastic Analysis

Disregarding the small amount of energy absorbed in elastic deformation, the kinetic energy of the missile is entirely balanced by the plastic work done in forming a spherically shaped dent in the surface. Perfectly plastic behavior of the impacted material is assumed. The kinetic energy of the missile just before impact is determined as:

$$KE := \frac{1}{2} \cdot M \cdot V_0^2$$

$$KE = 257.338 \text{ ft} \cdot \text{lbf}$$

Using Mathcad's built-in solver, determination of the depth of penetration begins with an estimate:

Assume $d := 0.18 \text{ in}$

Given

$$KE = S_y \cdot \pi \cdot \left(D \cdot \frac{d^2}{2} - \frac{d^3}{3} \right)$$

where the right hand side is the plastic work. The final deformation is characterized by the depth (d1) of the spherical dent in the cask surface, which is obtained as the value d (which solves the energy balance equation):

$$d1 := \text{Find}(d) \quad d1 = 0.271 \text{ in}$$

Note that the solution to the equation, d1, that is obtained by using the "Find(d)" command, can be checked by direct substitution of d1 for d in the equation. The maximum load, assuming that a constant stress is maintained until all of the impact energy is absorbed, is therefore:

$$P_{\max} := S_y \cdot \pi \cdot (D \cdot d1 - d1^2)$$

$$P_{\max} = 20249 \text{ lbf}$$

3.G.5.4 Conclusion: 1-in. Diameter Sphere Missile Impact

The 0.271 in. depth of penetration of the small missile, which is required to absorb all of the impact energy, is less than the thinnest section of material on the exterior surface of the cask. Therefore, the small missile will dent, but not penetrate, the cask. Global stresses in the overpack that arise from the 1-in. missile strike are assumed to be negligible.

3.G.6 Impact of an 8-in. Diameter Rigid Cylinder

3.G.6.1 Method

An 8-in. diameter cylindrical missile is postulated to impact the cask at the most vulnerable location, as shown in Figure 3.G.2.

Assuming the impacted material yields at the surface and then gross deformation occurs, the maximum force that can develop is the limit stress of the target material multiplied by the impact area. This limit stress is assumed to be the impacted material's "flow" stress, which is assumed to be the average of yield and ultimate strength.

This force is of sufficient magnitude to cause local denting of the immediate surface under the contact patch, and form a conical shaped region of gross deformation away from the contact patch. The large impact force occurs only for a short instant of time and will not cause a cask instability. The post-impact deformed shape is shown in Figure 3.G.3. The deformation is exaggerated for clarity.

The cylindrical punch may impact any exposed surface of the cask. The following three impact locations are investigated:

- a. Impact on outer overpack shell (no support from underlying neutron absorber is assumed),
- b. Impact on overpack closure plate, and
- c. Impact on the outside of the 8.5" overpack wall. For this strike location, the neutron absorber and outer shell are conservatively assumed not to slow the missile.

Penetration is examined by balancing the kinetic energy of the missile with the work required to punch out a slug of the target material.

Finally, global stresses in the overpack due to the 8-in. cylindrical missile impact are considered. Two impact locations are investigated, a side strike and an end strike.

3.G.6.2 Determination of Input Kinetic Energy and Applied Impact Force

The input data are specified as follows:

The diameter of the missile (from Table 2.2.5), $D := 8\text{-in}$

The weight of the missile (125 kg, from Table 2.2.5), $\text{Weight} := 125\text{-kg} \cdot 2.204 \frac{\text{lb}}{\text{kg}} \cdot g$

The velocity of the missile before impact (from Table 2.2.5), $V_0 := 126\text{-mph}$

The yield stress of the material at 400°F (from Table 3.3.4), $S_y := 32200\text{-psi}$

The ultimate stress of the material at 400°F (from Table 3.3.4), $S_u := 64600\text{-psi}$

The design stress intensity of the material at 400°F (from Table 3.3.4), $S_m := 21500$ ·psi

The flow stress is defined as the average of the yield stress and the ultimate stress.
The flow stress (S_{flow}) is therefore determined as:

$$S_{flow} := 0.5 \cdot (S_u + S_y)$$

$$S_{flow} = 48400 \text{ psi}$$

The force required to reach the flow stress of the material is determined by multiplying the flow stress by the impact area of the missile as:

$$\text{Force} := S_{flow} \cdot \pi \cdot \frac{D^2}{4}$$

$$\text{Force} = 2.433 \times 10^6 \text{ lbf}$$

3.G.6.3 Local Penetration

Local penetration is examined by requiring that the impact force developed be balanced by only the resistance force developed in shear along the side area of a plug that would be punched out from an otherwise rigid material. That is, a "shear plug" type failure mechanism is assumed. Figure 3.G.5 shows this type of failure pictorially. The failure mode is based on achievement of the ultimate stress in shear. The following three impact locations are examined:

- a. Penetration of the overpack outer shell,
- b. Penetration of the overpack inner shell plus five intermediate shells, and
- c. Penetration of the overpack closure plate.

- a. Penetration of the overpack outer shell:

The thickness of overpack outer shell, $t := 0.5$ ·in

The ultimate stress of the overpack outer shell (from Table 3.3.3), $S_u := 70000$ ·psi

Given $\pi \cdot D \cdot t \cdot \left(\frac{S_u}{2} \right) = \text{Force}$ the maximum depth of penetration can be determined.

$$h := \text{Find}(t)$$

$$h = 2.766 \text{ in}$$

Because the maximum depth of penetration (h) is greater than the shell thickness (t), the outer shell is penetrated if no resistance from the the neutron absorber is considered.

b. Penetration of overpack inner shell plus five intermediate shells:

The overpack outer shell and neutron absorber are assumed to offer no resistance to penetration.

The total thickness of the section (from BM-1476), $t := 8.5 \text{ in}$

The ultimate stress of the section at 400°F (from Table 3.3.4), $S_u := 68800 \text{ psi}$

The applied force (Force) is a known value. Therefore, the maximum penetration can be determined as:

$$\text{Given } \pi \cdot D \cdot t \cdot \left(\frac{S_u}{2} \right) = \text{Force} \quad h := \text{Find}(t) \quad h = 2.814 \text{ in}$$

Because the depth of penetration (h) is less than the total section thickness, the overpack inner shell is not penetrated.

c. Penetration of closure plate:

The closure plate thickness (from BM-1476), $t := 6 \text{ in}$

The ultimate stress of closure plate (from Table 3.3.4), $S_u := 64600 \text{ psi}$

The applied force (Force) is a known value. Therefore, the maximum penetration can be determined as:

$$\text{Given } \pi \cdot D \cdot t \cdot \left(\frac{S_u}{2} \right) = \text{Force} \quad h := \text{Find}(t) \quad h = 2.997 \text{ in}$$

Because the depth of penetration (h) is less than the closure plate thickness, the closure plate is not penetrated.

The results of the investigation of penetration at these three locations demonstrate that the HI-STAR 100 Overpack adequately protects the MPC from a direct missile strike. The following section demonstrates that the global stresses in the overpack remain below allowable limits in the missile strike event.

3.G.6.4 Stresses in the Overpack Due to 8-in. Diameter Missile Strike

Global stresses in the overpack due to missile strikes at two locations are examined in this subsection. The first location is a side strike at the level of the cask center of gravity (approximately 100 inches from the bottom of the baseplate), where the entire force is supported by the overpack inner shell acting as a simply supported beam (see Figure 3.G.4). The actual overpack wall consists of metal that is a minimum of 8.5 inches in thickness, but this analysis conservatively considers only the inner 2.5 inches.

The second location is an end strike at the center of the overpack closure plate.

a. First Location: Side Strike on Overpack

The length of the inner shell (assumed equal to the full cavity length), $L := 191.125 \text{ in}$

The inside diameter of the overpack (from Drawing 1397), $ID := 68.75 \text{ in}$

The thickness of the inner shell (from BM-1476), $t := 2.5 \text{ in}$

The applied force, $\text{Force} = 2.433 \times 10^6 \text{ lbf}$

We have previously shown that the missile will not penetrate through all of the intermediate shells. Therefore, in the computation of the global stress state induced by the missile strike, we include in the moment of inertia calculation of the overpack shells, the inner shell and the four intermediate shells that are welded to the baseplate.

The thickness of the intermediate shell (from BM-1476) is $t_i := 1.25 \text{ in}$

The outer diameter of the inner shell (D), and subsequently the area moment of inertia (I), are determined as:

$$D := 2 \cdot t + ID \qquad D_{\text{inner}} := D$$

Then the metal moment of inertia is computed as follows:

$$I := \frac{1}{4} \cdot \pi \cdot \left[\left(\frac{D}{2} \right)^4 - \left(\frac{D}{2} - t \right)^4 \right]$$
$$I = 3.555 \times 10^5 \text{ in}^4$$

The outer diameter of the innermost intermediate shell (D_i), and subsequently the area moment of inertia (I_i), are determined as:

$$D := 2 \cdot t_i + D \qquad D = 76.25 \text{ in}$$

Then the metal moment of inertia is computed as follows:

$$I_i := \frac{1}{4} \cdot \pi \cdot \left[\left(\frac{D}{2} \right)^4 - \left(\frac{D}{2} - t_i \right)^4 \right]$$
$$I_i = 2.071 \times 10^5 \text{ in}^4$$

The total area moment of inertia is obtained by summing the results from the two cylinders.

$$I := I + I_i \quad I = 5.627 \times 10^5 \text{ in}^4$$

The outer diameter of the next intermediate shell (D_i), and subsequently the area moment of inertia (I_i), are determined as:

$$D := 2 \cdot t_i + D \quad D = 78.75 \text{ in}$$

Then the metal moment of inertia is computed as follows:

$$I_i := \frac{1}{4} \cdot \pi \cdot \left[\left(\frac{D}{2} \right)^4 - \left(\frac{D}{2} - t_i \right)^4 \right]$$

$$I_i = 2.286 \times 10^5 \text{ in}^4$$

The total area moment of inertia is obtained by summing the results from the three cylinders.

$$I := I + I_i \quad I = 7.912 \times 10^5 \text{ in}^4$$

The outer diameter of the next intermediate shell (D_i), and subsequently the area moment of inertia (I_i), are determined as:

$$D := 2 \cdot t_i + D \quad D = 81.25 \text{ in}$$

Then the metal moment of inertia is computed as follows:

$$I_i := \frac{1}{4} \cdot \pi \cdot \left[\left(\frac{D}{2} \right)^4 - \left(\frac{D}{2} - t_i \right)^4 \right]$$

$$I_i = 2.514 \times 10^5 \text{ in}^4$$

The total area moment of inertia is obtained by summing the results from the four cylinders.

$$I := I + I_i \quad I = 1.043 \times 10^6 \text{ in}^4$$

The outer diameter of the final intermediate shell (D_i), and subsequently the area moment of inertia (I_i), are determined as:

$$D := 2 \cdot t_i + D \qquad D = 83.75 \text{ in} \qquad D_{\text{outer}} := D$$

Then the metal moment of inertia is computed as follows:

$$I_i := \frac{1}{4} \cdot \pi \cdot \left[\left(\frac{D}{2} \right)^4 - \left(\frac{D}{2} - t_i \right)^4 \right]$$

$$I_i = 2.757 \times 10^5 \text{ in}^4$$

The total area moment of inertia is obtained by summing the results from the five cylinders.

$$I := I + I_i \qquad I = 1.318 \times 10^6 \text{ in}^4$$

We assume the missile strike is at height L above the base of the shells. Then, assuming that the shells behave as a cantilever beam, the bending moment at the base is

$$\text{Moment} := \text{Force} \cdot L$$

The resultant stress in the inner shell can then be determined as:

$$\text{Stress} := \text{Moment} \cdot \frac{D_{\text{inner}} - t}{2 \cdot I} \qquad \text{Stress} = 12565 \text{ psi}$$

The allowable strength for this Level D condition is obtained by using the membrane stress intensity for SA203 at 400 degrees F from Table 3.1.7,

$$S_a := 48200 \text{ psi}$$

Therefore the safety factor for the membrane stress in the helium retention boundary inner shell is

$$\text{SF} := \frac{S_a}{\text{Stress}} \qquad \text{SF} = 3.836$$

This is conservative since the load will spread out into a pressure band at the smaller radius after the strike at the outside perimeter.

The resultant stress in the outermost intermediate shell can then be determined as:

$$\text{Stress} := \text{Moment} \cdot \frac{D_{\text{outer}} - t}{2 \cdot I} \quad \text{Stress} = 14329 \text{ psi}$$

The allowable strength for this Level D condition is obtained by using the membrane stress intensity for SA516 Grade 70 at 400 degrees F from Table 3.1.17,

$$S_a := 39100 \text{ psi}$$

Therefore the safety factor for the membrane stress in the helium retention boundary inner shell is

$$\text{SF} := \frac{S_a}{\text{Stress}} \quad \text{SF} = 2.729$$

This is conservative since the load will spread out into a pressure band at the smaller radius after the strike at the outside perimeter.

b. Second Location: End Strike on Overpack Closure Plate

The effect of a normal missile impact has been studied in Appendix 3.F where a conservative methodology used for shipping cask puncture has been applied assuming that the so called "puncture pin" is replaced by the "impacting missile". It is shown that the bolt stress remains within the required margins. For the analysis of the bolt stress, it is conservatively assumed that the closure plate develops a full clamping moment inboard of the bolt circle. Continuing with this conservatism, the stress at the edge of the outer closure plate section is determined using the conservative estimate of maximum impact force developed above. Stresses at the bolt circle can be determined using the calculated limiting impact load as a uniform pressure applied over an 8" circle at the center of the overpack closure plate. Assuming that the closure plate has a fixed edge at the bolt circle, and using case 17 from Reference [3.G.1] (Table 24, p.433), the stress at the bolt circle is determined as follows:

The closure plate thickness (from BM-1476), $t := 6 \text{ in}$

The applied moment, $M_r := \frac{\text{Force}}{4 \cdot \pi}$

The radial stress at bolt circle (from [3.G.1], p.398), $\sigma_r := 6 \cdot \frac{M_r}{t^2}$

The closure plate thickness is reduced inboard of the bolt circle; bending stress will increase here if the section is assumed clamped. However, this would not be classified as a primary bending stress. The stress intensity in the closure plate under an impact load is required to be less than 3.6 times the material design stress intensity (S_m , from Table 3.3.4) and less than the material ultimate stress.

$$S_m := 21500 \text{ psi}$$

$$3.6 \cdot S_m = 77400 \text{ psi}$$

$$S_u = 64600 \text{ psi}$$

$$\frac{3.6 \cdot S_m}{\sigma_r} = 2.399$$

$$\frac{S_u}{\sigma_r} = 2.002$$

These results indicate that the bolt stress and the minimum plate primary bending stress near the bolt circle remain below allowable strength values for the Level D impact condition investigated.

The stress state near the center of the closure plate is investigated by performing a dynamic analysis to ascertain the maximum load applied to the closure plate as it undergoes a global mode of deflection. It is assumed that the plate deforms like a simply supported plate for this analysis. The initial striking velocity and the striking weight of the missile is known. It is determined from [3.G.2], p.5-55, that 50% of the plate weight acts during the subsequent deformation. It remains to establish an appropriate spring constant to represent the plate elastic behavior in order to establish all of the necessary input for solving the dynamic problem representing the post-strike behavior of the plate-missile system. To determine the spring rate, apply Case 16 of Table 24 in [3.G.1] which is the static solution for a circular plate, simply supported at the edge, and subject to a load applied over a small circular region. Using the notation of [3.G.1] for the case in question, and assuming deformation only inboard of the top flange:

The diameter of contact (from Drawing 1397), $d_{con} := 8 \text{ in}$

The radius of simple support (from Drawing 1397), $a := \frac{72 \text{ in}}{2} \quad a = 36 \text{ in}$

The minimum closure plate thickness (from Drawing 1397), $h := 5.9375 \text{ in}$

The plate stiffness, $D := \frac{E \cdot h^3}{12 \cdot (1 - \nu^2)} \quad D = 5.003 \times 10^8 \text{ lbf} \cdot \text{in}$

The global stiffness of the plate (K) is simply the total load divided by the corresponding displacement at the plate center:

$$K := \frac{16 \cdot \pi \cdot D \cdot (1 + \nu)}{(3 + \nu) \cdot a^2}$$

$$K = 7.644 \times 10^6 \frac{\text{lbf}}{\text{in}}$$

To establish the appropriate structural damping value, a post-impact natural frequency is determined as follows:

The weight of the closure plate (7,984 lbf, from Table 3.3.3) that participates in the analysis,

$$W_{\text{clp}} := 0.5 \cdot 7984 \cdot \text{lbf}$$

$$W_{\text{clp}} = 3992 \text{ lbf}$$

Using the appropriate expression from [3.G.2], the natural frequency can be determined as:

$$f := \frac{1}{2 \cdot \pi} \sqrt{K \cdot \frac{g}{(\text{Weight} + W_{\text{clp}})}}$$

$$f = 132.354 \text{ Hz}$$

It is conservatively assumed that 4% structural damping is conservative for an impact scenario.

$$c := \left(\frac{.04}{\pi \cdot f} \right) \cdot K$$

$$c = 735.352 \text{ lbf} \cdot \frac{\text{sec}}{\text{in}}$$

The dynamics problem is solved using the Working Model program [3.G.3], with the impacting missile striking a target mass which is supported by the spring k to ground. The system is constrained to move vertically, and gravitational forces are included in the solution. Figure 3.G.6 shows a schematic of the model and a trace of the total force in the spring-damper element. The maximum force developed, $W := 1212000 \cdot \text{lbf}$.

The stress near the center of the closure plate is obtained by computing the bending moment due to W. For Level D conditions, only primary bending stress intensities are required to be compared to the allowable strength value. The stress directly under the loaded region, by the very nature of the form of solution ($\ln(a/r)$), should not be considered as a primary stress. Employing St.Venant's Principle of classical elasticity, the primary stress intensity state is considered to be established at the plate cross section at a radius 150% of the load patch radius. Therefore, the bending moment and the stress are computed at:

$$r := 1.5 \cdot \left(\frac{d_{con}}{2} \right)$$

$$r = 6 \text{ in}$$

The tangential moment exceeds the radial moment at this location, so the maximum moment and corresponding stress are:

$$M_t := \frac{W}{16 \cdot \pi} \left[(1 + \nu) \cdot \ln\left(\frac{a}{r}\right) \cdot 4 + (1 - \nu) \cdot \left[4 - \left(\frac{d_{con}}{2 \cdot r}\right)^2 \right] \right]$$

$$M_t = 2.847 \times 10^5 \text{ lbf} \cdot \frac{\text{in}}{\text{in}}$$

$$\sigma_t := 6 \cdot \frac{M_t}{h^2} \quad \sigma_t = 4.845 \times 10^4 \text{ psi}$$

This stress represents a stress intensity and when compared with the allowable strength for combined membrane plus bending for a Level D condition, yields a stress ratio of:

$$\frac{S_u}{\sigma_t} = 1.333$$

c. 8" Missile strike at other surface locations

If the 8" missile impacts at other locations, the global stress state will be less than the values computed here. A strike near a bolt location will impart additional compression on the lid surface near the bolt (since the bolt is protected. This additional compressive load cannot unload the seals. A direct strike on any of the small cover plates the protect various quick disconnects will not damage the quick disconnects since the unbacked diameter of the protective cover plate is less than 4"; therefore, all impact load will be directly onto the surrounding lid surface.

3.G.7 Conclusion

The above calculations demonstrate that the HI-STAR 100 Overpack provides an effective containment barrier for the HI-STAR 100 MPC after being subjected to various missile strikes. No missile strike compromises the integrity of the containment boundary; further, global stress intensities arising from the missile strikes satisfy ASME Code Level D allowable strengths away from the immediate vicinity of the loaded region.

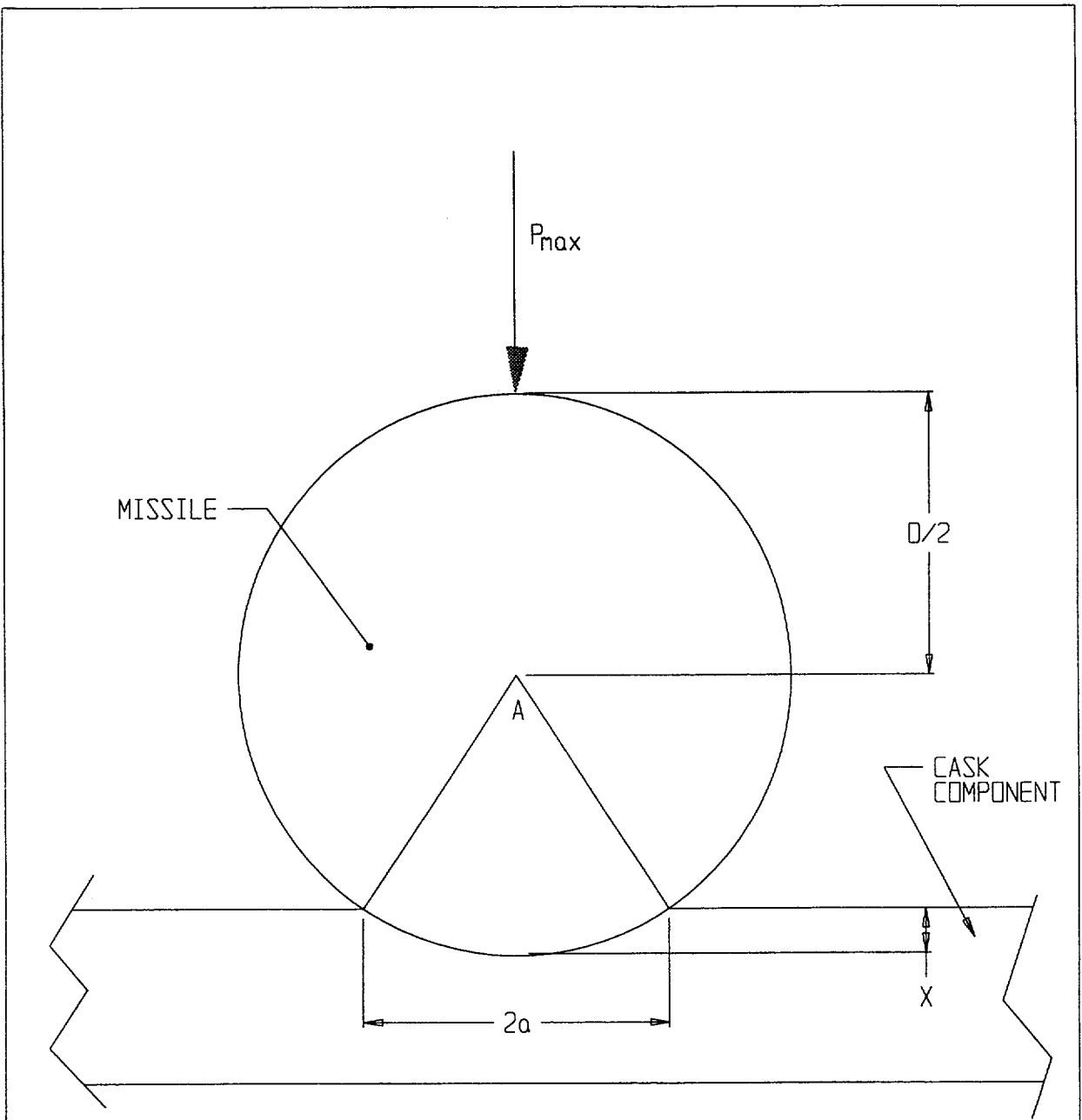


FIGURE 3.G.1; SMALL MISSILE IMPACT

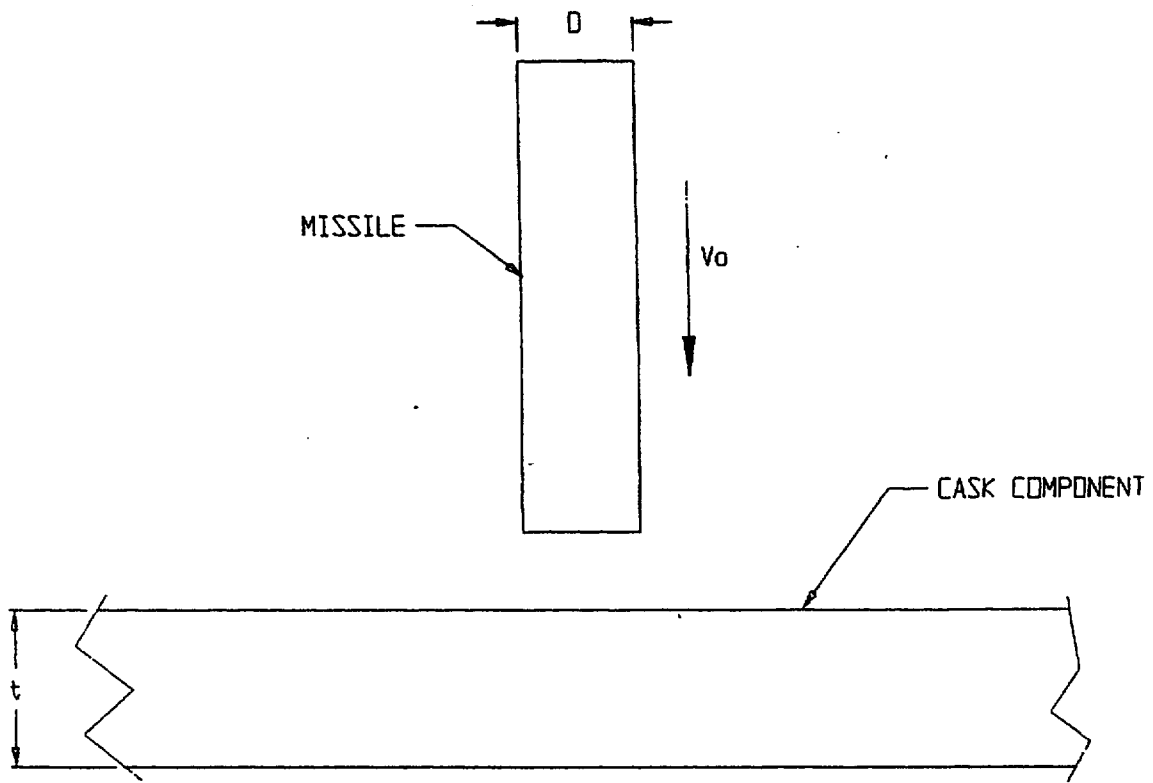


FIGURE 3.G.2; 8-inch DIAMETER MISSILE IMPACT

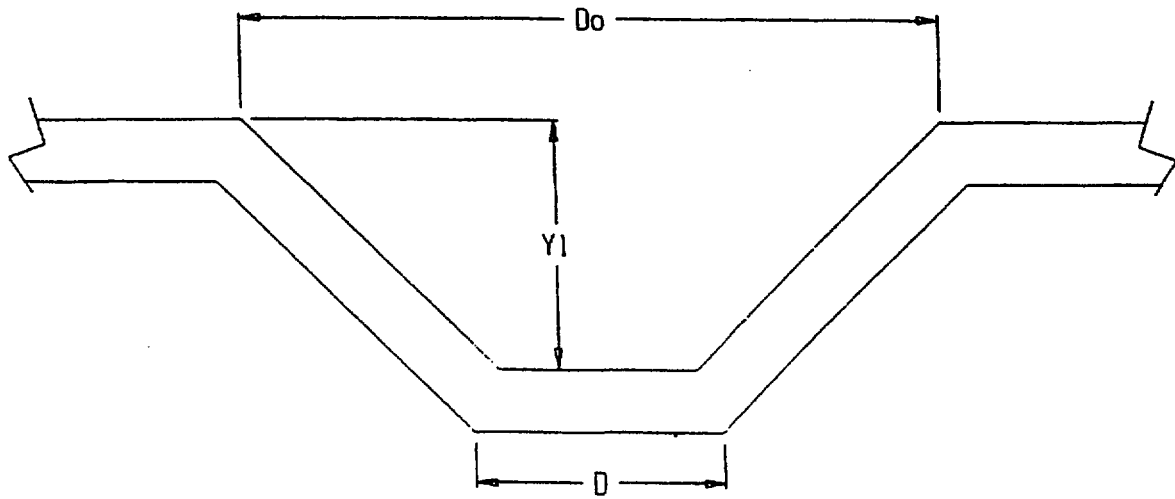


FIGURE 3.G.3; ASSUMED POST-IMPACT DEFORMED SHAPE

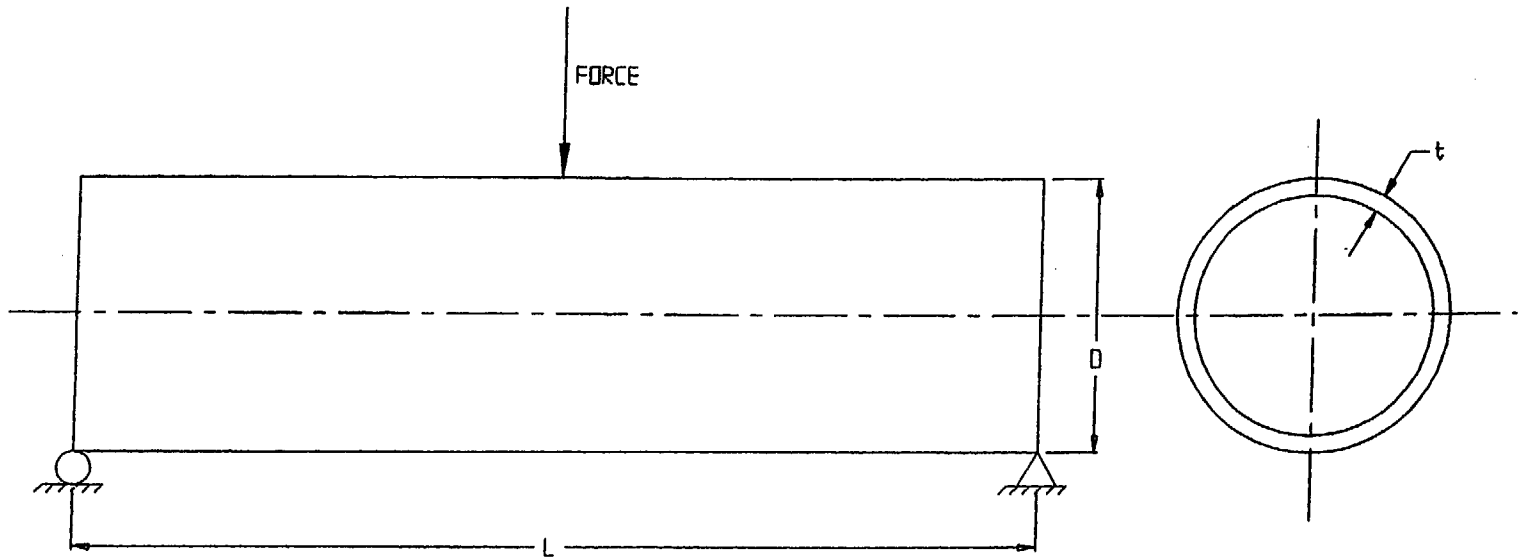


FIGURE 3.G.4; SIDE STRIKE GEOMETRY

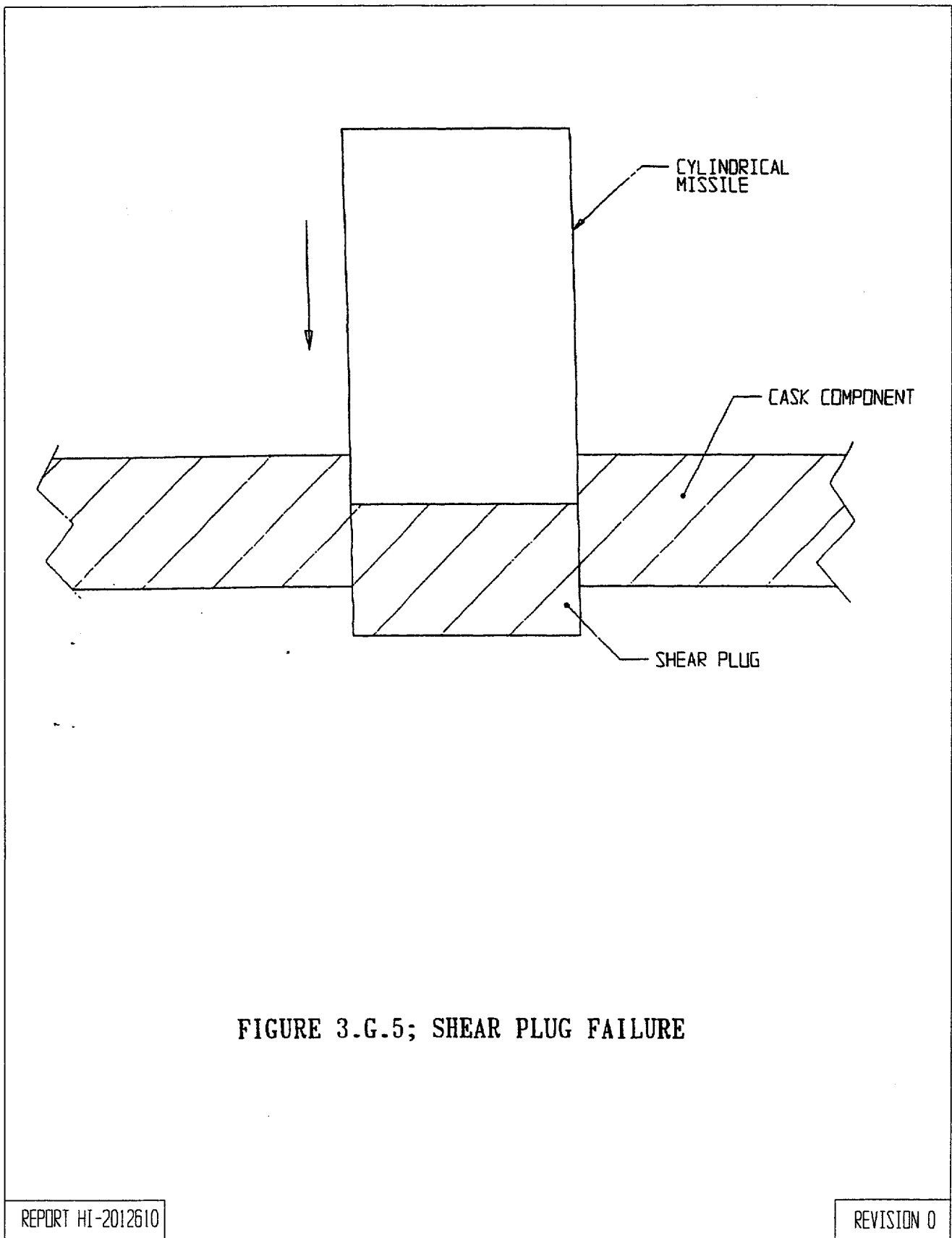


FIGURE 3.G.5; SHEAR PLUG FAILURE

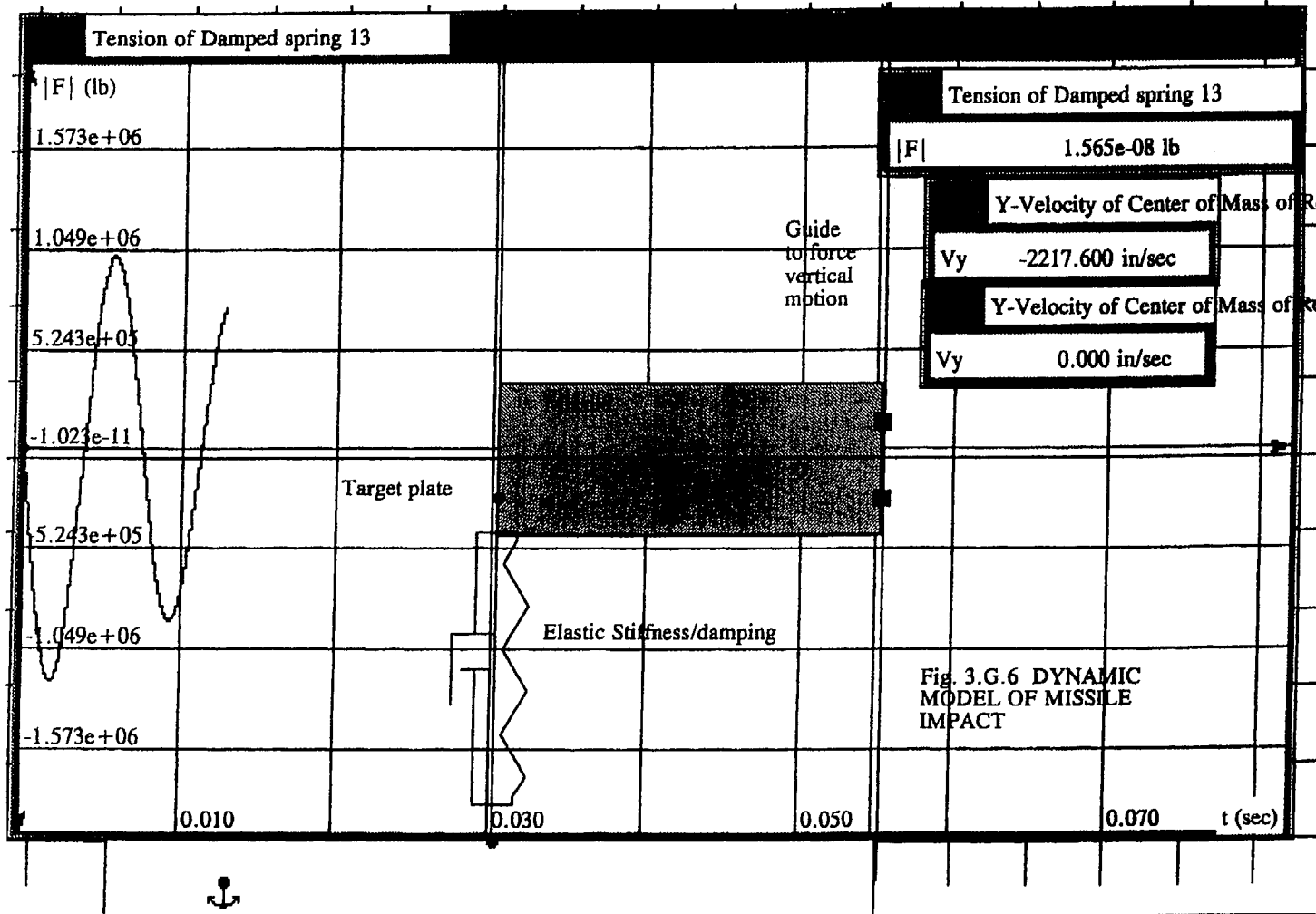


Fig. 3.G.6 DYNAMIC MODEL OF MISSILE IMPACT

FIGURE 3.G.6; DYNAMIC MODEL OF MISSILE IMPACT

APPENDIX 3.H - CODE CASE N-284 STABILITY CALCULATIONS

3.H.1 Scope

The purpose of this analysis is to determine the buckling capacity of the HI-STAR 100 System under the load combinations specified in Section 3. It is shown that both the overpack and the MPC meet the buckling requirements of USNRC Regulatory Guide 7.6 (C.5).

The most probable locations of failure due to buckling are the overpack inner shell, and the the MPC confinement shell. In this appendix, the stability of each shell is evaluated using the criteria set forth in ASME Code Case N-284, Metal Containment Shell Buckling Design Methods, Section III, Division 1, Class MC. In addition to axial loading, the Overpack is subject to a compressive circumferential stress due to external pressure and fabrication. The MPC confinement shell is also subject to a compressive circumferential stress due to a defined external pressure (although the net pressure across the shell will always lead to a tensile circumferential stress).

The symbols used in this appendix, where possible, are consistent with those used in ASME Code. Material properties for Alloy X and SA-203-E are taken from Tables in Section 3.

This appendix was created using the Mathcad (version 6.0+) software package. Mathcad uses the symbol ':=' as an assignment operator, and the equals symbol '=' retrieves values for constants or variables. The logical 'if' construction is also used in this appendix. The 'if' statement format is as follows:

...if(expression,true value,false value)

3.H.2 References

[3.H.1] ASME Boiler & Pressure Vessel Code, Code Case N-284, Metal Containment Shell Buckling Design Methods.

[3.H.2] MATHCAD, V7.0, Mathsoft, 1996.

3.H.3 Load Cases Considered

3.H.3.1 Overpack

Case 1 Fabrication Stress + 1.15G End Loading Due to Handling. This is a Level A event.

Case 2 Fabrication Stress + 60G End Drop. This is a Level D event.

Case 3 Fabrication Stress + Deep Submergence. This is a Level D event

3.H.3.2 MPC

Case 4 Design Internal Pressure + 1.15G End Loading Due to Handling. This is a Level A event.

Case 5 Design Internal Pressure + 60G End Drop. This is a Level D event.

Case 6 Accident External Pressure + 1G Dead Load. This is a Level D event.

Case 7 Design External Pressure + 1G Dead Load. This is a Level A event.

3.H.4 Stability of the Overpack Inner Shell

3.H.4.1 Method - ASME Code Case N-284

Code Case N-284 provides guidelines for determining the stability of metal confinement shells. This method applies to shells with radius-to-thickness ratios of up to 1000 and shell thicknesses greater than 0.25 in..

The buckling characteristics of any confinement shell are governed by the longitudinal membrane, circumferential membrane, and in-plane shear stresses which develop under loading. Only these three stress components are considered in the analysis.

The factors of safety against buckling required by the Code are the following

$FS_{LA} := 2.0$ Level A Service Limit

$FS_{LD} := 1.34$ Level D Service Limit

The analysis method provided by Case N-284 for treatment of confinement shells is further outlined below:

1. The stress components which cause buckling are identified, and each is multiplied by the appropriate factor of safety. As a minimum, the amplified longitudinal and circumferential membrane stresses must be less than the material yield stress, and the in-plane shear stress must be less than 60% of the yield stress. Failure to meet this condition requires a redesign of the system.
2. Capacity reduction factors are calculated in order to account for the difference between classical theory and actual predictions of instability stress.

3. The theoretical elastic buckling stresses are calculated. The stresses correspond to the minimum theoretical values for shells with simple support boundary conditions under uniform stress fields.
4. The amplified stress components are compared to the elastic limits of the material. In the event that any stress exceeds the proportional limit, plasticity reduction factors are introduced in order to account for any material nonlinearities.
5. The interaction equations for elastic and inelastic buckling set forth in the Code Case are used to calculate safety factors.

3.H.4.2 Assumptions

1. Under the postulated end drop, the weight of the overpack (minus the weight of the bottom plate) is supported vertically by the 2.5 in. thick inner shell. This assumption conservatively neglects the intermediate shells and enclosure shell as load bearing members.
2. By employing the method of Case N-284, the inner shell is assumed to be simply supported. The welded base of the inner shell more closely represents a clamped boundary. Therefore, elastic buckling stress limits are actually higher.
3. All material properties are chosen at the overpack design temperature (400 deg. F). The Young's modulus and the yield stress decrease with increasing temperature, therefore, the analysis is conservative.
4. Fabrication stresses are included in the calculation. This is very conservative since fabrication stress is secondary in nature (self-limiting). Therefore, these stress components are relieved as the shell begins to buckle.

3.H.4.3 Input Data

The following is a list of input parameters for the overpack inner shell that are common to each case. The dimensions are obtained from the design drawings in Section 1.5.

$R_i := \frac{68.75}{2} \text{ in}$	Inner radius of shell
$R_o := \frac{73.75}{2} \text{ in}$	Outer radius of shell
$L := 173.625 \text{ in}$	Axial length of shell (conservative)
$t := 2.5 \text{ in}$	Shell thickness

$W := 155000 \cdot \text{lbf} - 10000 \cdot \text{lbf}$	Bounding Weight of overpack (minus the bottom plate)	Table 3.2.4
$g := 386.4 \cdot \frac{\text{in}}{\text{sec}^2}$	Gravitational acceleration	
$E := 26.1 \cdot 10^6 \cdot \text{psi}$	Young's modulus (400° F) SA203-E	Table 3.3.4
$\sigma_y := 34300 \cdot \text{psi}$	Yield strength (400° F) SA203-E	Table 3.3.4

3.H.4.4 Analysis of Overpack Load Cases

3.H.4.4.1 Load Case 1 (Load Case 03 in Table 3.1.5)

The G level for Longitudinal Load is $G := 1.15 \cdot g$

The Factor of Safety for Design is $FS_D := FS_{LA}$ $FS_D = 2$

Stress components

The longitudinal membrane stress is the impact weight supported by the inner shell divided by the cross sectional area of the shell.

$$P := G \cdot \frac{W}{g} \quad P = 1.667 \times 10^5 \text{ lbf}$$

$$A := \pi \cdot (R_o^2 - R_i^2) \quad A = 559.596 \text{ in}^2$$

$$\sigma_\phi := \frac{P}{A} \quad \sigma_\phi = 297.982 \text{ psi} \quad \text{Longitudinal stress}$$

The circumferential membrane stress is equal to the mean fabrication stress (from Appendix 3 I.)

$$\sigma_\theta := 10506 \cdot \text{psi} \quad \text{Bounding circumferential mean stress from fabrication analysis}$$

$$\sigma_{\phi\theta} := 0 \cdot \text{psi} \quad \text{In-plane shear stress}$$

As an initial check, the amplified stress components must meet the allowable limits stated in Section 3.H.4.1 of the appendix.

$$\frac{\sigma_\phi \cdot FS_D}{\sigma_y} = 0.017 < 1.0 \quad \frac{|\sigma_\theta| \cdot FS_D}{\sigma_y} = 0.613 < 1.0 \quad \frac{\sigma_{\phi\theta} \cdot FS_D}{\sigma_y} = 0 < 0.6$$

Capacity reduction factors

The first step towards defining the capacity reduction factors is to calculate the following geometric parameters.

$$R := \frac{R_i + R_o}{2}$$

$$R = 35.625 \text{ in}$$

Mean radius

The unsupported longitudinal and circumferential lengths are

$$l_\phi := L$$

$$l_\phi = 173.625 \text{ in}$$

$$l_\theta := 2 \cdot \pi \cdot R$$

$$l_\theta = 223.838 \text{ in}$$

M_i is a dimensionless factor defined as follows

$$M_\phi := \frac{l_\phi}{(R \cdot t)^{0.5}}$$

$$M_\phi = 18.398$$

$$M_\theta := \frac{l_\theta}{(R \cdot t)^{0.5}}$$

$$M_\theta = 23.719$$

$$M := \text{if}(M_\phi < M_\theta, M_\phi, M_\theta)$$

$$M = 18.398$$

M equals smaller of two values

The radius-to-thickness ratio is $\frac{R}{t} = 14.25$

Next, the capacity reduction factors are computed per Sec. 1511(a), (b), and (c) of Code Case N-284.

Axial Compression

Effect of R/t ($R/t < 600$)

$$\alpha_1 := 1.52 - 0.473 \cdot \log\left(\frac{R}{t}\right)$$

$$\alpha_1 = 0.974$$

$$\alpha_2 := 1.0 \cdot 10^{-5} \cdot \frac{\sigma_y}{\text{psi}} - 0.033$$

$$\alpha_2 = 0.31$$

$$\alpha_{\phi L1} := \text{if}(\alpha_1 < \alpha_2, \alpha_1, \alpha_2)$$

$$\alpha_{\phi L1} = 0.31$$

$\alpha_{\phi L1}$ equals smaller of two values

Effect of Length ($M > 10$)

$$\alpha_{\phi L2} := 0.207$$

$$\alpha_{\phi L} := \text{if}(\alpha_{\phi L1} > \alpha_{\phi L2}, \alpha_{\phi L1}, \alpha_{\phi L2})$$

$$\alpha_{\phi L} = 0.31$$

$\alpha_{\phi L}$ equals larger of two values

Hoop Compression

$$\alpha_{\theta L} := 0.8$$

Shear ($R/t < 250$)

$$\alpha_{\phi eL} := 0.8$$

Theoretical elastic buckling stresses

The basic equations used are given in Sec. 1712.1.1 of Code Case N-284.

Axial Compression ($M_\phi > 1.73$)

$$C_\phi := 0.605$$

$$\sigma_{\phi eL} := C_\phi \cdot \frac{E \cdot t}{R}$$

$$\sigma_{\phi eL} = 1.108 \times 10^6 \text{ psi}$$

External Pressure

No End Pressure ($3.0 < M_\phi < 1.65 R/t$)

$$C_{er} := \frac{0.92}{M_\phi - 1.17}$$

$$C_{er} = 0.053$$

$$\sigma_{reL} := C_{er} \cdot \frac{E \cdot t}{R}$$

$$\sigma_{reL} = 9.781 \times 10^4 \text{ psi}$$

End Pressure Included ($3.5 < M_\phi < 1.65 R/t$)

$$C_{eh} := \frac{0.92}{M_\phi - 0.636}$$

$$C_{eh} = 0.052$$

$$\sigma_{heL} := C_{eh} \cdot \frac{E \cdot t}{R}$$

$$\sigma_{heL} = 9.487 \times 10^4 \text{ psi}$$

Shear ($1.5 < M_\phi < 26$)

$$C_{\phi\phi} := \frac{4.82}{M_\phi^2} \cdot (1 + 0.0239 \cdot M_\phi^3)^{0.5}$$

$$C_{\phi\phi} = 0.174$$

$$\sigma_{\phi\phi eL} := C_{\phi\phi} \cdot \frac{E \cdot t}{R}$$

$$\sigma_{\phi\phi eL} = 3.193 \times 10^5 \text{ psi}$$

Plasticity reduction factors

The plasticity reduction factors are calculated according to the equations provided by Sec. 1610(a), (b), and (c) of the Code Case.

Axial Compression

$$\eta_{\phi} := 1.0$$

$$\frac{\sigma_{\phi} \cdot \text{FS}_D}{\sigma_y} = 0.017 < .55$$

Hoop Compression

$$\eta_{\theta} := 1.0$$

$$\left(\frac{|\sigma_{\theta}| \cdot \text{FS}_D}{\sigma_y} < 0.67 \right)$$

Shear

$$\eta_{\phi\theta} := 1.0$$

$$\left(\frac{\sigma_{\phi\theta} \cdot \text{FS}_D}{\sigma_y} < 0.48 \right)$$

Interaction equations

The interaction equations for local buckling are supplied in Sec. 1713 of Code Case N-284.

Elastic Buckling

$$\sigma_{\phi s} := \frac{\sigma_{\phi} \cdot \text{FS}_D}{\alpha_{\phi L}}$$

$$\sigma_{\phi s} = 1.922 \times 10^3 \text{ psi}$$

$$\sigma_{\theta s} := \frac{\sigma_{\theta} \cdot \text{FS}_D}{\alpha_{\theta L}}$$

$$\sigma_{\theta s} = 2.626 \times 10^4 \text{ psi} < \sigma_{\text{heL}} = 9.487 \times 10^4 \text{ psi}$$

$$\sigma_{\phi\theta s} := \frac{\sigma_{\phi\theta} \cdot \text{FS}_D}{\alpha_{\phi\theta L}}$$

$$\sigma_{\phi\theta s} = 0 \text{ psi}$$

Axial Compression Plus Hoop Compression

$$\frac{\sigma_{\phi s} - 0.5 \cdot \sigma_{\text{heL}}}{\sigma_{\phi eL} - 0.5 \cdot \sigma_{\text{heL}}} + \left(\frac{\sigma_{\theta s}}{\sigma_{\text{heL}}} \right)^2 = 0.034 < 1.0$$

Axial Compression Plus Shear

$$\frac{\sigma_{\phi s}}{\sigma_{\phi eL}} + \left(\frac{\sigma_{\phi\theta s}}{\sigma_{\phi\theta eL}} \right)^2 = 1.735 \times 10^{-3} < 1.0$$

Hoop Compression Plus Shear

$$\frac{|\sigma_{\theta s}|}{\sigma_{reL}} + \left(\frac{\sigma_{\phi \theta s}}{\sigma_{\phi \theta eL}} \right)^2 = 0.269 < 1.0$$

Axial Compression Plus Hoop Compression Plus Shear

The shear constant, K, is computed as follows

$$K := 1 - \left(\frac{\sigma_{\phi \theta s}}{\sigma_{\phi \theta eL}} \right)^2 \quad K = 1$$

As a result of the shear stress equaling zero, the value of K equals one. Therefore, no further interaction checks are required for this combination of stresses.

Inelastic Buckling

$$\sigma_{\phi p} := \frac{\sigma_{\phi s}}{\eta_{\phi}} \quad \sigma_{\phi p} = 1.922 \times 10^3 \text{ psi}$$

$$\sigma_{\theta p} := \frac{\sigma_{\theta s}}{\eta_{\theta}} \quad \sigma_{\theta p} = 2.626 \times 10^4 \text{ psi}$$

$$\sigma_{\phi \theta p} := \frac{\sigma_{\phi \theta s}}{\eta_{\phi \theta}} \quad \sigma_{\phi \theta p} = 0 \text{ psi}$$

Axial Compression Plus Shear

$$\left(\frac{\sigma_{\theta p}}{\sigma_{\theta eL}} \right)^2 + \left(\frac{\sigma_{\phi \theta p}}{\sigma_{\phi \theta eL}} \right)^2 = 3.01 \times 10^{-6} < 1.0$$

Hoop Compression Plus Shear

$$\left(\frac{\sigma_{\phi p}}{\sigma_{\phi eL}} \right)^2 + \left(\frac{\sigma_{\phi \theta p}}{\sigma_{\phi \theta eL}} \right)^2 = 0.072 < 1.0$$

Analysis of the overpack inner shell shows that under this load case, the interaction equations for elastic and inelastic buckling are satisfied (less than 1.0). Therefore, stability of the inner shell is assured.

3.H.4.4.2 Load Case 2 (Load Case 04.a in Table 3.1.5)

The G level for Drop Load is	$G := 60\text{-g}$	Table 3.1.2
The Factor of Safety for Design is	$FS_D := FS_{LD}$	$FS_D = 1.34$

Stress components

The longitudinal membrane stress is the impact weight supported by the inner shell divided by the cross sectional area of the shell.

$$P := G \cdot \frac{W}{g} \quad P = 8.7 \times 10^6 \text{ lbf} \quad A := \pi \cdot (R_o^2 - R_i^2) \quad A = 559.596 \text{ in}^2$$

$$\sigma_\phi := \frac{P}{A} \quad \sigma_\phi = 1.555 \times 10^4 \text{ psi} \quad \text{Longitudinal stress}$$

The circumferential membrane stress is equal to the mean fabrication stress (from Appendix 3 I.)

$$\sigma_\theta := 10506\text{-psi} \quad \text{Bounding circumferential mean stress from fabrication analysis}$$

$$\sigma_{\phi\theta} := 0\text{-psi} \quad \text{In-plane shear stress}$$

The amplified stress components must meet the allowable limits in Section 3.H.4.1 of the appendix.

$$\frac{\sigma_\phi \cdot FS_D}{\sigma_y} = 0.607 < 1.0 \quad \frac{|\sigma_\theta| \cdot FS_D}{\sigma_y} = 0.41 < 1.0 \quad \frac{\sigma_{\phi\theta} \cdot FS_D}{\sigma_y} = 0 < 0.6$$

Capacity reduction factors

The factors are as calculated previously for load case 1 since the geometry is the same

Theoretical elastic buckling stresses

The basic equations used are given in Sec. 1712.1.1 of Code Case N-284 and are functions of geometry; therefore, there is no change from the load case 1 calculation..

Plasticity reduction factors

The plasticity reduction factors are calculated according to the equations provided by Sec. 1610(a), (b), and (c) of the Code Case. Since these are a function of the current load state, they need to be recomputed.

Axial Compression

$$\eta_\phi := \frac{0.18}{\left(1 - \frac{0.45 \cdot \sigma_y}{\sigma_\phi \cdot FS_D}\right)} \quad \eta_\phi = 0.695 \quad \left(0.55 < \frac{\sigma_\phi \cdot FS_D}{\sigma_y} < 0.738\right)$$

Hoop Compression

$$\eta_{\theta} := 1.0$$

$$\left(\frac{|\sigma_{\theta}| \cdot \text{FS}_D}{\sigma_y} < 0.67 \right)$$

Shear

$$\eta_{\phi\theta} := 1.0$$

$$\left(\frac{\sigma_{\phi\theta} \cdot \text{FS}_D}{\sigma_y} < 0.48 \right)$$

Interaction equations

The interaction equations for local buckling are supplied in Sec. 1713 of Code Case N-284.

Elastic Buckling

$$\sigma_{\phi s} := \frac{\sigma_{\phi} \cdot \text{FS}_D}{\alpha_{\phi L}} \quad \sigma_{\phi s} = 6.72 \times 10^4 \text{ psi}$$

$$\sigma_{\theta s} := \frac{\sigma_{\theta} \cdot \text{FS}_D}{\alpha_{\theta L}} \quad \sigma_{\theta s} = 1.76 \times 10^4 \text{ psi} < \sigma_{\text{heL}} = 9.487 \times 10^4 \text{ psi}$$

$$\sigma_{\phi\theta s} := \frac{\sigma_{\phi\theta} \cdot \text{FS}_D}{\alpha_{\phi\theta L}} \quad \sigma_{\phi\theta s} = 0 \text{ psi}$$

Axial Compression Plus Hoop Compression - ($\sigma_{\theta} > 0.5 \sigma_{\phi}$)

$$\frac{\sigma_{\theta s} - 0.5 \cdot \sigma_{\text{heL}}}{\sigma_{\phi eL} - 0.5 \cdot \sigma_{\text{heL}}} + \left(\frac{\sigma_{\theta s}}{\sigma_{\text{heL}}} \right)^2 = 0.053 < 1.0$$

Axial Compression Plus Shear

$$\frac{\sigma_{\phi s}}{\sigma_{\phi eL}} + \left(\frac{\sigma_{\phi\theta s}}{\sigma_{\phi\theta eL}} \right)^2 = 0.061 < 1.0$$

Hoop Compression Plus Shear

$$\frac{|\sigma_{\theta s}|}{\sigma_{\text{reL}}} + \left(\frac{\sigma_{\phi\theta s}}{\sigma_{\phi\theta eL}} \right)^2 = 0.18 < 1.0$$

Axial Compression Plus Hoop Compression Plus Shear

The shear constant, K, is computed as follows

$$K := 1 - \left(\frac{\sigma_{\phi s}}{\sigma_{\phi eL}} \right)^2 \quad K = 1$$

As a result of the shear stress equaling zero, the value of K equals one. Therefore, no further interaction checks are required for this combination of stresses.

Inelastic Buckling

$$\sigma_{\phi p} := \frac{\sigma_{\phi s}}{\eta_{\phi}} \quad \sigma_{\phi p} = 9.674 \times 10^4 \text{ psi}$$

$$\sigma_{\theta p} := \frac{\sigma_{\theta s}}{\eta_{\theta}} \quad \sigma_{\theta p} = 1.76 \times 10^4 \text{ psi}$$

$$\sigma_{\phi \theta p} := \frac{\sigma_{\phi \theta s}}{\eta_{\phi \theta}} \quad \sigma_{\phi \theta p} = 0 \text{ psi}$$

Axial Compression Plus Shear

$$\left(\frac{\sigma_{\phi p}}{\sigma_{\phi eL}} \right)^2 + \left(\frac{\sigma_{\phi \theta p}}{\sigma_{\phi \theta eL}} \right)^2 = 7.621 \times 10^{-3} < 1.0$$

Hoop Compression Plus Shear

$$\left(\frac{\sigma_{\theta p}}{\sigma_{\theta eL}} \right)^2 + \left(\frac{\sigma_{\phi \theta p}}{\sigma_{\phi \theta eL}} \right)^2 = 0.032 < 1.0$$

Analysis of the overpack inner shell shows that under this load case, the interaction equations for elastic and inelastic buckling are satisfied (less than 1.0). Therefore, stability of the inner shell is assured.

3.H.4.4.3 Load Case3 (Load Case 02 in Table 3.1.5)

The external pressure is	$p_{\text{ext}} := 300 \text{ psi}$	Table 2.2.1
The G level for Longitudinal Load is	$G := 1 \cdot g$	
The Factor of Safety for Design is	$FS_D := FS_{LD}$	$FS_D = 1.34$

Stress components

The longitudinal membrane stress is the impact weight supported by the inner shell divided by the cross sectional area of the shell plus the effects of the submergence pressure..

$$P := G \cdot \frac{W}{g} \quad P = 1.45 \times 10^5 \text{ lbf} \quad A := \pi \cdot (R_o^2 - R_i^2) \quad A = 559.596 \text{ in}^2$$
$$\sigma_\phi := \frac{P}{A} + p_{\text{ext}} \frac{R_o^2}{2 \cdot t \cdot R} \quad \sigma_\phi = 2.549 \times 10^3 \text{ psi} \quad \text{Longitudinal stress}$$

The circumferential membrane stress is equal to the mean fabrication stress (from Appendix 3.L) plus the submergence pressure.

$$\sigma_\theta := 10506 \cdot \text{psi} + p_{\text{ext}} \frac{R}{t} \quad \sigma_\theta = 1.478 \times 10^4 \text{ psi}$$

$$\sigma_{\phi\theta} := 0 \cdot \text{psi} \quad \text{In-plane shear stress}$$

As an initial check, the amplified stress components must meet the allowable limits stated in Section 3.H.4.1 of the appendix.

$$\frac{\sigma_\phi \cdot \text{FS}_D}{\sigma_y} = 0.1 < 1.0 \quad \frac{|\sigma_\theta| \cdot \text{FS}_D}{\sigma_y} = 0.577 < 1.0 \quad \frac{\sigma_{\phi\theta} \cdot \text{FS}_D}{\sigma_y} = 0 < 0.6$$

Capacity reduction factors

The factors are as calculated in load case 1 since the geometry is the same

Theoretical elastic buckling stresses

The basic equations used are given in Sec. 1712.1.1 of Code Case N-284 and are functions of geometry; therefore, there is no change from the load case 1 calculation..

Plasticity reduction factors

The plasticity reduction factors are calculated according to the equations provided by Sec. 1610(a), (b), and (c) of the Code Case. Since these are a function of the current load state, they need to be recomputed.

Axial Compression

$$\eta_\phi := 1.0 \quad \frac{\sigma_\phi \cdot \text{FS}_D}{\sigma_y} = 0.1 < .55$$

Hoop Compression

$$\eta_{\theta} := 1.0$$

$$\left(\frac{|\sigma_{\theta}| \cdot \text{FS}_D}{\sigma_y} < 0.67 \right)$$

Shear

$$\eta_{\phi\theta} := 1.0$$

$$\left(\frac{\sigma_{\phi\theta} \cdot \text{FS}_D}{\sigma_y} < 0.48 \right)$$

Interaction equations

The interaction equations for local buckling are supplied in Sec. 1713 of Code Case N-284.

Elastic Buckling

$$\sigma_{\phi s} := \frac{\sigma_{\phi} \cdot \text{FS}_D}{\alpha_{\phi L}}$$

$$\sigma_{\phi s} = 1.102 \times 10^4 \text{ psi}$$

$$\sigma_{\theta s} := \frac{\sigma_{\theta} \cdot \text{FS}_D}{\alpha_{\theta L}}$$

$$\sigma_{\theta s} = 2.476 \times 10^4 \text{ psi} < \sigma_{\text{heL}} = 9.487 \times 10^4 \text{ psi}$$

$$\sigma_{\phi\theta s} := \frac{\sigma_{\phi\theta} \cdot \text{FS}_D}{\alpha_{\phi\theta L}}$$

$$\sigma_{\phi\theta s} = 0 \text{ psi}$$

Axial Compression Plus Hoop Compression ($\sigma_s > 0.5 \sigma_u$)

$$\frac{\sigma_{\phi s} - 0.5 \cdot \sigma_{\text{heL}}}{\sigma_{\phi eL} - 0.5 \cdot \sigma_{\text{heL}}} + \left(\frac{\sigma_{\theta s}}{\sigma_{\text{heL}}} \right)^2 = 0.034 < 1.0$$

Axial Compression Plus Shear

$$\frac{\sigma_{\phi s}}{\sigma_{\phi eL}} + \left(\frac{\sigma_{\phi\theta s}}{\sigma_{\phi\theta eL}} \right)^2 = 9.944 \times 10^{-3} < 1.0$$

Hoop Compression Plus Shear

$$\frac{|\sigma_{\theta s}|}{\sigma_{\text{reL}}} + \left(\frac{\sigma_{\phi\theta s}}{\sigma_{\phi\theta eL}} \right)^2 = 0.253 < 1.0$$

Axial Compression Plus Hoop Compression Plus Shear

The shear constant, K, is computed as follows

$$K := 1 - \left(\frac{\sigma_{\phi\theta s}}{\sigma_{\phi\theta eL}} \right)^2 \quad K = 1$$

As a result of the shear stress equaling zero, the value of K equals one. Therefore, no further interaction checks are required for this combination of stresses.

Inelastic Buckling

$$\sigma_{\phi p} := \frac{\sigma_{\phi s}}{\eta_{\phi}} \quad \sigma_{\phi p} = 1.102 \times 10^4 \text{ psi}$$

$$\sigma_{\theta p} := \frac{\sigma_{\theta s}}{\eta_{\theta}} \quad \sigma_{\theta p} = 2.476 \times 10^4 \text{ psi}$$

$$\sigma_{\phi\theta p} := \frac{\sigma_{\phi\theta s}}{\eta_{\phi\theta}} \quad \sigma_{\phi\theta p} = 0 \text{ psi}$$

Axial Compression Plus Shear

$$\left(\frac{\sigma_{\phi p}}{\sigma_{\phi eL}} \right)^2 + \left(\frac{\sigma_{\phi\theta p}}{\sigma_{\phi\theta eL}} \right)^2 = 9.889 \times 10^{-5} < 1.0$$

Hoop Compression Plus Shear

$$\left(\frac{\sigma_{\theta p}}{\sigma_{\theta eL}} \right)^2 + \left(\frac{\sigma_{\phi\theta p}}{\sigma_{\phi\theta eL}} \right)^2 = 0.064 < 1.0$$

Analysis of the overpack inner shell shows that under this load case, the interaction equations for elastic and inelastic buckling are satisfied (less than 1.0). Therefore, stability of the inner shell is assured.

3.H.5 Stability of the MPC Containment Shell

3.H.5.1 Method - ASME Code Case N-284

A description is provided in the previous section.

3.H.5.2 Assumptions

1. Under the postulated end drop, the appropriate weight of the MPC confinement vessel (minus the weight of the baseplate) is supported vertically by the 0.5 in. thick shell. Lateral pressure is neglected since design internal pressure exceeds design external pressure.
2. By employing the method of Case N-284, the confinement shell is assumed to be simply supported. The welded base of the shell more closely represents a clamped boundary. Therefore, elastic buckling stress limits are actually higher.
3. The channels and other shims welded axially to the inside surface of the confinement shell act as stiffeners. The effect of these axial stiffeners is neglected. This is a conservative and a simplifying assumption.
4. Material properties are chosen at the bounding temperature for normal heat condition or for the fire condition of the MPC confinement boundary. The Young's modulus and the yield stress decrease with increasing temperature, therefore, the analysis is conservative.

3.H.5.3 Input Data

The following is a list of input parameters for the MPC confinement shell. The dimensions are obtained from the design drawings in Section 1.5.

$R_i := \frac{67.375}{2} \text{ in}$	Inner radius of shell
$R_o := \frac{68.375}{2} \text{ in}$	Outer radius of shell
$L := 188 \text{ in}$	Axial length of shell
$t := 0.5 \text{ in}$	Shell thickness
$W := 10400 \text{ lbf} + 5900 \text{ lbf} \dots$ $+ 3700 \text{ lbf}$	Bounding weight of MPC components. This weight excludes the fuel basket and the baseplate but includes the closure lid and all of the basket support structure. The values are obtained from Table 3.2.4.
$g := 386.4 \cdot \frac{\text{in}}{\text{sec}^2}$	Gravitational acceleration

$p_{ext} := 40$ -psi Design basis external pressure Table 2.2.1

Multiplier on external design pressure to define accident pressure $mp := 1.5$

$E := 26.75 \cdot 10^6$ -psi Young's modulus (350 deg. F), Alloy X Table 3.3.1

$\sigma_y := 21600$ -psi Yield strength (350 deg. F) Alloy X Table 3.3.1

3.H.5.4 Analysis

3.H.5.4.1 Load Case 4 (Load Case E2 in Table 3.1.4)

The external pressure is $p_{ext} = 40$ psi

The G level for Longitudinal Load is $G := 1.15 \cdot g$

The Factor of Safety for Design is $FS_D := FS_{LA}$ $FS_D = 2$

Stress components

The longitudinal membrane stress is the impact weight supported by the confinement shell divided by the cross sectional area of the shell.

$$P := G \cdot \frac{W}{g} \qquad P = 2.3 \times 10^4 \text{ lbf}$$

$$A := \pi \cdot (R_o^2 - R_i^2) \qquad A = 106.618 \text{ in}^2$$

$$\sigma_\phi := \frac{P}{A} + p_{ext} \frac{R_i + R_o}{4 \cdot t} \cdot 0.0 \qquad \sigma_\phi = 215.724 \text{ psi} \qquad \text{Longitudinal stress}$$

No lateral pressure is assumed since use of actual internal pressure is not conservative.

$$\sigma_\theta := \frac{p_{ext} \cdot (R_i + R_o) \cdot 0.0}{2 \cdot t} \qquad \sigma_\theta = 0 \text{ psi} \qquad \text{Circumferential stress}$$

The shear stresses on the gross section of the inner shell are equal to zero.

$$\sigma_{\phi\theta} := 0 \cdot \text{psi} \qquad \text{In-plane shear stress}$$

As an initial check, the amplified stress components must meet the allowable limits stated in Section 3.H.4.1 of the appendix.

$$\frac{\sigma_{\phi} \cdot \text{FS}_D}{\sigma_y} = 0.02 < 1.0 \quad \frac{|\sigma_{\theta}| \cdot \text{FS}_D}{\sigma_y} = 0 < 1.0 \quad \frac{\sigma_{\phi\theta} \cdot \text{FS}_D}{\sigma_y} = 0 < 0.6$$

Capacity reduction factors

$$R := \frac{R_i + R_o}{2} \quad R = 33.938 \text{ in} \quad \text{Mean radius}$$

The unsupported longitudinal and circumferential lengths are

$$l_{\phi} := L \quad l_{\theta} = 188 \text{ in}$$

$$l_{\theta} := 2 \cdot \pi \cdot R \quad l_{\theta} = 213.236 \text{ in} \quad \text{Neglect stiffeners}$$

M_i is a dimensionless factor defined as follows

$$M_{\phi} := \frac{l_{\phi}}{(R \cdot t)^{0.5}} \quad M_{\phi} = 45.639$$

$$M_{\theta} := \frac{l_{\theta}}{(R \cdot t)^{0.5}} \quad M_{\theta} = 51.765$$

$$M := \text{if}(M_{\phi} < M_{\theta}, M_{\phi}, M_{\theta}) \quad M = 45.639 \quad M \text{ equals smaller of two values}$$

The radius-to-thickness ratio is

$$\frac{R}{t} = 67.875$$

Next, the capacity reduction factors are computed per Sec. 1511(a), (b), and (c) of Code Case N-284.

Axial Compression

Effect of R/t ($R/t < 600$)

$$\alpha_1 := 1.52 - 0.473 \cdot \log\left(\frac{R}{t}\right) \quad \alpha_1 = 0.654$$

$$\alpha_2 := 1.0 \cdot 10^{-5} \cdot \frac{\sigma_y}{\text{psi}} - 0.033 \quad \alpha_2 = 0.183$$

$$\alpha_{\phi L1} := \text{if}(\alpha_1 < \alpha_2, \alpha_1, \alpha_2) \quad \alpha_{\phi L1} = 0.183 \quad \alpha_{\phi L1} \text{ equals smaller of two values}$$

Effect of Length ($M > 10$)

$$\alpha_{\phi L2} := \frac{0.826}{M^{0.6}}$$

$$\alpha_{\phi L2} = 0.083$$

$$\alpha_{\phi L} := \text{if}(\alpha_{\phi L1} > \alpha_{\phi L2}, \alpha_{\phi L1}, \alpha_{\phi L2})$$

$$\alpha_{\phi L} = 0.183$$

$\alpha_{\phi L}$ equals larger of two values

Hoop Compression

$$\alpha_{\theta L} := 0.8$$

Shear ($R/t < 250$)

$$\alpha_{\phi \theta L} := 0.8$$

Theoretical elastic buckling stresses

The basic equations used are given in Sec. 1712.1.1 of Code Case N-284.

Axial Compression

$$M_{\phi} = 45.639$$

$$C_{\phi} := .605$$

$$C_{\phi} = 0.605$$

$$\sigma_{\phi eL} := C_{\phi} \cdot \frac{E \cdot t}{R}$$

$$\sigma_{\phi eL} = 2.384 \times 10^5 \text{ psi}$$

External Pressure

$$1.65 \cdot \frac{R}{t} = 111.994$$

No End Pressure

$$C_{\theta r} := \frac{.92}{M_{\phi} - 1.17}$$

$$C_{\theta r} = 0.021$$

$$\sigma_{reL} := C_{\theta r} \cdot \frac{E \cdot t}{R}$$

$$\sigma_{reL} = 8.154 \times 10^3 \text{ psi}$$

End Pressure Included

$$C_{\theta r} := \frac{.92}{M_{\phi} - .636}$$

$$C_{\theta h} = 0.052$$

$$\sigma_{heL} := C_{\theta h} \frac{E \cdot t}{R}$$

$$\sigma_{heL} = 2.041 \times 10^4 \text{ psi}$$

Shear ($26 < M_{\phi} < 8.69 R/t$)

$$C_{\phi\theta} := \frac{0.746}{M_{\phi}^{0.5}}$$

$$C_{\phi\theta} = 0.11$$

$$\sigma_{\phi\theta eL} := C_{\phi\theta} \frac{E \cdot t}{R}$$

$$\sigma_{\phi\theta eL} = 4.352 \times 10^4 \text{ psi}$$

Plasticity reduction factors

The plasticity reduction factors are calculated according to the equations provided by Sec. 1610(a), (b), and (c) of the Code Case.

Axial Compression

$$\eta_{\phi} := 1$$

$$\frac{\sigma_{\phi} \cdot FS_D}{\sigma_y} = 0.02$$

Hoop Compression

$$\eta_{\theta} := 1.0$$

$$\left(\frac{|\sigma_{\theta}| \cdot FS_D}{\sigma_y} < 0.67 \right)$$

Shear

$$\eta_{\phi\theta} := 1.0$$

$$\left(\frac{\sigma_{\phi\theta} \cdot FS_D}{\sigma_y} < 0.48 \right)$$

Interaction equations

The interaction equations for local buckling are supplied in Sec. 1713 of Code Case N-284.

Elastic Buckling

$$\sigma_{\phi s} := \frac{\sigma_{\phi} \cdot FS_D}{\alpha_{\phi L}}$$

$$\sigma_{\phi s} = 2.358 \times 10^3 \text{ psi}$$

$$\sigma_{\theta s} := \frac{\sigma_{\theta} \cdot FS_D}{\alpha_{\theta L}}$$

$$\sigma_{\theta s} = 0 \text{ psi}$$

$$< \sigma_{heL} = 2.041 \times 10^4 \text{ psi}$$

$$\sigma_{\phi s} := \frac{\sigma_{\phi s} \cdot \text{FS}_D}{\alpha_{\phi eL}} \quad \sigma_{\phi s} = 0 \text{ psi}$$

Axial Compression Plus Hoop Compression ($\sigma_s > 0.5 \sigma_d$)

$$\frac{\sigma_{\phi s} - 0.5 \cdot \sigma_{heL}}{\sigma_{\phi eL} - 0.5 \cdot \sigma_{heL}} + \left(\frac{\sigma_{es}}{\sigma_{heL}} \right)^2 = -0.034 < 1.0 \quad \text{No need to check this per Code Case.}$$

Axial Compression Plus Shear

$$\frac{\sigma_{\phi s}}{\sigma_{\phi eL}} + \left(\frac{\sigma_{\phi s}}{\sigma_{\phi eL}} \right)^2 = 9.888 \times 10^{-3} < 1.0$$

Hoop Compression Plus Shear

$$\frac{|\sigma_{es}|}{\sigma_{reL}} + \left(\frac{\sigma_{\phi s}}{\sigma_{\phi eL}} \right)^2 = 0 < 1.0$$

Axial Compression Plus Hoop Compression Plus Shear

The shear constant, K, is computed as follows

$$K := 1 - \left(\frac{\sigma_{\phi s}}{\sigma_{\phi eL}} \right)^2 \quad K = 1$$

As a result of the shear stress equaling zero, the value of K equals one. Therefore, no further interaction checks are required for this combination of stresses.

Inelastic Buckling

$$\sigma_{\phi p} := \frac{\sigma_{es}}{\eta_{\phi}} \quad \sigma_{\phi p} = 2.358 \times 10^3 \text{ psi}$$

$$\sigma_{\theta p} := \frac{\sigma_{es}}{\eta_{\theta}} \quad \sigma_{\theta p} = 0 \text{ psi}$$

$$\sigma_{\phi \theta p} := \frac{\sigma_{\phi s}}{\eta_{\phi \theta}} \quad \sigma_{\phi \theta p} = 0 \text{ psi}$$

Axial Compression Plus Shear

$$\left(\frac{\sigma_{\phi p}}{\sigma_{\phi eL}}\right)^2 + \left(\frac{\sigma_{\phi \theta p}}{\sigma_{\phi \theta eL}}\right)^2 = 9.777 \times 10^{-5} < 1.0$$

Hoop Compression Plus Shear

$$\left(\frac{\sigma_{\theta p}}{\sigma_{\theta eL}}\right)^2 + \left(\frac{\sigma_{\phi \theta p}}{\sigma_{\phi \theta eL}}\right)^2 = 0 < 1.0$$

Conclusion

Analysis of the MPC confinement shell shows that the interaction equations for elastic and inelastic buckling are satisfied (less than 1.0). Therefore, stability of the inner shell is assured for load case 4.

3.H.5.4.2 Load Case 5 (Load Case E3.a in Table 3.1.4)

The external pressure is $p_{ext} = 40$ psi
The G level for Drop Load is $G := 60$ g
The Factor of Safety for Design is $FS_D := FS_{LD} \quad FS_D = 1.34$

Stress components

The longitudinal membrane stress is the impact weight supported by the confinement shell divided by the cross sectional area of the shell.

$$P := G \cdot \frac{W}{g} \quad P = 1.2 \times 10^6 \text{ lbf} \quad A := \pi \cdot (R_o^2 - R_i^2) \quad A = 106.618 \text{ in}^2$$

$$\sigma_{\phi} := \frac{P}{A} + p_{ext} \cdot \frac{R_i + R_o}{4 \cdot t} \cdot 0.0 \quad \sigma_{\phi} = 1.126 \times 10^4 \text{ psi} \quad \text{Longitudinal stress}$$

We neglect stresses due to pressure since the normal operation will have tensile circumferential stress in the shell.

$$\sigma_{\theta} := \frac{p_{ext} \cdot (R_i + R_o) \cdot 0.0}{2 \cdot t} \quad \sigma_{\theta} = 0 \text{ psi} \quad \text{Circumferential stress}$$

The shear stresses on the gross section of the inner shell are equal to zero.

$$\sigma_{\phi \theta} := 0 \text{ psi} \quad \text{In-plane shear stress}$$

As an initial check, the amplified stress components must meet the allowable limits stated in Section 3.H.4.1 of the appendix.

$$\frac{\sigma_{\phi} \cdot \text{FS}_D}{\sigma_y} = 0.698 < 1.0 \quad \frac{|\sigma_{\theta}| \cdot \text{FS}_D}{\sigma_y} = 0 < 1.0 \quad \frac{\sigma_{\phi\theta} \cdot \text{FS}_D}{\sigma_y} = 0 < 0.6$$

Plasticity reduction factors

The plasticity reduction factors are calculated according to the equations provided by Sec. 1610(a), (b), and (c) of the Code Case.

Axial Compression

$$\eta_{\phi} := 1.31 - 1.15 \cdot \sigma_{\phi} \cdot \frac{\text{FS}_D}{\sigma_y} \quad \eta_{\phi} = 0.507$$

Hoop Compression

$$\eta_{\theta} := 1.0 \quad \left(\frac{|\sigma_{\theta}| \cdot \text{FS}_D}{\sigma_y} < 0.67 \right)$$

Shear

$$\eta_{\phi\theta} := 1.0 \quad \left(\frac{\sigma_{\phi\theta} \cdot \text{FS}_D}{\sigma_y} < 0.48 \right)$$

Interaction equations

The interaction equations for local buckling are supplied in Sec. 1713 of Code Case N-284.

Elastic Buckling

$$\sigma_{\phi s} := \frac{\sigma_{\phi} \cdot \text{FS}_D}{\alpha_{\phi L}} \quad \sigma_{\phi s} = 8.241 \times 10^4 \text{ psi}$$

$$\sigma_{\theta s} := \frac{\sigma_{\theta} \cdot \text{FS}_D}{\alpha_{\theta L}} \quad \sigma_{\theta s} = 0 \text{ psi} < \sigma_{\theta eL} = 2.041 \times 10^4 \text{ psi}$$

$$\sigma_{\phi\theta s} := \frac{\sigma_{\phi\theta} \cdot \text{FS}_D}{\alpha_{\phi\theta L}} \quad \sigma_{\phi\theta s} = 0 \text{ psi}$$

Axial Compression Plus Hoop Compression ($\sigma_{\phi} > 0.5 \sigma_u$)

$$\frac{\sigma_{\phi s} - 0.5 \cdot \sigma_{heL}}{\sigma_{\phi eL} - 0.5 \cdot \sigma_{heL}} + \left(\frac{\sigma_{\phi s}}{\sigma_{heL}} \right)^2 = 0.316 < 1.0$$

Axial Compression Plus Shear

$$\frac{\sigma_{\phi s}}{\sigma_{\phi eL}} + \left(\frac{\sigma_{\phi s}}{\sigma_{\phi eL}} \right)^2 = 0.346 < 1.0$$

Hoop Compression Plus Shear

$$\frac{|\sigma_{\theta s}|}{\sigma_{reL}} + \left(\frac{\sigma_{\phi s}}{\sigma_{\phi eL}} \right)^2 = 0 < 1.0$$

Axial Compression Plus Hoop Compression Plus Shear

The shear constant, K, is computed as follows

$$K := 1 - \left(\frac{\sigma_{\phi s}}{\sigma_{\phi eL}} \right)^2 \quad K = 1$$

As a result of the shear stress equaling zero, the value of K equals one. Therefore, no further interaction checks are required for this combination of stresses.

Inelastic Buckling

$$\sigma_{\phi p} := \frac{\sigma_{\phi s}}{\eta_{\phi}} \quad \sigma_{\phi p} = 1.625 \times 10^5 \text{ psi} \quad \sigma_{\phi eL} = 2.384 \times 10^5 \text{ psi}$$

$$\sigma_{\theta p} := \frac{\sigma_{\theta s}}{\eta_{\theta}} \quad \sigma_{\theta p} = 0 \text{ psi}$$

$$\sigma_{\phi \theta p} := \frac{\sigma_{\phi \theta s}}{\eta_{\phi \theta}} \quad \sigma_{\phi \theta p} = 0 \text{ psi}$$

Axial Compression Plus Shear

$$\left(\frac{\sigma_{\phi p}}{\sigma_{\phi eL}} \right)^2 + \left(\frac{\sigma_{\phi \theta p}}{\sigma_{\phi \theta eL}} \right)^2 = 0.465 < 1.0$$

Hoop Compression Plus Shear

$$\left(\frac{\sigma_{\theta p}}{\sigma_{\theta eL}} \right)^2 + \left(\frac{\sigma_{\phi \theta p}}{\sigma_{\phi \theta eL}} \right)^2 = 0 < 1.0$$

Conclusion

Analysis of the MPC confinement shell shows that the interaction equations for elastic and inelastic buckling are satisfied (less than 1.0). Therefore, stability of the inner shell is assured for load case 5.

3.H.5.4.3 Load Case 6 (Load Case E5 in Table 3.1.4)

The external pressure is $P_{ext} := mp \cdot P_{ext}$ $P_{ext} = 60$ psi

The G level for Longitudinal Load is $G := 1 \cdot g$

The Factor of Safety for Design is $FS_D := FS_{LD}$ $FS_D = 1.34$

The Young's modulus and the yield strength are evaluated at (400°F), which bounds the MPC shell temperature during a fire accident (see Subsection 3.4.4.2.2).

$E := 26.5 \cdot 10^6$ psi Young's modulus (400 deg. F), Alloy X Table 3.3.1

$\sigma_y := 20700$ psi Yield strength (400 deg. F) Alloy X Table 3.3.1

Stress components

The longitudinal membrane stress is the impact weight supported by the confinement shell divided by the cross sectional area of the shell.

$$P := G \cdot \frac{W}{g} \quad P = 2 \times 10^4 \text{ lbf}$$

$$A := \pi \cdot (R_o^2 - R_i^2) \quad A = 106.618 \text{ in}^2$$

$$\sigma_{\phi} := \frac{P}{A} + P_{ext} \frac{R_i + R_o}{4 \cdot t} \quad \sigma_{\phi} = 2.224 \times 10^3 \text{ psi} \quad \text{Longitudinal stress}$$

A circumferential membrane stress develops in the MPC confinement shell due to external pressure.

$$\sigma_{\theta} := \frac{p_{ext}(R_i + R_o)}{2 \cdot t} \quad \sigma_{\theta} = 4.073 \times 10^3 \text{ psi} \quad \text{Circumferential stress}$$

The shear stresses on the gross section of the inner shell are equal to zero.

$$\sigma_{\phi\theta} := 0 \text{ psi} \quad \text{In-plane shear stress}$$

As an initial check, the amplified stress components must meet the allowable limits stated in Section 3.H.4.1 of the appendix.

$$\frac{\sigma_{\phi} \cdot FSD}{\sigma_y} = 0.144 < 1.0 \quad \frac{|\sigma_{\theta}| \cdot FSD}{\sigma_y} = 0.264 < 1.0 \quad \frac{\sigma_{\phi\theta} \cdot FSD}{\sigma_y} = 0 < 0.6$$

Capacity reduction factors

$$R := \frac{R_i + R_o}{2} \quad R = 33.938 \text{ in} \quad \text{Mean radius}$$

The unsupported longitudinal and circumferential lengths are

$$l_{\phi} := L \quad l_{\phi} = 188 \text{ in}$$

$$l_{\theta} := 2 \cdot \pi \cdot R \quad l_{\theta} = 213.236 \text{ in} \quad \text{No credit for stiffeners}$$

M_i is a dimensionless factor defined as follows

$$M_{\phi} := \frac{l_{\phi}}{(R \cdot t)^{0.5}} \quad M_{\phi} = 45.639$$

$$M_{\theta} := \frac{l_{\theta}}{(R \cdot t)^{0.5}} \quad M_{\theta} = 51.765$$

$$M := \text{if}(M_{\phi} < M_{\theta}, M_{\phi}, M_{\theta}) \quad M = 45.639 \quad \text{M equals smaller of two values}$$

The radius-to-thickness ratio is

$$\frac{R}{t} = 67.875$$

Next, the capacity reduction factors are computed per Sec. 1511(a), (b), and (c) of Code Case N-284.

Axial Compression

Effect of R/t ($R/t < 600$)

$$\alpha_1 := 1.52 - 0.473 \cdot \log\left(\frac{R}{t}\right)$$

$$\alpha_1 = 0.654$$

$$\alpha_2 := 1.0 \cdot 10^{-5} \cdot \frac{\sigma_y}{\text{psi}} - 0.033$$

$$\alpha_2 = 0.174$$

$$\alpha_{\phi L1} := \text{if}(\alpha_1 < \alpha_2, \alpha_1, \alpha_2)$$

$$\alpha_{\phi L1} = 0.174$$

$\alpha_{\phi L1}$ equals smaller of two value:

Effect of Length ($M > 10$)

$$\alpha_{\phi L2} := .207$$

$$\alpha_{\phi L2} = 0.207$$

$$\alpha_{\phi L} := \text{if}(\alpha_{\phi L1} > \alpha_{\phi L2}, \alpha_{\phi L1}, \alpha_{\phi L2})$$

$$\alpha_{\phi L} = 0.207$$

$\alpha_{\phi L}$ equals larger of two values

Hoop Compression

$$\alpha_{\theta L} := 0.8$$

Shear ($R/t < 250$)

$$\alpha_{\phi \theta L} := 0.8$$

Theoretical elastic buckling stresses

The basic equations used are given in Sec. 1712.1.1 of Code Case N-284.

Axial Compression

$$M_{\phi} = 45.639$$

$$C_{\phi} := .605$$

$$C_{\phi} = 0.605$$

$$\sigma_{\phi eL} := C_{\phi} \cdot \frac{E \cdot t}{R}$$

$$\sigma_{\phi eL} = 2.362 \times 10^5 \text{ psi}$$

External Pressure

$$1.65 \cdot \frac{R}{t} = 111.994$$

No End Pressure

$$C_{er} := \frac{.92}{M_\phi - 1.17}$$

$$C_{er} = 0.021$$

$$\sigma_{reL} := C_{er} \cdot \frac{E \cdot t}{R}$$

$$\sigma_{reL} = 8.077 \times 10^3 \text{ psi}$$

End Pressure Included

$$C_{er} := \frac{.92}{M_\phi - .636}$$

$$C_{er} = 0.052$$

$$\sigma_{heL} := C_{er} \cdot \frac{E \cdot t}{R}$$

$$\sigma_{heL} = 2.022 \times 10^4 \text{ psi}$$

Shear (26 < M_φ < 8.69 R/t)

$$C_{\phi\theta} := \frac{0.746}{M_\phi^{0.5}}$$

$$C_{\phi\theta} = 0.11$$

$$\sigma_{\phi\theta eL} := C_{\phi\theta} \cdot \frac{E \cdot t}{R}$$

$$\sigma_{\phi\theta eL} = 4.311 \times 10^4 \text{ psi}$$

Plasticity reduction factors

The plasticity reduction factors are calculated according to the equations provided by Sec. 1610(a), (b), and (c) of the Code Case.

Axial Compression

$$\eta_\phi := 1$$

$$\frac{\sigma_\phi \cdot FS_D}{\sigma_y} = 0.144 < .55$$

Hoop Compression

$$\eta_\theta := 1.0$$

$$\left(\frac{|\sigma_\theta| \cdot FS_D}{\sigma_y} < 0.67 \right)$$

Shear

$$\eta_{\phi\theta} := 1.0$$

$$\left(\frac{\sigma_{\phi\theta} \cdot \text{FS}_D}{\sigma_y} < 0.48 \right)$$

Interaction equations

The interaction equations for local buckling are supplied in Sec. 1713 of Code Case N-284.

Elastic Buckling

$$\sigma_{\phi s} := \frac{\sigma_{\phi} \cdot \text{FS}_D}{\alpha_{\phi L}} \quad \sigma_{\phi s} = 1.44 \times 10^4 \text{ psi}$$

$$\sigma_{\theta s} := \frac{\sigma_{\theta} \cdot \text{FS}_D}{\alpha_{\theta L}} \quad \sigma_{\theta s} = 6.821 \times 10^3 \text{ psi} < \sigma_{\theta eL} = 2.022 \times 10^4 \text{ psi}$$

$$\sigma_{\phi\theta s} := \frac{\sigma_{\phi\theta} \cdot \text{FS}_D}{\alpha_{\phi\theta L}} \quad \sigma_{\phi\theta s} = 0 \text{ psi}$$

Axial Compression Plus Hoop Compression ($\sigma_{\phi} > 0.5 \sigma_{\theta}$)

$$\frac{\sigma_{\phi s} - 0.5 \cdot \sigma_{\theta eL}}{\sigma_{\phi eL} - 0.5 \cdot \sigma_{\theta eL}} + \left(\frac{\sigma_{\theta s}}{\sigma_{\theta eL}} \right)^2 = 0.133 < 1.0$$

Axial Compression Plus Shear

$$\frac{\sigma_{\phi s}}{\sigma_{\phi eL}} + \left(\frac{\sigma_{\phi\theta s}}{\sigma_{\phi\theta eL}} \right)^2 = 0.061 < 1.0$$

Hoop Compression Plus Shear

$$\frac{|\sigma_{\theta s}|}{\sigma_{\theta eL}} + \left(\frac{\sigma_{\phi\theta s}}{\sigma_{\phi\theta eL}} \right)^2 = 0.845 < 1.0$$

Axial Compression Plus Hoop Compression Plus Shear

The shear constant, K, is computed as follows

$$K := 1 - \left(\frac{\sigma_{\phi s}}{\sigma_{\phi eL}} \right)^2 \quad K = 1$$

As a result of the shear stress equaling zero, the value of K equals one. Therefore, no further interaction checks are required for this combination of stresses.

Inelastic Buckling

$$\sigma_{\phi p} := \frac{\sigma_{\phi s}}{\eta_{\phi}} \quad \sigma_{\phi p} = 1.44 \times 10^4 \text{ psi} \quad \sigma_{\phi eL} = 2.362 \times 10^5 \text{ psi}$$

$$\sigma_{\theta p} := \frac{\sigma_{\theta s}}{\eta_{\theta}} \quad \sigma_{\theta p} = 6.821 \times 10^3 \text{ psi}$$

$$\sigma_{\phi \theta p} := \frac{\sigma_{\phi \theta s}}{\eta_{\phi \theta}} \quad \sigma_{\phi \theta p} = 0 \text{ psi}$$

Axial Compression Plus Shear

$$\left(\frac{\sigma_{\phi p}}{\sigma_{\phi eL}} \right)^2 + \left(\frac{\sigma_{\phi \theta p}}{\sigma_{\phi \theta eL}} \right)^2 = 3.714 \times 10^{-3} < 1.0$$

Hoop Compression Plus Shear

$$\left(\frac{\sigma_{\theta p}}{\sigma_{\theta eL}} \right)^2 + \left(\frac{\sigma_{\phi \theta p}}{\sigma_{\phi \theta eL}} \right)^2 = 0.713 < 1.0$$

Conclusion

Analysis of the MPC confinement shell shows that the interaction equations for elastic and inelastic buckling are satisfied (less than 1.0). Therefore, stability of the inner shell is assured for load case 6.

3.H.5.4.4 Load Case 7 (Load Case E1.b in Table 3.1.4)

The external pressure is $p_{\text{ext}} := 40 \cdot \text{psi}$ $p_{\text{ext}} = 40 \text{ psi}$

The G level for Longitudinal Load is $G := 1 \cdot g$

The Factor of Safety for Design is $FS_D := FS_{LA}$ $FS_D = 2$

The Young's modulus and the yield strength are evaluated at (300°F), which bounds all MPC temperatures during the normal heat condition.

$E := 26.75 \cdot 10^6 \cdot \text{psi}$ Young's modulus (350 deg. F), Alloy X Table 3.3.1

$\sigma_y := 21600 \cdot \text{psi}$ Yield strength (350 deg. F) Alloy X Table 3.3.1

Stress components

The longitudinal membrane stress is the impact weight supported by the confinement shell divided by the cross sectional area of the shell.

$$P := G \cdot \frac{W}{g} \quad P = 2 \times 10^4 \text{ lbf}$$

$$A := \pi \cdot (R_o^2 - R_i^2) \quad A = 106.618 \text{ in}^2$$

$$\sigma_\phi := \frac{P}{A} + p_{\text{ext}} \frac{R_i + R_o}{4 \cdot t} \quad \sigma_\phi = 1.545 \times 10^3 \text{ psi} \quad \text{Longitudinal stress}$$

A circumferential membrane stress develops in the MPC confinement shell due to external pressure.

$$\sigma_\theta := \frac{p_{\text{ext}} \cdot (R_i + R_o)}{2 \cdot t} \quad \sigma_\theta = 2.715 \times 10^3 \text{ psi} \quad \text{Circumferential stress}$$

The shear stresses on the gross section of the inner shell are equal to zero.

$$\sigma_{\phi\theta} := 0 \cdot \text{psi} \quad \text{In-plane shear stress}$$

As an initial check, the amplified stress components must meet the allowable limits stated in Section 3.H.4.1 of the appendix.

$$\frac{\sigma_\phi \cdot FS_D}{\sigma_y} = 0.143 < 1.0 \quad \frac{|\sigma_\theta| \cdot FS_D}{\sigma_y} = 0.251 < 1.0 \quad \frac{\sigma_{\phi\theta} \cdot FS_D}{\sigma_y} = 0 < 0.6$$

Capacity reduction factors

$$R := \frac{R_i + R_o}{2} \quad R = 33.938 \text{ in} \quad \text{Mean radius}$$

The unsupported longitudinal and circumferential lengths are

$$l_\phi := L \quad l_\phi = 188 \text{ in}$$

$$l_\theta := 2 \cdot \pi \cdot R \quad l_\theta = 213.236 \text{ in} \quad \text{No credit for stiffeners}$$

M_i is a dimensionless factor defined as follows

$$M_\phi := \frac{l_\phi}{(R \cdot t)^{0.5}} \quad M_\phi = 45.639$$

$$M_\theta := \frac{l_\theta}{(R \cdot t)^{0.5}} \quad M_\theta = 51.765$$

$$M := \text{if}(M_\phi < M_\theta, M_\phi, M_\theta) \quad M = 45.639 \quad M \text{ equals smaller of two values}$$

The radius-to-thickness ratio is

$$\frac{R}{t} = 67.875$$

Next, the capacity reduction factors are computed per Sec. 1511(a), (b), and (c) of Code Case N-284.

Axial Compression

Effect of R/t ($R/t < 600$)

$$\alpha_1 := 1.52 - 0.473 \cdot \log\left(\frac{R}{t}\right) \quad \alpha_1 = 0.654$$

$$\alpha_2 := 1.0 \cdot 10^{-5} \cdot \frac{\sigma_y}{\text{psi}} - 0.033 \quad \alpha_2 = 0.183$$

$$\alpha_{\phi L1} := \text{if}(\alpha_1 < \alpha_2, \alpha_1, \alpha_2) \quad \alpha_{\phi L1} = 0.183 \quad \alpha_{\phi L1} \text{ equals smaller of two values}$$

Effect of Length ($M > 10$)

$$\alpha_{\phi L2} := .207 \quad \alpha_{\phi L2} = 0.207$$

$$\alpha_{\phi L} := \text{if}(\alpha_{\phi L1} > \alpha_{\phi L2}, \alpha_{\phi L1}, \alpha_{\phi L2})$$

$$\alpha_{\phi L} = 0.207$$

$\alpha_{\phi L}$ equals larger of two values

Hoop Compression

$$\alpha_{\theta L} := 0.8$$

Shear (R/t < 250)

$$\alpha_{\phi \theta L} := 0.8$$

Theoretical elastic buckling stresses

The basic equations used are given in Sec. 1712.1.1 of Code Case N-284.

Axial Compression

$$M_{\phi} = 45.639$$

$$C_{\phi} := .605$$

$$C_{\phi} = 0.605$$

$$\sigma_{\phi eL} := C_{\phi} \cdot \frac{E \cdot t}{R}$$

$$\sigma_{\phi eL} = 2.384 \times 10^5 \text{ psi}$$

External Pressure

$$1.65 \cdot \frac{R}{t} = 111.994$$

No End Pressure

$$C_{\theta r} := \frac{.92}{M_{\phi} - 1.17}$$

$$C_{\theta r} = 0.021$$

$$\sigma_{reL} := C_{\theta r} \cdot \frac{E \cdot t}{R}$$

$$\sigma_{reL} = 8.154 \times 10^3 \text{ psi}$$

End Pressure Included

$$C_{\theta h} := \frac{.92}{M_{\phi} - .636}$$

$$C_{\theta h} = 0.052$$

$$\sigma_{heL} := C_{\theta h} \cdot \frac{E \cdot t}{R}$$

$$\sigma_{heL} = 2.041 \times 10^4 \text{ psi}$$

Shear ($26 < M_s < 8.69 R/t$)

$$C_{\phi\theta} := \frac{0.746}{M_s^{0.5}}$$

$$C_{\phi\theta} = 0.11$$

$$\sigma_{\phi\theta eL} := C_{\phi\theta} \cdot \frac{E \cdot t}{R}$$

$$\sigma_{\phi\theta eL} = 4.352 \times 10^4 \text{ psi}$$

Plasticity reduction factors

The plasticity reduction factors are calculated according to the equations provided by Sec. 1610(a), (b), and (c) of the Code Case.

Axial Compression

$$\eta_{\phi} := 1$$

$$\frac{\sigma_{\phi} \cdot FS_D}{\sigma_y} = 0.143 < .55$$

Hoop Compression

$$\eta_{\theta} := 1.0$$

$$\left(\frac{|\sigma_{\theta}| \cdot FS_D}{\sigma_y} < 0.67 \right)$$

Shear

$$\eta_{\phi\theta} := 1.0$$

$$\left(\frac{\sigma_{\phi\theta} \cdot FS_D}{\sigma_y} < 0.48 \right)$$

Interaction equations

The interaction equations for local buckling are supplied in Sec. 1713 of Code Case N-284.

Elastic Buckling

$$\sigma_{\phi s} := \frac{\sigma_{\phi} \cdot FS_D}{\alpha_{\phi L}}$$

$$\sigma_{\phi s} = 1.493 \times 10^4 \text{ psi}$$

$$\sigma_{\theta s} := \frac{\sigma_{\theta} \cdot FS_D}{\alpha_{\theta L}}$$

$$\sigma_{\theta s} = 6.787 \times 10^3 \text{ psi} < \sigma_{\theta eL} = 2.041 \times 10^4 \text{ psi}$$

$$\sigma_{\phi\theta s} := \frac{\sigma_{\phi\theta} \cdot FS_D}{\alpha_{\phi\theta L}}$$

$$\sigma_{\phi\theta s} = 0 \text{ psi}$$

Axial Compression Plus Hoop Compression ($\sigma_{\phi} > 0.5 \sigma_{\theta}$)

$$\frac{\sigma_{\phi s} - 0.5 \cdot \sigma_{\theta eL}}{\sigma_{\phi eL} - 0.5 \cdot \sigma_{\theta eL}} + \left(\frac{\sigma_{\phi s}}{\sigma_{\theta eL}} \right)^2 = 0.131 < 1.0$$

Axial Compression Plus Shear

$$\frac{\sigma_{\phi s}}{\sigma_{\phi eL}} + \left(\frac{\sigma_{\phi s}}{\sigma_{\phi eL}} \right)^2 = 0.063 < 1.0$$

Hoop Compression Plus Shear

$$\frac{|\sigma_{\theta s}|}{\sigma_{\theta eL}} + \left(\frac{\sigma_{\phi s}}{\sigma_{\phi eL}} \right)^2 = 0.832 < 1.0$$

Axial Compression Plus Hoop Compression Plus Shear

The shear constant, K, is computed as follows

$$K := 1 - \left(\frac{\sigma_{\phi s}}{\sigma_{\phi eL}} \right)^2 \quad K = 1$$

As a result of the shear stress equaling zero, the value of K equals one. Therefore, no further interaction checks are required for this combination of stresses.

Inelastic Buckling

$$\sigma_{\phi p} := \frac{\sigma_{\phi s}}{\eta_{\phi}} \quad \sigma_{\phi p} = 1.493 \times 10^4 \text{ psi} \quad \sigma_{\phi eL} = 2.384 \times 10^5 \text{ psi}$$

$$\sigma_{\theta p} := \frac{\sigma_{\theta s}}{\eta_{\theta}} \quad \sigma_{\theta p} = 6.787 \times 10^3 \text{ psi}$$

$$\sigma_{\phi \theta p} := \frac{\sigma_{\phi s}}{\eta_{\phi \theta}} \quad \sigma_{\phi \theta p} = 0 \text{ psi}$$

Axial Compression Plus Shear

$$\left(\frac{\sigma_{\phi p}}{\sigma_{\phi eL}} \right)^2 + \left(\frac{\sigma_{\phi \theta p}}{\sigma_{\phi \theta eL}} \right)^2 = 3.92 \times 10^{-3} < 1.0$$

Hoop Compression Plus Shear

$$\left(\frac{\sigma_{\theta p}}{\sigma_{\theta eL}} \right)^2 + \left(\frac{\sigma_{\phi \theta p}}{\sigma_{\phi \theta eL}} \right)^2 = 0.693 < 1.0$$

Conclusion

Analysis of the MPC confinement shell shows that the interaction equations for elastic and inelastic buckling are satisfied (less than 1.0). Therefore, stability of the inner shell is assured for load case 7.

3.H.6 Conclusions

Three bounding load cases have been defined for the Overpack, and a corresponding set of four cases defined for the MPC. The characteristics of the load cases are that they combine a large mean axial stress with a high circumferential stress both of which extend over the entire vessel both axially and circumferentially.

Although some stiffening effect is expected from the basket support ribs, the effect of such stiffening on the MPC buckling is conservatively neglected.

All required safety margins are met for the load cases considered.

APPENDIX 3.I: STRUCTURAL QUALIFICATION OF MPC BASEPLATE

3.I.1 SCOPE

This appendix provides the structural qualification of the MPC baseplate for a bounding set of loadings. The results demonstrate that the baseplate thickness is adequately sized to insure satisfaction of stress intensity allowables.

3.I.2 Methodology

A stress analysis of the MPC baseplate and adjoining local regions of the MPC canister is carried out using a finite element model and the finite element code ANSYS [3.I.1]. The configuration is shown in Figure 3.I.1. Values extracted from the "raw" results of this finite element analysis are then used to form the final combined stresses.

3.I.3 References

[3.I.1] ANSYS 5.2, Ansys, Inc., 1995.

3.I.4 Acceptance Criteria

Loads are identified for Level A analyses and for Level D analyses. It is required that the following stress combinations be examined:

1. Primary Membrane Stress Intensity plus Primary Bending Stress Intensity
2. Primary Membrane Stress Intensity plus Primary Bending Stress Intensity plus Secondary Stress Intensity

The following allowable stress intensity values are used to calculate the margin of safety resulting from each loading condition. The values are obtained from Tables 3.1.15 and 3.1.16 for Levels A and D, respectively.

Level A

Primary Membrane Allowable, $Sm_{am} = 18700$ psi

Primary Membrane and Bending Allowable, $Sm_{amb} = 1.5 \times Sm_{am} = 28050$ psi

Primary Membrane and Bending and Secondary Allowable, $Sm_{as} = 2 \times Sm_{amb} = 56100$ psi

Level D

Primary Membrane Allowable, $S_{dm} = 2.4 S_{am} = 44,880$ psi

Primary Membrane and Bending Allowable, $Sm_{dmb} = 2.4 \times Sm_{amb} = 67320$ psi

Primary Membrane and Bending Allowable (775F), $S_m \text{ fire} = 54,225$ psi

3.I.5 Assumptions

1. The baseplate and the lower portion of the canister are modeled as plate and shell structures. The SHELL51 axisymmetric shell element is used.
2. All loadings are assumed to be applied in an axisymmetric manner.
3. Allowable strength values for Alloy X at 400 degrees F are used except for the fire evaluation.
4. The canister is included in the model only to the extent necessary to adequately capture secondary bending stress intensities in the analysis.

3.I.6 Input Load Data

3.I.6.1 Level A Loads

For the Level A condition, the following loadings must be accounted for:

Accident Pressure = (P_{ACC}) = 125 psi	Table 2.2.1
Design Internal Pressure (P) = 100 psi	Table 2.2.1
MPC Basket Weight (W_{basket}) = 13,000 lb.	Table 3.2.4
MPC Baseplate Weight (W_{base}) = 3,000 lb.	Table 3.2.4
Fuel Weight = 54,000 lb.	Table 3.2.4

The total bounding lifted load is determined by summing the weights of the fuel, the basket, and the baseplate. Note that this value anticipates the potential scenario where a fully loaded MPC is lifted from the threaded connections on top of the MPC lid.

3.I.6.2 Level D Load

The only identified Level D load condition that could lead to significant stress in the MPC baseplate is a 60-g top end drop of a HI-STAR 100. The drop loading on the baseplate is the weight of the baseplate multiplied by 60.

$$\text{Top End Drop Load } (L_{\text{drop}}) = W_{\text{base}} \times 60 = 180,000 \text{ lb.}$$

3.I.7 Input Geometry

The pertinent geometric input values are obtained from the Design Drawings in Section 1.5.

$$\text{Baseplate Thickness } (t_{\text{base}}) = 2.5 \text{ in.}$$

$$\text{Canister Thickness } (t_{\text{can}}) = 0.5 \text{ in.}$$

$$\text{Mean Radius to Canister Mid-Plane } (R_{\text{mean}}) = 1/2 \times 68.375 - t_{\text{can}}/2 = 33.9375 \text{ in.}$$

3.I.8 Analysis and Results

An axisymmetric finite element analysis is performed for three load cases. From the results of these evaluations, the stresses from all loads listed above can be either evaluated or bounded. The first evaluated load case applies a 60-g gravitational load to the baseplate. This gravitational load is not applied to the canister. The second load case applies a 125 psi external pressure to both the baseplate and the canister. The final load case applies a 1,000 lb. ring load to the baseplate at a radius of 23 inches. This represents a "unit load" case which describes the basket-induced load on the baseplate. The results of these three finite element solutions are examined and are either amplified or attenuated to form (or bound) the required combinations.

3.I.8.1 Load Case E1 (Design Internal Pressure)

Based on the finite element analysis of the 125 psi external pressure load case, the stress intensity and corresponding margin of safety of the baseplate under the design internal pressure loading (P) can be determined. The maximum value of the combined membrane and bending stress intensities in the baseplate, obtained from the finite element analysis, is 26427 psi. The corresponding combined stress intensity for the design internal pressure case can be determined by multiplying the calculated value by the ratio of the pressures.

$$\sigma_{\text{E1mb}} = 26427 \times P \div 125 \text{ psi} = 21141.6 \text{ psi}$$

The corresponding margin of safety is:

$$MS_{E1mb} = (Sm_{amb} \div \acute{o}_{E1mb}) - 1 = 0.326$$

The maximum value of the combined primary membrane, primary bending and secondary bending stress intensities in the canister, obtained from the finite element analysis, is 39948 psi. This maximum values occurs near the baseplate-to-canister connection. Using the same method of multiplying the stress intensity by the pressure ratio, the stress intensity and margin of safety for this canister under design internal pressure can be determined as:

$$\acute{o}_{E1S} = 39948 \times P \div 125 \text{ psi} = 31958.4 \quad \text{psi}$$

$$MS_{E1S} = (Sm_{aS} \div \acute{o}_{E1S}) - 1 = 0.755$$

The primary membrane stress intensity in the canister under design internal pressure must be calculated if it is to be considered individually. This value is determined as:

$$\acute{o}_{E1m} = (P \times R_{mean} \div t_{can}) + P = 6887.5 \text{ psi}$$

and the corresponding margin of safety is:

$$MS_{E1m} = (Sm_{am} \div \acute{o}_{E1m}) - 1 = 1.715$$

It should be noted that the margin of safety for all three of these stress intensities is greater than zero, as required.

3.1.8.2 Load Case E2 (Normal Handling)

This load condition consists of the design internal pressure combined with an effective pressure due to the weight of the fuel and baseplate and a ring load due to the MPC basket. Once again, the results of the three finite element evaluations are combined, with the use of appropriate multipliers, to obtain the desired stress results.

The load supported by the baseplate as a distributed load is the weight of the fuel plus the weight of the baseplate. If a dynamic load factor of 1.15 (based on the Crane Manufacturer's Association of America Standard (CMAA #70) for a low-speed lift) is applied to this value, it then increases to:

$$W_{dyn} = (W_{fuel} + W_{base}) \times 1.15 = 65,550 \text{ lb.}$$

The finite element solution for the first load case (60-g gravitational loading on a baseplate of weight of 2,662 lb.) gives a total support reaction load of 157394 lb. from the amplified gravitational load. An effective gravitational multiplier can be determined by calculating the ratio of W_{dyn} to the support reaction load.

$$g_{\text{eff}} = W_{\text{dyn}} \div 157394 \text{ lb.} = 0.416 \quad (g_{\text{eff}} \text{ allows finite element results to be ratioed for the case considered here)}$$

The maximum stress intensity produced by the 1,000 lb. ring load is 49.5 psi (this can be used with the proper multiplier to evaluate the case here). From the results of the finite-element analyses we again determine the stress intensity and resulting margin of safety in the baseplate using the attenuation method. The maximum combined baseplate membrane and bending stress intensity is determined from the finite-element analysis of the 60-g gravitational load as 9375 psi. The corresponding maximum stress intensity from the finite-element analysis of the external pressure case is 26552 psi. The maximum combined primary membrane and primary bending stress intensity and the resultant margin of safety of the baseplate, under the design internal pressure and dynamic lift weight, are determined as:

$$\sigma_{E2mb} = 9375 \text{ psi} \times g_{\text{eff}} + 26,427 \text{ psi} \times P \div 125 \text{ psi} + 49.5 \text{ psi} \times \frac{1.15 W_{\text{basket}}}{1,000 \text{ lb.}} = 25,781 \text{ psi}$$

$$MS_{E2mb} = (S_{m_{amb}} \div \sigma_{E2mb}) - 1 = 0.088$$

Similarly, the finite-element analysis results give the maximum stress intensities in the canister, for the combination of primary membrane and primary bending, for the 60-g load, the external pressure load and the ring load, as 12299 psi, 39948 psi, and 84 psi, respectively. Again using the appropriate attenuation factors, the maximum canister stress intensity and resultant margin of safety are:

$$\sigma_{E2S} = 12299 \text{ psi} \times g_{\text{eff}} + 39948 \times P \div 125 \text{ psi} + 84 \text{ psi} \times \frac{1.15 W_{\text{basket}}}{1,000 \text{ lb.}} = 38,331 \text{ psi}$$

$$MS_{E2S} = (S_{m_{as}} \div \sigma_{E2S}) - 1 = 0.46$$

3.I.8.3 Load Case E3 (drop events)

The limiting Level D loading condition for the baseplate is a postulated end drop condition. In the storage mode the MPC baseplate will not experience loadings in a credible end drop because the MPC baseplate will be supported by the overpack baseplate. In the transport mode, however, a top end drop of the HI-STAR 100 System is a credible postulated accident. For this case, the baseplate must meet Level D structural design requirements under the amplified g loading acting

on the baseplate weight together with the mandated surface pressure.

The two finite element solutions correspond to the 60-g drop loading and the accident design internal pressure of 125 psi, respectively. Therefore, no attenuation multipliers are used to form the desired stress intensity combinations.

Using the results of the finite-element analyses, the combined stress intensity at the center of the baseplate from the applied g-loading and pressure is:

$$\sigma_{E3mb} = 9375 \text{ psi} + 26552 \text{ psi} = 35927 \text{ psi}$$

and the resultant margin of safety is therefore:

$$MS_{E3mb} = (Sm_{dmb} \div \sigma_{E3mb}) - 1 = 0.874$$

The combined stress intensity in the canister from the applied g-loading and pressure is:

$$\sigma_{E3S} = 12299 \text{ psi} + 39948 \text{ psi} = 52247 \text{ psi}$$

Note that the secondary stress intensity due to the discontinuity at the baseplate-to-canister joint has been included in this combination, even though such inclusion is not required for a Level D condition. Therefore, the margin of safety is conservatively computed at this location as:

$$MS_{E3S} = (Sm_{Edmb} \div \sigma_{E3S}) - 1 = 0.288$$

3.I.8.4 Load Case E5 (Fire Accident)

During a fire the MPC baseplate is assumed to be subjected to the fire pressure, dead load, and fire temperature. The stress results reported for normal handling can be used to find the stress by eliminating the 1.15 load factor.

$$\sigma_{E5} = \frac{9,375 \text{ psi} \times g_{\text{eff}}}{1.15} + 26,427 \text{ psi} \times \frac{P_{\text{acc}}}{125 \text{ psi}} + 49.5 \text{ psi} \times \frac{W_{\text{basket}}}{1,000 \text{ lb.}} = 30,461 \text{ psi}$$

$$E5 = \left(\frac{Sm_{\text{fire}}}{\sigma_{E5}} \right) - 1 = 0.78$$

3.I.9

Conclusion

Safety margins for all defined Design, limiting Level A and limiting Level D loading conditions have safety margins greater than zero, as required.

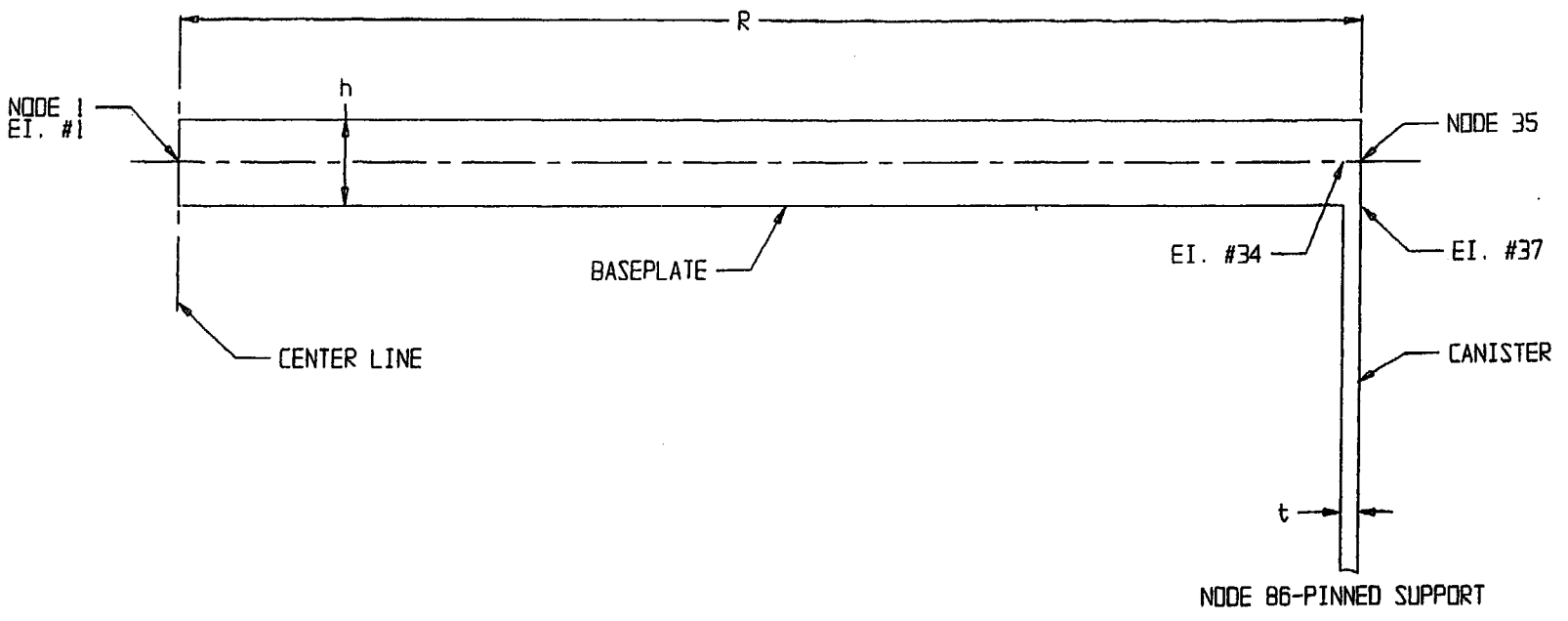


FIGURE 3.1.1; FINITE ELEMENT MODEL

APPENDIX 3.J

FUEL SUPPORT SPACER STRENGTH EVALUATIONS

3.J.1 Fuel Spacer Strength Analysis

The upper and lower fuel spacers are illustrated in the design drawings with lengths specified in Tables 2.1.9 and 2.1.10. The following calculations are presented to show that the spacer designs are structurally adequate for their intended function under the design loadings. The spacers are not required to be designed in accordance with ASME Code, Section III, Subsection NG; however, the Subsection NG stress limits are conservatively applied.

The fuel spacers must maintain the axial position of the fuel assembly during normal, off-normal, and accident loading conditions. The maximum fuel assembly weights are taken from Table 2.1.6 as:

PWR assembly	1680 lbs.
BWR assembly	700 lbs.

The fuel spacers are manufactured from Alloy X. The normal, off-normal, and accident design temperature is 725°F. The normal and off-normal loading condition is simply the maximum weight of the fuel assembly multiplied by a deceleration factor of 10g's. The accident loading is the inertia loading corresponding to an axial fuel assembly deceleration of 60g's, which would accompany the design basis cask drop.

The fuel spacers are shown to meet ASME Code Subsection NG stress limits for normal and off-normal loads. For the accident condition loading, it is necessary to show that:

- a. The maximum axial load induced in the spacer is less than the elastic buckling load.
- b. The axial stress in the smallest section under the maximum axial load in the spacer is less than the Subsection NG stress limit for accident loads.

The above criteria, (a) and (b), shall be referred to as the "stability" and "strength" compliance, respectively.

3.J.2 Normal and Off-Normal Loading Condition

ASME Code Subsection NG, Article NG-3133.6 lists the maximum allowable compressive stress for cylinders as the lesser of the values for the stress intensity, S_m , at the design temperature or the factor B.

The normal and off-normal loads are the following, where $W_{PWR} = 1680$ lb., H (deceleration factor) = 10, and $W_{BWR} = 700$ lb.

$$F_{PWR} = W_{PWR} H \quad \text{and} \quad F_{BWR} = W_{BWR} H$$

$$F_{PWR} = 16,800 \text{ lb.} \quad F_{BWR} = 7,000 \text{ lb.}$$

The MPC fuel spacers are depicted in the Design Drawings of Section 1.5. The cross sectional area of the PWR and BWR fuel spacers are as follows:

$${}^\dagger AL_{p\ell} = 6^2 - 5.5^2 = 5.75 \text{ in}^2$$

$$AL_{b\ell} = 4^2 - 3.5^2 = 3.75 \text{ in}^2$$

$$AL_{pu} = AL_{bu} = \delta (1.75^2 - 1.45^2) = 3.016 \text{ in}^2$$

Using the fuel spacer with the smallest area, the maximum axial load which a spacer can withstand without exceeding the NG Level A limit, listed in Table 2.1.18, for axial stress is

$$\text{BWR or PWR:} \quad F_{\max} = AL_{pu} S_m = (3.016 \text{ in}^2) (15.4 \text{ ksi}) = 46,446 \text{ lb.}$$

Comparison of the load with the allowable follows:

<u>PWR</u>	<u>BWR</u>
$F_{PWR} = 16,800 \text{ lb.}$	$F_{BWR} = 7,000 \text{ lb.}$
$F_{\max} = 46,446 \text{ lb.}$	$F_{\max} = 46,446 \text{ lb.}$
$F_{PWR} < F_{\max}$	$F_{BWR} < F_{\max}$

[†] Subscripts p and b refer to PWR and BWR cases, respectively. Second subscript u or ℓ indicates upper and lower fuel spacer, respectively.

Therefore, the normal and off-normal loads do not exceed the values for S_m at design temperatures.

The factor B is determined in accordance with Article NG-3133.6, as follows.

An equivalent thin walled cylinder is determined for the lower fuel spacer by using equivalent moments of inertia. S_o equals the outer side length and S_i equals the inner side length of the lower fuel spacer square tube.

$$I_{pl} = (S_o^4 - S_i^4)/12 = (6^4 - 5.5^4)/12$$
$$I_{pl} = 31.74 \text{ in}^4$$

$$I_{bl} = (S_o^4 - S_i^4) / 12 = (4^4 - 3.5^4)/12$$
$$I_{bl} = 8.83 \text{ in}^4$$

Equivalent Thin Walled Cylinder

$$\text{Equiv. } I_{pl} = \frac{\delta}{4} (R_o^4 - R_i^4) = 31.74 \text{ in}^4$$

$$\text{Equiv. } I_{bl} = \frac{\delta}{4} (R_o^4 - R_i^4) = 8.83 \text{ in}^4$$

Assume $t = 0.25$, the thickness of the square tube in the lower fuel spacer, yields

$$R_o = R_i + 0.25 \text{ in.}$$

$$\text{Equiv. } R_{pl} = R_o = 3.55 \text{ in.}$$

$$\text{Equiv. } R_{bl} = R_o = 2.365 \text{ in.}$$

$$R_{pu} = R_{bu} = 1.75 \text{ in.}$$

$$t_{pu} = t_{bu} = 0.3 \text{ in.}$$

Article NG-3133.6 states the following, where T = the thickness and R = the inner radius (R_i).

$$AI = \frac{0.125}{(R/T)}$$

Using the inner radius for the equivalent thin walled cylinder and the inner radius of the upper fuel spacer, yields

$$AI_{pl} = 0.0095 \quad AI_{pu} = AI_{bu} = 0.0259$$

$$AI_{bl} = 0.0148$$

Using the value A with Figures HA-1 and HA-2 on page 628 of Part D, ASME Section II, the value B is determined to be the following (the lower value from the two figures is utilized):

$$B_{pl} = 8,000 \quad B_{pu} = B_{bu} = 8,500$$

$$B_{bl} = 8,100$$

The area as calculated earlier is:

$$AL_{pl} = 5.75 \text{ in}^2$$

$$AL_{bl} = 3.75 \text{ in}^2$$

$$AL_{pu} = AL_{bu} = 3.016 \text{ in}^2$$

The compressive stress is the following:

$$S_{pl} = F_{PWR}/AL_{pl} = 16,800/5.75 = 2,922 \text{ psi}$$

$$S_{bl} = F_{BWR}/AL_{bl} = 7,000/3.75 = 1,867 \text{ psi}$$

$$S_{pu} = F_{PWR}/AL_{pu} = 16,800/3.016 = 5,570 \text{ psi}$$

$$S_{bu} = F_{BWR}/AL_{bu} = 7,000/3.016 = 2,321 \text{ psi}$$

The maximum compressive stress of the fuel spacers, S_{pu}, is less than the minimum B value, B_{pl}. Therefore, the fuel spacers meet the B value allowables of Article NG-3133.6 for the normal and off-normal conditions.

3.J.3 Accident Loading Condition

Table 3.3.1 provides the following properties for the Alloy X material, required for our computations.

Young's Modulus, $E @ 725^\circ\text{F} = 24.625 \times 10^6 \text{ psi}$
Ultimate Strength, $S_u @ 725^\circ\text{F} = 62,350 \text{ psi}$

Other properties, namely net minimum cross sectional area and moment of inertia, are calculated as follows:

$AL_{pl} = 5.75 \text{ in}^2$, as calculated earlier

$$\text{Moment of Inertia, } I_p = \frac{1}{12} (h_o^4 - h_i^4)$$

where h_o and h_i are outside and inside side dimensions of the square tubes.

$$\text{or } I_{pl} = \frac{1}{12} (6^4 - 5.5^4)$$

$$\text{or } I_{pl} = \frac{1}{12} (1296 - 915.1)$$

$$\text{or } I_{pl} = 31.8 \text{ in}^4$$

The corresponding data for the BWR lower fuel spacer is 4 inch square tube, 1/4 in. wall, $I_{bl} = 8.8 \text{ in}^4$, $AL_{bl} = 3.75 \text{ in}^2$

The upper spacer for both PWRs and BWRs is 3 inch Sch. 80 pipe (3.5 inch O.D. x 0.3 inch wall):

$$AL_{pu} = AL_{bu} = 3.016 \text{ in}^2$$

Moment of inertia, $I_{pu} = I_{bu} = 3.9 \text{ in}^4$

Strength Compliance

The minimum area, A_{min} , for the spacers is 3.016 in^2 for the PWR and BWR upper fuel spacer. The maximum axial load which a spacer of this net area can withstand without exceeding the NG Level D limit for axial stress is

BWR or PWR: $F_{\max} = (3.016 \text{ in}^2) (36,950 \text{ psi})$
 $F_{\max} = 111,441 \text{ lb.}$

Let W_{\max} be the maximum fuel assembly weight, then at 60 g's

$$W_{\max} = \frac{F_{\max}}{60}$$

BWR or PWR: $W_{\max} = 111,441/60 = 1,857$

As can be seen from Table 2.1.6, all fuel assemblies weigh less than the W_{\max} .

Stability Compliance

The critical buckling load for the spacers is computed using the classical Euler formula for slender columns (see, for example, Seely F.B. and Smith J.D., "Advanced Mechanics of Materials", Wiley (1965), p. 587).

$$F_{cr} = \frac{\delta^2 E I}{l^2}$$

where

- E: Young's Modulus of the spacer material at temperature (725°F)
- I: Planar moment of inertia

Referring to Tables 2.1.9 and 2.1.10, the maximum upper fuel spacer length is 40.5 inches. Therefore, using the longest spacer length to obtain the lowest critical load, we have

$$F_{cr} = \frac{(\delta^2) (24.625 \times 10^6) (3.9)}{40.5^2}$$

or

$$F_{cr} = 5.77 \times 10^5 \text{ lb.}$$

Allowable fuel weight W_{\max} is again given by (for 60g axial inertial deceleration)

$$W_{\max} = \frac{F_{cr}}{60}$$

or

$$W_{\max} = 9,616 \text{ lb.}$$

This weight bounds all PWR and BWR assemblies, even allowing for a factor of safety of 1.5.

Referring to Table 2.1.9, the maximum length of the lower spacer for PWR fuel is 20.25" ($\ell = 20.25$ ").

The critical load is given by

$$\begin{aligned} F_{cr} &= \frac{\delta^2 E I_{pl}}{\ell^2} = \frac{(\delta^2) (24.625 \times 10^6) (31.8)}{20.25^2} \\ &= 1.88 \times 10^7 \end{aligned}$$

The maximum allowable fuel assembly weight for 60g deceleration is, therefore,

$$\begin{aligned} W_{\max} &= 1.88 \times 10^7 / 60 \\ &= 313,333 \text{ lb.} \end{aligned}$$

W_{\max} bounds all PWR fuel assemblies, even allowing for a large safety margin.

Finally, the critical load for lower fuel spacer is computed using the Euler formula, $\ell = 40.5$ " (maximum length from Table 2.1.10)

$$\begin{aligned} F_{cr} &= \frac{(\delta^2) (24.625 \times 10^6) (8.8)}{40.5^2} \\ &= 1.30 \times 10^6 \text{ lb.} \end{aligned}$$

Therefore

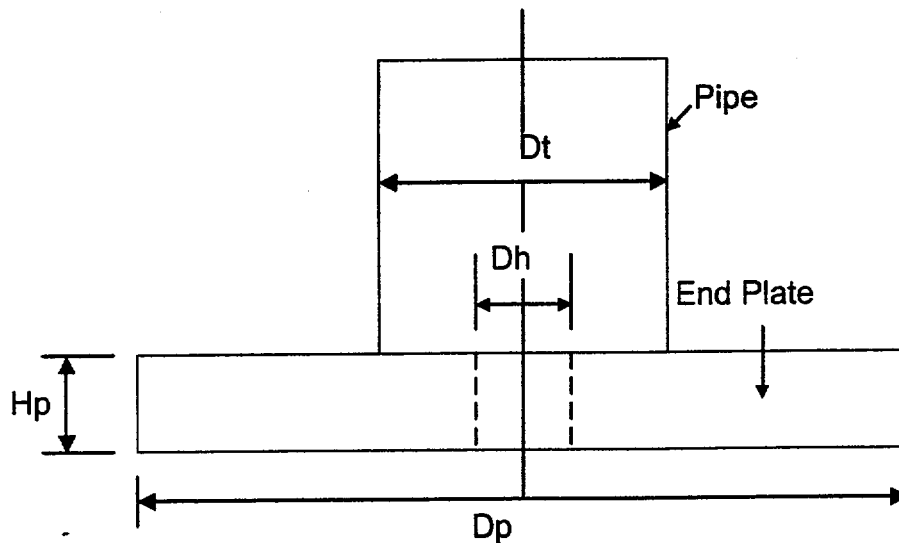
$$W_{\max} = \frac{1.30 \times 10^6}{60} = 21,667 \text{ lb.}$$

W_{\max} bounds all BWR fuel assembly weights.

Therefore, it is concluded that the upper and lower fuel spacers have sufficient axial strength to withstand the axial inertia loads without suffering plastic collapse or elastic instability.

3.J.4 Analysis of Upper Spacer End Plate for PWR Spacers

Some PWR fuel types are not supportable by the current upper spacer design having a simple pipe extension. To insure that all PWR fuel types are captured, an end plate having sufficient diameter is welded to the end of the pipe to extend the contact area. This section of the appendix addresses the stress analysis of the end plate to insure that it performs as desired under a handling accident that results in a direct impact of the fuel assembly onto the end plate. The configuration is shown below:



The dimensions are: (note that outer radius is taken equal to inside radius of limiting fuel assembly contact circle)

$$H_p := 0.75 \cdot \text{in} \quad D_p := 4.1 \cdot \text{in} \quad D_t := 3.5 \cdot \text{in} \quad D_h := 1 \cdot \text{in}$$

Under the postulated handling accident, the total applied load is (design basis deceleration of 60 g's):

$$P := 60 \cdot 1680 \cdot \text{lbf} \quad P = 1.008 \times 10^5 \text{ lbf}$$

This load may be applied as a line load around the outer periphery

$$q_o := \frac{P}{\pi \cdot D_p} \quad q_o = 7.826 \times 10^3 \frac{\text{lbf}}{\text{in}}$$

or it may be applied as a line load at a diameter of 1.8" (from a survey of fuel assembly types)

$$q_i := \frac{P}{\pi \cdot 1.8 \cdot \text{in}} \quad q_i = 1.783 \times 10^4 \frac{\text{lbf}}{\text{in}}$$

In either case, the shear load at the pipe connection is approximately

$$q_p := \frac{P}{\pi \cdot Dt} \quad q_p = 9.167 \times 10^3 \frac{\text{lb}}{\text{in}}$$

At the design temperature, the ultimate strength is, (conservatively neglect any increase in ultimate strength due to strain rate effects

$$S_u := 62350 \cdot \text{psi}$$

The spacer pipe has been designed to NG, Level D requirements for axial strength and to the appropriate ASME Code requirements for gross stability. The function of the end plate is to insure that the fuel assembly impacts the spacer; the only requirement is that under an accident condition, no permanent deformation of this end plate occurs to the extent that the positioning limits of the fuel assembly is compromised. This is insured if we demonstrate that the ultimate shear capacity of the added end plate and the ultimate moment capacity of the end plate is not exceeded during the impact. Satisfaction of these stress limits will insure that no large axial movement of the assembly can occur because of the impact.

The ultimate shear capacity of the section is taken as $0.577S_u$, and the ultimate moment capacity is calculated assuming perfectly plastic behavior at the ultimate stress. Therefore, at any section of the plate the shear capacity is:

$$q_{cap} := .577 \cdot S_u \cdot Hp \quad q_{cap} = 2.698 \times 10^4 \frac{\text{lb}}{\text{in}}$$

Comparison of this limit with the peripheral shear loads computed previously demonstrates that the end plate will not experience a gross shear failure at any section. The minimum safety factor "SF" is

$$\frac{q_{cap}}{q_i} = 1.514$$

The ultimate moment capacity is (assume rectangular distribution through the thickness):

$$M_u := S_u \cdot \frac{Hp^2}{4} \quad M_u = 8.768 \times 10^3 \text{ in} \cdot \frac{\text{lb}}{\text{in}}$$

The weight of the added end plate is:

$$\text{Weight} := 0.29 \cdot \frac{\text{lb}}{\text{in}^3} \cdot \frac{\pi}{4} \cdot Hp \cdot (Dp^2 - Dh^2) \quad \text{Weight} = 2.701 \text{ lb}$$

The following calculations are performed to establish the maximum bending moment in the end plate based on the two extreme locations of impact load. The electronic version of Roark's Handbook (6th Edition) that is a Mathcad add-on, is used for this computation. Mathcad 2000 is used for this section of Appendix 3.J.

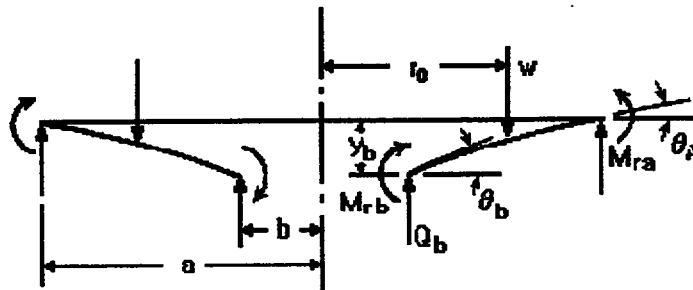
Table 24 Formulas for shear, moment and deflection of flat circular plates of constant thickness



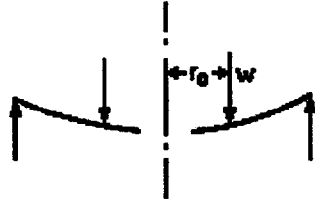
Cases 1a - 1d Annular Plate With Uniform Annular Line Load w at Radius r_0 ; Outer Edge Simply Supported

This file corresponds to Cases 1a - 1d in *Roark's Formulas for Stress and Strain*.

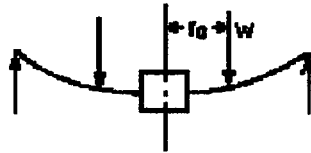
Annular plate with a uniform annular line load w at a radius r_0



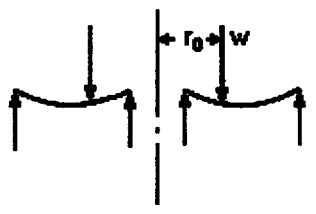
Outer edge simply supported, inner edge free



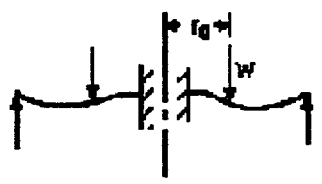
Outer edge simply supported, inner edge guided



Outer edge simply supported, inner edge simply supported



Outer edge simply supported, inner edge fixed



CASE 1A applies to the impact load at the outer periphery. The pipe diameter is the applied load location

**Enter dimensions,
properties and
loading**

Plate dimensions:

thickness: $t \equiv 0.75 \cdot \text{in}$

outer radius: $a \equiv 2.05 \cdot \text{in}$

inner radius: $b \equiv 0.5 \cdot \text{in}$

Applied unit load: $w \equiv 9167 \cdot \frac{\text{lbf}}{\text{in}}$

Modulus of elasticity: $E \equiv 24.625 \cdot 10^6 \cdot \frac{\text{lbf}}{\text{in}^2}$

Poisson's ratio: $\nu \equiv 0.3$

Radial location of applied load: $r_o \equiv .5 \cdot 3.5 \cdot \text{in}$

Constants

Shear modulus: $G \equiv \frac{E}{2 \cdot (1 + \nu)}$

D is a plate constant used in determining boundary values; it is also used in the general equations for deflection, slope, moment and shear. K_{sb} and K_{sro} are tangential shear constants used in determining the deflection due to shear:

$$D \equiv \frac{E \cdot t^3}{12 \cdot (1 - \nu^2)} \qquad D = 9.513 \times 10^5 \text{ lbf} \cdot \text{in}$$

$$K_{sro} \equiv -1.2 \cdot \frac{r_o}{a} \cdot \ln \left(\frac{a}{r_o} \right) \qquad K_{sb} \equiv K_{sro}$$

**General formulas and graphs
for deflection, slope, moment,
shear and stress as a function
of r**

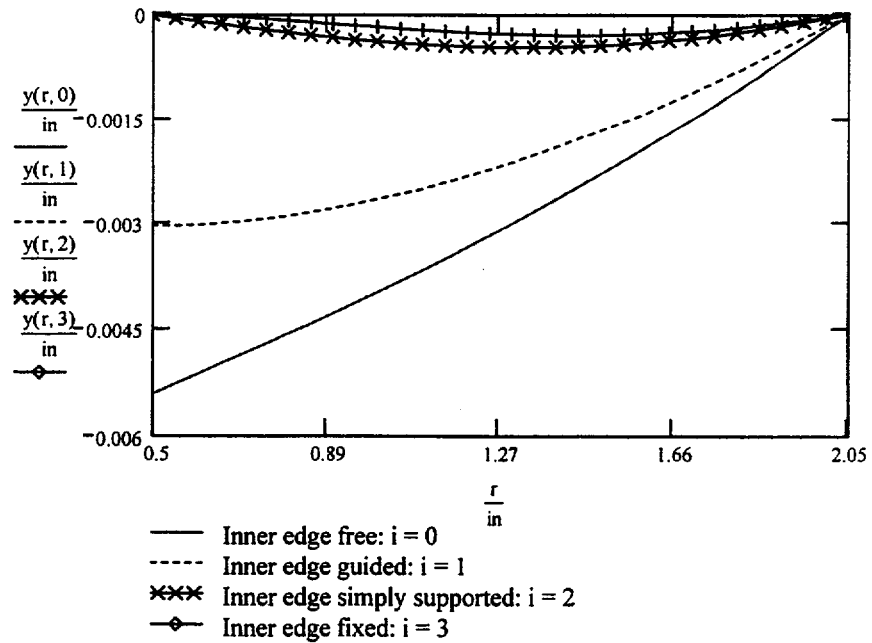
Define r, the range of the radius and i, the vector index:

$$r \equiv b, 1.1 \cdot b .. a$$

$$i \equiv 0..3$$

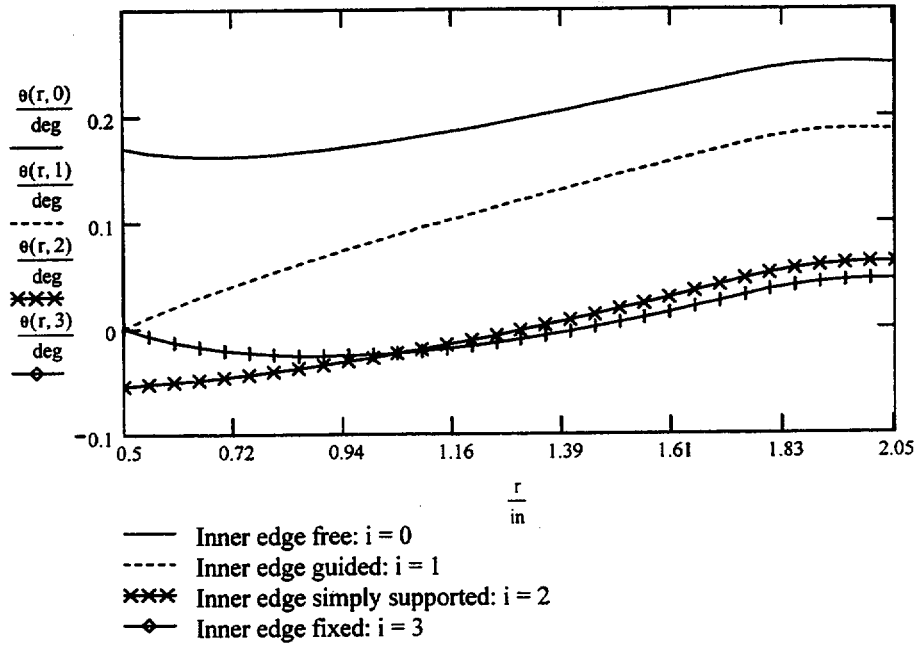
Deflection

$$y(r, i) := y_{b_i} + \theta_{b_i} \cdot r \cdot F_1(r) + M_{rb_i} \cdot \frac{r^2}{D} \cdot F_2(r) + Q_{b_i} \cdot \frac{r^3}{D} \cdot F_3(r) - w \cdot \frac{r^3}{D} \cdot G_3(r)$$



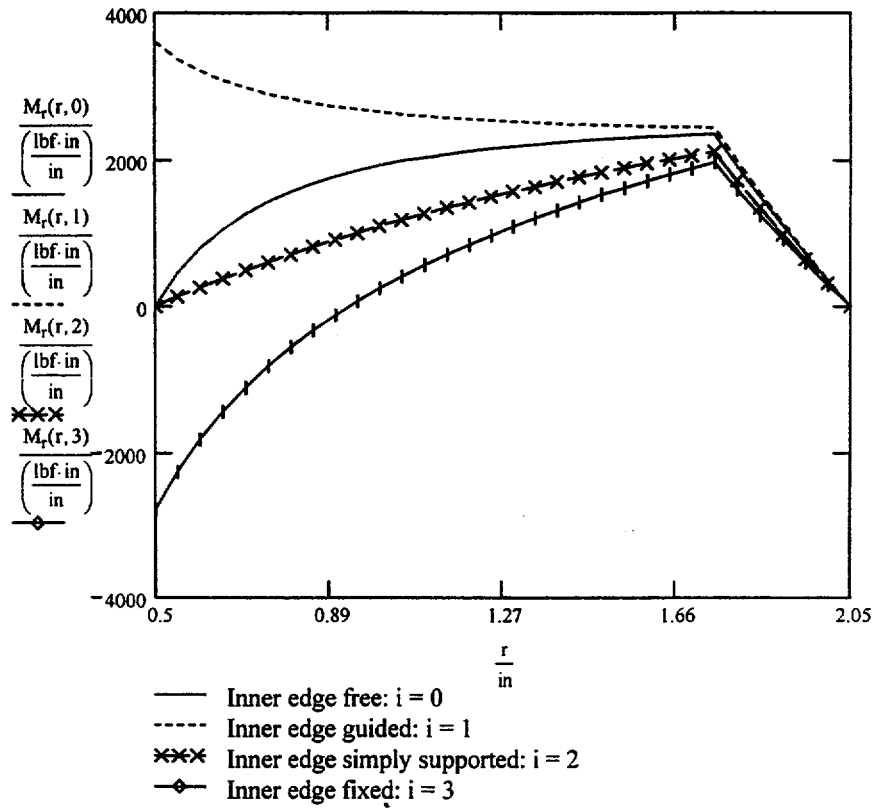
Slope

$$\theta(r, i) := \theta_{b_i} \cdot F_4(r) + M_{rb_i} \cdot \frac{r}{D} \cdot F_5(r) + Q_{b_i} \cdot \frac{r^2}{D} \cdot F_6(r) - w \cdot \frac{r^2}{D} \cdot G_6(r)$$



Radial moment

$$M_r(r, i) := \theta_{b_i} \cdot \frac{D}{r} \cdot F_7(r) + M_{rb_i} \cdot F_8(r) + Q_{b_i} \cdot r \cdot F_9(r) - w \cdot r \cdot G_9(r)$$



The following values are listed in order of inner edge:

- **free (i = 0)**
- **guided (i = 1)**
- **simply supported (i = 2)**
- **fixed (i = 3)**

Moment at points b and a (inner and outer radius):

$$\frac{M_{rb}}{\left(\frac{\text{lbf}\cdot\text{in}}{\text{in}}\right)} = \begin{pmatrix} 0 \\ 3.595 \times 10^3 \\ 0 \\ -2.798 \times 10^3 \end{pmatrix} \quad \frac{M_{ra}}{\left(\frac{\text{lbf}\cdot\text{in}}{\text{in}}\right)} = \begin{pmatrix} 0 \\ 0 \\ 0 \\ 0 \end{pmatrix}$$

Maximum radial moment (magnitude):

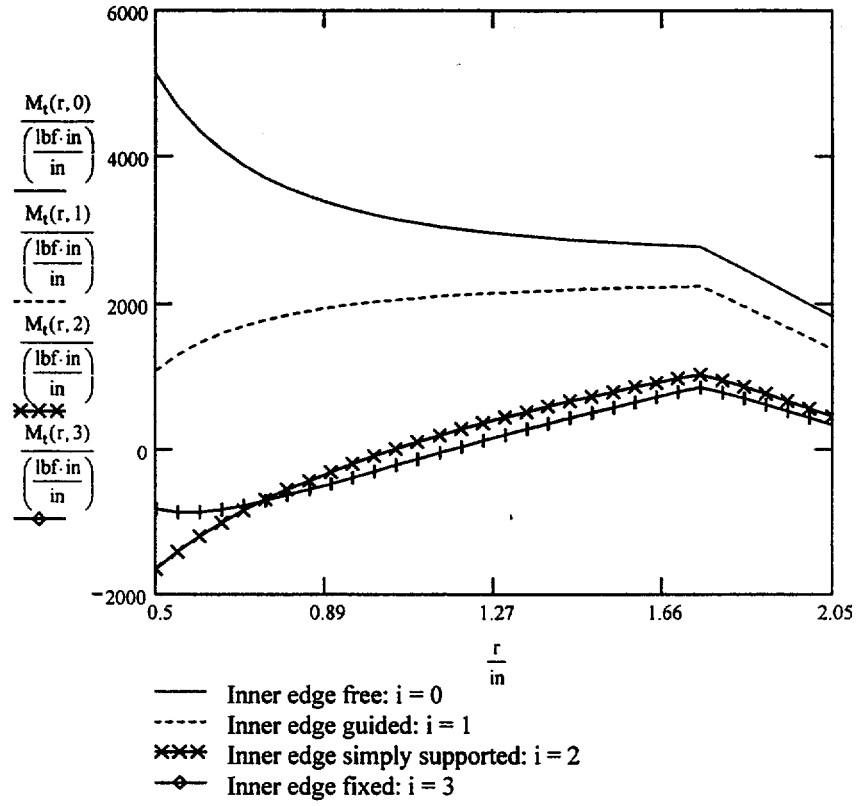
$$Mr_{(r-b)\frac{100}{\text{in}},i} := M_r(r,i) \quad A_{mr_i} := \max(Mr^{(i)}) \quad B_{mr_i} := \min(Mr^{(i)})$$

$$Mr_{\max_i} := (A_{mr_i} > -B_{mr_i}) \cdot A_{mr_i} + (A_{mr_i} \leq -B_{mr_i}) \cdot B_{mr_i}$$

$$\frac{Mr_{\max}}{\left(\frac{\text{lbf}\cdot\text{in}}{\text{in}}\right)} = \begin{pmatrix} 2.355 \times 10^3 \\ 3.595 \times 10^3 \\ 2.115 \times 10^3 \\ -2.798 \times 10^3 \end{pmatrix}$$

Transverse moment

$$M_t(r, i) := \frac{\theta(r, i) \cdot D \cdot (1 - \nu^2)}{r} + \nu \cdot M_r(r, i)$$



The following values are listed in order of inner edge:

- free (i = 0)
- guided (i = 1)
- simply supported (i = 2)
- fixed (i = 3)

Transverse moment at points b and a (inner and outer radius) due to bending:

$\frac{M_t(b,i)}{\left(\frac{\text{lbf}\cdot\text{in}}{\text{in}}\right)}$	$\frac{M_t(a,i)}{\left(\frac{\text{lbf}\cdot\text{in}}{\text{in}}\right)}$
$5.128 \cdot 10^3$	$1.828 \cdot 10^3$
$1.078 \cdot 10^3$	$1.373 \cdot 10^3$
$-1.661 \cdot 10^3$	452.798
-839.265	334.706

Maximum tangential moment (magnitude):

$$M_{t \frac{100}{(r-b) \cdot \text{in}}, i} := M_t(r, i) \quad A_{mt_i} := \max(M_t \langle i \rangle) \quad B_{mt_i} := \min(M_t \langle i \rangle)$$

$$M_{t_{\max}_i} := (A_{mt_i} > -B_{mt_i}) \cdot A_{mt_i} + (A_{mt_i} \leq -B_{mt_i}) \cdot B_{mt_i}$$

$$\frac{M_{t_{\max}}}{\frac{\text{lbf}\cdot\text{in}}{\text{in}}} = \begin{pmatrix} 5.128 \times 10^3 \\ 2.234 \times 10^3 \\ -1.661 \times 10^3 \\ -884.013 \end{pmatrix} \quad SF := \frac{M_u}{5128 \cdot \text{lbf}} \quad SF = 1.71$$

The remainder of the document displays the general plate functions and constants used in the equations above.

$$C_1 \equiv \frac{1+v}{2} \cdot \frac{b}{a} \cdot \ln\left(\frac{a}{b}\right) + \frac{1-v}{4} \cdot \left(\frac{a}{b} - \frac{b}{a}\right)$$

$$C_7 \equiv \frac{1}{2} \cdot (1-v^2) \cdot \left(\frac{a}{b} - \frac{b}{a}\right)$$

$$C_2 \equiv \frac{1}{4} \cdot \left[1 - \left(\frac{b}{a}\right)^2 \cdot \left(1 + 2 \cdot \ln\left(\frac{a}{b}\right)\right) \right]$$

$$C_8 \equiv \frac{1}{2} \cdot \left[1 + v + (1-v) \cdot \left(\frac{b}{a}\right)^2 \right]$$

$$C_3 \equiv \frac{b}{4 \cdot a} \cdot \left[\left[\left(\frac{b}{a}\right)^2 + 1 \right] \cdot \ln\left(\frac{a}{b}\right) + \left(\frac{b}{a}\right)^2 - 1 \right]$$

$$C_9 \equiv \frac{b}{a} \cdot \left[\frac{1+v}{2} \cdot \ln\left(\frac{a}{b}\right) + \left(\frac{1-v}{4}\right) \cdot \left[1 - \left(\frac{b}{a}\right)^2 \right] \right]$$

$$C_4 \equiv \frac{1}{2} \cdot \left[(1+v) \cdot \frac{b}{a} + (1-v) \cdot \frac{a}{b} \right]$$

$$L_3 \equiv \frac{r_o}{4 \cdot a} \cdot \left[\left[\left(\frac{r_o}{a}\right)^2 + 1 \right] \cdot \ln\left(\frac{a}{r_o}\right) + \left(\frac{r_o}{a}\right)^2 - 1 \right]$$

$$C_5 \equiv \frac{1}{2} \cdot \left[1 - \left(\frac{b}{a}\right)^2 \right]$$

$$L_6 \equiv \frac{r_o}{4 \cdot a} \cdot \left[\left(\frac{r_o}{a}\right)^2 - 1 + 2 \cdot \ln\left(\frac{a}{r_o}\right) \right]$$

$$C_6 \equiv \frac{b}{4 \cdot a} \cdot \left[\left(\frac{b}{a}\right)^2 - 1 + 2 \cdot \ln\left(\frac{a}{b}\right) \right]$$

$$L_9 \equiv \frac{r_o}{a} \cdot \left[\frac{1+v}{2} \cdot \ln\left(\frac{a}{r_o}\right) + \frac{1-v}{4} \cdot \left[1 - \left(\frac{r_o}{a}\right)^2 \right] \right]$$

Boundary values due to bending:

At the inner edge of the plate:

$$Q_b \equiv \begin{bmatrix} 0 \cdot \frac{\text{lb} \cdot \text{f}}{\text{in}} \\ 0 \cdot \frac{\text{lb} \cdot \text{f}}{\text{in}} \\ w \cdot \left(\frac{C_1 \cdot L_9 - C_7 \cdot L_3}{C_1 \cdot C_9 - C_3 \cdot C_7} \right) \\ w \cdot \left(\frac{C_2 \cdot L_9 - C_8 \cdot L_3}{C_2 \cdot C_9 - C_3 \cdot C_8} \right) \end{bmatrix}$$

$$M_{rb} \equiv \begin{bmatrix} 0 \cdot \frac{\text{lb} \cdot \text{f} \cdot \text{in}}{\text{in}} \\ \frac{w \cdot a}{C_8} \cdot L_9 \\ 0 \cdot \frac{\text{lb} \cdot \text{f} \cdot \text{in}}{\text{in}} \\ -w \cdot a \cdot \left(\frac{C_3 \cdot L_9 - C_9 \cdot L_3}{C_2 \cdot C_9 - C_3 \cdot C_8} \right) \end{bmatrix}$$

$$y_b \equiv \begin{bmatrix} \frac{-w \cdot a^3}{D} \cdot \left(\frac{C_1 \cdot L_9}{C_7} - L_3 \right) \\ \frac{-w \cdot a^3}{D} \cdot \left(\frac{C_2 \cdot L_9}{C_8} - L_3 \right) \\ 0 \cdot \text{in} \\ 0 \cdot \text{in} \end{bmatrix}$$

$$\theta_b \equiv \begin{bmatrix} \frac{w \cdot a^2}{D \cdot C_7} \cdot L_9 \\ 0 \cdot \text{deg} \\ \frac{-w \cdot a^2}{D} \cdot \left(\frac{C_3 \cdot L_9 - C_9 \cdot L_3}{C_1 \cdot C_9 - C_3 \cdot C_7} \right) \\ 0 \cdot \text{deg} \end{bmatrix}$$

At the outer edge of the plate:

$$y_a \equiv \begin{pmatrix} 0 \cdot \text{in} \\ 0 \cdot \text{in} \\ 0 \cdot \text{in} \\ 0 \cdot \text{in} \end{pmatrix}$$

$$\theta_a \equiv \begin{pmatrix} \frac{w \cdot a^2}{D} \left(\frac{C_4 \cdot L_9}{C_7} - L_6 \right) \\ \frac{w \cdot a^2}{D} \left(\frac{C_5 \cdot L_9}{C_8} - L_6 \right) \\ \theta_{b_2} \cdot C_4 + Q_{b_2} \cdot \frac{a^2}{D} \cdot C_6 - \frac{w \cdot a^2}{D} \cdot L_6 \\ M_{rb_3} \cdot \frac{a}{D} \cdot C_5 + Q_{b_3} \cdot \frac{a^2}{D} \cdot C_6 - \frac{w \cdot a^2}{D} \cdot L_6 \end{pmatrix}$$

$$Q_a \equiv \begin{pmatrix} -w \cdot \frac{r_o}{a} \\ -w \cdot \frac{r_o}{a} \\ Q_{b_2} \cdot \frac{b}{a} - \frac{w \cdot r_o}{a} \\ Q_{b_3} \cdot \frac{b}{a} - \frac{w \cdot r_o}{a} \end{pmatrix}$$

$$M_{ra} \equiv \begin{pmatrix} 0 \cdot \frac{\text{lb} \cdot \text{in}}{\text{in}} \\ 0 \cdot \frac{\text{lb} \cdot \text{in}}{\text{in}} \\ 0 \cdot \frac{\text{lb} \cdot \text{in}}{\text{in}} \\ 0 \cdot \frac{\text{lb} \cdot \text{in}}{\text{in}} \end{pmatrix}$$

Due to tangential shear stresses:

$$y_{sb} \equiv \begin{pmatrix} \frac{K_{sb} \cdot w \cdot a}{t \cdot G} \\ \frac{K_{sb} \cdot w \cdot a}{t \cdot G} \\ 0 \cdot \text{in} \\ 0 \cdot \text{in} \end{pmatrix}$$

$$y_{sro} \equiv \begin{pmatrix} \frac{K_{sro} \cdot w \cdot r_o}{t \cdot G} \\ \frac{K_{sro} \cdot w \cdot r_o}{t \cdot G} \\ 0 \cdot \text{in} \\ 0 \cdot \text{in} \end{pmatrix}$$

$$F_1(r) \equiv \frac{1+v}{2} \cdot \frac{b}{r} \cdot \ln\left(\frac{r}{b}\right) + \frac{1-v}{4} \cdot \left(\frac{r}{b} - \frac{b}{r}\right)$$

$$F_6(r) \equiv \frac{b}{4 \cdot r} \cdot \left[\left(\frac{b}{r}\right)^2 - 1 + 2 \cdot \ln\left(\frac{r}{b}\right) \right]$$

$$F_2(r) \equiv \frac{1}{4} \cdot \left[1 - \left(\frac{b}{r}\right)^2 \cdot \left(1 + 2 \cdot \ln\left(\frac{r}{b}\right)\right) \right]$$

$$F_7(r) \equiv \frac{1}{2} \cdot (1 - v^2) \cdot \left(\frac{r}{b} - \frac{b}{r}\right)$$

$$F_3(r) \equiv \frac{b}{4 \cdot r} \cdot \left[\left(\frac{b}{r}\right)^2 + 1 \right] \cdot \ln\left(\frac{r}{b}\right) + \left(\frac{b}{r}\right)^2 - 1$$

$$F_8(r) \equiv \frac{1}{2} \cdot \left[1 + v + (1 - v) \cdot \left(\frac{b}{r}\right)^2 \right]$$

$$F_4(r) \equiv \frac{1}{2} \cdot \left[(1 + v) \cdot \frac{b}{r} + (1 - v) \cdot \frac{r}{b} \right]$$

$$F_9(r) \equiv \frac{b}{r} \cdot \left[\frac{1+v}{2} \cdot \ln\left(\frac{r}{b}\right) + \frac{1-v}{4} \cdot \left[1 - \left(\frac{b}{r}\right)^2 \right] \right]$$

$$F_5(r) \equiv \frac{1}{2} \cdot \left[1 - \left(\frac{b}{r}\right)^2 \right]$$

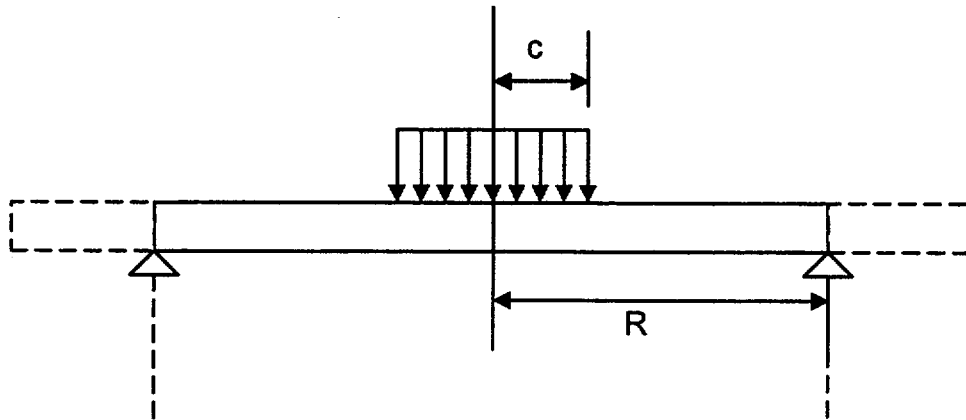
$$G_3(r) \equiv \frac{r_0}{4 \cdot r} \cdot \left[\left(\frac{r_0}{r}\right)^2 + 1 \right] \cdot \ln\left(\frac{r}{r_0}\right) + \left(\frac{r_0}{r}\right)^2 - 1 \cdot (r > r_0)$$

$$G_6(r) \equiv \frac{r_0}{4 \cdot r} \cdot \left[\left(\frac{r_0}{r}\right)^2 - 1 + 2 \cdot \ln\left(\frac{r}{r_0}\right) \right] \cdot (r > r_0)$$

$$G_9(r) \equiv \frac{r_0}{r} \cdot \left[\frac{1+v}{2} \cdot \ln\left(\frac{r}{r_0}\right) + \frac{1-v}{4} \cdot \left[1 - \left(\frac{r_0}{r}\right)^2 \right] \right] \cdot (r > r_0)$$

The actual safety factor against a complete collapse of the ring like plate is much larger since unlimited large rotations will only occur when a substantial region of the plate has the circumferential moment reach capacity (this can be shown by a limit analysis solution of the plate equations).

The second impact scenario has the loading applied over a region inside the outer diameter of the pipe. To qualify this load case, we consider the plate as simply supported at the pipe diameter and conservatively neglect the overhanging portion of the pipe. Further, we assume the loading is conservatively applied as a uniform pressure over an area equal to the minimum impact diameter of 1.8". For simplicity, we neglect the inner hole in this calculation. Therefore, the limit analysis model for the second impact scenario is shown below:



Calculate effective load area at middle surface assuming a 45 degree spread of load patch

$$H_p = 0.75 \text{ in}$$

$$R := 0.5 \cdot [(3.5 - 2 \cdot 0.226) \cdot \text{in}]$$

$$P = 1.008 \times 10^5 \text{ lbf}$$

$$c := 0.5 \cdot (1.8 \cdot \text{in} + H_p)$$

Use inside radius of pipe for this calc.

$$M_u = 8.768 \times 10^3 \text{ lbf} \cdot \frac{\text{in}}{\text{in}}$$

Using a solution in the text "Introduction to Plasticity" by W. Prager, Addison Wesley, 1959, p. 61, the limit load is

$$P_{lim} := 6 \cdot \pi \cdot \frac{M_u}{\left(3 - 2 \cdot \frac{c}{R}\right)}$$

Therefore, the safety factor for this case is

$$\frac{P_{lim}}{P} = 1.236$$

Therefore it is concluded that an end plate of diameter and thickness equal to

$$D_p = 4.1 \text{ in}$$

$$H_p = 0.75 \text{ in}$$

will perform the intended load transfer and limit the movement of the fuel assembly.

APPENDIX 3.K - LIFTING BOLTS - MPC LID and OVERPACK TOP CLOSURE

3.K.1 Scope of Appendix

In this Appendix, the bolts on the MPC top lid that are used for lifting a fully loaded MPC are analyzed for strength and engagement length. The required number of bolts are set at a specific radius of the MPC lid. Only the bolts are considered; the mating lifting device is not a part of this submittal. Bolt sizes required for lifting of the overpack top closure alone (during the fuel loading operation) are also determined.

3.K.2 Configuration

The required data for analysis is 1) the number of bolts NB; 2) the bolt diameter db; 3) the lifted weight; and 4), the details of the individual bolts.

3.K.3 Acceptance Criteria

The lifting bolts are considered as part of a special lifting device; therefore, NUREG-0612 applies. The acceptance criteria is that the bolts and the adjacent lid threads must have stresses less than $1/6$ x material yield strength and $1/10$ x material ultimate strength.

3.K.4 Composition of Appendix

This appendix is created using the Mathcad (version 6.0+) software package. Mathcad uses the symbol ':=' as an assignment operator, and the equals symbol '=' retrieves values for constants or variables.

3.K.5 References

- [3.K.1] E. Oberg and F.D. Jones, *Machinery's Handbook*, Fifteenth Edition, Industrial Press, 1957, pp987-990.
- [3.K.2] FED-STD-H28/2A, *Federal Standard Screw-Thread Standards for Federal Services*, United States Government Printing Office, April, 1984.

3.K.6 Input Data for Lifting of a Fully Loaded MPC

Lifted Weight: (use a value that bounds all MPC's per Table 3.2.4 - this is the only load)

$W_{\text{lift}} := 1.15 \cdot 90000 \cdot \text{lbf}$ includes any anticipated inertia load factor

Bolt diameter $db := 1.75 \cdot \text{in}$

Number of Bolts NB := 4

It is anticipated that the eventual lifting device will enable a straight (90 deg) lift. For conservatism the minimum lift angle (from the horizontal) is assumed to be 75 deg.

$$\text{ang} := 75 \cdot \text{deg}$$

Therefore, the load inducing direct shear in the unthreaded bolt region is:

$$T_h := \frac{W_{\text{lift}}}{\tan(\text{ang})} \quad T_h = 2.773 \times 10^4 \text{ lbf}$$

$$A_d := \pi \cdot \frac{d_b^2}{4} = 2.405 \text{ in}^2 \quad \text{is the area of the unthreaded portion of the bolt}$$

$$A_{\text{stress}} := 1.8983 \cdot \text{in}^2 \quad \text{is the stress area of the bolt}$$

$$d_{\text{pitch}} := 1.6201 \cdot \text{in} \quad \text{is the pitch diameter of the bolt}$$

$$d_{\text{mext}} := 1.5046 \cdot \text{in} \quad \text{is the minor diameter of the bolt}$$

$$d_{\text{mint}} := 1.5335 \cdot \text{in} \quad \text{is the minor diameter of the hole}$$

The design temperature of the MPC closure ring, located atop the MPC lid, is 400 deg. F. The lifting bolts, however, penetrate several inches into the lid. Therefore, for conservatism, the material properties and allowable stresses for the MPC lid and bolt materials used in the qualification are taken at 450 deg F.

The yield and ultimate strengths of the MPC lid and bolt materials are reduced by factors of 6 and 10, respectively.

$$S_{\text{ulid}} := \frac{64000}{10} \cdot \text{psi} \quad S_{\text{ubolt}} := \frac{169650}{10} \cdot \text{psi} \quad S_{\text{mbolt}} := 46100 \cdot \text{psi}$$

$$S_{\text{ylid}} := \frac{20050}{6} \cdot \text{psi} \quad S_{\text{ybolt}} := \frac{137550}{6} \cdot \text{psi}$$

Since this is an analysis using allowable strengths based on fractions of yield or ultimate strengths, the allowable strength in shear is taken as 57.7% of the postulated tensile allowable strengths.

3.K.7 Calculations

3.K.7.1 Length of Engagement/Strength Calculations

In this section, it is shown that the length of thread engagement is adequate. The method and terminology of Reference 3.K.2 is followed.

$$N := 5 \cdot \frac{1}{\text{in}} \quad \text{is the number of threads per inch (UNC)}$$

$$p := \frac{1}{N} \quad \text{is the thread pitch}$$

$$H := 4 \cdot 0.21651 \cdot p \quad H = 0.173 \text{ in}$$

$$\text{Depth}_{\text{ext}} := \frac{17}{24} \cdot H \quad \text{Depth}_{\text{ext}} = 0.123 \text{ in}$$

$$\text{Depth}_{\text{int}} := \frac{5}{8} \cdot H \quad \text{Depth}_{\text{int}} = 0.108 \text{ in}$$

$$\text{dmaj}_{\text{ext}} := \text{dm}_{\text{ext}} + 2 \cdot \text{Depth}_{\text{ext}} \quad \text{dmaj}_{\text{ext}} = 1.75 \text{ in}$$

$$L_{\text{eng}} := 3.0 \cdot \text{in} \quad \text{is the length of engagement}$$

Using page 103 of reference 3.K.2,

$$\text{Bolt_thrd_shr_A} := \pi \cdot N \cdot L_{\text{eng}} \cdot \text{dm}_{\text{int}} \left[\frac{1}{2 \cdot N} + .57735 \cdot (\text{d}_{\text{pitch}} - \text{dm}_{\text{int}}) \right]$$

$$\text{Bolt_thrd_shr_A} = 10.84 \text{ in}^2$$

$$\text{Ext_thrd_shr_A} := \pi \cdot N \cdot L_{\text{eng}} \cdot \text{dmaj}_{\text{ext}} \left[\frac{1}{2 \cdot N} + 0.57735 \cdot (\text{dmaj}_{\text{ext}} - \text{d}_{\text{pitch}}) \right]$$

$$\text{Ext_thrd_shr_A} = 14.43 \text{ in}^2$$

The load capacities of the bolt and the lid material based on yield strength are:

$$\text{Load_Capacity}_{\text{bolt}} := S_{\text{ybolt}} \cdot A_{\text{stress}} \quad \text{Load_Capacity}_{\text{bolt}} = 4.352 \times 10^4 \text{ lbf}$$

$$\text{Load_Capacity}_{\text{boltshear}} := .577 \cdot S_{\text{ybolt}} \cdot A_d \quad \text{Load_Capacity}_{\text{boltshear}} = 3.182 \times 10^4 \text{ lbf}$$

$$\text{Load_Capacity}_{\text{boltthrd}} := (0.577 \cdot S_{\text{ybolt}}) \cdot \text{Bolt_thrd_shr_A} \quad \text{Load_Capacity}_{\text{boltthrd}} = 1.434 \times 10^5 \text{ lbf}$$

$$\text{Load_Capacity}_{\text{lid}} := (0.577 \cdot S_{\text{ylid}}) \cdot \text{Ext_thrd_shr_A} \quad \text{Load_Capacity}_{\text{lid}} = 2.782 \times 10^4 \text{ lbf}$$

Therefore, the lifting capacity of the configuration is based on thread shear in the lid material.

$$\text{Max_Lift_Load} := \text{NB} \cdot \text{Load_Capacity}_{\text{lid}} \quad \text{Max_Lift_Load} = 1.113 \times 10^5 \text{ lbf}$$

$$\text{MS} := \frac{\text{Max_Lift_Load}}{W_{\text{lift}}} - 1 \quad \text{MS} = 0.075 > 0$$

The load capacities of the bolt and the lid material based on ultimate strength are:

$$\text{Load_Capacity}_{\text{bolt}} := S_{\text{ubolt}} \cdot A_{\text{stress}} \quad \text{Load_Capacity}_{\text{bolt}} = 3.22 \times 10^4 \text{ lbf}$$

$$\text{Load_Capacity}_{\text{boltthrd}} := (0.577 \cdot S_{\text{ubolt}}) \cdot \text{Bolt_thrd_shr_A} \quad \text{Load_Capacity}_{\text{boltthrd}} = 1.061 \times 10^5 \text{ lbf}$$

$$\text{Load_Capacity}_{\text{boltshear}} := .577 \cdot S_{\text{ubolt}} \cdot A_d \quad \text{Load_Capacity}_{\text{boltshear}} = 2.354 \times 10^4 \text{ lbf}$$

$$\text{Load_Capacity}_{\text{lid}} := (0.577 \cdot S_{\text{ulid}}) \cdot \text{Ext_thrd_shr_A} \quad \text{Load_Capacity}_{\text{lid}} = 5.329 \times 10^4 \text{ lbf}$$

Therefore, the load capacity is based on bolt tensile strength or bolt shear due to the lift angle.

$$\text{Max_Lift_Load} := \text{NB} \cdot \text{Load_Capacity}_{\text{bolt}} \quad \text{Max_Lift_Load} = 1.288 \times 10^5 \text{ lbf}$$

$$\text{Max_Lift_Load}_{\text{boltshear}} := \text{NB} \cdot \text{Load_Capacity}_{\text{boltshear}}$$

$$\text{Max_Lift_Load}_{\text{boltshear}} = 9.418 \times 10^4 \text{ lbf}$$

$$\text{MS} := \frac{\text{Max_Lift_Load}}{W_{\text{lift}}} - 1 \quad \text{MS} = 0.245$$

or

$$\text{MS} := \frac{\text{Max_Lift_Load}_{\text{boltshear}}}{T_h} - 1 \quad \text{MS} = 2.396$$

The previous calculations indicate that external thread shear stresses govern the design when yield strength is used as the criteria and bolt tension governs the design when ultimate strength is used as the criteria.

3.K.7.2 Preload Stress

$$\text{Bolt}_{\text{pl}} := \frac{W_{\text{lift}}}{\text{NB}} \quad \text{Bolt}_{\text{pl}} = 25875 \text{ lbf}$$

The minimum preload stress required is:

$$\sigma := \frac{\text{Bolt}_{\text{pl}}}{A_{\text{stress}}} \quad \sigma = 13630.6 \text{ psi}$$

If preload of the bolt is specified, using an unlubricated joint, the preload torque is:

$$T_{\text{pre}} := .2 \cdot \left(\frac{W_{\text{lift}}}{\text{NB}} \right) \cdot d_b \quad T_{\text{pre}} = 754.687 \text{ ft} \cdot \text{lbf}$$

3.K.8 Input Data for Lifting of an Overpack Top Closure Alone

diameter_lid := 77.375·in

thickness_of_lid := 6·in

Bill of Materials
BM-1476

ang := 45·deg

Minimum Lift Angle from Horizontal

inertia_load_factor := 0.15 appropriate for slow speed operation of lifting equipment

Weight := 8000·lbf

Table 3.2.4

$W_{\text{lift}} := \text{Weight} \cdot (1.0 + \text{inertia_load_factor})$

$W_{\text{lift}} = 9.2 \times 10^3 \text{ lbf}$

includes any anticipated inertia load factor

$T_h := \frac{W_{\text{lift}}}{\tan(\text{ang})}$

$T_h = 9.2 \times 10^3 \text{ lbf}$

Bolt diameter

db := .625·in

Number of Bolts

NB := 4

$A_d := \pi \cdot \frac{db^2}{4} = 0.307 \text{ in}^2$

is the area of the unthreaded portion of the bolt

$A_{\text{stress}} := .2256 \cdot \text{in}^2$

is the stress area of the bolt

$d_{\text{pitch}} := .5660 \cdot \text{in}$

is the pitch diameter of the bolt

$dm_{\text{ext}} := .5135 \cdot \text{in}$

is the major diameter of the bolt

$dm_{\text{int}} := .5266 \cdot \text{in}$

is the minor diameter of the threaded hole

3.K.9 Calculations

3.K.9.1 Length of Engagement/Strength Calculations

In this section, it is shown that the length of thread engagement is adequate. The method and terminology of reference 3.K.2 is followed.

$$N := 11 \cdot \frac{1}{\text{in}} \quad \text{is the number of threads per inch}$$

$$p := \frac{1}{N} \quad \text{is the thread pitch}$$

$$H := 4 \cdot 0.21651 \cdot p \quad H = 0.079 \text{ in}$$

$$\text{Depth}_{\text{ext}} := \frac{17}{24} \cdot H \quad \text{Depth}_{\text{ext}} = 0.056 \text{ in}$$

$$\text{Depth}_{\text{int}} := \frac{5}{8} \cdot H \quad \text{Depth}_{\text{int}} = 0.049 \text{ in}$$

$$d_{\text{maj}_{\text{ext}}} := d_{\text{ext}} + 2 \cdot \text{Depth}_{\text{ext}} \quad d_{\text{maj}_{\text{ext}}} = 0.625 \text{ in}$$

$$L_{\text{eng}} := 1.00 \cdot \text{in} \quad \text{is the length of engagement}$$

Using page 103 of reference 3.K.2,

$$\text{Bolt_thrd_shr_A} := \pi \cdot N \cdot L_{\text{eng}} \cdot d_{\text{m}_{\text{int}}} \left[\frac{1}{2 \cdot N} + .57735 \cdot (d_{\text{pitch}} - d_{\text{m}_{\text{int}}}) \right]$$

$$\text{Bolt_thrd_shr_A} = 1.241 \text{ in}^2$$

$$\text{Ext_thrd_shr_A} := \pi \cdot N \cdot L_{\text{eng}} \cdot d_{\text{maj}_{\text{ext}}} \left[\frac{1}{2 \cdot N} + 0.57735 \cdot (d_{\text{maj}_{\text{ext}}} - d_{\text{pitch}}) \right]$$

$$\text{Ext_thrd_shr_A} = 1.718 \text{ in}^2$$

The load capacities of the bolt and the lid material based on yield strength are:

$$\text{Load_Capacity}_{\text{bolt}} := S_{\text{ybolt}} \cdot A_{\text{stress}} \quad \text{Load_Capacity}_{\text{bolt}} = 5.172 \times 10^3 \text{ lbf}$$

$$\text{Load_Capacity}_{\text{boltshear}} := .577 \cdot S_{\text{ybolt}} \cdot A_d \quad \text{Load_Capacity}_{\text{boltshear}} = 4.058 \times 10^3 \text{ lbf}$$

$$\text{Load_Capacity}_{\text{boltthrd}} := (0.577 \cdot S_{\text{ybolt}}) \cdot \text{Bolt_thrd_shr_A} \quad \text{Load_Capacity}_{\text{boltthrd}} = 1.642 \times 10^4 \text{ lbf}$$

$$\text{Load_Capacity}_{\text{lid}} := (0.577 \cdot S_{\text{ylid}}) \cdot \text{Ext_thrd_shr_A} \quad \text{Load_Capacity}_{\text{lid}} = 3.313 \times 10^3 \text{ lbf}$$

Therefore, the lifting capacity of the configuration is based on thread shear in the lid.

$$\text{Max_Lift_Load} := \text{NB} \cdot \text{Load_Capacity}_{\text{lid}} \quad \text{Max_Lift_Load} = 1.325 \times 10^4 \text{ lbf}$$

$$\text{Max_Lift_Load}_{\text{boltshear}} := \text{NB} \cdot \text{Load_Capacity}_{\text{boltshear}} \quad \text{Max_Lift_Load}_{\text{boltshear}} = 1.623 \times 10^4 \text{ lbf}$$

$$\text{MS} := \frac{\text{Max_Lift_Load}}{W_{\text{lift}}} - 1 \quad \text{MS} = 0.44 > 0$$

The load capacities of the bolt and the lid material based on ultimate strength are:

$$\text{Load_Capacity}_{\text{bolt}} := S_{\text{ubolt}} \cdot A_{\text{stress}} \quad \text{Load_Capacity}_{\text{bolt}} = 3.827 \times 10^3 \text{ lbf}$$

$$\text{Load_Capacity}_{\text{boltshear}} := .577 \cdot S_{\text{ubolt}} \cdot A_d \quad \text{Load_Capacity}_{\text{boltshear}} = 3.003 \times 10^3 \text{ lbf}$$

$$\text{Load_Capacity}_{\text{boltthrd}} := (0.577 \cdot S_{\text{ubolt}}) \cdot \text{Bolt_thrd_shr_A} \quad \text{Load_Capacity}_{\text{boltthrd}} = 1.215 \times 10^4 \text{ lbf}$$

$$\text{Load_Capacity}_{\text{lid}} := (0.577 \cdot S_{\text{ulid}}) \cdot \text{Ext_thrd_shr_A}$$

$$\text{Load_Capacity}_{\text{lid}} = 6.344 \times 10^3 \text{ lbf}$$

Therefore, the load capacity is based on bolt tensile strength or bolt shear strength due to inclined lift cable.

$$\text{Max_Lift_Load} := \text{NB} \cdot \text{Load_Capacity}_{\text{bolt}} \quad \text{Max_Lift_Load} = 1.531 \times 10^4 \text{ lbf}$$

$$\text{Max_Lift_Load}_{\text{boltshear}} := \text{NB} \cdot \text{Load_Capacity}_{\text{boltshear}}$$

$$\text{Max_Lift_Load}_{\text{boltshear}} = 1.201 \times 10^4 \text{ lbf}$$

$$\text{MS} := \frac{\text{Max_Lift_Load}}{W_{\text{lift}}} - 1 \quad \text{MS} = 0.664 > 0$$

or

$$\text{MS} := \frac{\text{Max_Lift_Load}_{\text{boltshear}}}{T_h} - 1 \quad \text{MS} = 0.306$$

3.K.9.2 Preload Stress

$$\text{Bolt}_{\text{pl}} := \frac{W_{\text{lift}}}{\text{NB}} \quad \text{Bolt}_{\text{pl}} = 2300 \text{ lbf}$$

The minimum preload stress required is:

$$\sigma := \frac{\text{Bolt}_{\text{pl}}}{A_{\text{stress}}} \quad \sigma = 10195 \text{ psi}$$

If preload of the bolt is specified, using an unlubricated joint, the minimum preload torque is:

$$T_{\text{pre}} := .2 \cdot \left(\frac{W_{\text{lift}}}{\text{NB}} \right) \cdot d_b \quad T_{\text{pre}} = 23.958 \text{ ft} \cdot \text{lbf}$$

3.K.10 Conclusion

The preceding analysis demonstrates that the length of thread engagement at the lifting locations is conservatively set. In addition, the minimum bolt preload requirements based on the lifted load are set. When lifting of a loaded MPC is not part of the operating procedure, plugs of a non-galling material with properties equal to or better than Alloy X shall be in-place to provide a filler material.

APPENDIX 3.L: FABRICATION STRESSES

3.L.1 INTRODUCTION

The HI-STAR 100 System overpack intermediate shells are constructed by layering circular shell sections around the inner confinement shell. The shell longitudinal welding process pulls each shell together and establishes a radial contact pressure between each layer and circumferential stresses in each layer. Girth welds at each end of the intermediate shells (top and bottom) further connect the layers to each other and to the top flange and to the bottom plate. In accordance with NRC requirements, fabrication stresses arising in the intermediate shells must be included in load combinations when performing structural evaluation of the overpack. This appendix documents the stress analysis. The results from this evaluation are included as added stresses in the overpack finite element analysis and the results of the overpack stress analysis includes the fabrication stresses in the final safety margins.

3.L.2 Methodology

A two-dimensional finite element analysis of the inner confinement shell and the five intermediate shells is performed to establish the level of fabrication circumferential stress developing during the assembly process. Figure 3.L.1 shows a 180 degree section through the overpack consisting of six layers of metal. The ANSYS finite element code is used to model the fabrication process; each layer is modeled using PLANE42 four node quadrilateral elements. Contact (or lack of contact) is modeled by CONTAC48 point-to-surface elements. Symmetry boundary conditions apply at 90° , and radial movement of the inner nodepoint of the confinement layer is restrained. At -90° , the inner confinement layer is restrained while the remaining layers are subject to a prescribed circumferential displacement d to stretch the layer and to simulate the shrinkage caused by the weld process. Although the actual fabrication process locates the longitudinal weld in each layer at different circumferential orientation, in the analytical simulations all layer welds are located together. This is acceptable for analysis since the stress of interest is the primary membrane component. Figure 3.L.2 shows a partial free body of a small section of one of the layers. Normal pressures p develop between each layer due to the welding process; shear stresses due to friction between the layers also develop since there is relative circumferential movement between the layers. The free body also shows the section forces and moment that develop within the layer.

3.L.3 Analysis and Results

The fabrication stress distribution is a function of the coefficient-of-friction between the layers. For a large enough coefficient-of-friction the effects of the assembly process are localized near

the weld. Localized stresses are not considered as primary stresses. For a coefficient-of-friction = 0.0, the membrane hoop stress in the component shells is non-local in nature. Therefore, the fabrication stress computation conservatively considers only the case coefficient of friction (COF) = 0.0 since this will develop the largest in-plane primary membrane stress in each layer. The simulation is nonlinear in that each of the contact elements is checked for closure during increments of applied loading (the weld displacement).

Results for maximum primary membrane stress S_m in each layer are presented in Table 3.L.1 for circumferential locations -90° , -80° , 0° , 90° . There is no significant variation through the layer thickness except near the actual weld location. For the purposes of load combination with other mandated load cases, the maximum circumferential stress at the middle surface in each layer is designated as the fabrication membrane stress level for the layer and is used in the load combination process in the overpack finite element post-processor. The fabrication stresses generated here are also included in the appropriate Code Case N-284 evaluations since a compressive stress state is developed. The notations "inner, outer, and middle" used in the tables refer to inner surface, outer surface, and mid-plane stress locations for the respective layers.

3.L.4 Conclusions

The finite element solution has identified appropriate circumferential stresses in the various shells of the overpack due to the fabrication process. These stresses are required to be added to the stress components obtained from the finite element analysis of other load cases, and the safety margins on stress intensity reported include the fabrication stress effect.

Where appropriate, the fabrication stresses reported herein need to be included in the Code Case N-284 evaluations of the overpack confinement shell.

Table 3.L.1

FABRICATION STRESS S_m (psi) IN THE
OVERPACK CONFINEMENT AND INTERMEDIATE SHELLS
(COF = 0.0)

Location (degrees)	Confinement Shell	Intermediate Shells				
		1	2	3	4	Outer
-90	Inner -16266	11219	9369	8539	7787	6189
	Outer -4569	172	-351	-165.0	-115	294
	Middle -10418	5695	4509	4187	3836	3241
-80	Inner -14256	8218	7300	6776	6068	5048
	Outer -6756	3895	1606	1496	1506	1358
	Middle -10506	6057	4453	4136	3787	3203
0	Inner -8716	3063	4571	3932	4229	2583
	Outer -11185	6133	4678	3858	3823	4295
	Middle -9951	4598	4625	3895	4026	3439
90	Inner -11399	1597	5371	4693	4694	4637
	Outer -7416	5171	4295	3489	2445	2738
	Middle -9408	3384	4833	4091	3570	3687

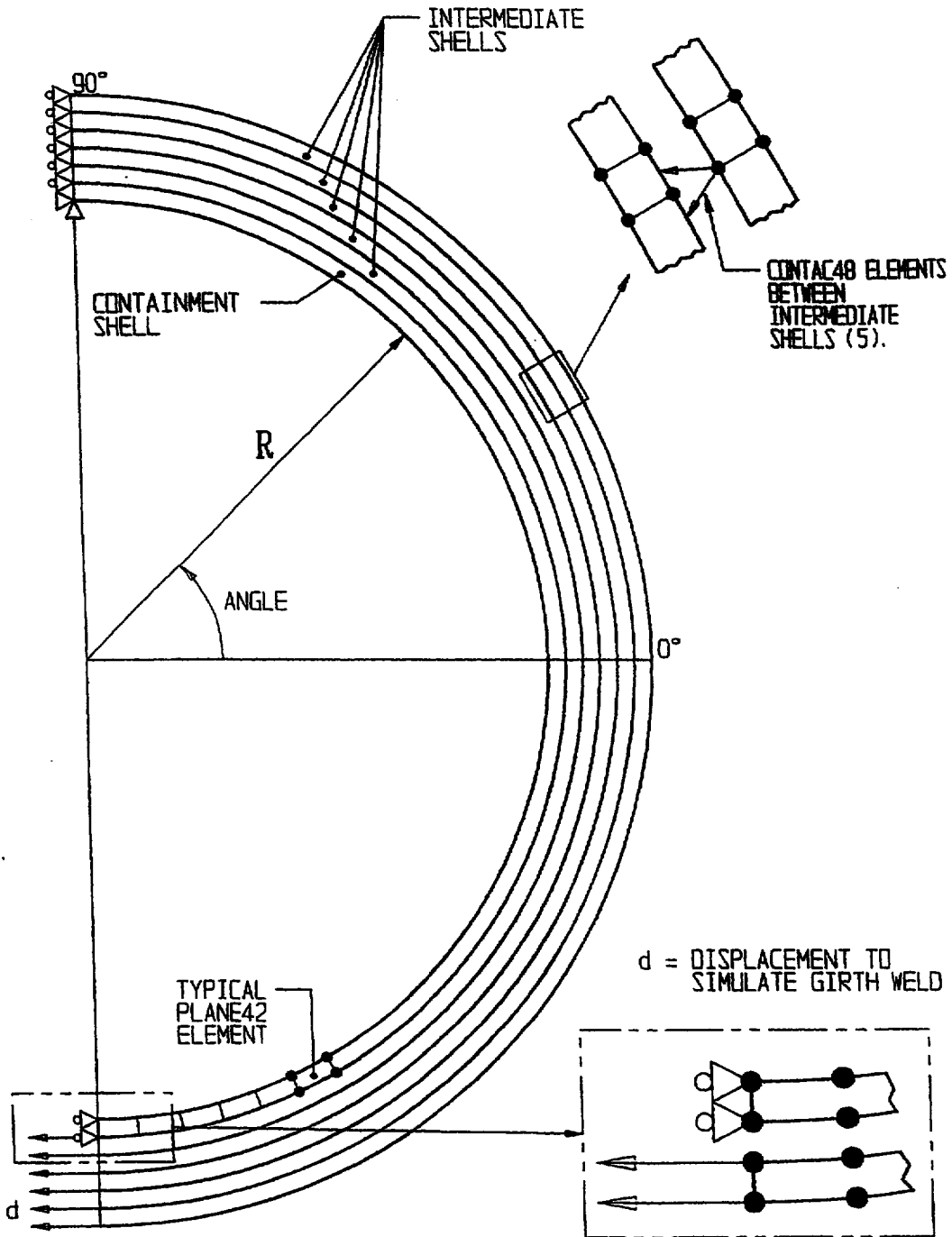
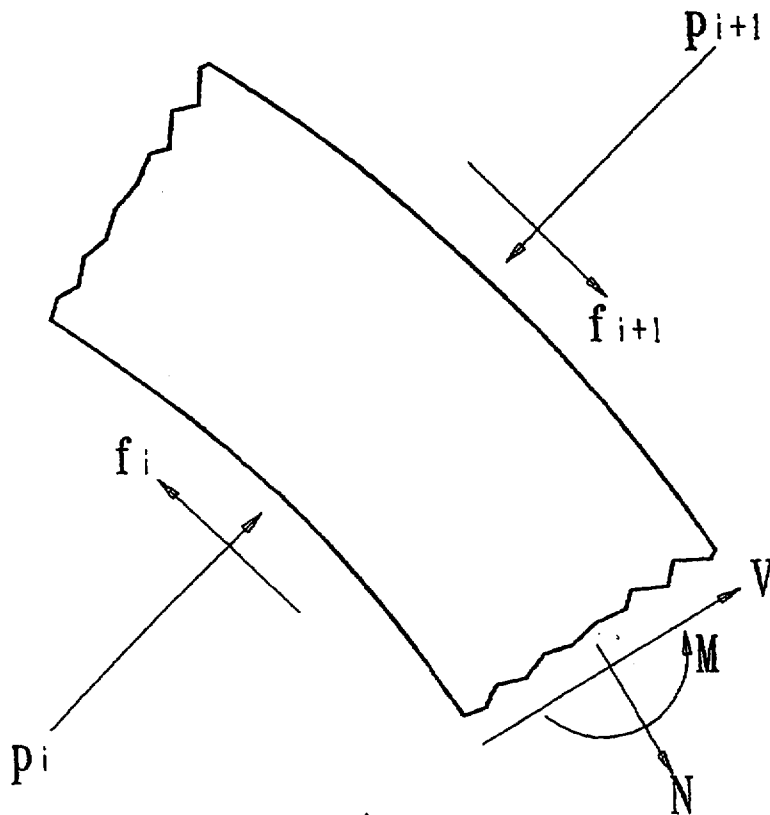


FIGURE 3.L.1; SIMULATION MODEL FOR FABRICATION STRESSES IN THE OVERPACK



$$|f_i| \leq \text{COF} * |p_i|$$

COF = COEFFICIENT OF FRICTION

FIGURE 3.L.2; PARTIAL FREE BODY DIAGRAM OF A SHELL SECTION

APPENDIX 3.M: MISCELLANEOUS CALCULATIONS

3.M.1 CALCULATION FOR THE FILLET WELDS IN THE FUEL BASKET

The fillet welds in the fuel basket honeycomb are made by an autogenous operation that has shown to produce highly consistent and porosity free weld lines. However, Subsection NG of the ASME Code permits only 40% quality credit on double fillet welds that can be only visually examined. Subsection NG, however, fails to provide specific stress limit on such fillet welds. In the absence of a Code mandated limit, Holtec International's standard design procedure requires that the weld section possess as much load resistance capability as the parent metal section. Since the loading on the honeycomb panels is essentially that of section bending, it is possible to develop a closed form expression for the required weld throat t corresponding to panel thickness h .

We refer to Figure 3.M.1 that shows a unit depth of panel-to-panel joint subjected to moment M .

The stress distribution in the panel is given by the classical Kirchoff beam formula

$$S_p = \frac{6M}{h^2}$$

or

$$M = \frac{S_p h^2}{6}$$

S_p is the extreme fiber stress in the panel.

Assuming that the panel edge-to-panel contact region develops no resistive pressure, Figure 3.M.1(c) shows the free body of the dual fillet welds. F is the net compressive or tensile force acting on the surface of the leg of the weld.

From moment equilibrium

$$M = F(h + t)$$

Following standard weld design practice, we assume that the shear stress on the throat of the weld

is equal to the force F divided by the weld throat area. If we assume 40% weld efficiency, minimum weld throat, and define S_w as the average shear stress on the weld throat, then for a unit depth of weld,

$$F = S_w (0.707)(0.4) t$$

$$F = 0.283 S_w t$$

Then, since M is given in terms of F , we can write M in terms of S_w . Also, a relation exists between M and S_p . Between these two expressions for M , we can eliminate M and arrive at a relationship between S_w , S_p , the weld size t , and the basket panel thickness h :

$$M = 0.283 S_w t (h + t)$$

$$0.283 S_w (ht + t^2) = \frac{S_p h^2}{6}$$

This is to be solved for the weld by thickness t that is required for a panel thickness h . The relationship between S_p and S_w is evaluated using the most limiting hypothetical accident condition. The allowable base metal membrane plus bending stress intensity is (Table 3.1.16):

$$S_p = 55,450 \text{ psi at } 725^\circ \text{F}$$

The appropriate limit for the weld stress S_w is set at

$$S_w = 0.42 S_u$$

Table 3.3.1 gives a value for the ultimate strength of the base metal as 62,350 psi at 725°F. The weld metal used at the panel connections is one grade higher in ultimate tensile stress than the adjacent

base metal (80,000 psi at room temperature compared with 75,000 for the base metal at room temperature).

The strength of the weld is assumed to decrease with temperature the same as the base metal.

$$S_w = .42 \times 80,000 \left(\frac{62,350}{75,000} \right) = 27,930 \text{ psi}$$

Therefore, the corresponding limit stress on the weld throat is

$$h^2 = (0.283) (6) \frac{S_w}{S_p} (ht + t^2)$$

$$h^2 = 1.698 \frac{S_w}{S_p} (ht + t^2)$$

The equation given above establishes the relationship between the weld size “t”, the fuel basket panel wall thickness “h”, and the ratio of allowable weld strength “S_w” to base metal allowable strength “S_p”. We now apply this formula to establish the *minimum* fillet weld size to be specified on the design drawings to insure a factor of safety of 1.0 subsequent to incorporation of the appropriate dynamic load amplifier. Table 3.4.9 gives fuel basket safety factors “SF” for primary membrane plus bending stress intensities corresponding to the base metal allowable strength S_p at 725 degrees F. Similarly, Appendix 3.X provides dynamic amplification factors “DAF” for each fuel basket type. To establish the minimum permissible weld size, S_p is replaced in the above formula by (S_px(DAF/SF)), and t/h computed for each basket. The following results are obtained:

MINIMUM WELD SIZE FOR FUEL BASKETS					
Item	SF (Table 3.4.9)	DAF (Appendix 3.X)	t/h	h (inch)	t (inch)
MPC-24	1.17	1.03	0.631	10/32	0.197
MPC-68	1.56	1.08	0.529	8/32	0.132

Sheathing Weld Capacity

Simple force equilibrium relationships are used to demonstrate that the sheathing weld is adequate to support a 60g deceleration load applied vertically and horizontally to the sheathing and to the confined Boral.

Definitions

h = height of weld line (in.)

w = width of weld line (in.)

t_w = weld size

e = 0.3 = quality factor for single fillet weld

W_b = weight of a Boral panel (lbf)

W_s = weight of sheathing confining a Boral panel (lbf)

G = 60

S_w = weld shear stress (psi)

Equations

Weld area = $2 (0.707 t_w e) (h)$ (Neglect the top and bottom of the sheathing)

Load on weld = $(W_b + W_s) G$

Weld stress from combined action of vertical plus horizontal load in each of the two directions

$$S_w = \sqrt{(3)} \frac{G (W_b + W_s)}{2 (.707) e t_w (h)}$$

For a PWR panel, the weights are calculated as

$$W_b = 11.35 \text{ lb.}$$

$$W_s = 28.0 \text{ lb.}$$

The weld size is conservatively assumed as a 1/16" fillet weld, and the length and width of the weld line is

$$h = 156 \text{ in.}$$

$$w = 7.5 \text{ in.}$$

Therefore,

$$S_w = \frac{60 \times (11.35 + 28) \times 1.732}{1.414 \times 0.3 \times (1/16)(156)} = 989 \text{ psi}$$

For an MPC-68 panel, the corresponding values are

$$W_b = 7.56 \text{ lb.}$$

$$W_s = 17.48 \text{ lb.}$$

$$h = 156 \text{ in.}$$

$$W = 5 \text{ in.}$$

$$S_w = \frac{60 \times (7.56 + 17.48) \times 1.732}{1.414 \times 0.3 \times (1/16 \text{ in.})(139 \text{ in.})} = 706 \text{ psi}$$

The actual welding specified along the length of a sheathing panel is 2" weld on 8" pitch. The effect of the intermittent weld is to raise the average weld shear stress by a factor of 4. From the above results, it is concluded that the sheathing weld stress is negligible during the most severe drop accident.

3.M.2 Calculation for MPC Cover Plates in MPC Lid

The MPC cover plates are welded to the MPC lid during loading operations. The cover plates are part of the confinement boundary for the MPC. No credit is taken for the pressure retaining abilities of the quick disconnect couplings for the MPC vent and drain. Therefore, the MPC cover plates must meet ASME Code, Section III, Subsection NB limits for normal, off-normal, and accident conditions.

The normal and off-normal condition design basis MPC internal pressure is 100 psi. The accident condition design basis MPC internal pressure is 125 psi. Conservatively, the accident condition pressure loading is applied and it is demonstrated that the Level A limits for Subsection NB are met.

The MPC cover plate is depicted in the Design Drawings. The cover plate is stepped and has a maximum and minimum thickness of 0.38 inches and 0.1875 inches, respectively. Conservatively, the minimum thickness is utilized for these calculations.

To verify the MPC cover plate maintains the MPC internal pressure while meeting the ASME Code, Subsection NB limits, the cover plate bending stress and shear stress, and weld stress are calculated and compared to allowables.

Definitions

P = accident condition MPC internal pressure (psi) = 125 psi

r = cover plate radius (in.) = 2 in.

t = cover plate minimum thickness (in.) = 0.1875 in.

t_w = weld size (in.) = 0.1875 in.

The design temperature of the MPC cover plate is conservatively taken as equal to the MPC lid, 550°F. The peak temperature of the MPC lid is experienced on the internal portion of the MPC lid, and the actual operating temperature of the top surface is less than 400°F.

For the design temperature of 550°F, the Alloy X allowable membrane stress intensity is

$$S_m = 16,950 \text{ psi}$$

The allowable weld shear stress is 0.3 S_u per Subsection NF of the ASME Code for Level A conditions.

Calculations

Using Timoshenko, Strength of Materials, Part II, Advanced Theory and Problems, Third Edition, page 99, the formula for the bending stress in the cover plate is:

$$S_b = \frac{(9.9)(P)(r^2)}{(8)(t^2)} \quad (\nu = 0.3)$$

$$S_b = \frac{(9.9)(125 \text{ psi})(2 \text{ in})^2}{(8)(0.1875 \text{ in})^2}$$

$$S_b = 17,600 \text{ psi}$$

The allowable bending stress is $1.5S_m$; therefore, $S_b < 1.5S_m$ (i.e., $17,600 \text{ psi} < 24,425 \text{ psi}$).

The shear stress in the cover plate due to the accident MPC internal pressure is calculated as follows

$$\tau = \frac{P \pi r^2}{2 \pi r t}$$

$$\tau = \frac{(125 \text{ psi})(\pi)(2 \text{ in})^2}{(2)(\pi)(2 \text{ in})(0.1875 \text{ in})^2}$$

$$\tau = 667 \text{ psi}$$

This shear stress is less than the Level A limit of $0.4S_m = 6,780 \text{ psi}$.

The weld size is equal to the minimum cover plate thickness and therefore the weld stress can be calculated from the cover plate shear stress. The stress in the weld is calculated by dividing the shear stress in the cover plate by 0.707 and applying a quality factor 0.3.

$$S_w = \frac{667 \text{ psi}}{0.707 \times 0.3}$$

$$S_w = 3,145 \text{ psi}$$

$$S_w < 0.3S_u = 0.3 \times 63,300 \text{ psi} = 18,990 \text{ psi}$$

The Level A weld stress limit of 30% of the ultimate strength (at 550°F) has been taken from Section NF of the ASME Code, the only section that specifically addresses stress limits for welds.

The stress developed as a result of the accident condition MPC internal pressure has been conservatively shown to be below the Level A, Subsection NB, ASME Code limits. The MPC cover plates meet the stress limits for normal, off-normal, and accident conditions at design temperature.

PAGE 3.M-8 IS INTENTIONALLY LEFT BLANK

3.M.3 Fuel Basket Angle Support Stress Calculations

The fuel basket internal to the MPC canister is supported by a combination of angle fuel basket supports and flat plate or solid bar fuel basket supports. These fuel basket supports are subject to significant load only when a lateral acceleration is applied to the fuel basket and the contained fuel. The quasi-static finite element analyses of the MPC's, under lateral inertia loading, focused on the structural details of the fuel basket and the MPC shell. Basket supports were modeled in less detail which served only to properly model the load transfer path between fuel basket and canister. Safety factors reported for the fuel basket supports from the finite element analyses, are overly conservative, and do not reflect available capacity of the fuel basket angle support. A more detailed stress analysis of the fuel basket angle supports is performed herein. We perform a strength of materials analysis of the fuel basket angle supports that complements the finite element results. We compute weld stresses at the support-to-shell interface, and membrane and bending stresses in the basket support angle plate itself. Using this strength of materials approach, we demonstrate that the safety factors for the fuel basket angle supports are larger than indicated by the finite element analysis.

The fuel basket supports of interest are angled plate components that are welded to the MPC shell using continuous single fillet welds. The design drawings and bill of materials in Section 1.5 of this submittal define the location of these supports for all MPC constructions. These basket supports experience no loading except when the fuel assembly basket and contained fuel is subject to lateral deceleration loads either from normal handling or accident events.

In this section, the analysis proceeds in the following manner. The fuel basket support loading is obtained by first computing the fuel basket weight (cell walls plus Boral plus sheathing) and adding to it the fuel weight. To maximize the support load, the MPC is assumed to be fully populated with fuel assemblies. This total calculated weight is then amplified by the design basis deceleration load and divided by the length of the fuel basket support. The resulting value is the load per unit length that must be resisted by all of the fuel basket supports. We next conservatively estimate, from the drawings for each MPC, the number of cells in a direct line (in the direction of the deceleration) that is resisted by the most highly loaded fuel basket angle support. We then compute the resisting load on the particular support induced by the inertia load from this number of cells. Force equilibrium on a simplified model of the fuel basket angle support then provides the weld load and the axial force and bending moment in the fuel basket support.

The computation of safety factors is performed for a 60G load that bounds the non-mechanistic tip-over accident in the HI-STAR 100.

This entire section of Appendix 3.M has been written using Mathcad; all computations are performed directly within the document. The notation "==" represents an equality.

We first establish as input data common to all three MPC's, the allowable weld shear stress. In section 3.M.1, the allowable weld stress for a Level D accident event defined. We further reduce this allowable stress by an appropriate weld efficiency obtained from the ASME Code, Section III, Subsection NG, Table NG-3352-1.

Weld efficiency $e := 0.35$ (single fillet weld, visual inspection only)

The fuel support brackets are constructed from Alloy "X". At the canister interface,

Ultimate Strength $S_u := 64000 \cdot \text{psi}$ Alloy X @ 450 degrees F (Table 3.3.1)

Note that here we use the design temperature for the MPC shell under normal conditions (Table 2.2.3) since the fire accident temperature is not applicable during the tip-over. The allowable weld shear stress, incorporating the weld efficiency is (use the base metal ultimate strength for additional conservatism) determined as:

$$\tau_{\text{all}} := .42 \cdot S_u \cdot e \quad \tau_{\text{all}} = 9.408 \times 10^3 \text{ psi}$$

For the non-mechanistic tip-over, the design basis deceleration in "g's" is

$$G := 60 \quad (\text{Table 3.1.2})$$

The total load to be resisted by the fuel basket supports is obtained by first computing the moving weight, relative to the MPC canister, for each MPC.

The weights of the fuel baskets and total fuel load are (the notation "lbf" = "pound force")

Fuel Basket	Fuel	
$W_{\text{mpc68}} := 15263 \cdot \text{lbf}$	$W_{\text{f68}} := 47600 \cdot \text{lbf}$	MPC-68
$W_{\text{mpc24}} := 18725 \cdot \text{lbf}$	$W_{\text{f24}} := 40320 \cdot \text{lbf}$	MPC-24

The minimum length of the fuel basket support is $L := 168 \cdot \text{in}$

Dwg. 1396, sheet 1 Note that for the MPC-68, the support length is increased by 1/2"

Therefore, the load per unit length that acts along the line of action of the deceleration, and is resisted by the total of all supports, is computed as

$$Q_{68} := \frac{(W_{mpc68} + W_{f68}) \cdot G}{(L + 0.5 \cdot \text{in})}$$

$$Q_{68} = 2.238 \times 10^4 \frac{\text{lbf}}{\text{in}}$$

$$Q_{24} := \frac{(W_{mpc24} + W_{f24}) \cdot G}{L}$$

$$Q_{24} = 2.109 \times 10^4 \frac{\text{lbf}}{\text{in}}$$

The subscript associated with the above items is used as the identifier for the particular MPC.

An examination of the MPC construction drawings 1395, 1401, (sheet 1 of each drawing) indicates that the deceleration load is supported by shims and by fuel basket angle supports. By inspection of the relevant drawing, we can determine that the most highly loaded fuel basket angle support will resist the deceleration load from "NC" cells where NC for each basket type is obtained by counting the cells and portions of cells "above" the support in the direction of the deceleration. The following values for NC are used in the subsequent computation of fuel basket angle support stress:

$$NC_{68} := 8$$

$$NC_{24} := 7$$

The total normal load per unit length on the fuel basket support for each MPC type is therefore computed as:

$$P_{68} := Q_{68} \cdot \frac{NC_{68}}{68}$$

$$P_{68} = 2.633 \times 10^3 \frac{\text{lbf}}{\text{in}}$$

$$P_{24} := Q_{24} \cdot \frac{NC_{24}}{24}$$

$$P_{24} = 6.151 \times 10^3 \frac{\text{lbf}}{\text{in}}$$

Here again, the subscript notation identifies the particular MPC.

Figure 3.M.2 shows a typical fuel basket support with the support reactions at the base of the leg. The applied load and the loads necessary to put the support in equilibrium is not subscripted since the figure is meant to be typical of any MPC fuel basket angle support. The free body is drawn in a conservative manner by assuming that the load P is applied at the quarter point of the top flat portion. In reality, as the load is applied, the top flat portion deforms and the load shifts completely to the outer edges of the top flat section of the support. From the design drawings, we use the appropriate dimensions and perform the following analyses (subscripts are introduced as necessary as MPC identifiers):

The free body diagram shows the bending moment that will arise at the location where the idealized top flat section and the angled support are assumed to meet. Compatibility of joint rotation at the connection between the top flat and the angled portion of the support plus force and moment equilibrium equations from classical beam theory provide sufficient equations to solve for the bending moment at the connection (point O in Figure 3.M.2), the load R at the weld, and the bending moment under the load P/2.

$$M_o := \frac{9}{16} \cdot \frac{Pw^2}{(S + 3 \cdot w)}$$

Note that the small block after the equation indicates that this is a text equation rather than an evaluated equation. This is a Mathcad identifier.

The load in the weld, R, is expressed in the form

$$R := \frac{P \cdot H}{2 \cdot L} + \frac{M_o}{L}$$

Finally, the bending moment under the load, on the top flat portion, is given as

$$M_p := \frac{P}{2} \cdot \frac{w}{2} - M_o$$

Performing the indicated computations and evaluations for each of the MPC's gives:

MPC-24 (Dwg.1395 sheet 4)

$$\theta_{24} := 9 \text{ deg} \quad L_{24} := 4 \text{ in} \quad w_{24} := \left(0.25 + .125 + .5 \cdot \frac{5}{16} \right) \text{ in}$$

Therefore

$$H_{24} := L_{24} \tan(\theta_{24}) \quad H_{24} = 0.634 \text{ in} \quad w_{24} = 0.531 \text{ in}$$

$$S := \sqrt{L_{24}^2 + H_{24}^2} \quad S = 4.05 \text{ in}$$

$$M_o := \frac{9}{16} \cdot \frac{(P_{24} \cdot w_{24}^2)}{(S + 3 \cdot w_{24})} \quad M_o = 173.012 \text{ lbf} \cdot \frac{\text{in}}{\text{in}}$$

$$R_{24} := \frac{P_{24} \cdot H_{24}}{2 \cdot L_{24}} + \frac{M_o}{L_{24}} \quad R_{24} = 530.326 \frac{\text{lbf}}{\text{in}}$$

$$M_p := \frac{P_{24}}{2} \cdot \frac{w_{24}}{2} - M_o \quad M_p = 643.854 \text{ lbf} \cdot \frac{\text{in}}{\text{in}}$$

The fillet weld throat thickness is

$$t_w := 0.125 \cdot \text{in} \cdot 0.7071$$

The weld stress is

$$\tau_{\text{weld}} := \frac{R_{24}}{t_w} \quad \tau_{\text{weld}} = 6 \times 10^3 \text{ psi}$$

For this event, the safety factor on the weld is

$$SF_{\text{weld}} := \frac{\tau_{\text{all}}}{\tau_{\text{weld}}} \quad SF_{\text{weld}} = 1.568$$

For computation of member stresses, the wall thickness is

$$t_{\text{wall}} := \frac{5}{16} \cdot \text{in}$$

The maximum bending stress in the angled member is

$$\sigma_{\text{bending}} := 6 \cdot \frac{M_o}{t_{\text{wall}}^2} \quad \sigma_{\text{bending}} = 1.063 \times 10^4 \text{ psi}$$

The direct stress in the basket support angled section is

$$\sigma_{\text{direct}} := \frac{(R_{24} \cdot \sin(\theta_{24}) + .5 \cdot P_{24} \cdot \cos(\theta_{24}))}{t_{\text{wall}}} \quad \sigma_{\text{direct}} = 9.985 \times 10^3 \text{ psi}$$

From Table 3.1.16, the allowable membrane stress intensity for this condition is

$$S_{\text{membrane}} := 39400 \cdot \text{psi} \quad (\text{use the value at 600 degree F to conservatively bound the Safety Factor})$$

$$SF_{\text{membrane}} := \frac{S_{\text{membrane}}}{\sigma_{\text{direct}}} \quad SF_{\text{membrane}} = 3.946$$

From Table 3.1.16, the allowable combined stress intensity for this accident condition is

$$S_{\text{combined}} := 59100 \cdot \text{psi} \quad (\text{use the value at 600 degree F to conservatively bound the Safety Factor})$$

$$SF_{\text{combined}} := \frac{S_{\text{combined}}}{\sigma_{\text{direct}} + \sigma_{\text{bending}}} \quad SF_{\text{combined}} = 2.867$$

Note that for this model, it is appropriate to compare the computed stress with allowable stress intensities since we are dealing with beams and there are no surface pressure stresses

$$SF_{\text{membrane}} := \frac{S_{\text{membrane}}}{\sigma_{\text{direct}}} \quad SF_{\text{membrane}} = 3.946$$

$$SF_{\text{combined}} := \frac{S_{\text{combined}}}{\sigma_{\text{direct}} + \sigma_{\text{bending}}} \quad SF_{\text{combined}} = 2.867$$

The maximum bending stress in the top flat section is

$$\sigma_{\text{bending}} := 6 \cdot \frac{M_p}{t_{\text{wall}}^2} \quad \sigma_{\text{bending}} = 3.956 \times 10^4 \text{ psi}$$

The direct stress in the basket support top flat section is

$$\sigma_{\text{direct}} := \frac{R_{24}}{t_{\text{wall}}} \quad \sigma_{\text{direct}} = 1.697 \times 10^3 \text{ psi}$$

Computing the safety factors gives:

$$SF_{\text{membrane}} := \frac{S_{\text{membrane}}}{\sigma_{\text{direct}}} \quad SF_{\text{membrane}} = 23.217$$

$$SF_{\text{combined}} := \frac{S_{\text{combined}}}{\sigma_{\text{direct}} + \sigma_{\text{bending}}} \quad SF_{\text{combined}} = 1.433$$

All safety factors are greater than 1.0; therefore, the design is acceptable

MPC-68 (Dwg 1401 sheet 4)

$$\theta_{68} := 12.5 \cdot \text{deg} \quad L_{68} := 4.75 \cdot \text{in (estimated)} \quad w_{68} := \left(0.75 - .5 \cdot \frac{5}{16} \right) \cdot \text{in}$$

Note that in the MPC-68, there is no real top flat portion to the angle support. "w" is computed as the radius of the bend less 50% of the wall thickness. However, in the remaining calculations, the applied load is assumed a distance w/2 from the center on each side of the support centerline in Figure 3.M.2.

Therefore

$$H_{68} := L_{68} \cdot \tan(\theta_{68}) \quad H_{68} = 1.053 \text{ in} \quad w_{68} = 0.594 \text{ in}$$

$$S := \sqrt{L_{68}^2 + H_{68}^2} \quad S = 4.865 \text{ in}$$

$$M_o := \frac{9}{16} \cdot \frac{P_{68} \cdot w_{68}^2}{(S + 3 \cdot w_{68})} \quad M_o = 78.57 \text{ lbf} \cdot \frac{\text{in}}{\text{in}}$$

$$R_{68} := \frac{P_{68} \cdot H_{68}}{2 \cdot L_{68}} + \frac{M_o}{L_{68}} * \quad R_{68} = 308.454 \frac{\text{lbf}}{\text{in}}$$

$$M_p := \frac{P_{68}}{2} \cdot \frac{w_{68}}{2} - M_o * \quad M_p = 312.334 \text{ lbf} \cdot \frac{\text{in}}{\text{in}}$$

The weld stress is

$$\tau_{\text{weld}} := \frac{R_{68}}{t_w} \quad \tau_{\text{weld}} = 3.49 \times 10^3 \text{ psi}$$

The safety factor on the weld is

$$SF_{\text{weld}} := \frac{\tau_{\text{all}}}{\tau_{\text{weld}}} \quad SF_{\text{weld}} = 2.696$$

The maximum bending stress in the angled member is

$$\sigma_{\text{bending}} := 6 \cdot \frac{M_o}{t_{\text{wall}}^2} \quad \sigma_{\text{bending}} = 4.827 \times 10^3 \text{ psi}$$

The direct stress in the basket support angled section is

$$\sigma_{\text{direct}} := \frac{(R_{68} \cdot \sin(\theta_{68}) + .5 \cdot P_{68} \cdot \cos(\theta_{68}))}{t_{\text{wall}}} \quad \sigma_{\text{direct}} = 4.327 \times 10^3 \text{ psi}$$

$$SF_{\text{membrane}} := \frac{S_{\text{membrane}}}{\sigma_{\text{direct}}} \quad SF_{\text{membrane}} = 9.105$$

$$SF_{\text{combined}} := \frac{S_{\text{combined}}}{\sigma_{\text{direct}} + \sigma_{\text{bending}}} \quad SF_{\text{combined}} = 6.456$$

The maximum bending stress in the idealized top flat section is

$$\sigma_{\text{bending}} := 6 \cdot \frac{M_p}{t_{\text{wall}}^2} \quad \sigma_{\text{bending}} = 1.919 \times 10^4 \text{ psi}$$

The direct stress in the basket support top flat section is

$$\sigma_{\text{direct}} := \frac{R_{68}}{t_{\text{wall}}} \quad \sigma_{\text{direct}} = 987.052 \text{ psi}$$

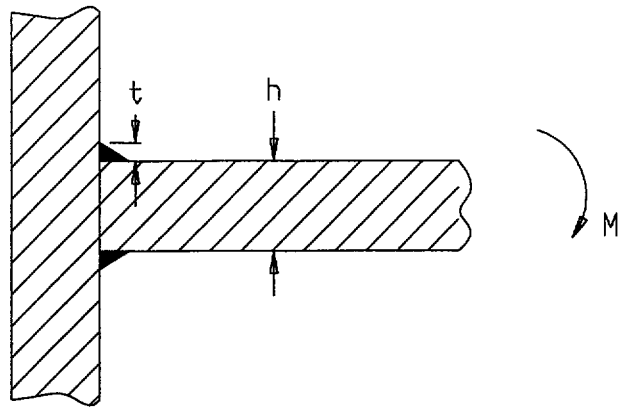
$$SF_{\text{membrane}} := \frac{S_{\text{membrane}}}{\sigma_{\text{direct}}} \quad SF_{\text{membrane}} = 39.917$$

$$SF_{\text{combined}} := \frac{S_{\text{combined}}}{\sigma_{\text{direct}} + \sigma_{\text{bending}}} \quad SF_{\text{combined}} = 2.929$$

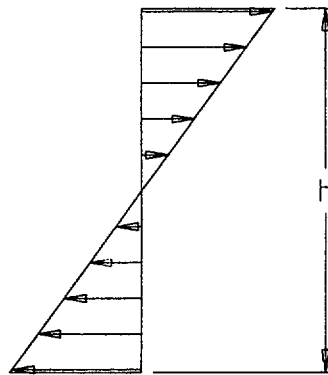
All safety factors are greater than 1.0; therefore, the design is acceptable

SUMMARY OF RESULTS

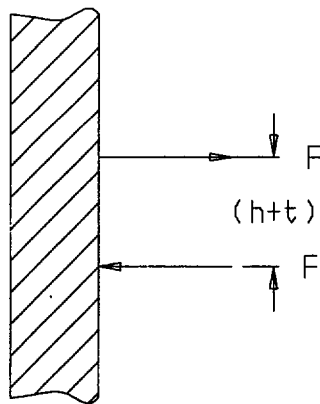
The above calculations demonstrate that for all MPC fuel basket angle supports, the minimum safety margin is 1.43 (MPC-24 combined membrane plus bending in the top flat section). This is a larger safety factor than predicted from the finite element solution. The reason for this increase is attributed to the fact that the finite element analysis used a less robust structural model of the supports for stress analysis purposes since the emphasis there was on analysis of the fuel basket itself and the MPC canister. Therefore, in reporting safety factors, or safety margins, the minimum safety factor of 1.43 can be used for this component in any summary table.



(a) Loading Configuration

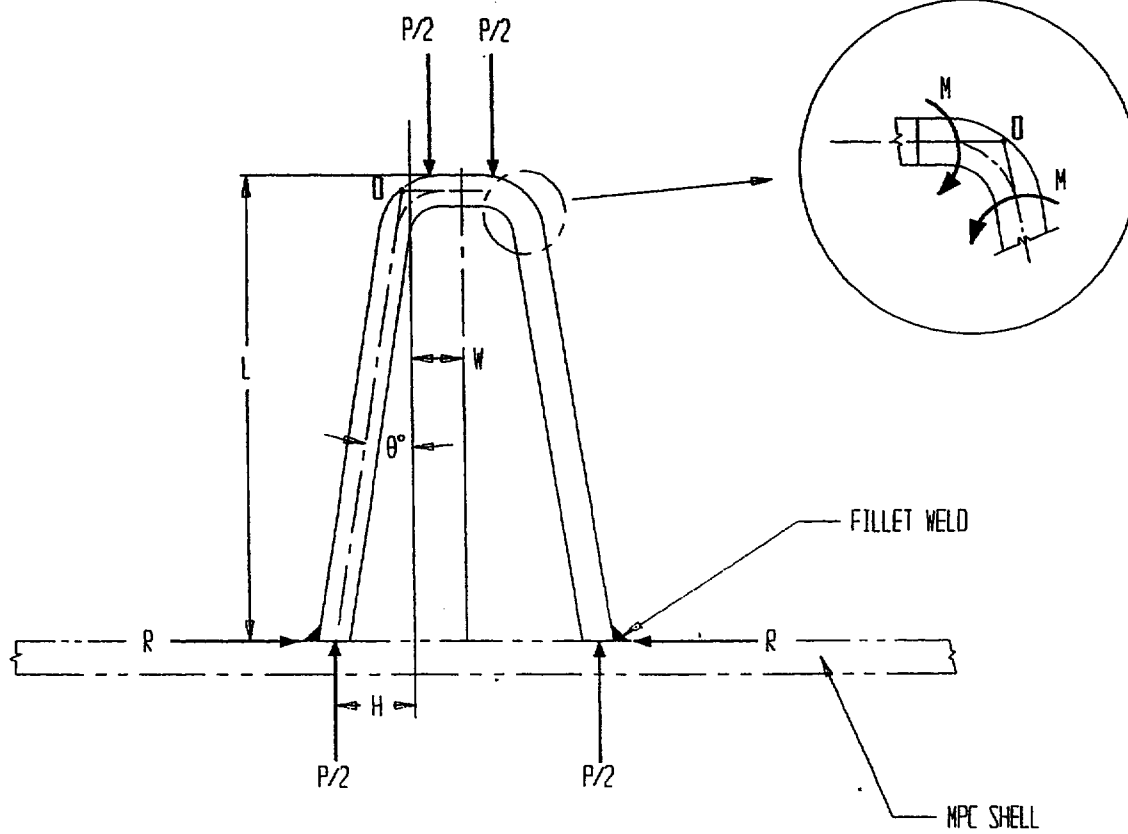


(b) Bending Stress in the Panel



(c) Reaction in the Welds

**FIGURE 3.M.1; FREEBODY OF STRESS DISTRIBUTION IN THE WELD
AND THE HONEYCOMB PANEL**



$$S^2 = L^2 + H^2$$

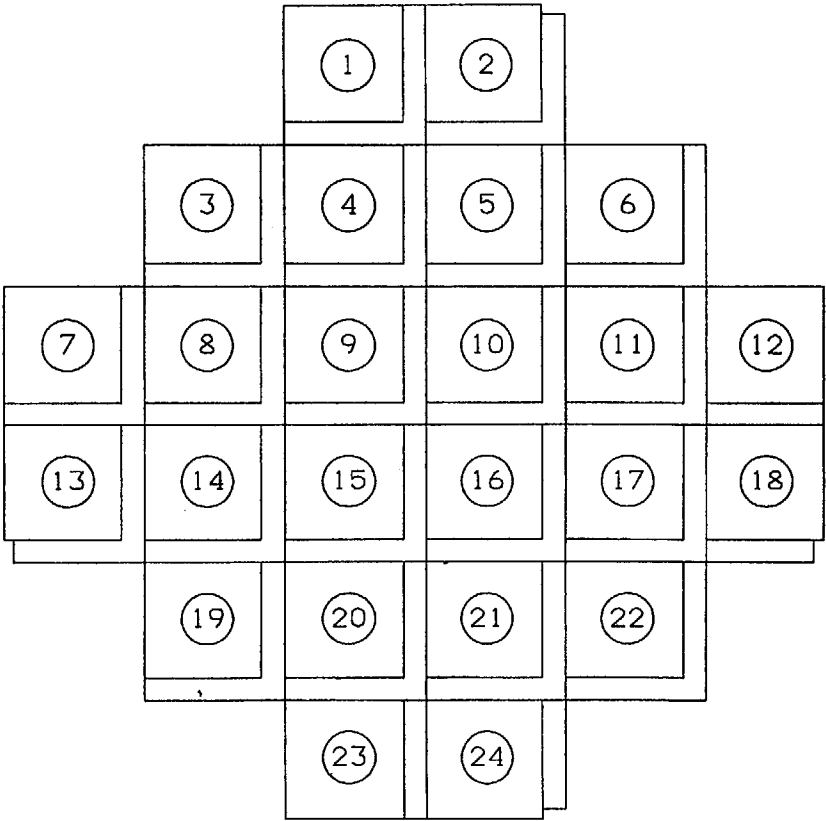
WHERE

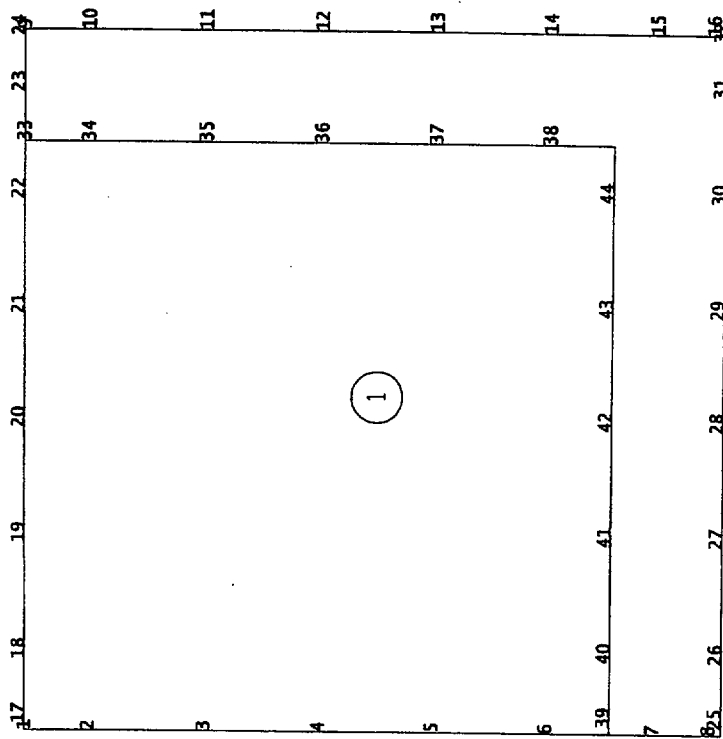
S = LENGTH OF ANGLED SECTION

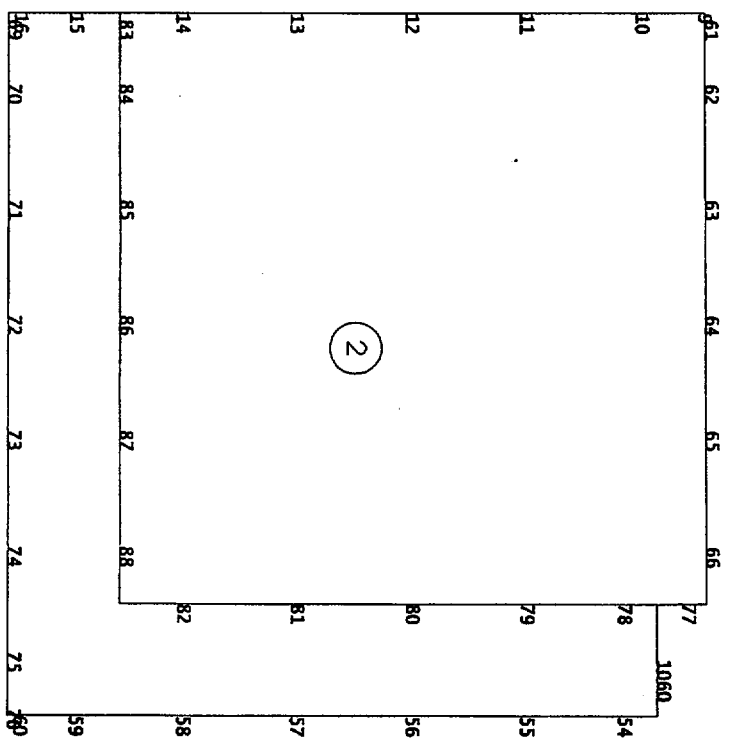
FIGURE 3.M.2: FREEBODY OF IDEALIZED FUEL BASKET SUPPORT

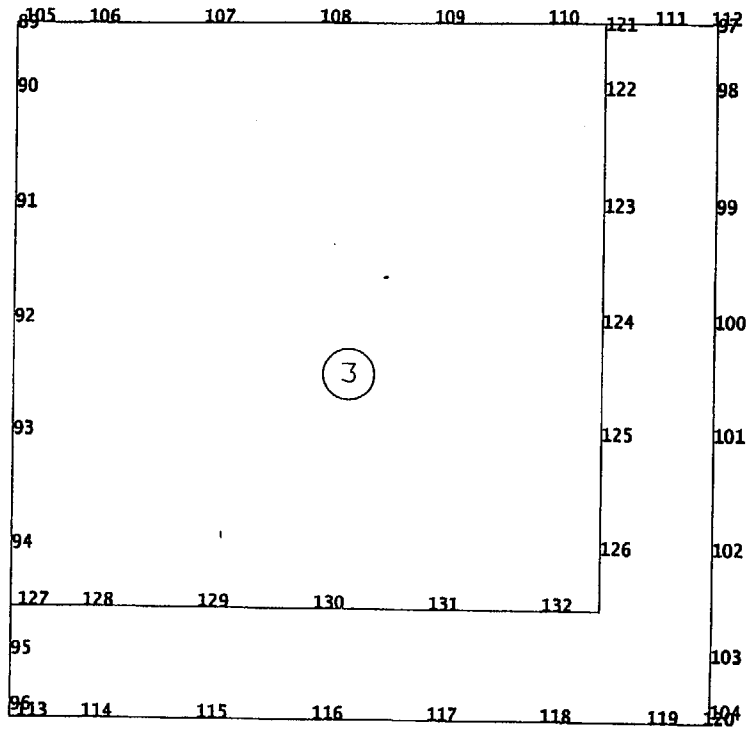
Appendix 3.N – Detailed Finite Element Listings for the MPC-24 Fuel Basket

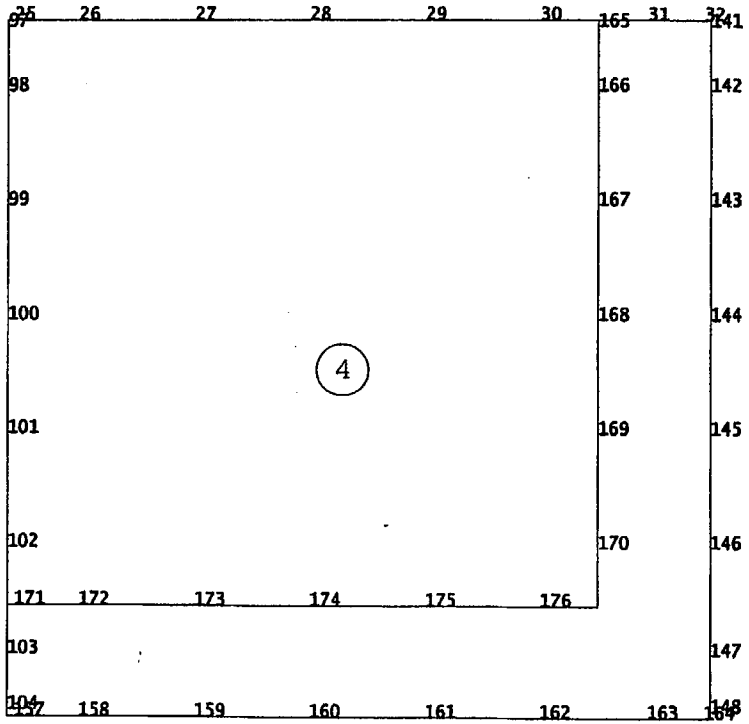
Twenty six (26) pages total including cover page

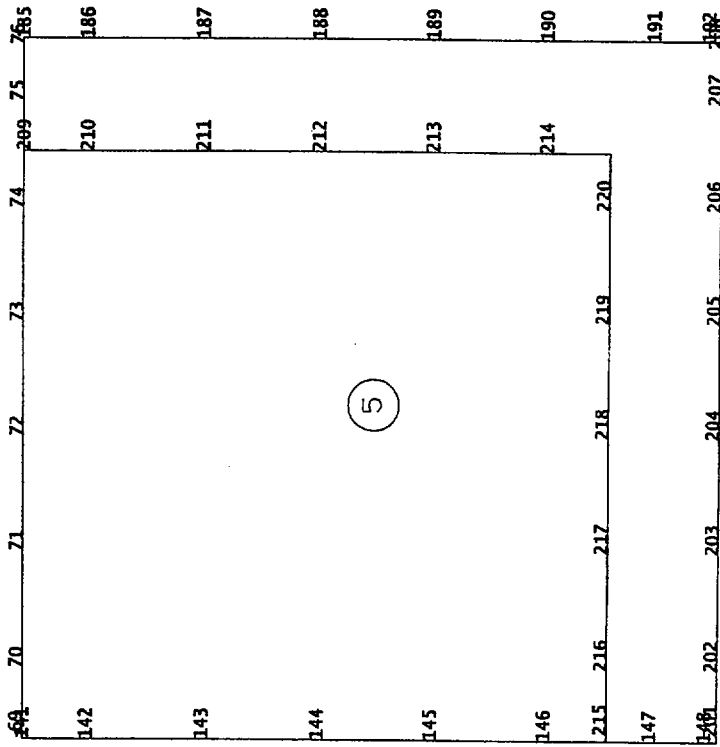


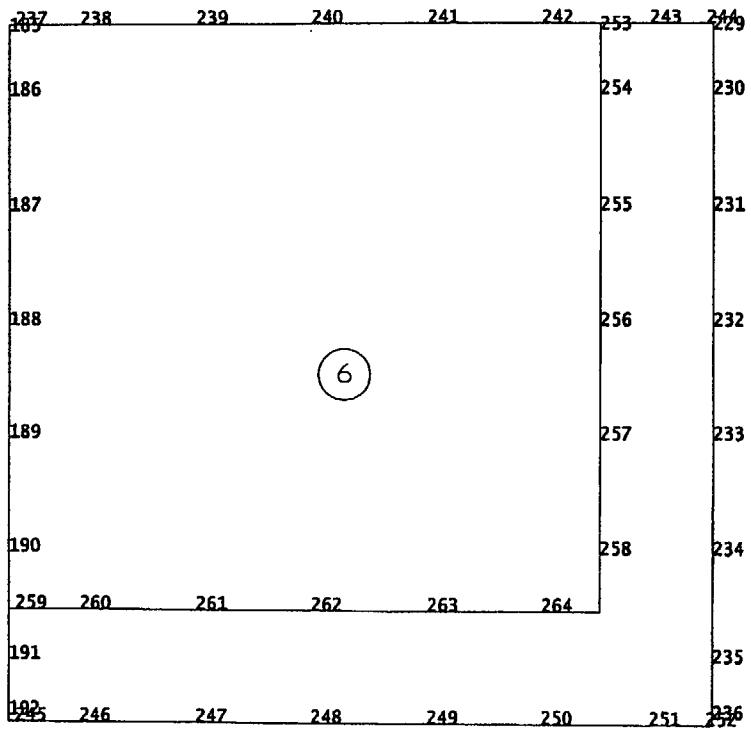


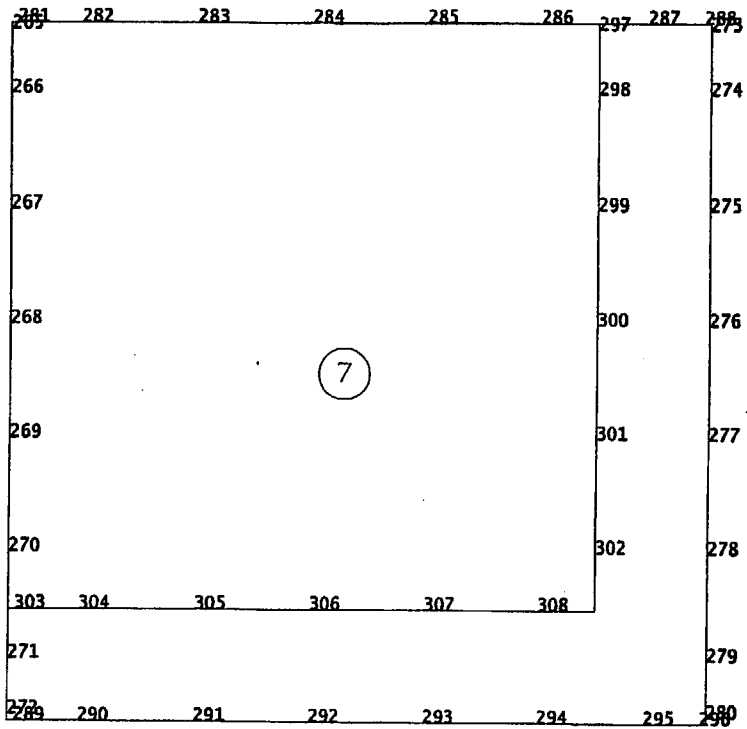


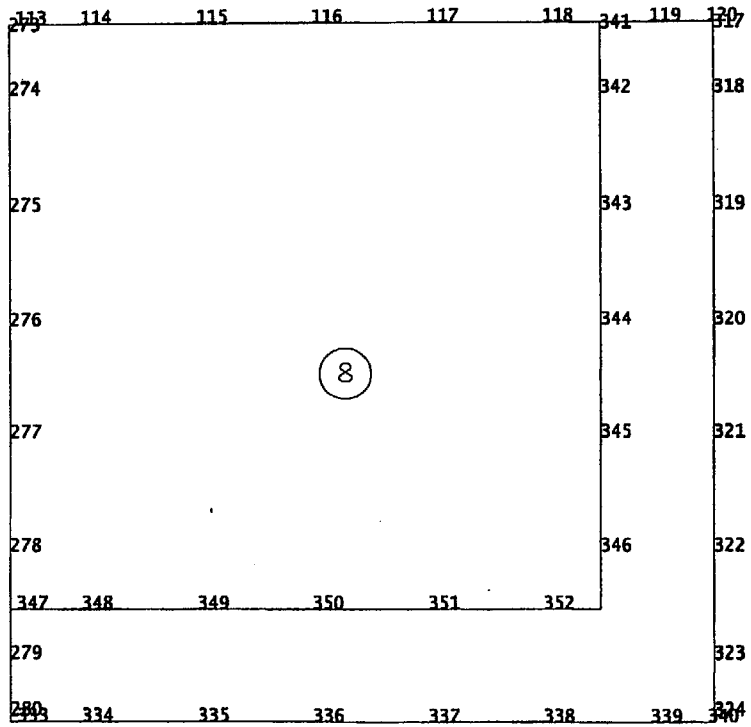


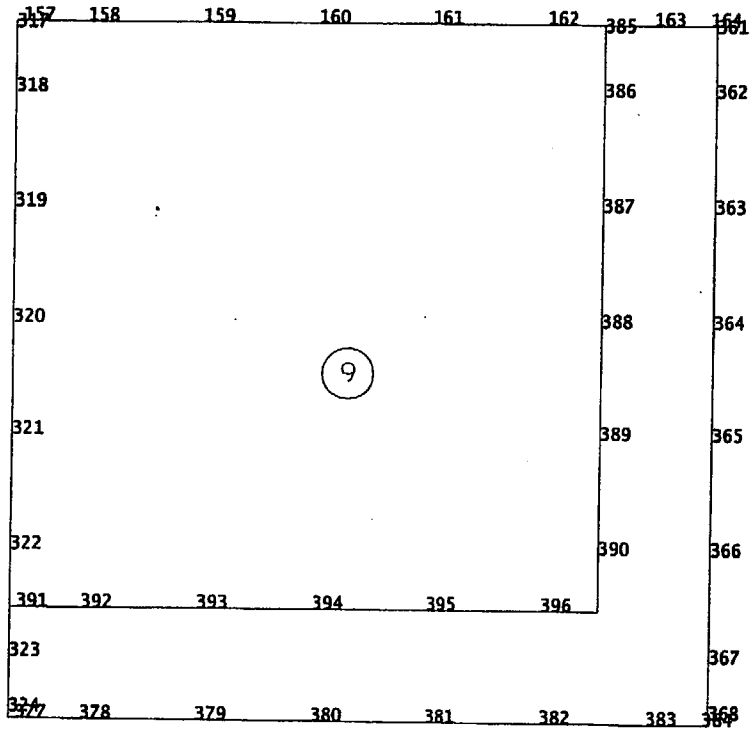


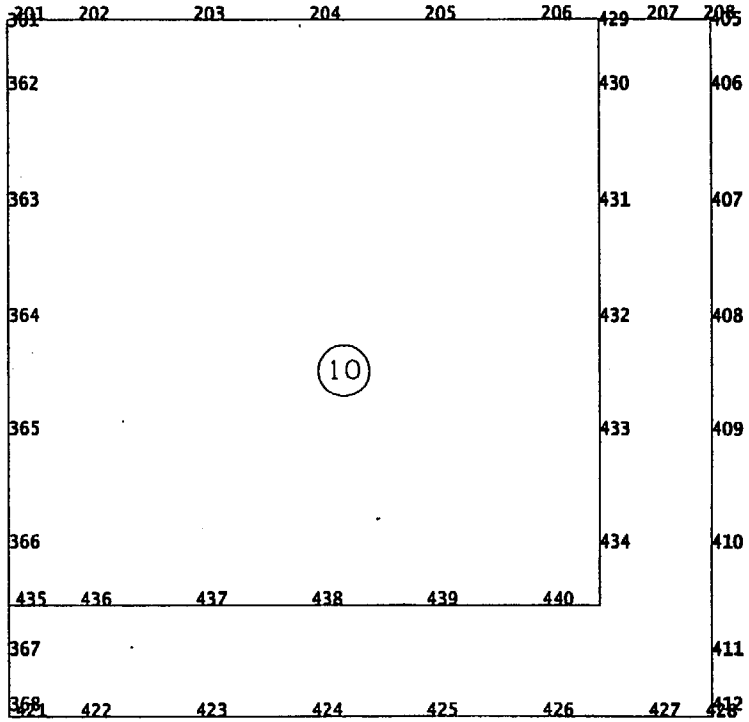


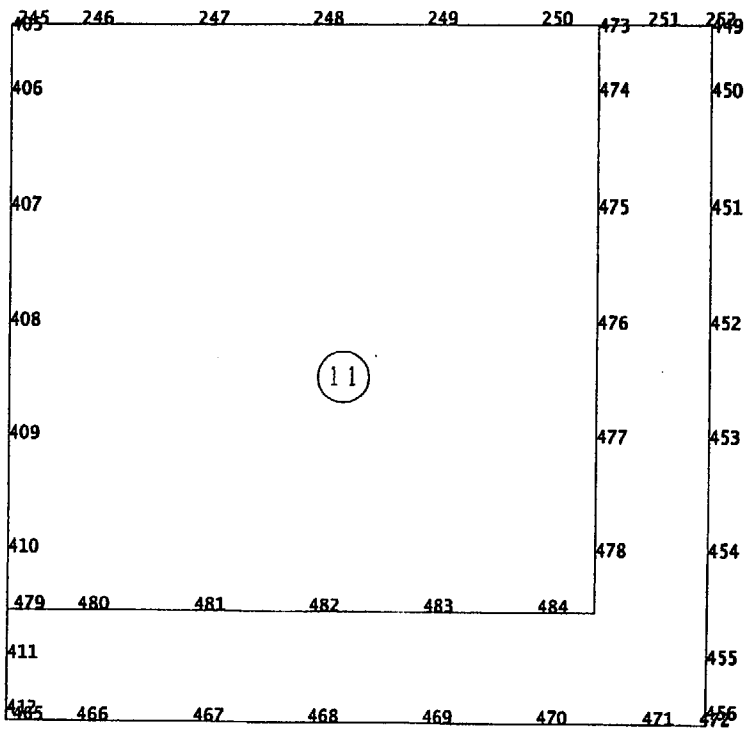


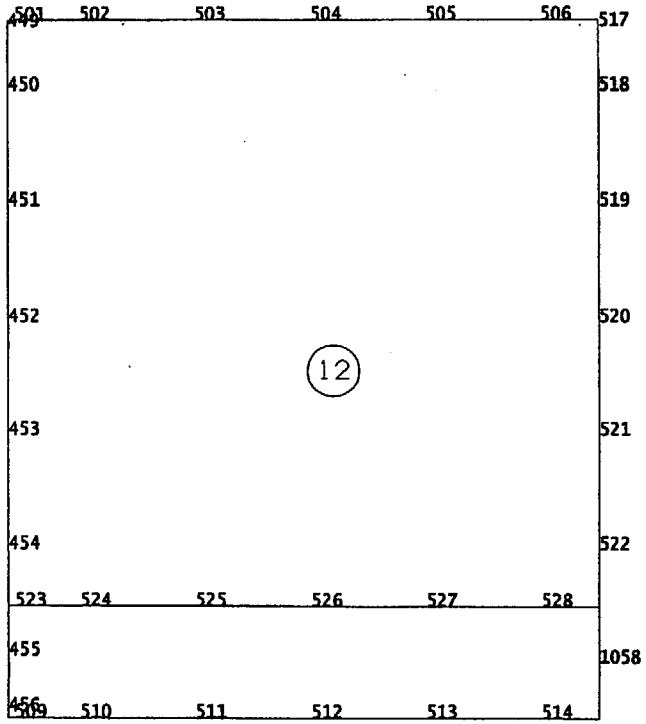


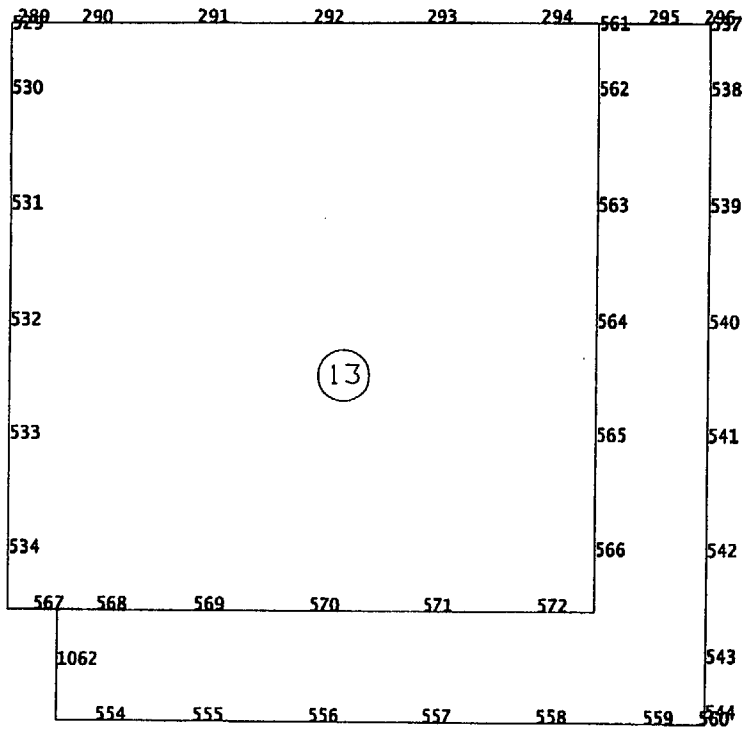


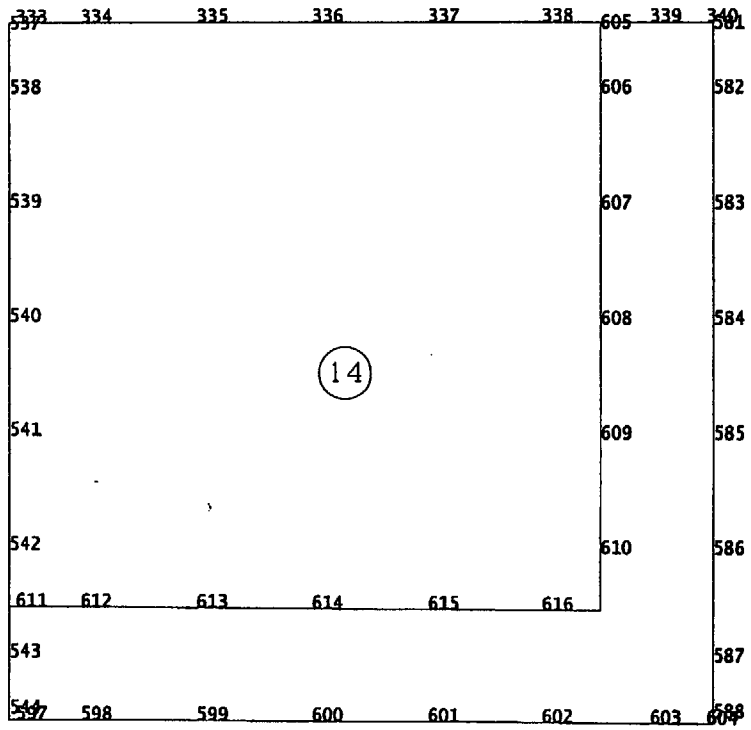


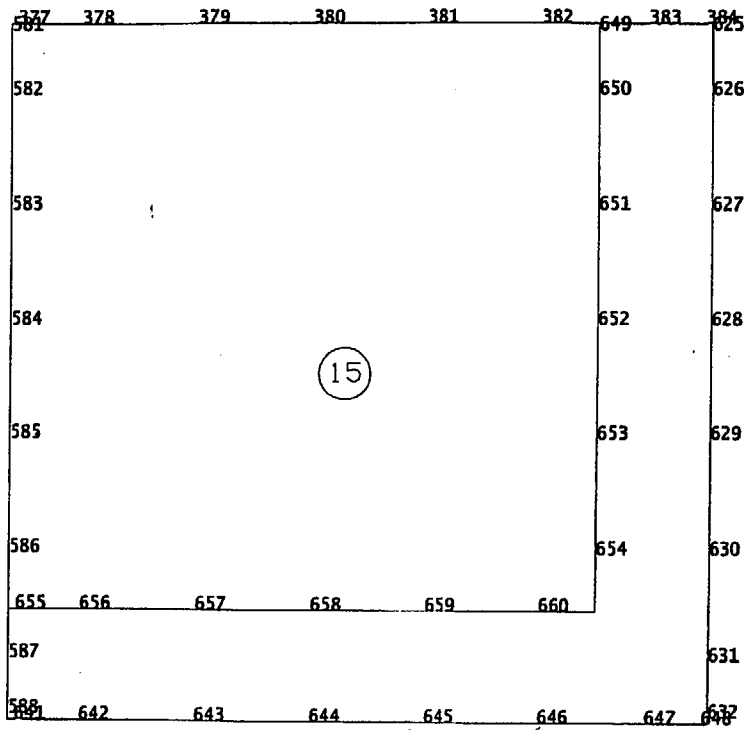


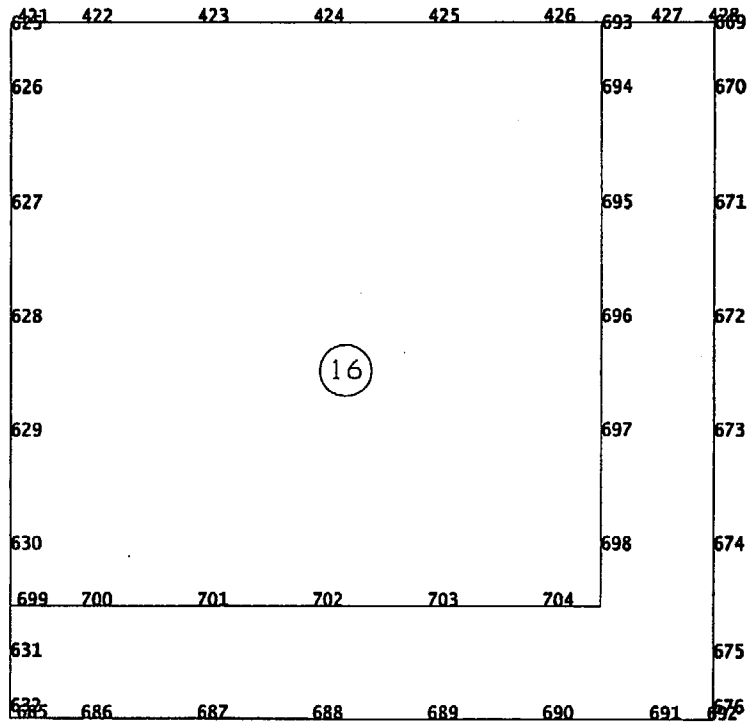


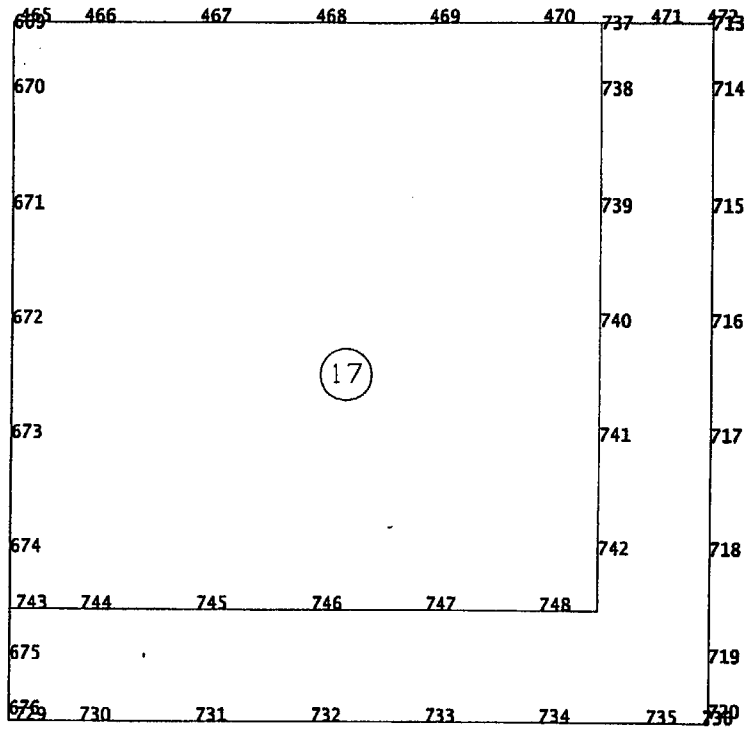


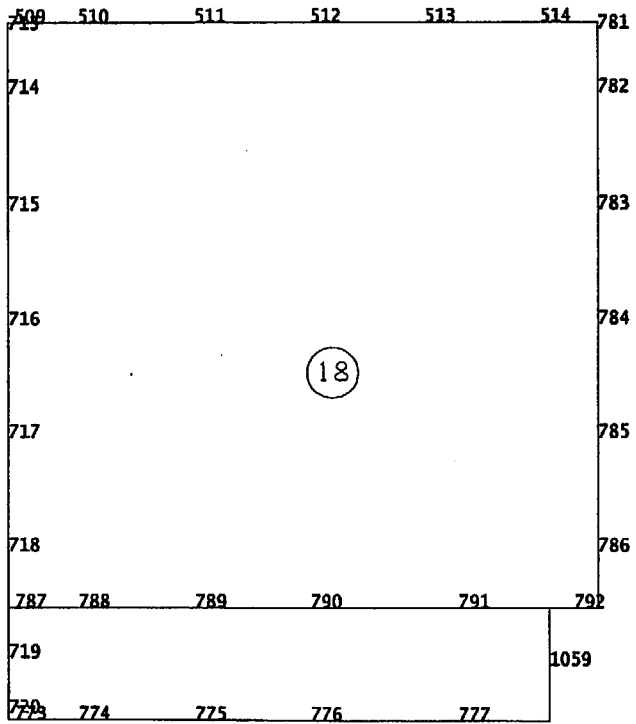


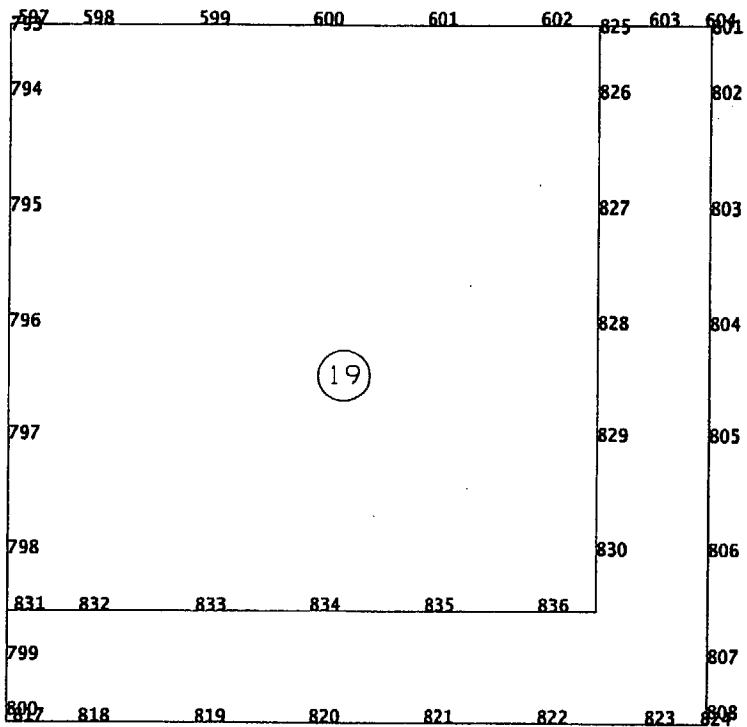


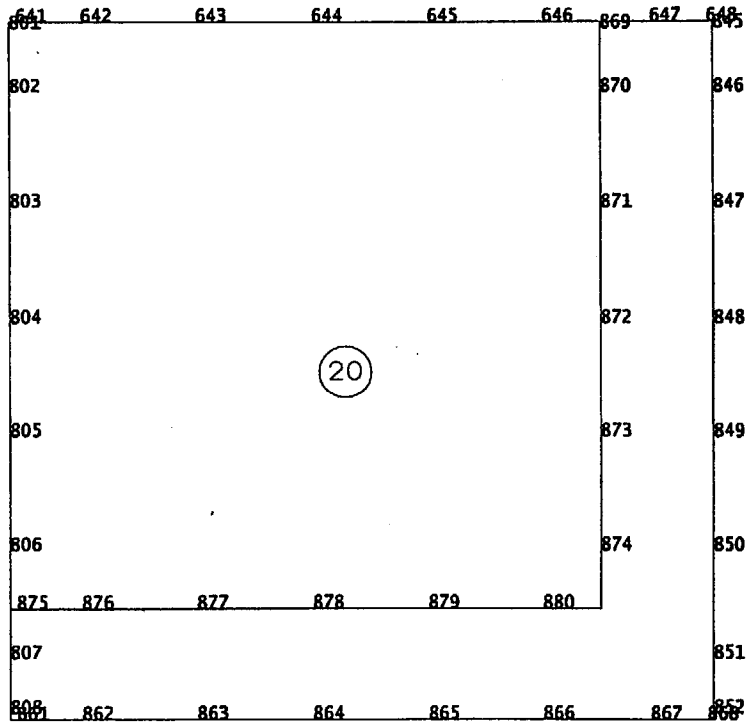


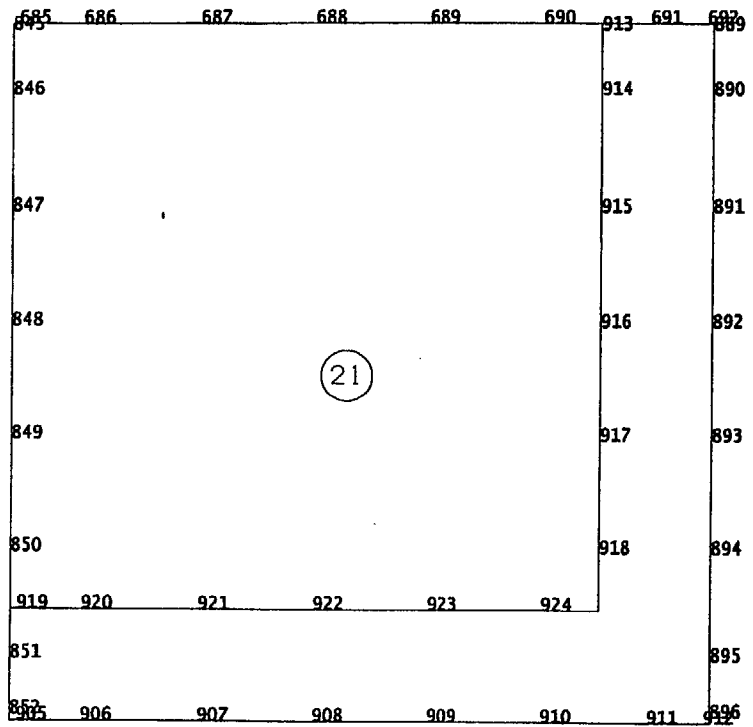


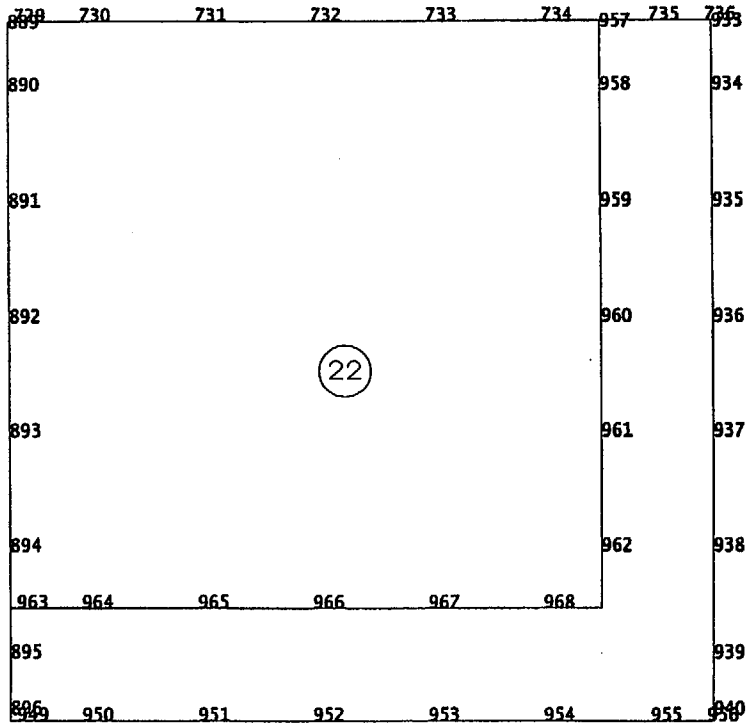


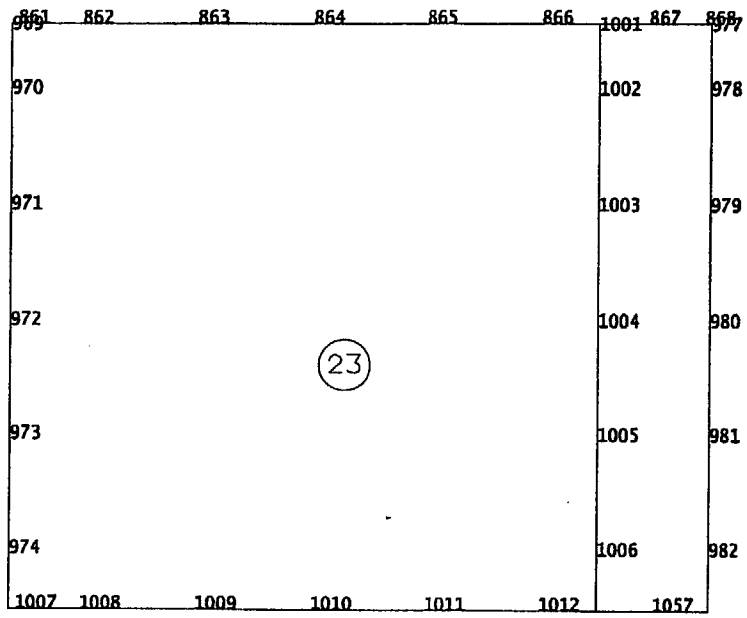


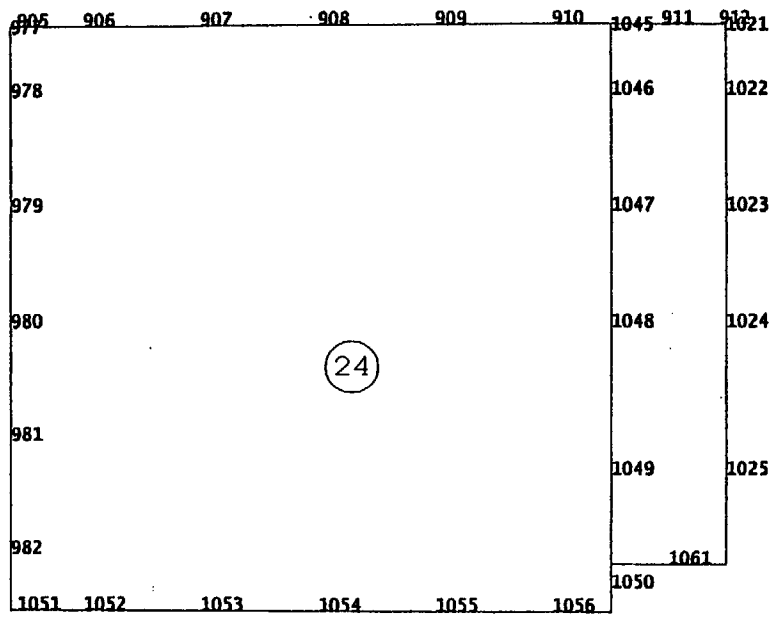






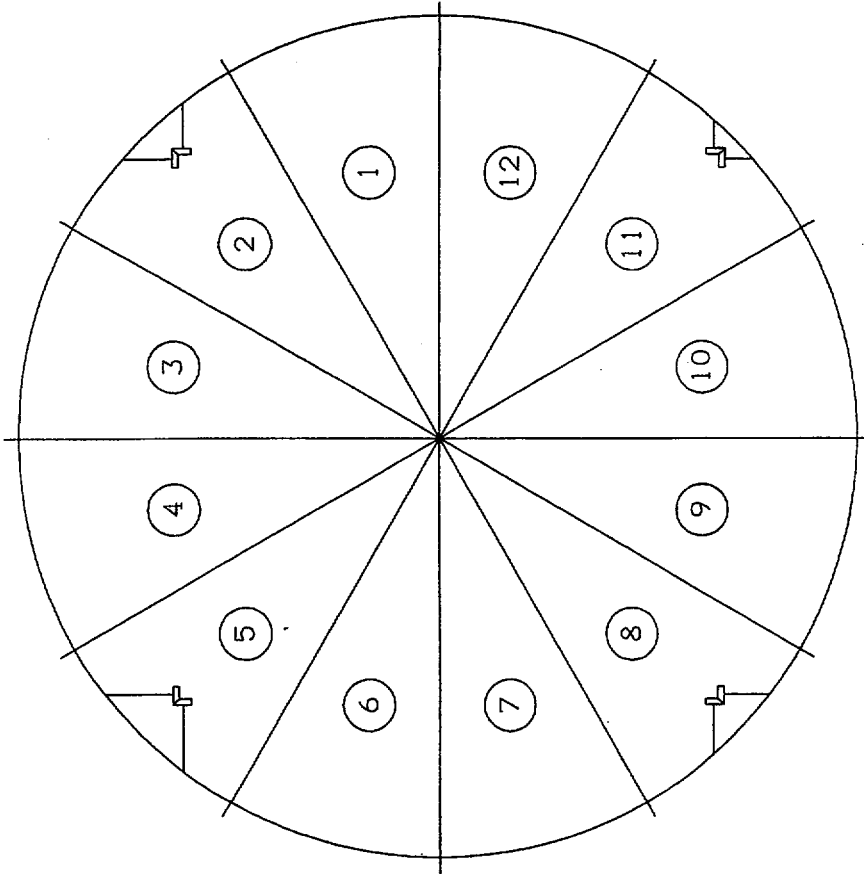


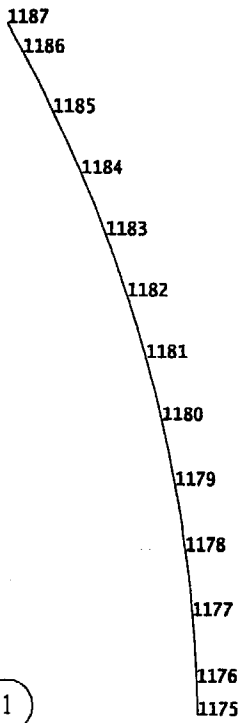




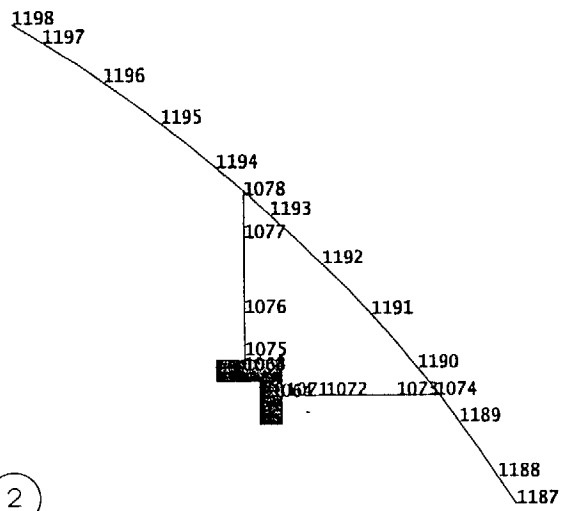
Appendix 3.O – Detailed Finite Element Listings For The MPC-24 Enclosure Vessel

Fourteen (14) pages total including cover page





2

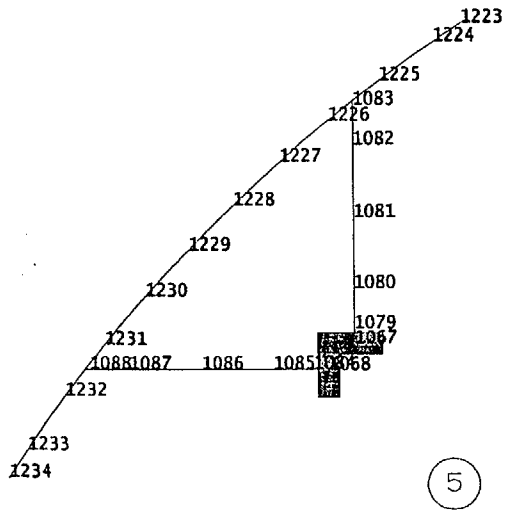


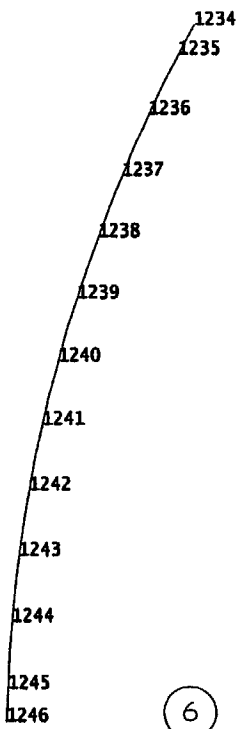
121110 1209 1208 1207 1206 1205 1204 1203 1202 1201 1200 1199 1198

3

1210 1211 1212 1213 1214 1215 1216 1217 1218 1219 1220 1221 1222 1223

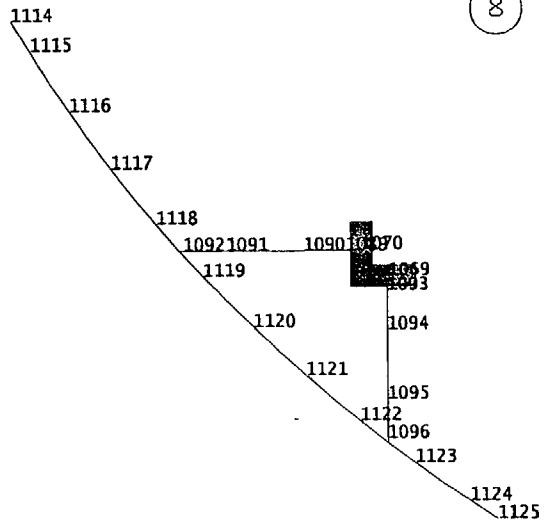
4





7

1246
1103
1104
1105
1106
1107
1108
1109
1110
1111
1112
1113
1114

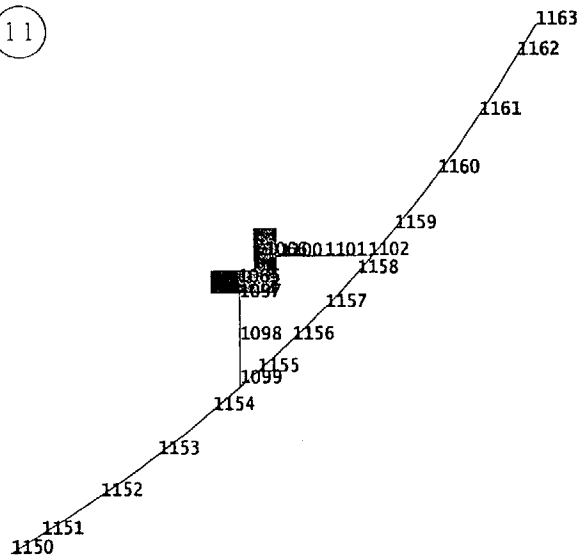


1125
1126
1127
1128
1129
1130
1131
1132
1133
1134
1135
1136 113738

10

113738 1139 1140 1141 1142 1143 1144 1145 1146 1147 1148 1149 1150

11



1175
1174
1173
1172
1171
1170
1169
1168
1167
1166
1165
1164
1163

12

Appendix 3.P -

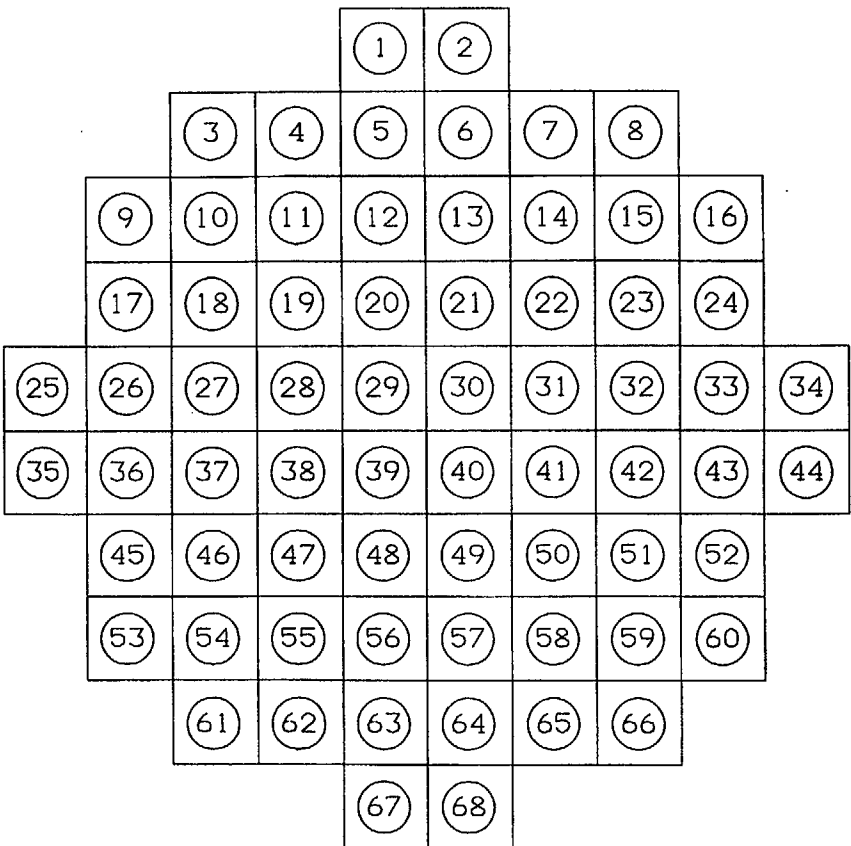
DELETED

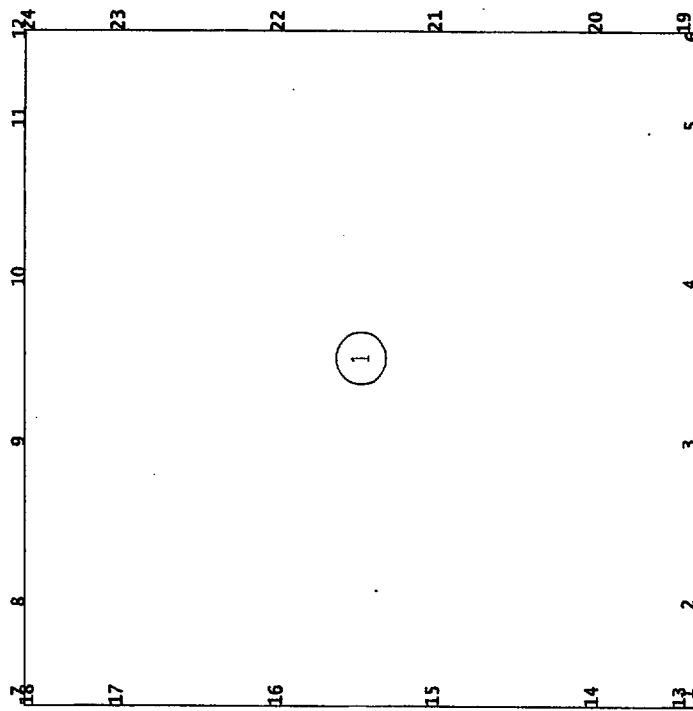
Appendix 3.Q -

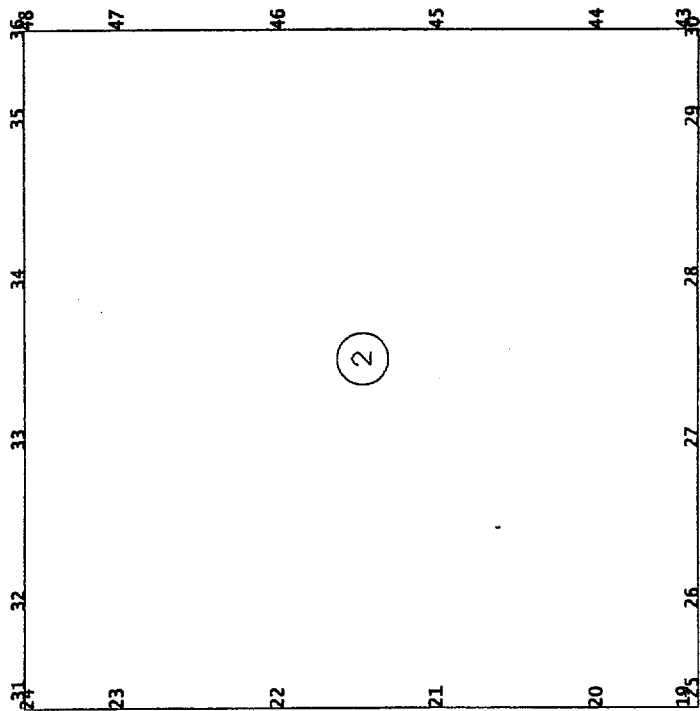
DELETED

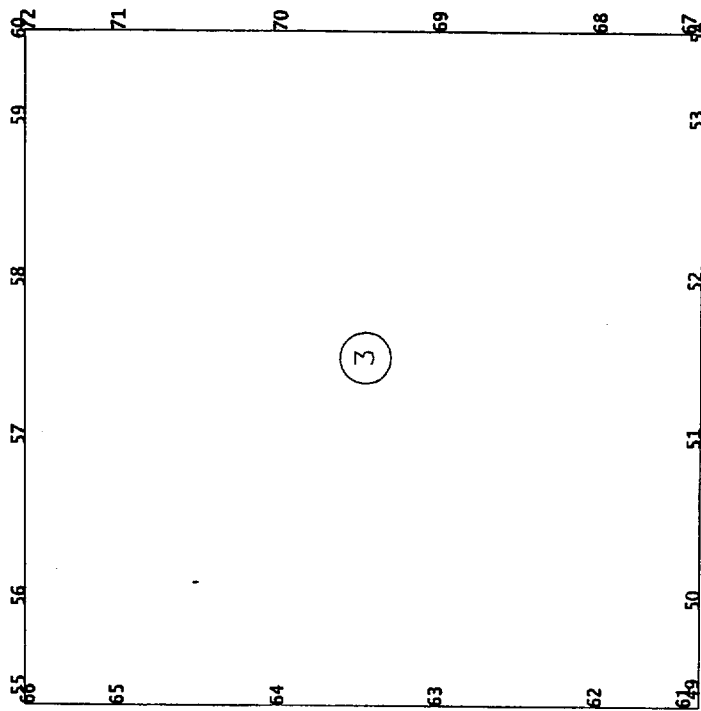
Appendix 3.R – Detailed Finite Element Listings For The MPC-68 Fuel Basket

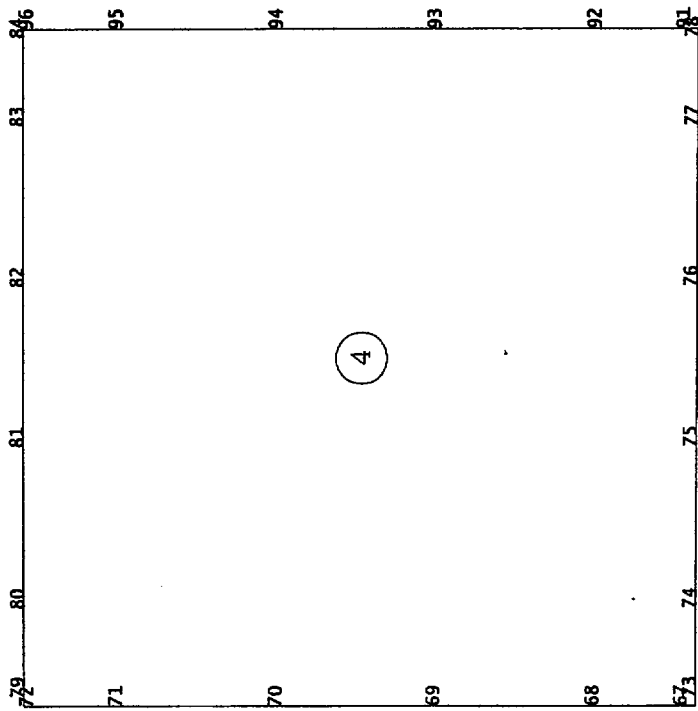
Seventy (70) pages total including cover page

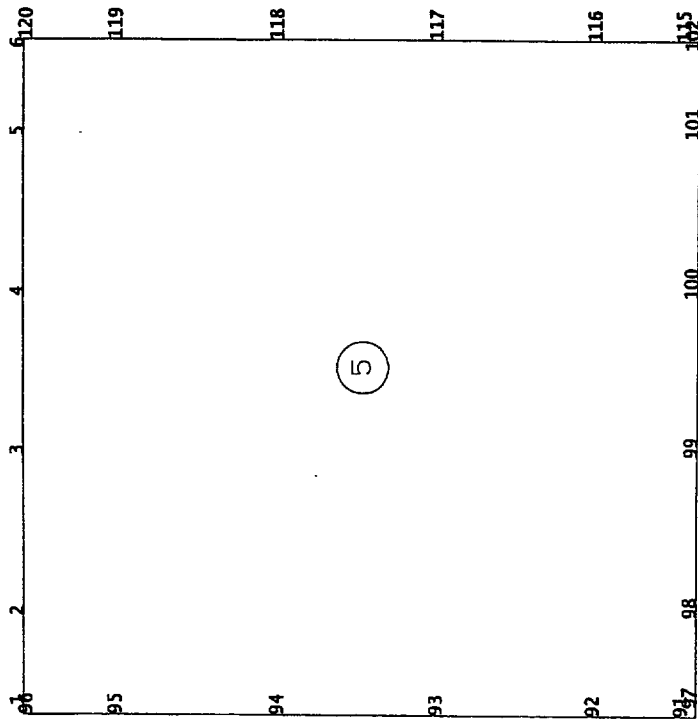


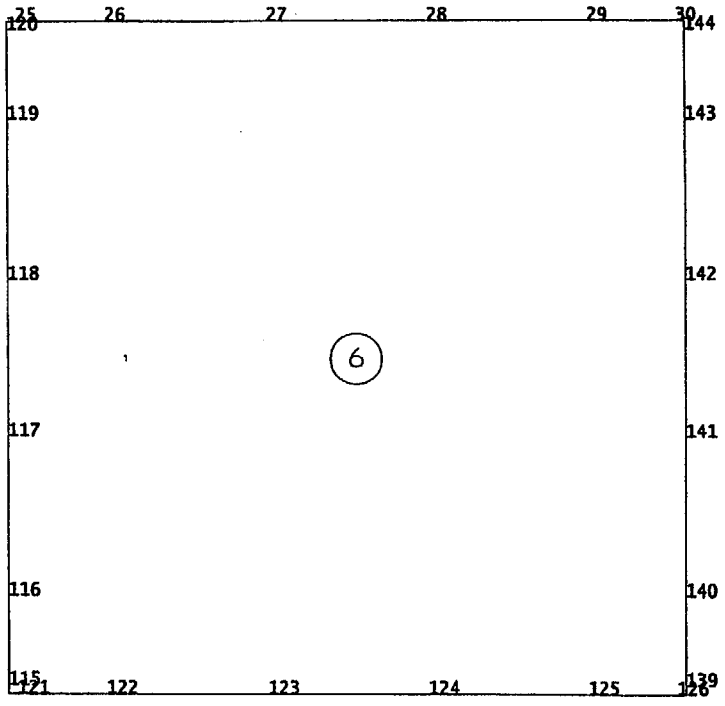


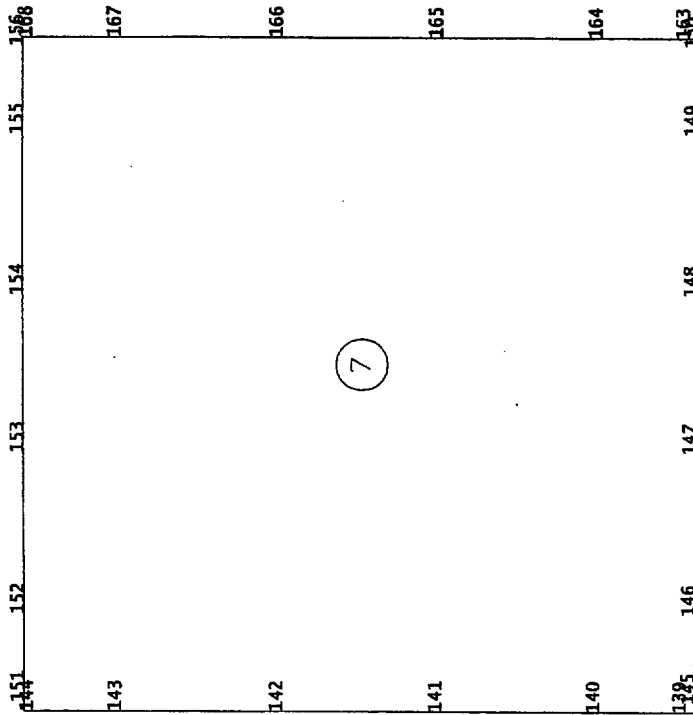


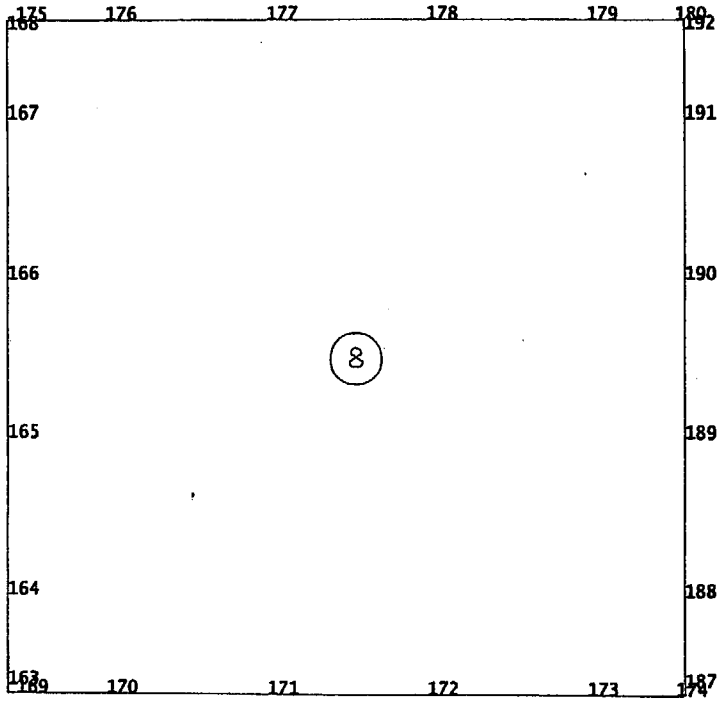


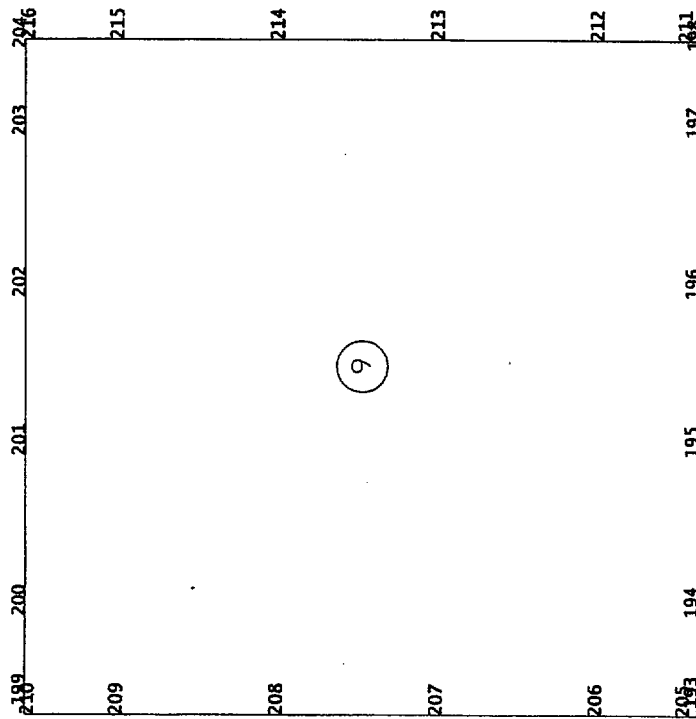


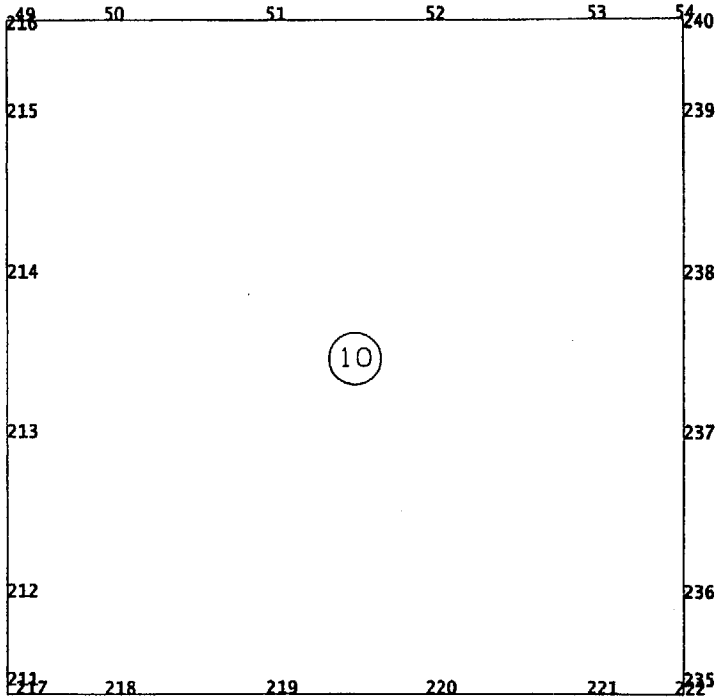


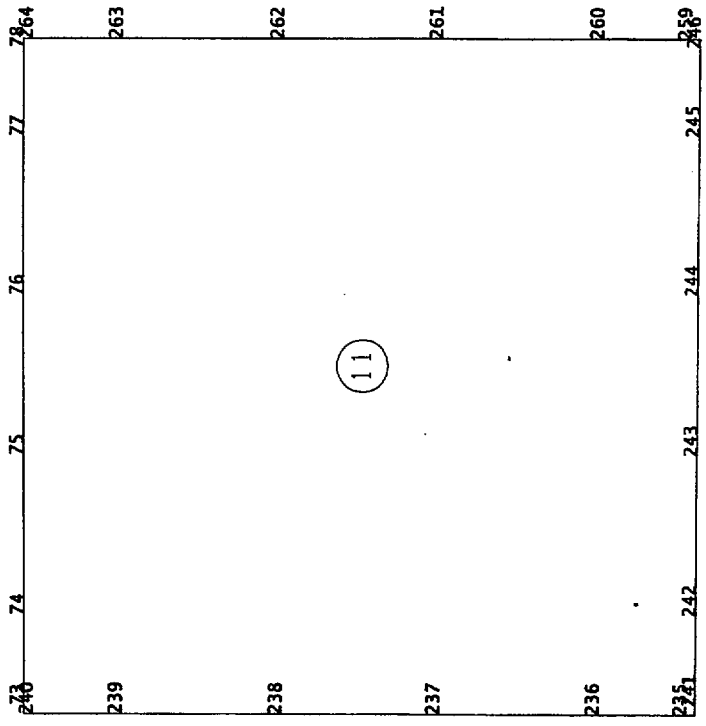


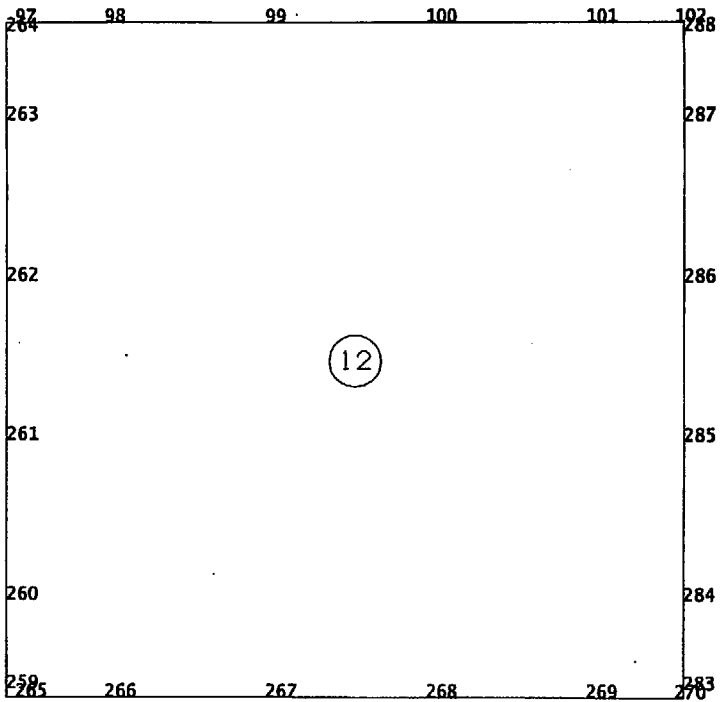


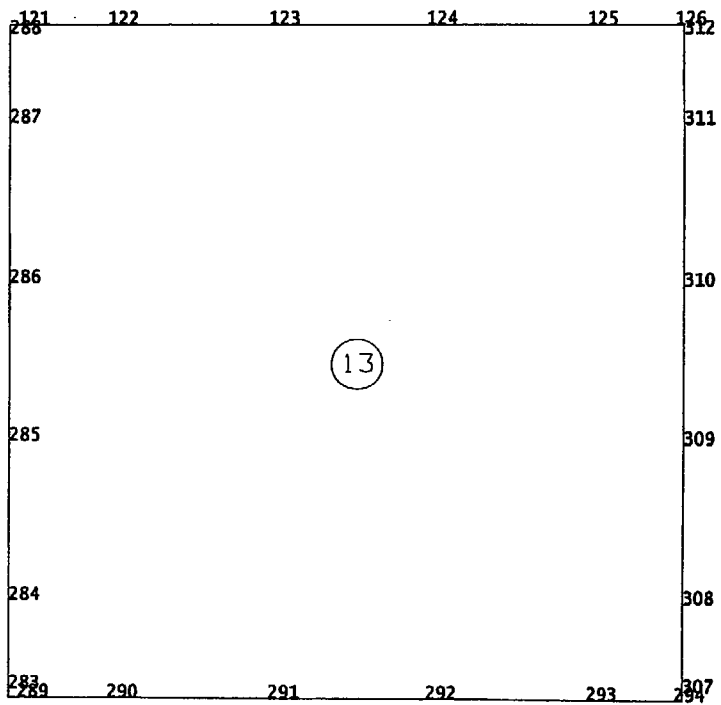


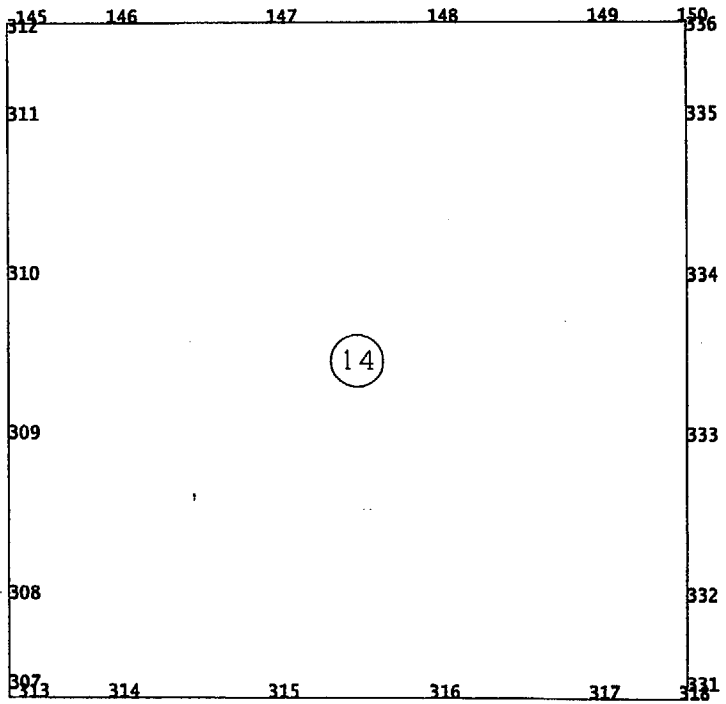


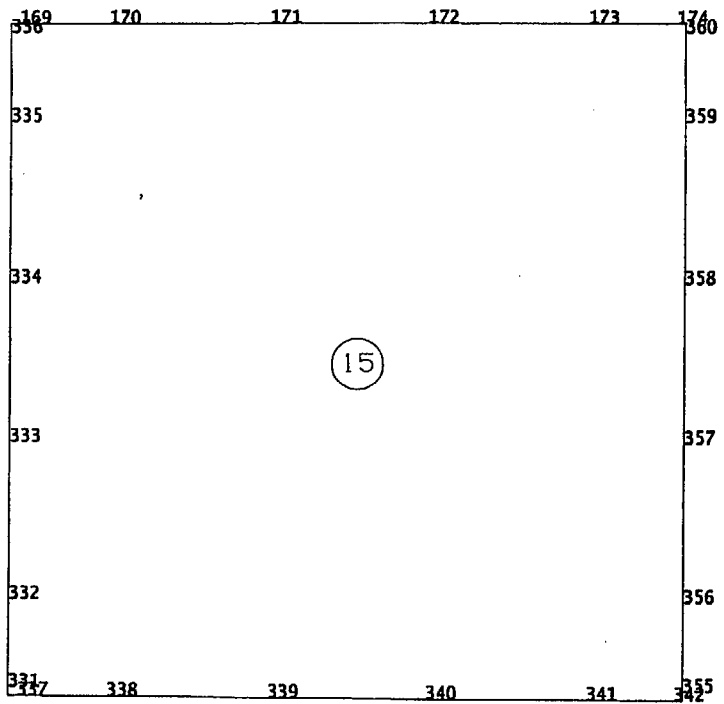


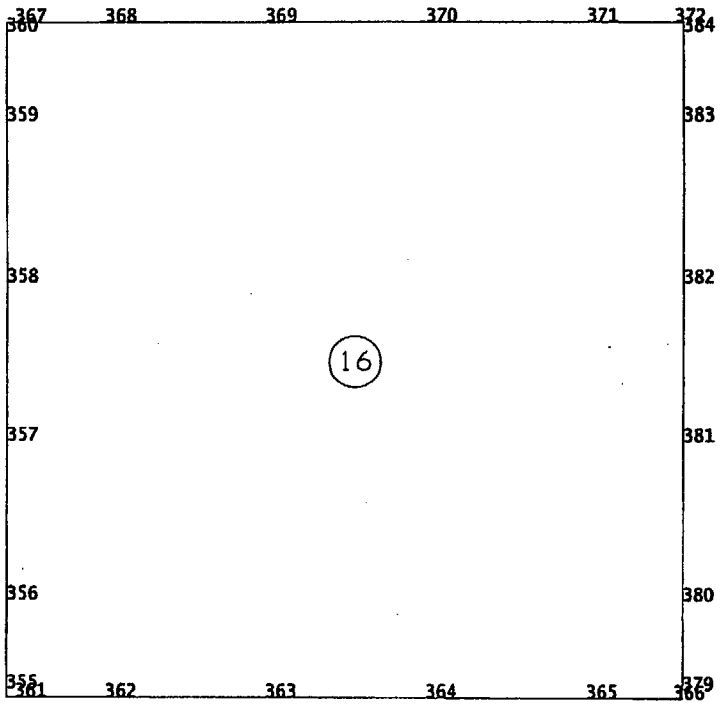


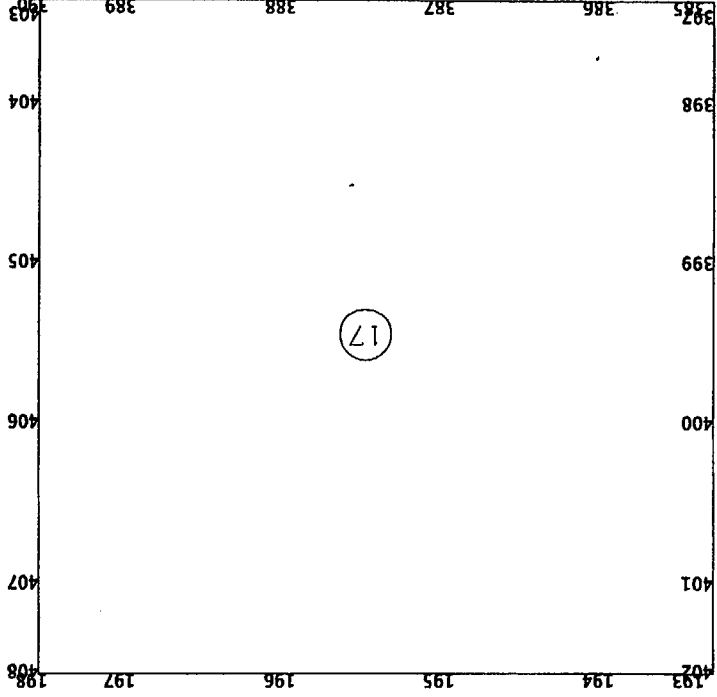


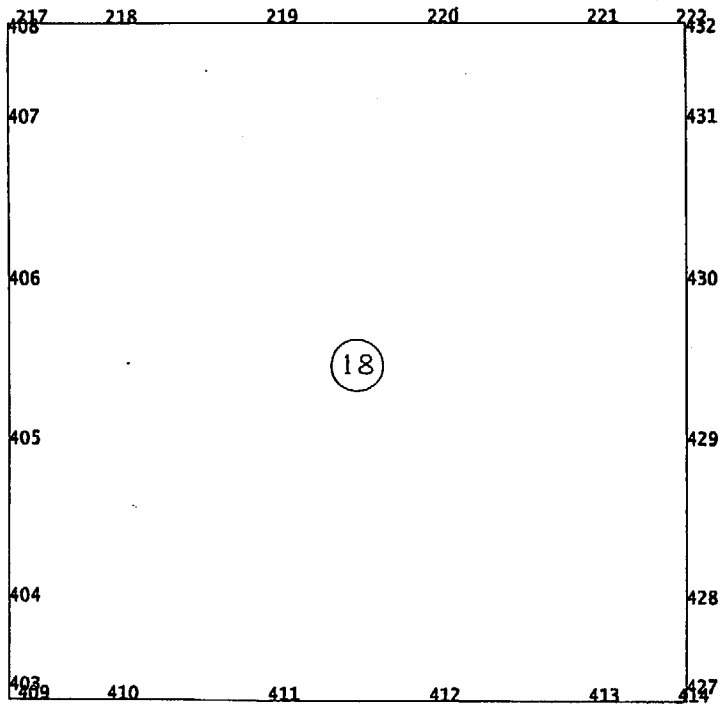


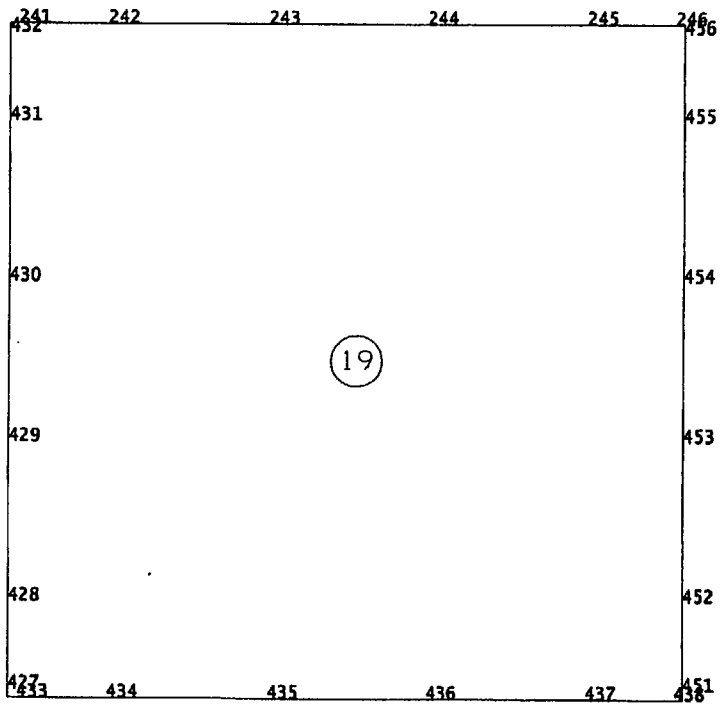


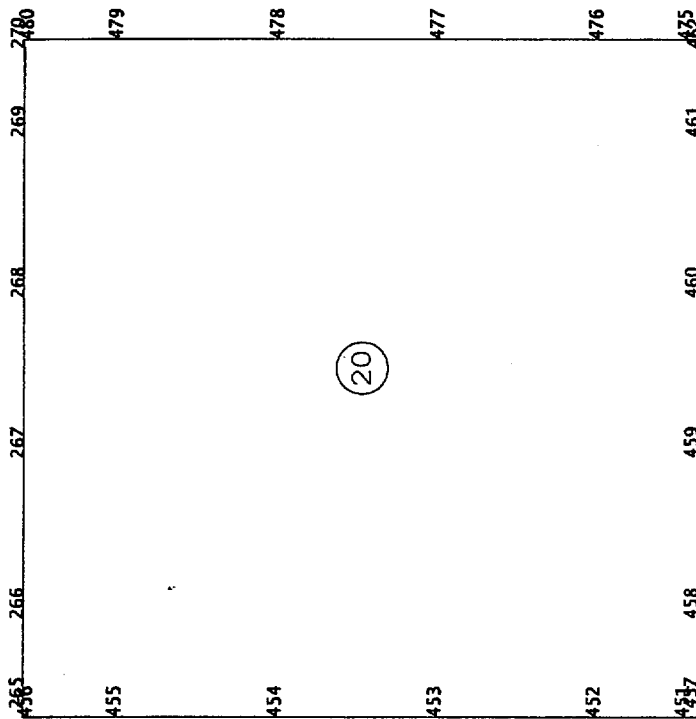


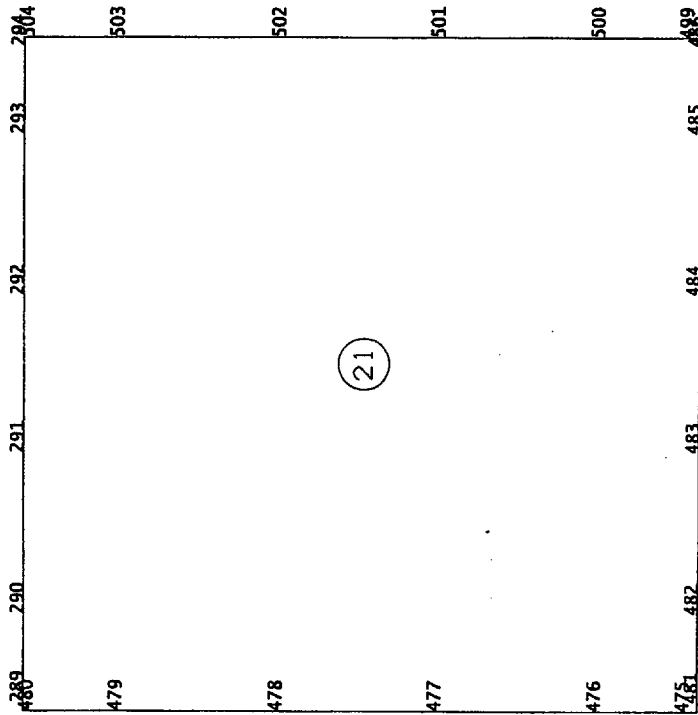


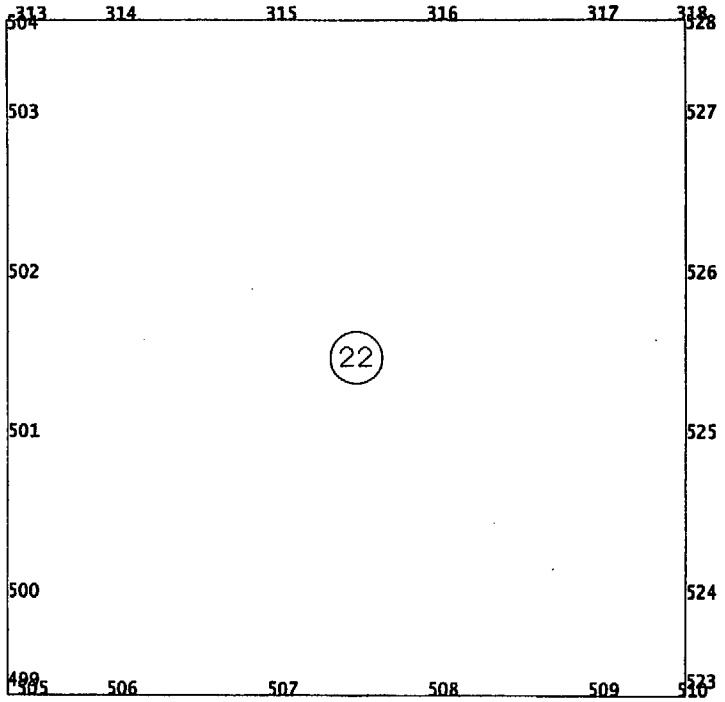


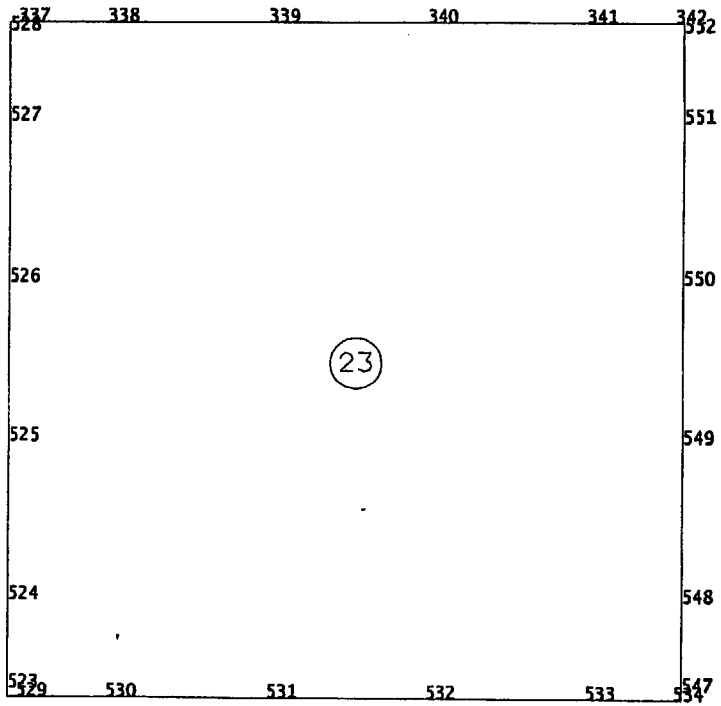


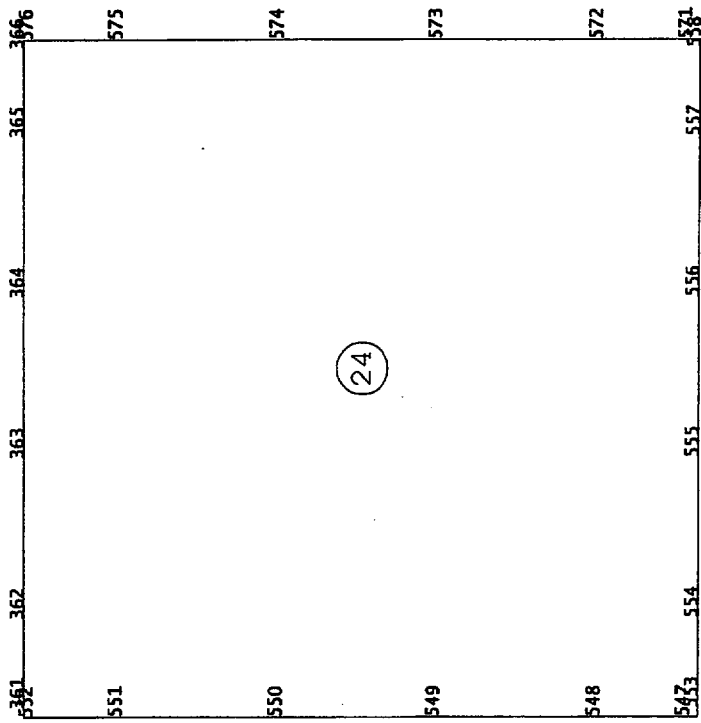


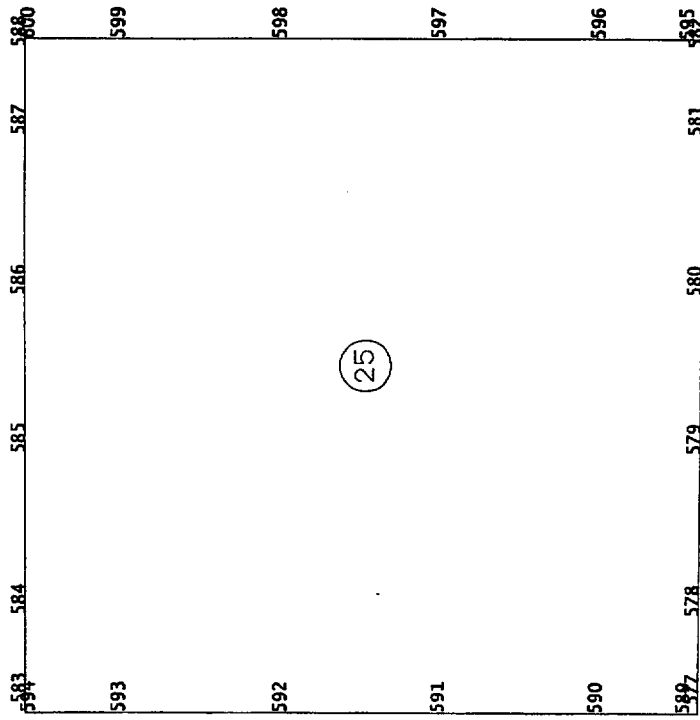


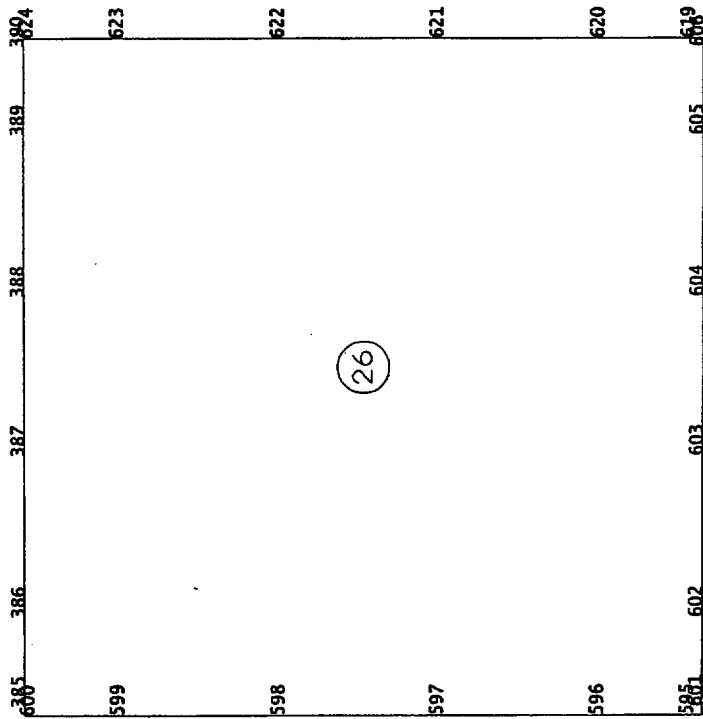


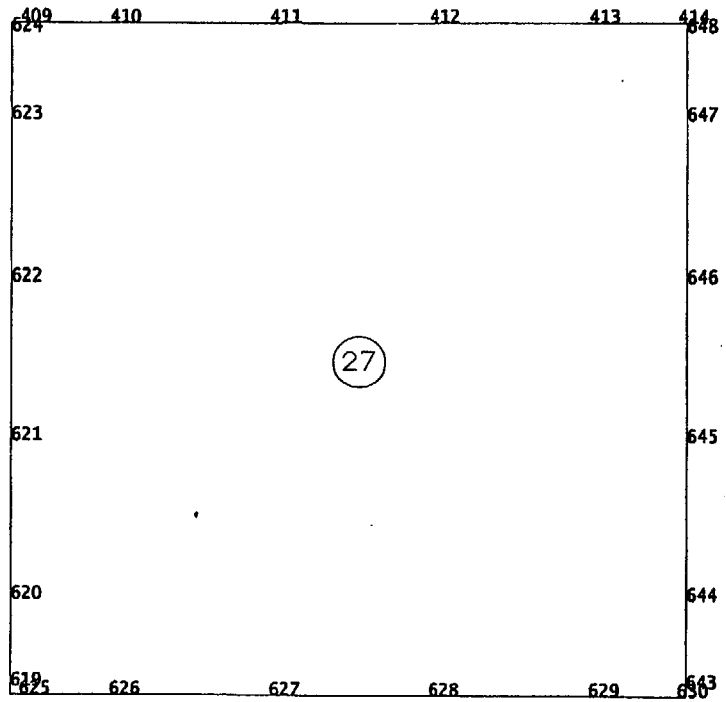


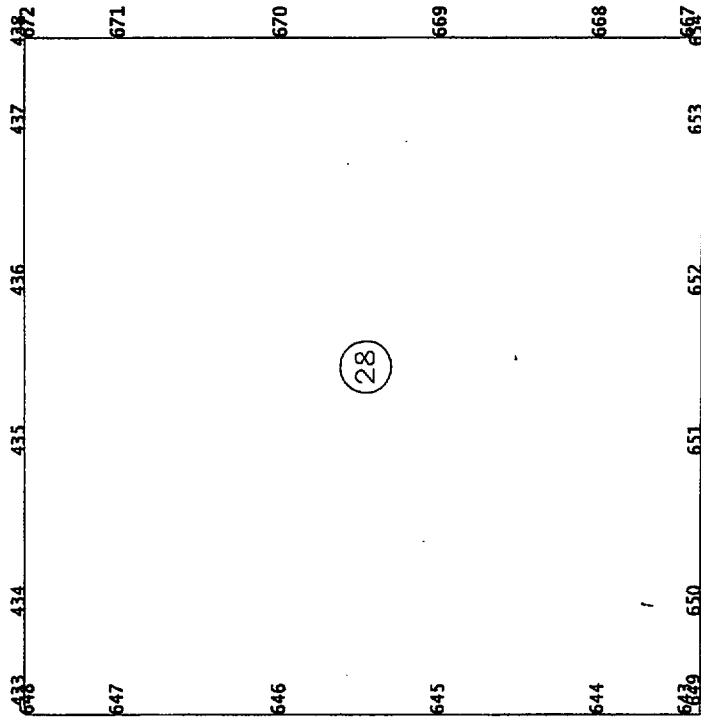


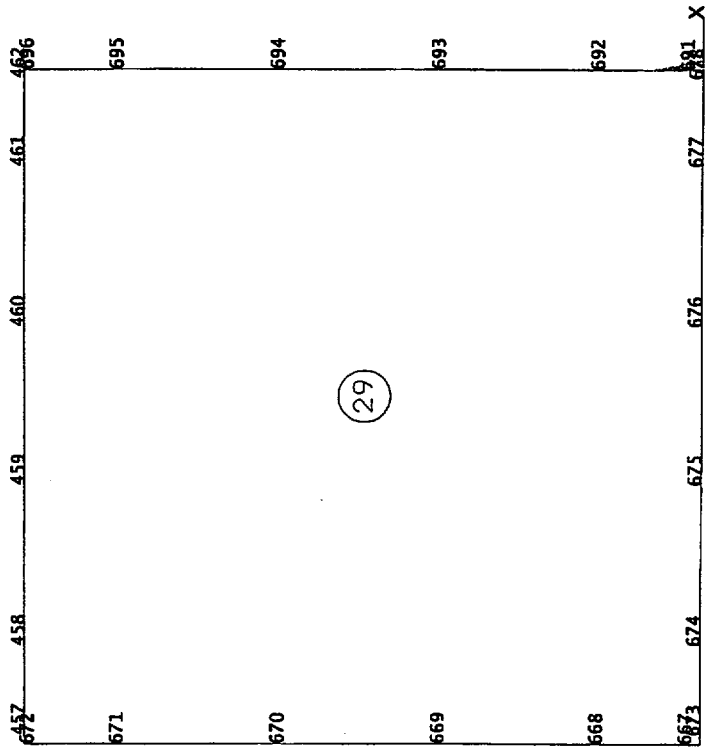


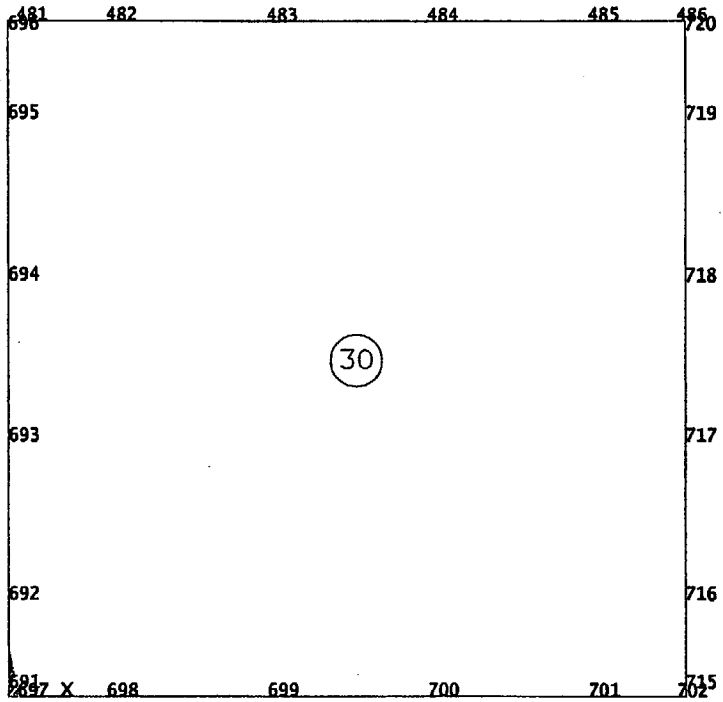


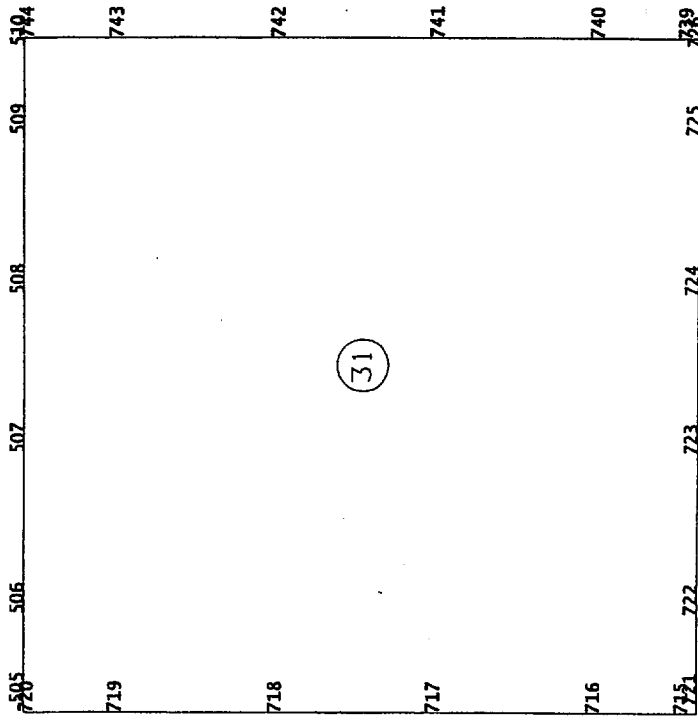


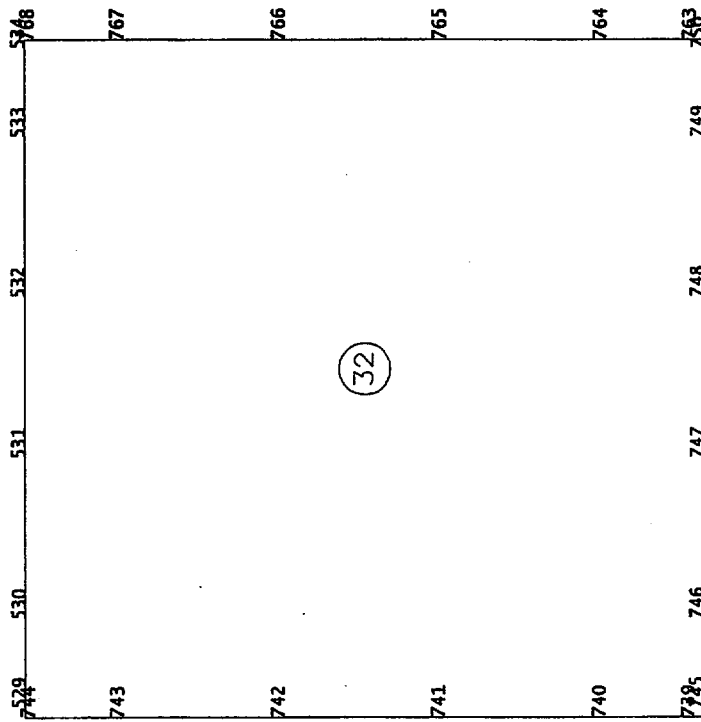


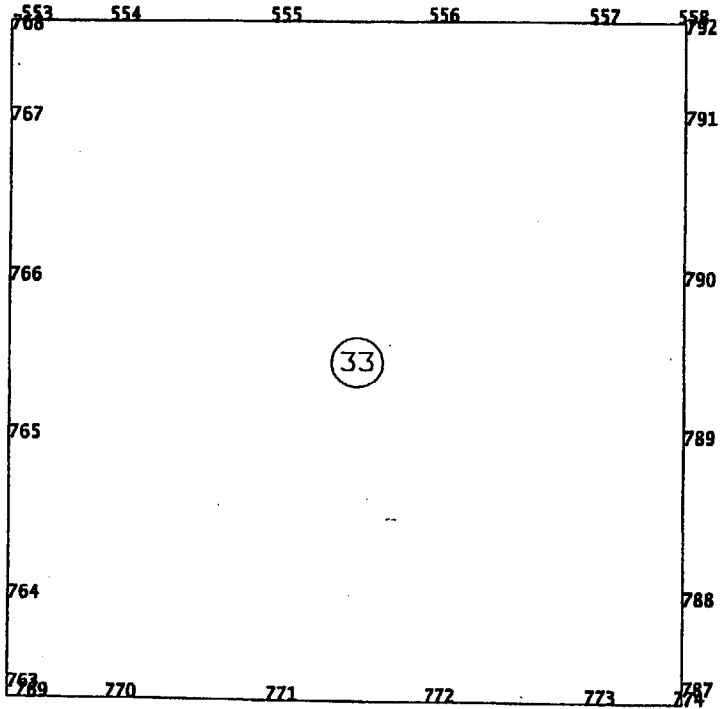


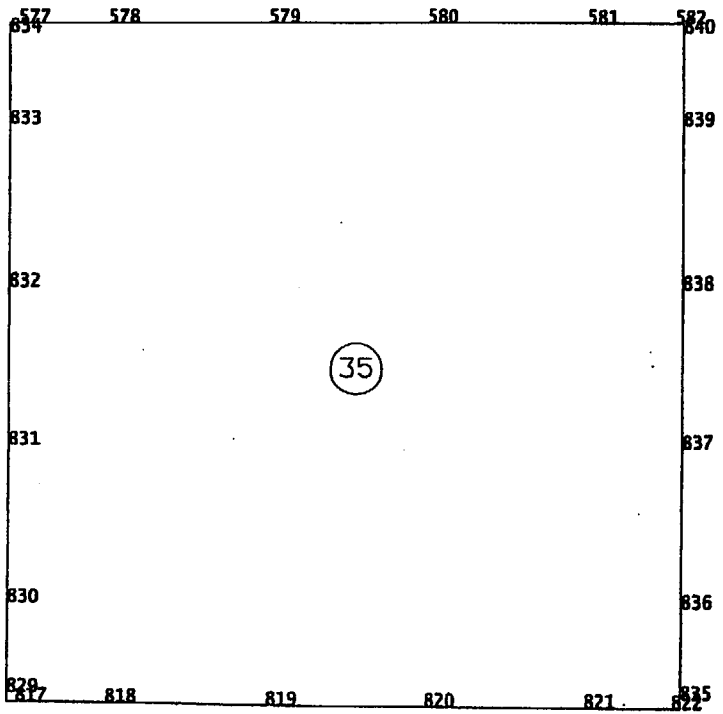


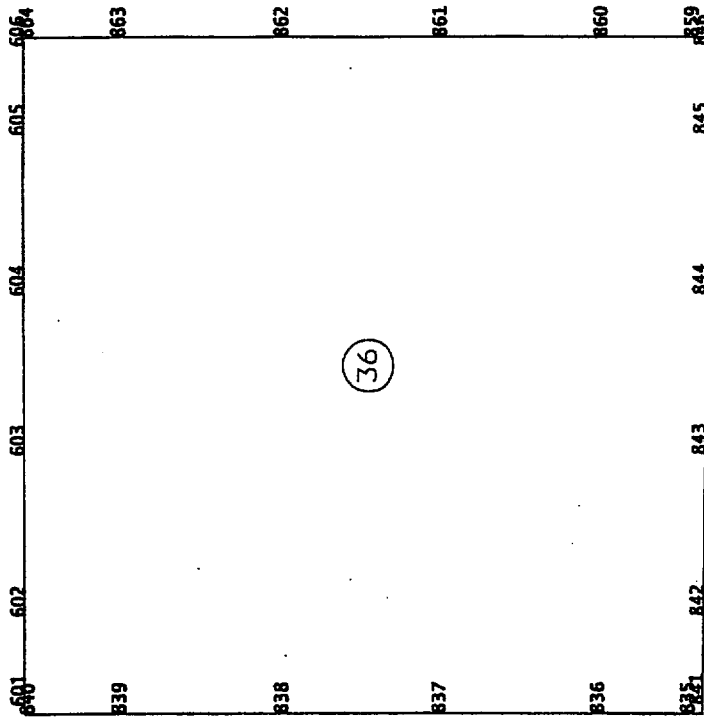


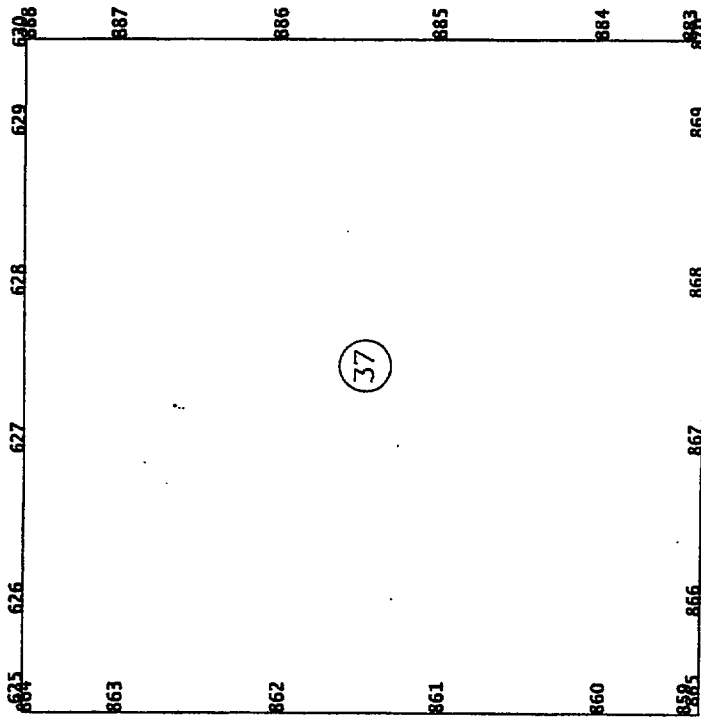


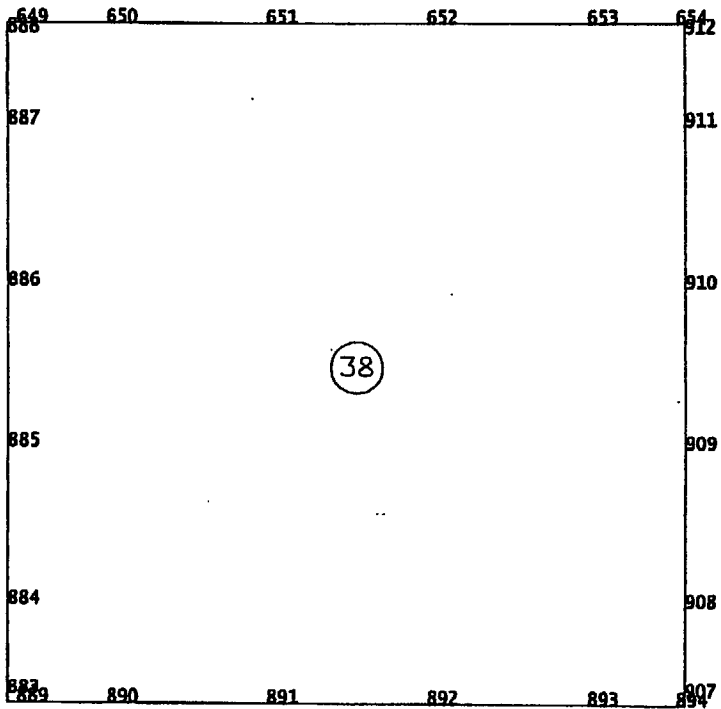


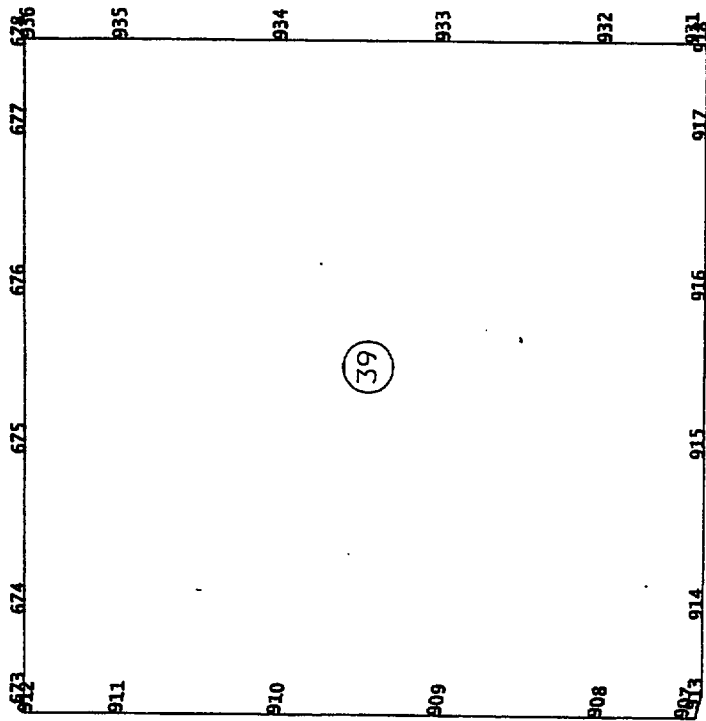


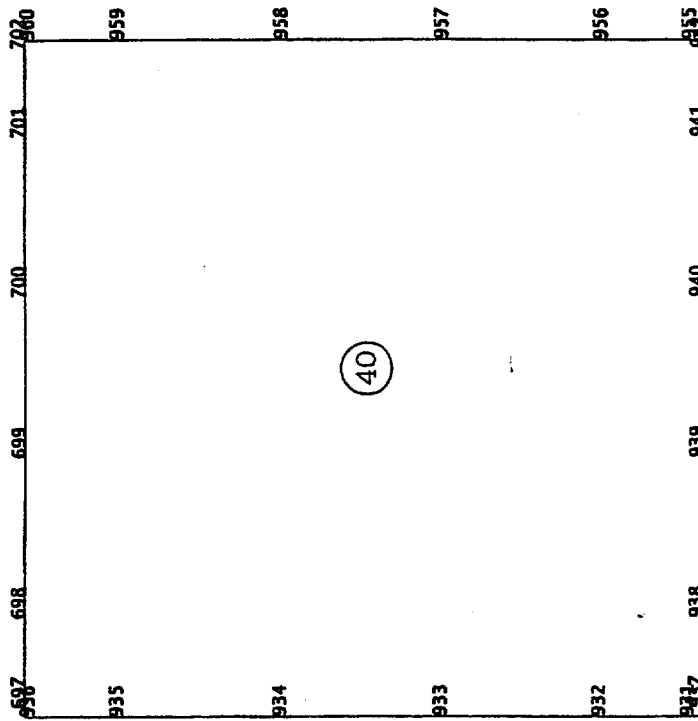


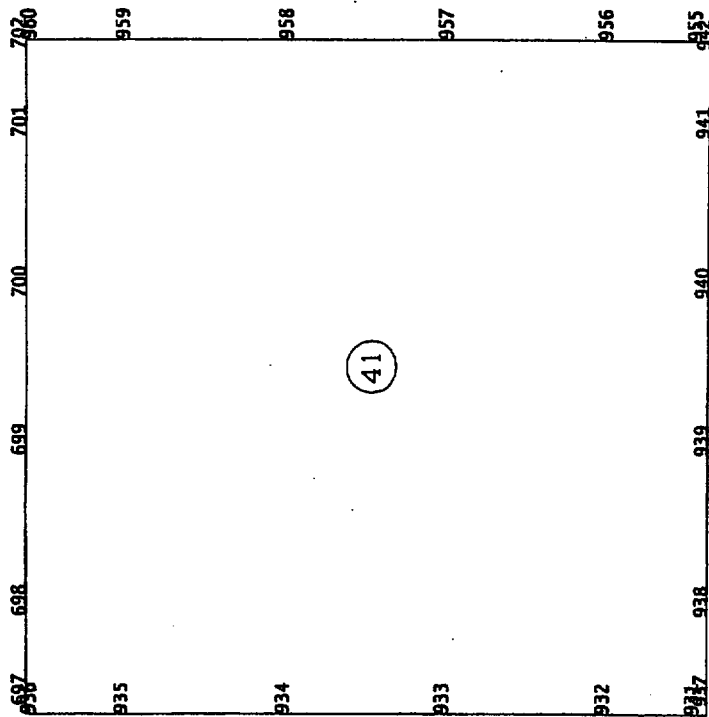


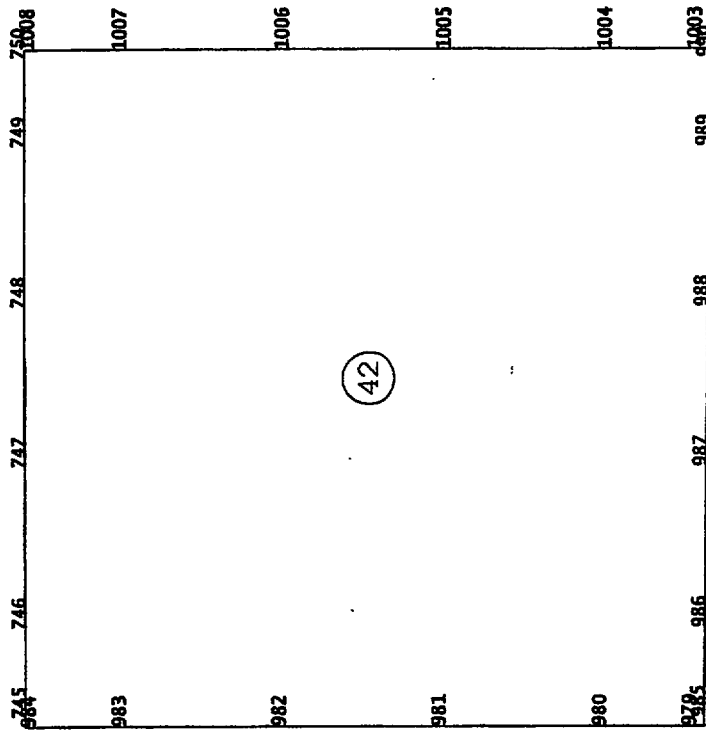


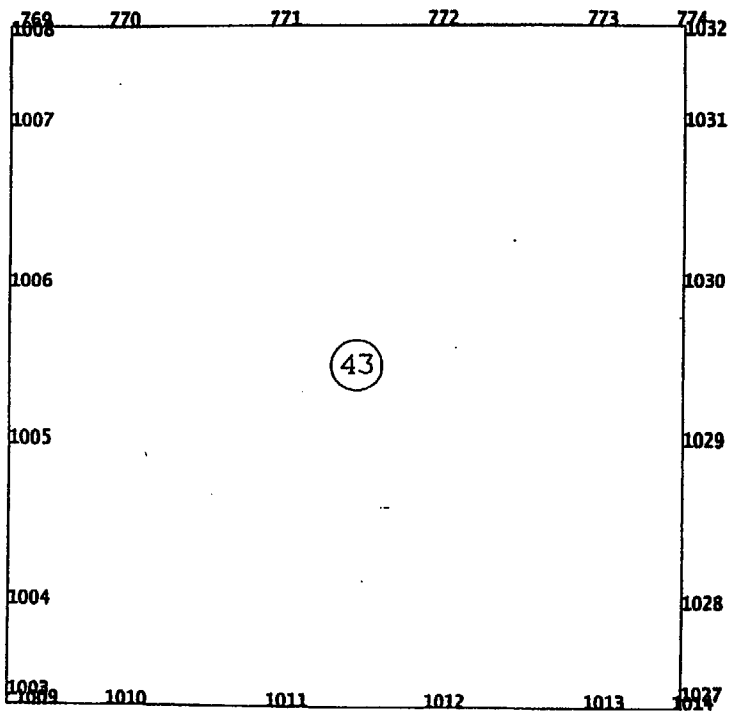


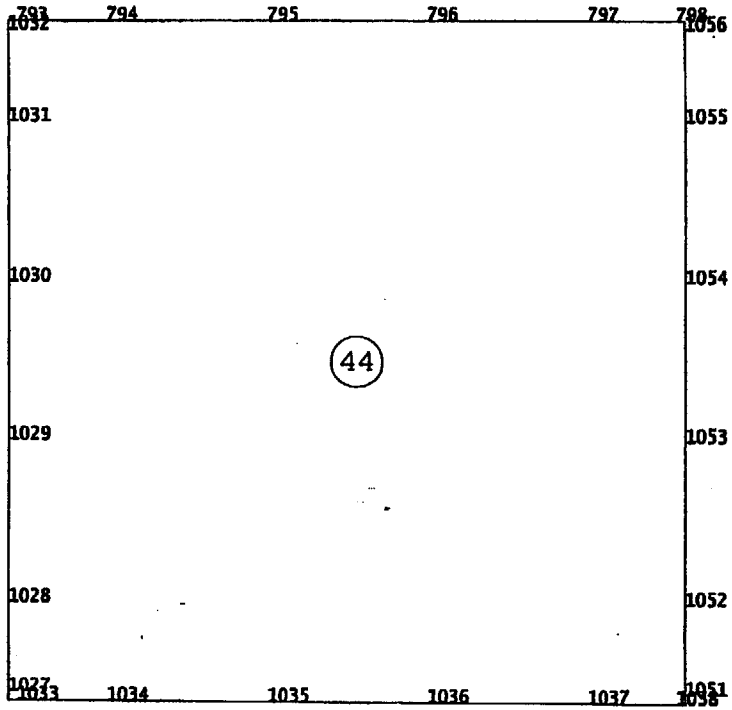


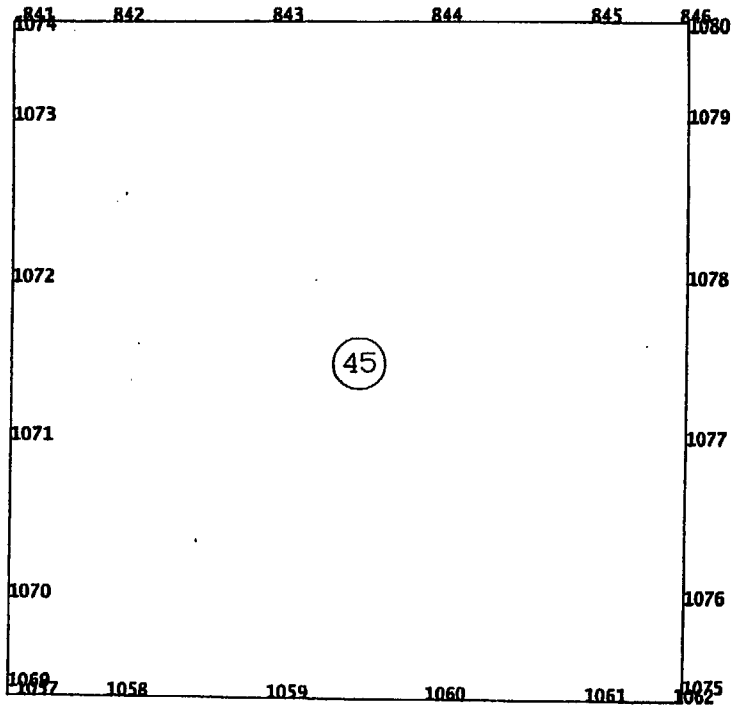


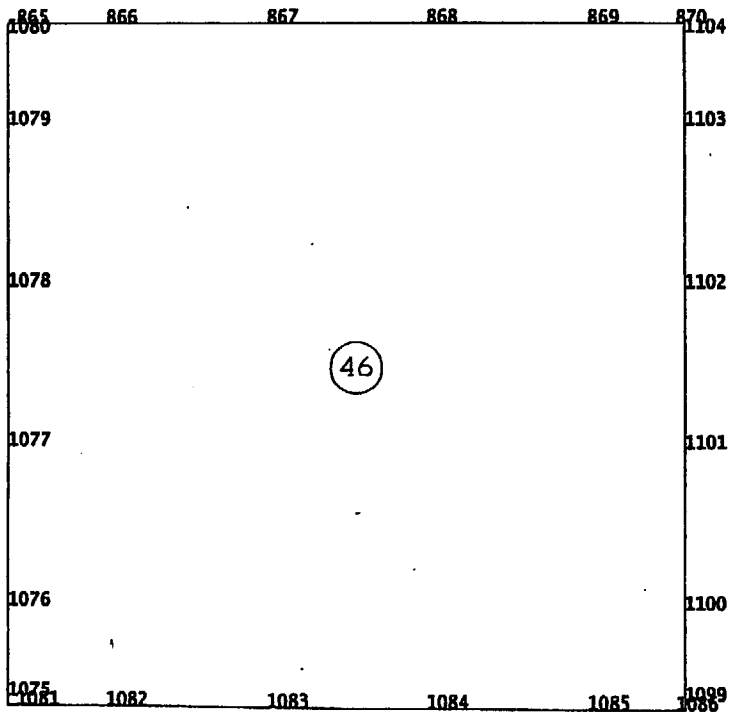


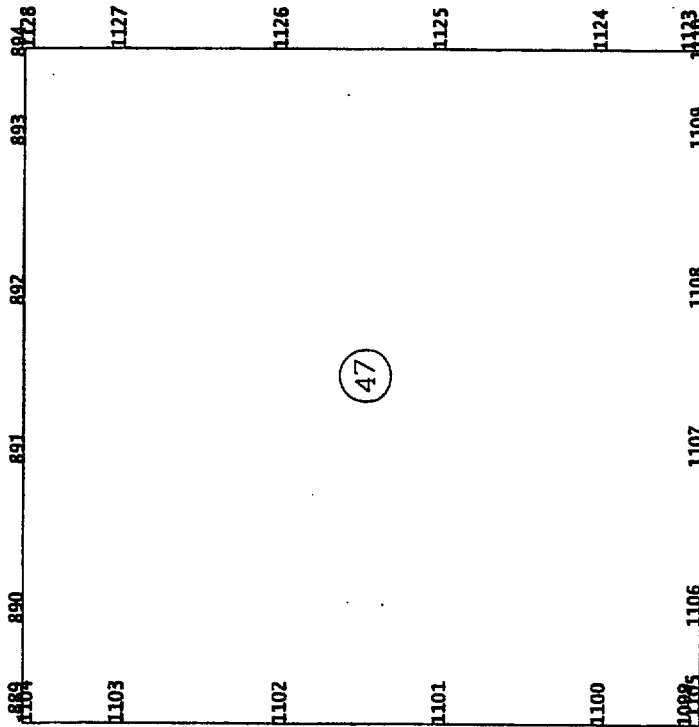


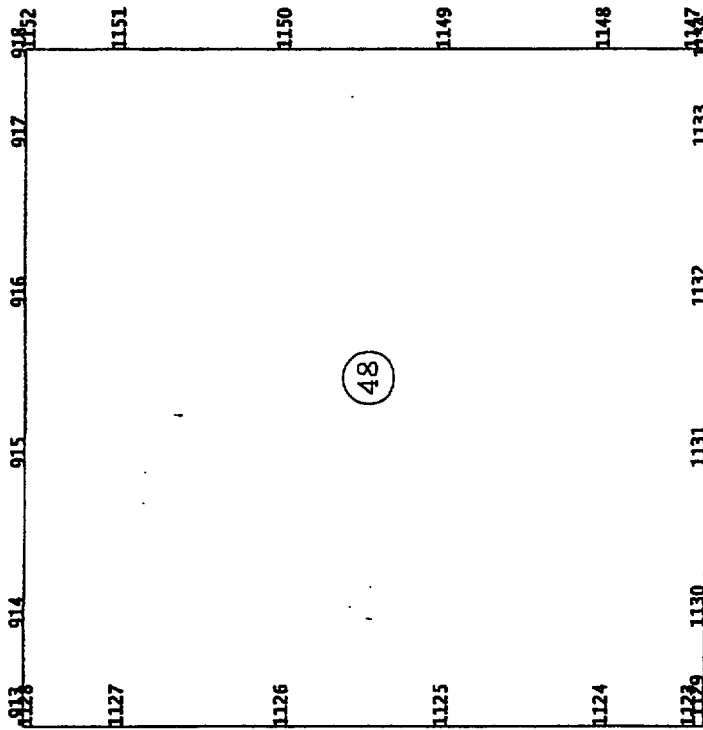


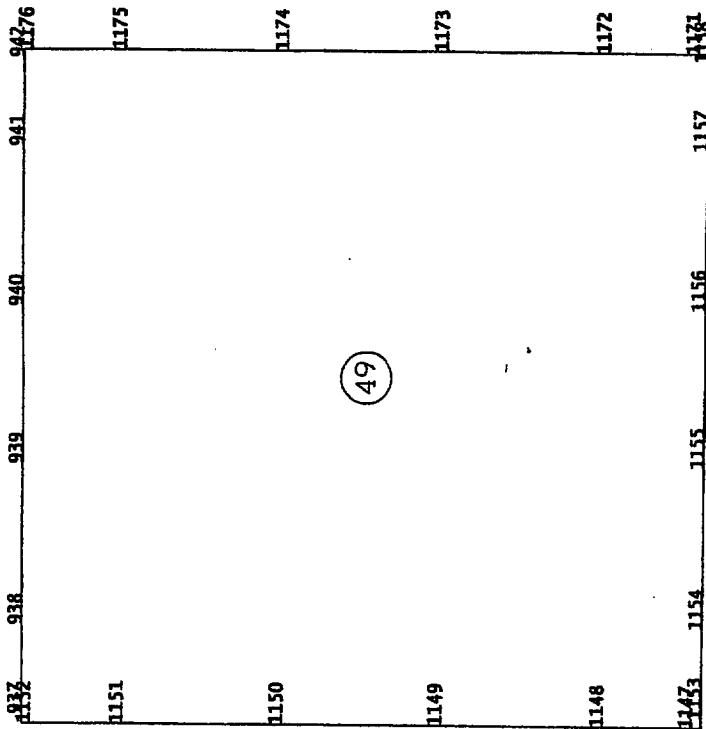


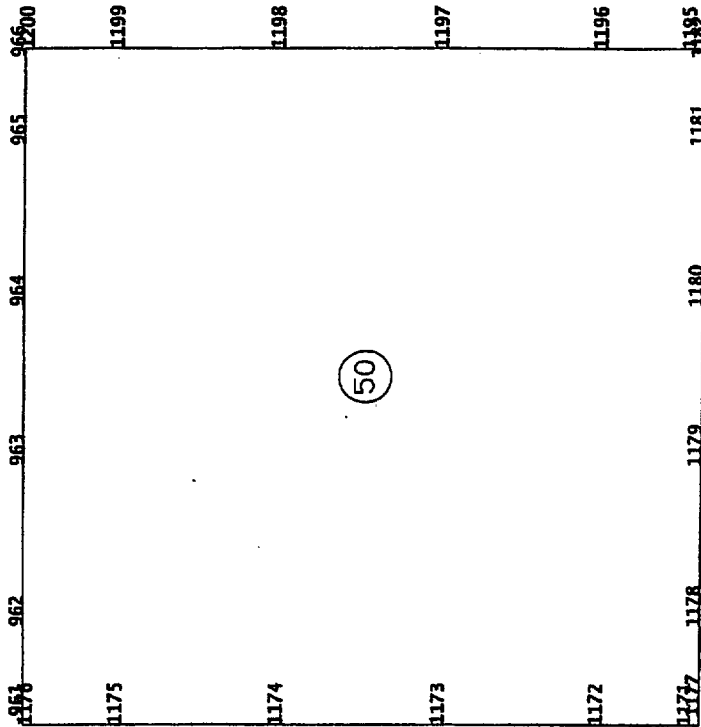


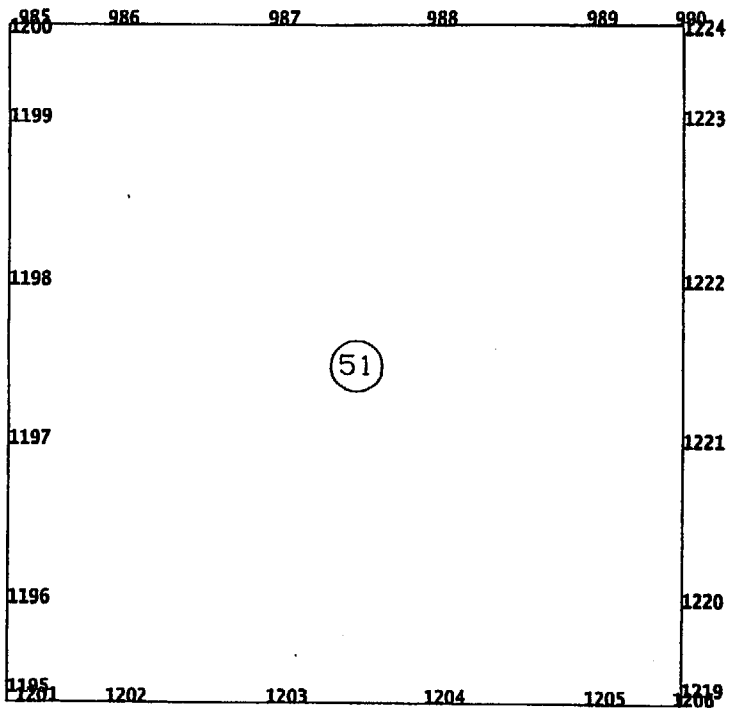


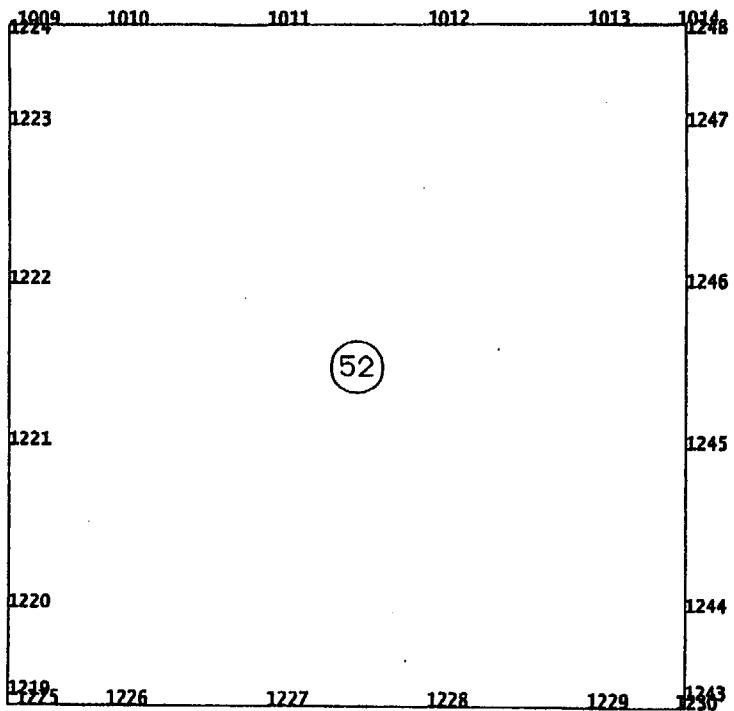


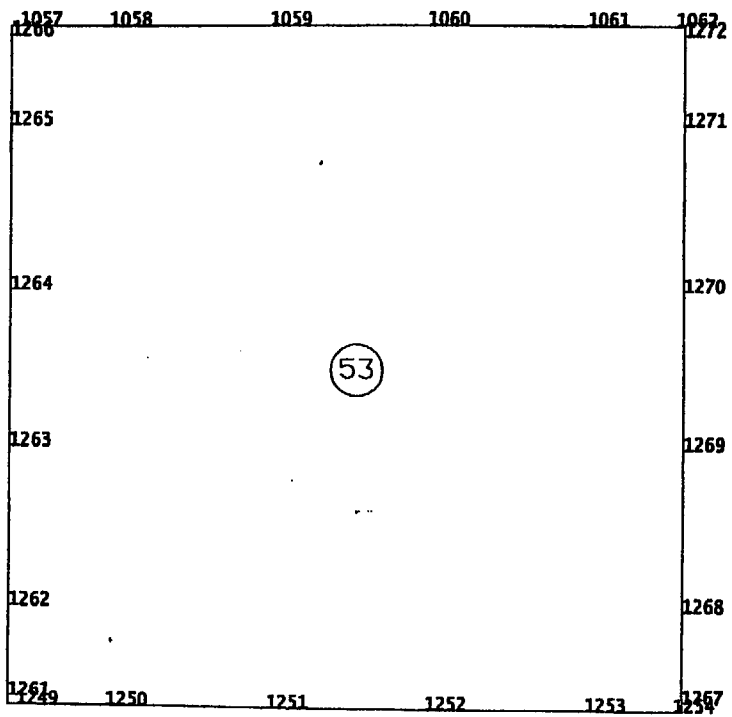


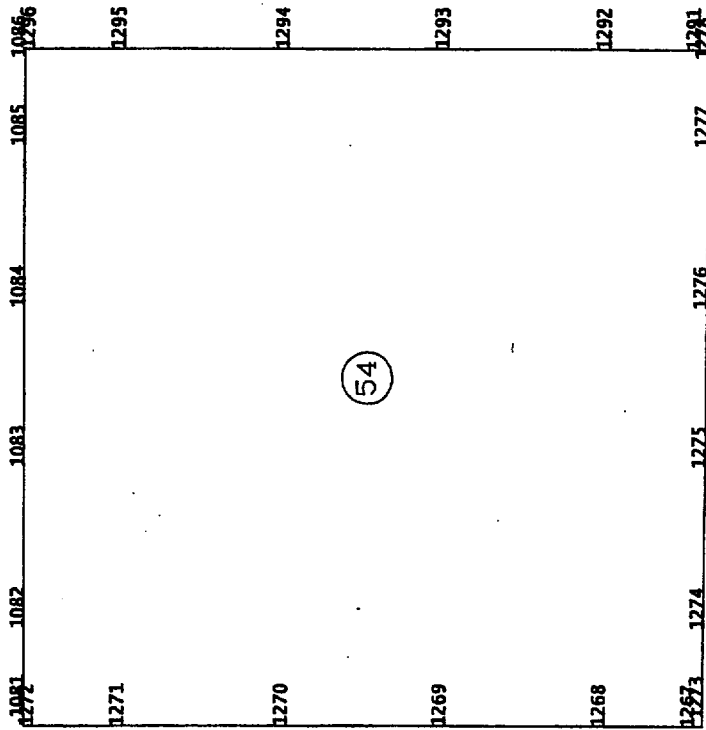


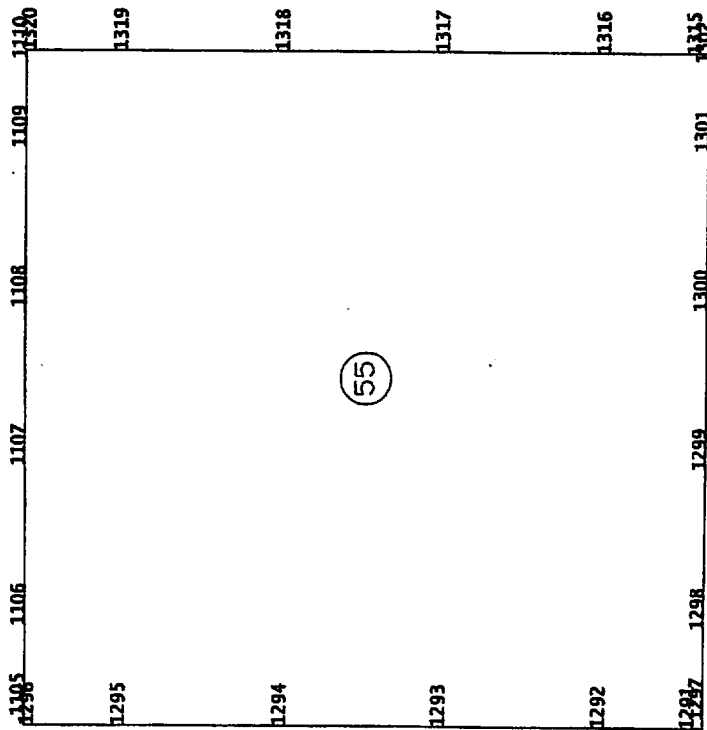


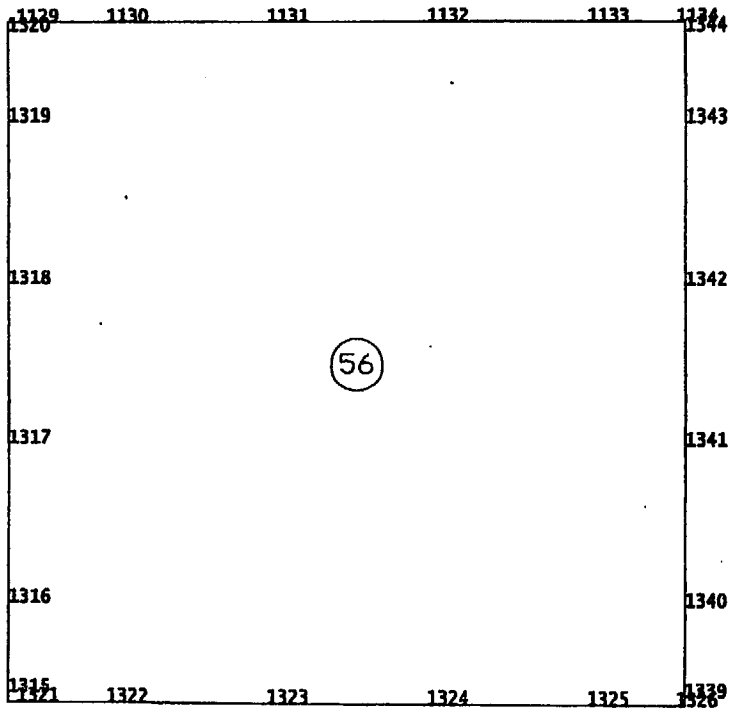


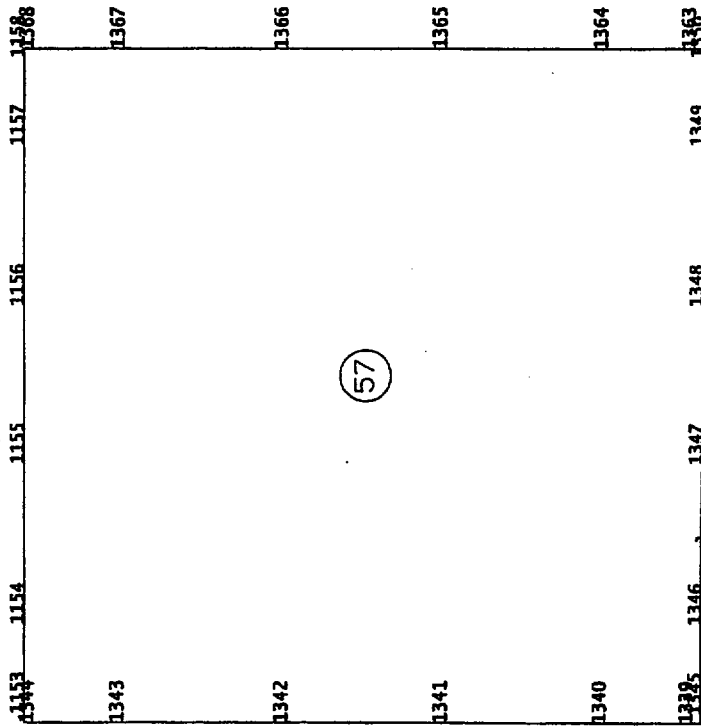


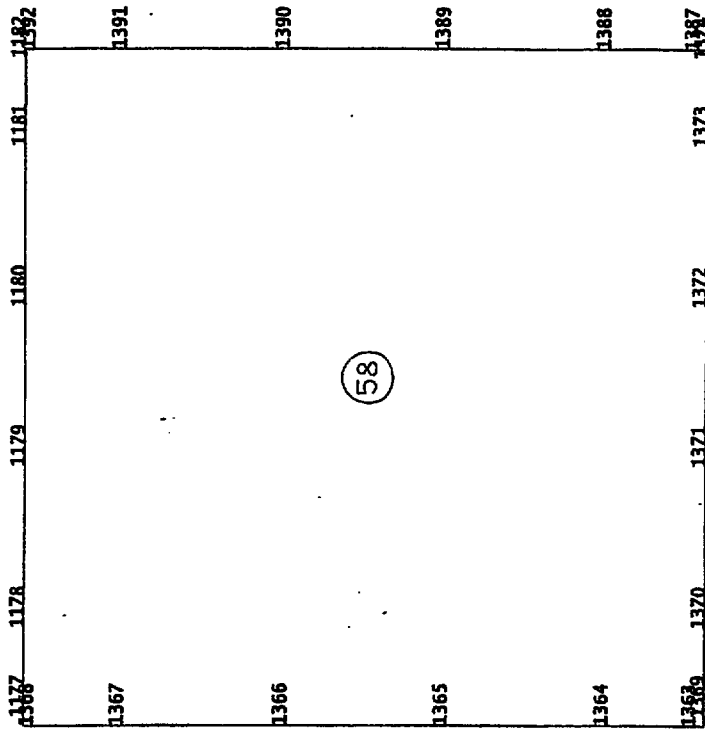


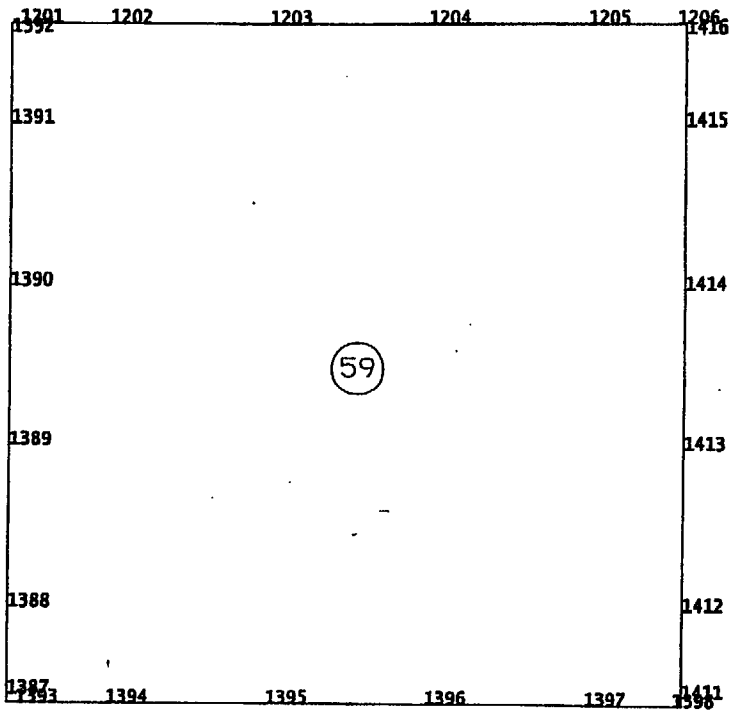


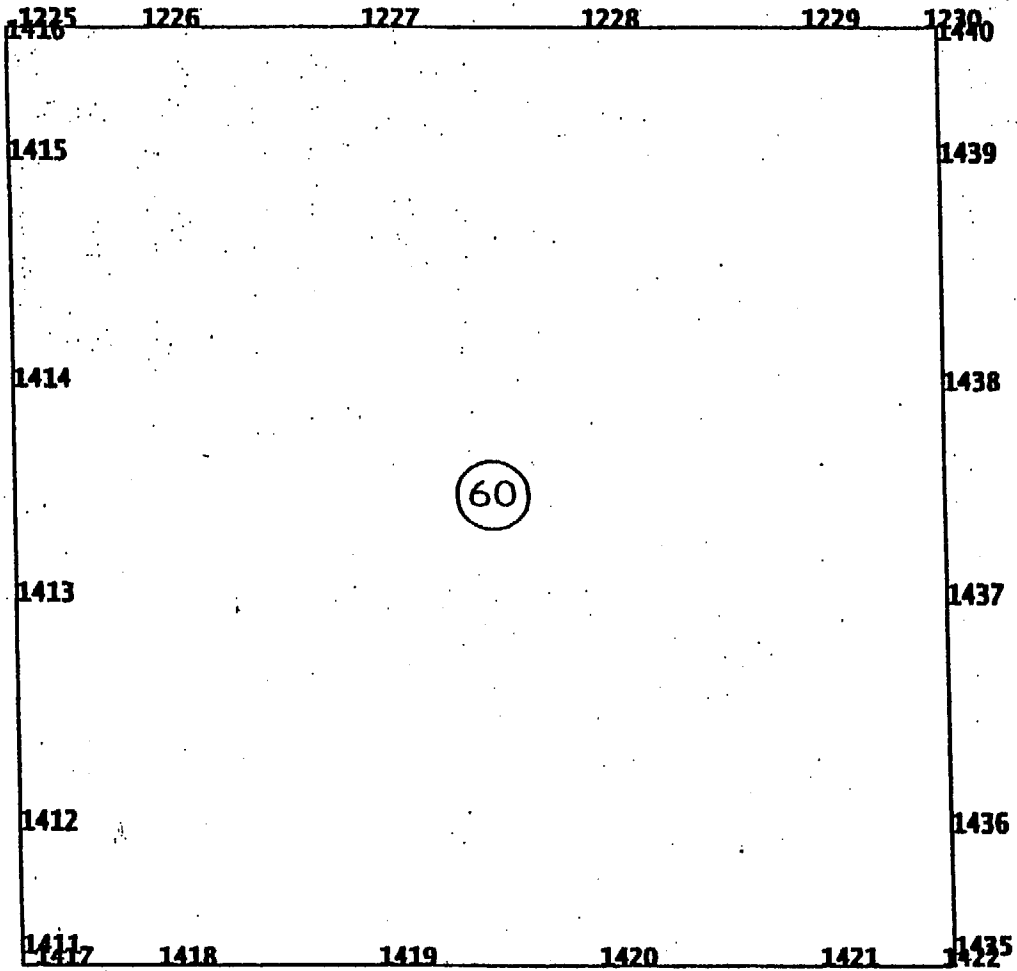


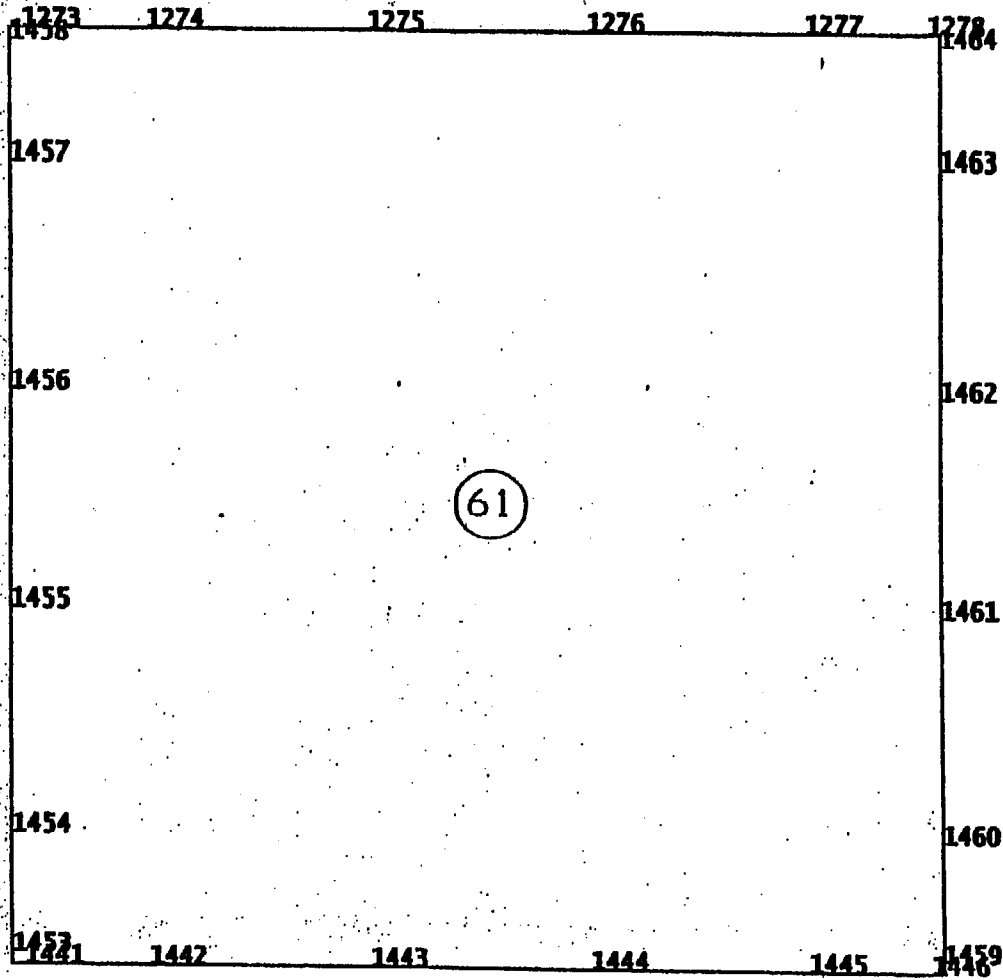


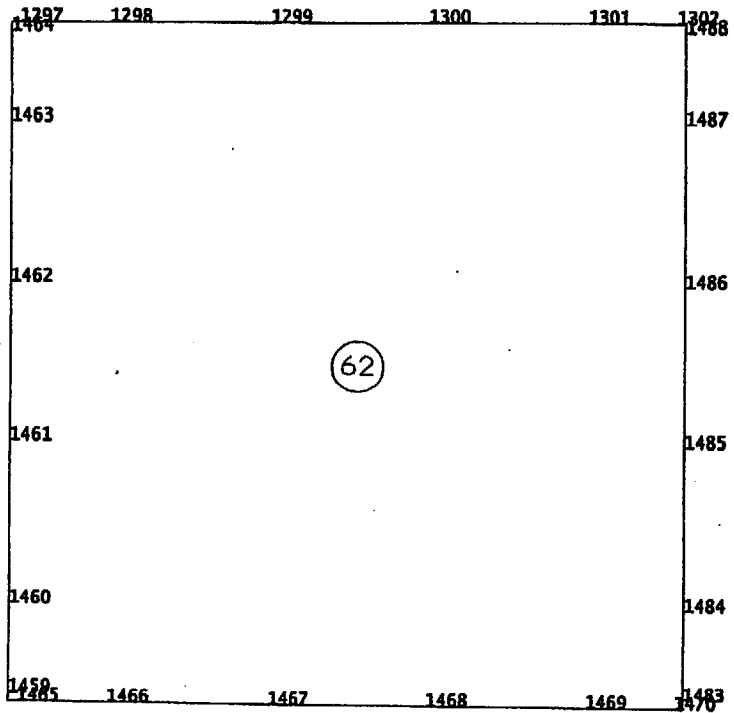


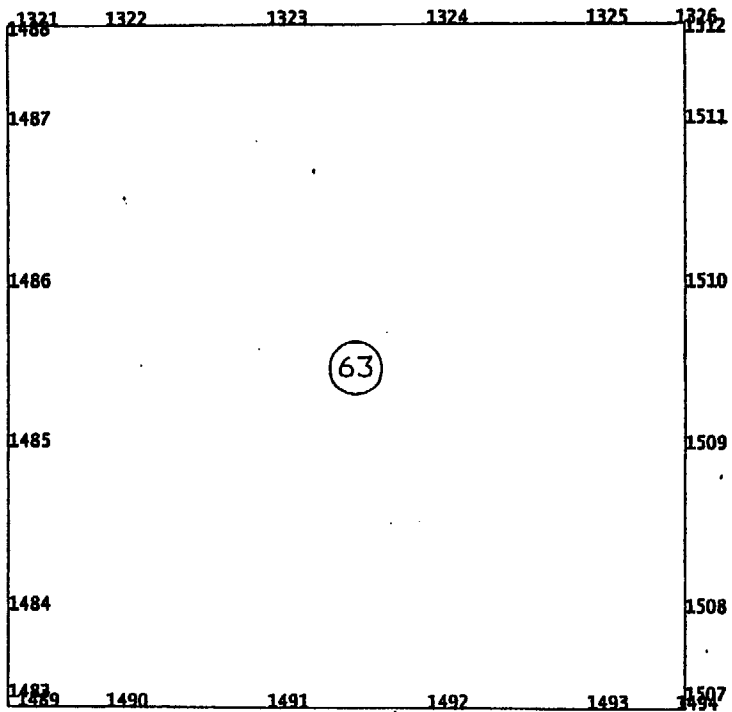


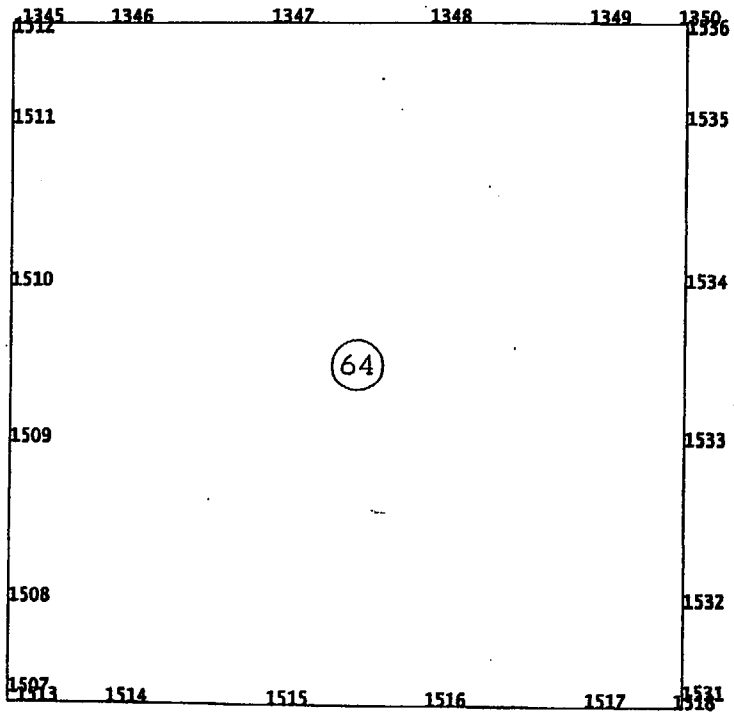












HI-STAR FSAR
REPORT HI-2012610

3.R-67

Rev. 0

